



HAL
open science

Integrated modelling of lipid metabolism in Plasmodium, the causative parasite of malaria

Partho Sen

► **To cite this version:**

Partho Sen. Integrated modelling of lipid metabolism in Plasmodium, the causative parasite of malaria. Parasitology. Université Montpellier II - Sciences et Techniques du Languedoc, 2013. English. NNT : 2013MON20153 . tel-01132704

HAL Id: tel-01132704

<https://theses.hal.science/tel-01132704>

Submitted on 17 Mar 2015

HAL is a multi-disciplinary open access archive for the deposit and dissemination of scientific research documents, whether they are published or not. The documents may come from teaching and research institutions in France or abroad, or from public or private research centers.

L'archive ouverte pluridisciplinaire **HAL**, est destinée au dépôt et à la diffusion de documents scientifiques de niveau recherche, publiés ou non, émanant des établissements d'enseignement et de recherche français ou étrangers, des laboratoires publics ou privés.

THÈSE

Pour obtenir le grade de
Docteur

Délivré par **L'UNIVERSITE MONTPELLIER 2**

Préparée au sein de l'école doctorale
Sciences Chimiques et Biologiques pour la Santé

Et de l'unité de recherche
**Dynamique des Interactions Membranaires Normales et
Pathologiques, (DIMNP-UMR 5235)**

Spécialité : **Biologie Santé**

Présentée par
Partho SEN

**Modélisation intégrée du métabolisme des lipides chez
Plasmodium, parasite causal du paludisme**

**Integrated modelling of lipid metabolism in *Plasmodium*,
the causative parasite of malaria.**

Soutenue le 17 Décembre devant le jury composé de

- | | |
|---|---------------------------|
| Prof. Jean-Pierre MAZAT
Institut de Biochimie et Génétique Cellulaires,
CNRS, Université Bordeaux Segalen, France | Rapporteur |
| Prof. Vassily HATZIMANIKATIS
Ecole polytechnique fédérale de Lausanne & Institut
des sciences et ingénierie chimiques, Laussane, Suisse. | Rapporteur |
| Dr. Cyrille BOTTE
Laboratoire Adaptation et Pathogenie des
Microorganismes, CNRS, Université.
Grenoble, France | Examineur |
| Dr. Henri VIAL
DR INSERM, DIMNP UMR 5235, CNRS, Université
Montpellier 1 & 2, Montpellier, France | Président du jury |
| Prof. Ovidiu RADULESCU
DIMNP UMR 5235, CNRS, Université Montpellier2
Montpellier, France. | Directeur de thèse |

**UNIVERSITE MONTPELLIER 2
SCIENCES ET TECHNIQUES DU LANGUEDOC**

THESE

pour obtenir le grade de

DOCTEUR DE L'UNIVERSITE MONTPELLIER 2

Spécialité: Biologie Santé

Ecole Doctorale: CBS2 - Sciences Chimiques et Biologiques pour la Santé

Titre:

**Modélisation intégrée du métabolisme des lipides chez *Plasmodium*,
parasite causal du paludisme**

**Integrated modelling of lipid metabolism in *Plasmodium*, the causative
parasite of malaria.**

présentée et soutenue publiquement par

Partho SEN

le 17 Décembre 2013

JURY

Prof. Jean-Pierre MAZAT

*Institut de Biochimie et Génétique Cellulaires,
CNRS, Université Bordeaux Segalen, France*

Rapporteur

Prof. Vassily HATZIMANIKATIS

*Ecole polytechnique fédérale de Lausanne & Institut des
sciences et ingénierie chimiques, Laussane, Suisse.*

Rapporteur

Dr. Cyrille BOTTE

*Laboratoire Adaptation et Pathogenie des
Microorganismes, CNRS, Université. Grenoble, France*

Examineur

Dr. Henri VIAL

*DR INSERM, DIMNP UMR 5235, CNRS, Université
Montpellier 1 & 2, Montpellier, France*

Président du jury

Prof. Ovidiu RADULESCU

*DIMNP UMR 5235, CNRS, Université Montpellier2
Montpellier, France.*

Directeur de thèse

Acknowledgements

The period approaching towards end of Ph.D is mingled with emotions. To extend this feelings, I would like to thank all those who made this thesis possible. First and foremost, my research supervisor, Prof.Ovidiu Radulescu who has been extremely encouraging and supportive. His early realization of my research inclination gave me a platform to perform interdisciplinary science in an effective environment. The basic discussions and motivations helped me to orient my thinking to cope up with this fascinating discipline. His constructive criticism helped me to attain the highest possible level of perfection. He had always granted the freedom and encouragement to work independently. These helped me to develop as an independent thinker and a confident researcher. All in all, it was a great experience to work with him and have him as my supervisor.

I am deeply grateful to Dr.Henri Vial, for his support and guidance throughout my PhD thesis. His tremendous knowledge in biology, guided me in troubleshooting conceptual issues. He is always motivating and inspiring. Thanks for providing time from your busy schedule and discussing with me as or when needed. With him I got a chance to meet with other fellow biologist, which enhanced my vision on various aspects in parasitology.

I acknowledge the referees of the jury, Prof.Jean-Pierre Mazat, Prof.Vassily Hatzi-manikatis, Dr.Cyrille Botte, who devoted their valuable time to examine the thesis.

I am also thankful to Prof.Catherine Braun-Breton, director of the lab DIMN-P-UMR-5235, for providing a cordial atmosphere in the lab. Prof.Andrea Parmeggiani for his kind help and useful discussions. Dr.Laurence Berry for useful suggestions. Christine Bousquet for all the administrative work.

Friends form an important part of life, and my friends have always been great companions to me. Thanks ! Vincent Noel for helping me out as or when required. Olivier Dauloudet for cheering me up, with coffee breaks. I pay a similar consideration to my fiancée-Palki, who remained non-demanding and understood the time crunch, I was going through.

Résumé en Français

Le paludisme est responsable de la mort de près d'un million de personnes chaque année. Cette maladie est causée par *Plasmodium*, parasite protozoaire appartenant à la famille des Apicomplexes. Dans cette thèse, nous avons développé des approches de biologie des systèmes pour l'étude du métabolisme des phospholipides (PL) et de sa régulation chez *Plasmodium*. Ces voies métaboliques sont d'une importance primordiale pour la survie du parasite. Lors du développement intra-érythrocytaire, les espèces de *Plasmodium* exploitent un nombre important de voies de synthèse phospholipidique, qui sont rarement trouvées ensemble dans un seul organisme : (i) la voie ancestrale CDP-diacylglycérol des procaryotes ii) les voies eucaryotes *de novo* dite de Kennedy, impliquant CDP- choline ou CDP-éthanolamine (iii) de plus, *P. falciparum* et *P. knowlesi* utilisent une voie transversale impliquant sérine décarboxylase et phospho-éthanolamine-méthyltransférase (SDPM), caractéristique des plantes, et source additionnelle de phosphatidyl-éthanolamine (PE) et de phosphatidyl-choline (PC). Pour comprendre la dynamique d'acquisition et le métabolisme des phospholipides chez *Plasmodium*, nous avons construit un modèle cinétique quantitatif basé sur des données de flux métaboliques (fluxomique) obtenues chez *P. knowlesi*. La dynamique *in vitro* d'incorporation de phospholipides révèle plusieurs voies de synthèse. Nous avons construit un réseau métabolique détaillé et nous avons identifié les valeurs de ses paramètres cinétiques (taux maximaux et constantes de Michaelis). Afin d'effectuer une recherche globale dans l'espace des paramètres, nous avons conçu une méthode hybride d'optimisation, discrète et continue. Des paramètres discrets ont été utilisés pour échantillonner le cône des flux admissibles, alors que les constantes de Michaelis et les taux maximaux ont été obtenus par la minimisation locale d'une fonction objectif, du type moindres carrés. Cette méthode nous a également permis de prédire la répartition des flux au sein du réseau, pour différentes concentrations des précurseurs métaboliques. Cette analyse quantitative a également été utilisée pour comprendre les liens de complémentarité entre les différentes voies. La principale source de PC est la voie de synthèse *de novo* (Kennedy). Des expériences de knock-out *in silico* ont montré l'importance comparable des voies phosphoéthanolamine-N-méthyltransférase

(PMT) et phosphatidyléthanolamine-N-méthyltransférase (PEMT) pour la synthèse de PC. Les valeurs des flux indiquent que la plus grande partie de PE dérivée de la sérine est formée suite à une décarboxylation de sérine, alors que la synthèse de PS paraît surtout impliquer des réactions d'échange de base. L'analyse des flux de la voie CDP-choline montre que la réaction d'entrée de la choline dans le parasite et la réaction cytidylyltransférase de la phosphocholine ont, dans cet ordre, les influences les plus importantes sur le flux de cette voie, mais ne permet pas de distinguer une réaction comme l'unique étape limitante. Ayant comme objectif la compréhension de la régulation de l'expression génique chez *P. falciparum* et son influence sur le fonctionnement métabolique, nous avons aussi effectué une étude bioinformatique intégrative des données du transcriptome et du métabolome pour les principales enzymes impliquées dans le métabolisme PL. L'étude de la dépendance temporelle des variables métaboliques et transcriptomiques au cours du cycle intra-érythrocytaire, a mis en évidence deux modes d'activation des voies PL. Les voies Kennedy sont activées pendant la phase schizogonique et au début de la phase anneau, alors que les voies SDPM et d'échange de bases sont activées vers la fin de la phase anneau et lors de la phase trophozoïte.

Résumé en Anglais

Malaria is responsible of the death of up to one million people each year. This disease is caused by *Plasmodium*, a protozoan parasite. In this thesis we have developed and applied Systems Biology approaches to the study of phospholipid (PL) metabolism and its regulation in *Plasmodium*. These pathways are of primary importance for the survival of the parasite. At the blood stage, *Plasmodium* species display a bewildering number of PL synthetic pathways that are rarely found together in a single organism (i) the ancestral prokaryotic CDP-diacylglycerol dependent pathway (ii) the eukaryotic type *de novo* CDP-choline and CDP-ethanolamine (Kennedy) pathways (iii) *Plasmodium falciparum* and *Plasmodium knowlesi* exhibits additional reactions that bridge some of these routes. A plant-like pathway that relies on serine to provide additional PC and PE, is named the serine decarboxylase-phosphoethanolamine-methyltransferase (SDPM) pathway. To understand the dynamics of PL acquisition and metabolism in *Plasmodium* we have used fluxomic data to build a quantitative kinetic model. *In vitro* incorporation dynamics of phospholipids unravels multiple synthetic pathways. A detailed metabolic network with values of the kinetic parameters (maximum rates and Michaelis constants) has been built. In order to obtain a global search in the parameter space, we have designed a hybrid (discrete and continuous), optimisation method. Discrete parameters were used to sample the cone of admissible fluxes, whereas the continuous Michaelis and maximum rates constants were obtained by local minimization of an objective function. The model was used to predict the distribution of fluxes within the network of various metabolic precursors. The quantitative analysis was used to understand eventual links between different pathways. The major source of phosphatidylcholine (PC) is the CDP-choline Kennedy pathway. *In silico* knock-out experiments showed comparable importance of phosphoethanolamine-N-methyltransferase (PMT) and phosphatidylethanolamine-N-methyltransferase (PEMT) for PC synthesis. The flux values indicate that, major part of serine derived phosphatidylethanolamine (PE) is formed via serine decarboxylation, whereas the phosphatidylserine (PS) is mainly predominated by base-exchange reactions. Metabolic control analysis of CDP-choline pathway shows that the carrier-

mediated choline entry into the parasite and the phosphocholine cytidyltransferase reaction have the largest control coefficients in this pathway, but does not distinguish a reaction as an unique rate-limiting step.

With a vision to understand regulation of gene expression in *P.falciparum* and its influence on the metabolite expression, we have performed an integrative study of the transcriptome and metabolome data for the main enzymes involved in PL metabolism. The study of the correlated time dependence of metabolic and transcriptomic variables during the intraerythrocytic cycle showed that there are two modes of activation of PL pathways. Kennedy pathways are activated during schizogony and early ring stages, whereas SDPM and base exchange pathways are activated during late ring and trophozoite stages.

— *DIMNP-UMR 5235, University of Montpellier2.*

Contents

Acknowledgements	i
Résumé en Français	ii
Résumé en Anglais	iv
List of Tables	x
List of Figures	xi
Abbreviations	1
1 Introduction to Malaria	1
1.1 History of malaria	2
1.2 <i>Plasmodium</i> , the causative organism	4
1.2.1 Lifecycle of <i>Plasmodium falciparum</i>	5
1.2.1.1 The Asexual stages	6
1.2.1.2 The Sexual stages	11
1.3 Symptoms and pathology	12
1.4 Global malarial control strategy	14
1.4.1 Vector control	14
1.4.2 Malarial Vaccine	15
1.4.3 Chemotherapy	16
1.4.3.1 Pharmacology of antimalarials	17

2	Glycerophospholipid metabolism in <i>Plasmodium</i>	20
2.1	Introduction to Glycerophospholipids	21
2.1.1	Phospholipid (PL) acquisition in Prokaryotes and Eukaryotes . .	23
2.1.1.1	PL acquisition in Prokaryotes	23
2.1.1.2	PL acquisition in Eukaryotes	26
2.1.1.3	PL acquisition in <i>Plasmodium</i> species	28
2.1.2	PL biogenesis in <i>Plasmodium</i>	32
2.1.2.1	Biochemical scheme of glycerophospholipid metabolism in <i>Plasmodium</i>	33
2.1.2.2	Different pathways involve in PL metabolism	34
2.1.2.3	Enzymes involved in PL metabolic pathways	37
2.1.3	Pharmacology of choline uptake	41
2.1.3.1	Albitiazolium (bis-thiazolium compound), an antimalar- ial drug candidate designed by Vial and group	43
2.2	Regulation of PL metabolic pathways	46
2.3	Future scope	49
3	Kinetic modelling of Phospholipid synthesis in <i>P.knowlesi</i>	51
3.1	Introduction and Background	52
3.2	The Model description	53
3.3	The hybrid method of optimization.	54
3.4	Flux Balance Analysis.	60
3.5	Results and Discussion	61
3.5.1	Model simplification	62
3.5.2	Training the PL model	63
3.5.3	Model predictions and analysis	66
3.5.4	Source of PC production in absence of CDP-choline pathway. . .	69
3.5.5	Rate-limiting steps for PC synthesis	73
3.6	Conclusion	76

4	Insights of <i>Plasmodium</i> omics from High-throughput analysis	78
4.1	An overview of <i>Plasmodium</i> genome	79
4.2	Functional genomics in <i>Plasmodium</i>	80
4.2.1	Genome diversity and genetic polymorphism	81
4.2.2	Epigenetics and epigenomics of <i>P. falciparum</i>	83
4.2.3	Comparative genomics of <i>P. falciparum</i> isolates	84
4.2.4	Transcriptomics	85
4.2.5	Proteomics	86
4.2.6	Regulation of gene expression in <i>P. falciparum</i>	89
4.2.6.1	Mechanism of transcriptional and post-transcriptional regulation	90
4.2.6.2	Mechanism of translational and post-translational reg- ulation	91
4.2.7	Metabolomics	93
4.2.8	Fluxomics	95
4.3	Methodology for identification, quantification and integration of OMICS	95
4.3.1	Processing and quantification of transcripts or gene expression.	96
4.3.1.1	DNA-Microarray	96
4.3.1.2	Next-Generation sequencing (NGS)	98
4.3.1.3	qPCR	103
4.3.2	Processing and quantification of protein expression	104
4.3.3	Quantification and analysis of metabolic response.	107
4.3.4	Quantification of Fluxes in the Metabolic network.	110
4.3.4.1	Modelling approaches to metabolism of <i>P. falciparum</i> .	111
4.3.5	Conclusion and future perspectives for functional genomics of <i>Plasmodium</i>	112
5	Integrating transcriptome, proteome and metabolome in blood stages of <i>P. falciparum</i>	115
5.1	Introduction and background	116

5.2	A model for translation control during ring to trophozoite transition. . .	119
5.2.1	Dynamical equations relating transcriptome and proteome . . .	119
5.2.2	Ranking transcriptome and proteome according to phase	120
5.3	The experimental study of the relation between transcriptome and metabolome	125
5.3.1	Materials and Methods	125
5.3.2	Processing and quantification of metabolomics data	125
5.3.3	Processing and quantification of qPCR data	127
5.3.4	Results and Discussions	127
5.3.4.1	Metabolomics of Host erythrocyte/RBC	127
5.3.5	Regulation of LP genes and metabolites along cell-cycle	130
5.3.5.1	Regulation of CDP-choline and CDP-ethanolmaine path- way	131
5.3.5.2	Regulation of serine and base-exchange reactions . . .	137
5.3.5.3	Regulation of LP genes and metabolites in Serine de- carboxylation pathway	137
5.4	Conclusion	138
6	General Conclusion	140
	Bibliography	145
	Article published/submitted	174
	Appendix A	175
	Appendix B	183

List of Tables

1	Abbreviation List	xiv
2	List of enzymes involved in PL metabolism and their corresponding ORFs .	40
3	List of the K_m and V_m of some of the enzymes involved in phospholipid metabolism of <i>P.falciparum</i>	49
4	Parameter values for the ODE (PL) Model.	66
5	Transcript counts in during development stage of <i>P. falciparum</i>	86
6	Peptide spectral count during the Intra-development cycle (IDC) of <i>P. falciparum</i>	88
7	RNAseq evidences in <i>P. falciparum</i> , source: <i>PlasmoDB</i>	100
8	Evidences of post-infection quantitative proteomics in <i>P. falciparum</i> . .	105
9	Factors for volume corrections that corresponds to T1...T7, seven different time-points. Volume of <i>Plasmodial</i> cell varies from 3–40 femto liters.	127
10	List of enzymes and ORF indicated in <i>P. falciparum</i>	130

List of Figures

1	An illustration of global malaria burden	3
2	Figure of <i>P.falciparum</i> with major organelles	4
3	Several asexual and sexual stages of development of <i>P.falciparum</i> . . .	6
4	The sporozoite journey to the hepatocyte and subsequent liver stage development.	8
5	Structure of glycerophospholipids	22
6	Scheme of PL metabolism in Prokaryotes	24
7	Scheme of PL metabolism in Eukaryotes	26
8	Composition of phospholipids in <i>P.falciparum</i> infected erythrocytes . .	29
9	FAS II systems in <i>Plasmodium</i>	31
10	Schematic overview of PL metabolism in <i>Plasmodium</i>	33
11	Kennedy pathway in <i>P.knowlesi</i>	34
12	SDPM pathway in <i>Plasmodium</i>	35
13	Base-exchanges in <i>Plasmodium</i>	36
14	Scheme of choline transport in <i>P.knowlesi</i> and <i>P.falciparum</i>	41
15	Scheme of Albitiazolium entry in <i>P.falciparum</i>	45
16	Discretization of the cone of admissible fluxes	57
17	Inversion of the <i>Michaelis-Menten</i> relation.	58
18	Flowchart illustrating the hybrid optimisation method	58
19	Schematic overview of <i>P.knowlesi</i> reactions in structural phospholipid biosynthesis as demonstrated by experimental work	63

20	Fit between the steady state concentration of serine and choline incorporated metabolites with the extracellular serine and choline	64
21	Distribution of fluxes in the network with four different concentrations of SerE, 0 – 100 μ M	68
22	<i>In silico</i> knock-out of PMT (R5)	71
23	<i>In silico</i> knock-out of PEMT/PLMT (R9)	72
24	Sensitivity coefficients matrix	75
25	A schematic representation of contribution of Functional genomics . . .	81
26	Genetic diversity within Gene Ontology (GO) classified on functional categories	82
27	Functional profiles of the expressed proteins. Proteins identified in each stage are plotted as a function of its functional class.	89
28	Schematic overview of process of translation in <i>Plasmodium</i>	90
29	Schematic overview and the scope of identification, quantification and integration of <i>Plasmodium</i> 'OMICS'	96
30	Illustration of DNA Microarray, a general protocol	97
31	Translating ribosome bound mRNA	100
32	Step by step flow of quantification of NGS data	102
33	Illustration of identification and quantification of metabolites	118
34	Transcriptome and proteome data for 121 oscillatory genes during intra-erythrocytic stage of <i>P. falciparum</i>	121
35	Volume of the parasite during intra-erythrocytic stage of <i>P. falciparum</i> as a function of time	123
36	Transition in expression of genes and proteins	124
37	Transmission X-ray tomography of asexual stages of <i>P. falciparum</i> . . .	126
38	Biochemical scheme showing glycerophospholipid metabolism in <i>P. falciparum</i>	129
39	The 48 hours cell cycle of <i>P. falciparum</i>	131

40	The fold change in expression of PL genes and metabolites obtained by qPCR and LC/MS–MS along the 48 hours cell cycle in <i>P.falciparum</i> 3D7	132
41	Regulation of genes and metabolites of CDP-choline pathway along the cell cycle	132
42	Regulation of genes and metabolites of CDP-ethanolamine pathway along the cell cycle	133
43	Regulation of serine	137
44	Dynamic ranges of substrate concentrations.	178
45	Parameter profiles and confidence intervals for a uncorrelated, multiplicative perturbation scheme	179
46	Parameter profiles and confidence intervals for a correlated, multiplicative perturbation scheme	180

Abbreviation Table

Abbreviations	Names	Abbreviations	Names
ACT	Artemisinin-based combination therapy	PA	Phosphatidic acid
ADP	Adenosine bisphosphate	PAP	PA phosphatase
AGPAT	1-acyl-G-3-P acyltransferase	PC	Phosphatidylcholine
ATP	Adenosine triphosphate	PCS	PC synthase
CCT	CTP:phosphocholine cytidyltransferase	PCho/P-Cho/CholP	Phosphocholine
CDP	Cytidine bisphosphate	PE	Phosphatidylethanolamine
CDP-Cho	CDP-choline	PMT	Phosphoethanolamine -N-methyltransferase
CDP-DAG	CDP-diacylglycerol	PEtn/P-Etn/EthaP	Phosphoethanolamine
CDP-Etn	CDP-ethanolamine	PEMT	PE N-methyltransferase
CDS	CDP-DAG synthase	PG	Phosphatidylglycerol
CEPT	Choline/ethanolamine-phosphotransferase	PGPS	PGP synthase
Cho	Choline	PGP	Phosphatidylglycerolphosphate
CK	Choline kinase	PGPPase	PGP phosphatase
CL	Cardiolipin	PI	Phosphatidylinositol
CLS	Cardiolipin synthase	PIS	PI synthase
CPT	Cholinephosphotransferase	PL(s)	Phospholipid(s)
CTP	Cytidine triphosphate	PLMT	PL N-methyltransferase
DAG	Diacylglycerol	PS	Phosphatidylserine
DHAP	Dihydroxyacetone phosphate	PSD	PS decarboxylase
DHAPAT	DHAP acyltransferase	PSS	PS synthase
Etn	Ethanolamine	PPM	Parasite's plasma membrane
EK	Ethanolamine kinase	PV	Parasitophorous vacuole
ECT	CTP:phosphoethanolamine cytidyltransferase	PVM	Parasitophorus- vacuolar-membrane
EPT	Ethanolaminephosphotransferase	Ser	Serine
FA	Fatty acid	SDPM	Serine decarboxylase - phosphoethanolamine- methyltransferase pathway
FAS II	Type II Fatty-acid biosynthesis	SD	Serine decarboxylase
FBA	Flux Balance Analysis	K_m	Affinity constant
FV	Food vacuoles	V_m	Maximum velocity/rate
Glu	Glucose		
GPAT	G-3-P acyltransferase		
G-3-P	Glycerol-3-phosphate		
HT	Hexose transporter		
Ino	Inositol		
IS	Inositol synthase		
IDC	Intra developmental cycle		
ITN	Insecticide treated net		
IRS	Insecticide resistant spray		
IRBC	Infected Red Blood Cells		
NPP	New Permeation Pathway(s)		
OCT	Organic-Cation Transporter		
ODE	Ordinary Differential Equations		

Table 1: List of abbreviations

Chapter 1

Introduction to Malaria

The chapter gives an overview of malaria, its origin and pathology. It discusses about life cycle of causative organism (*Plasmodium*) in human host and vector causing malaria. It also highlights the controls and measures undertaken to combat human malaria. The later part focus on mechanisms of various anitmalerials that has been used for chemotherapy.

1.1 History of malaria

C.Laveran, a French army surgeon stationed in Constantine, Algeria, was the first to notice parasites in the blood of a patient suffering from malaria. This occurred on 6th of November 1880. For his discovery, *Laveran* was awarded the Nobel Prize in 1907. On August 20th, 1897, *Ronald Ross*, a British officer in the Indian Medical Service, was the first to demonstrate that malaria parasites could be transmitted from infected patients to mosquitoes. In further work with bird malaria, *Ross* showed that mosquitoes could transmit malaria parasites from bird to bird. This necessitated a sporogonic cycle (the time interval during which the parasite developed in the mosquito). Thus, the problem of malaria transmission was solved. For his discovery, he was awarded the Nobel Prize in 1902.

The history of malaria predates humanity, as this ancient disease evolved before humans. The ancestors of malaria parasites were about half a billion years old. The pathology and symptoms of malaria was first described in China about 5000 years ago. Then it was reported in Egypt (3500 – 4000 years ago). The enlarge spleens of Egyptians mummies are known to caused by malarial infections. The disease reached India about 3000 years ago, northern Europe between 500 – 1000 years ago.

Global distribution of malaria

According to World Malaria Report (*WHO*, 2010) there were about 219 million cases of malaria (with an uncertainty range of 154 – 289 million) and an estimated 6.6 million deaths (with an uncertainty range of 4.9 – 8.36 million). Most deaths occur among

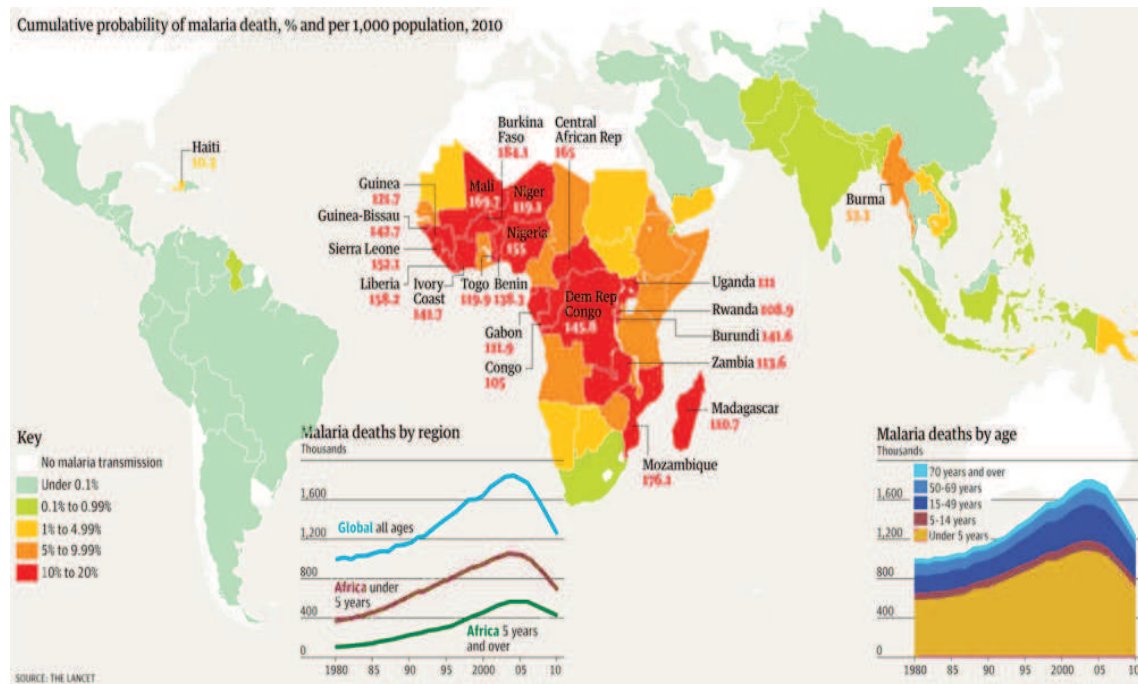


Figure 1: An illustration of malaria transmission, death occurred by region in accordance with WHO, World Malaria Report, 2010, (Courtesy: Jenny Ridley)

children living in Africa where a child dies every minute from malaria. Country level burden estimates (available for 2010) shows that 80% of malaria deaths occur in 14 countries. Together, the Democratic Republic of the Congo and Nigeria account for over 40%.

In 2011, 99 countries and territories had ongoing malaria transmission. Specific population risk groups include : –

- Young children in stable transmission areas who have not yet developed protective immunity against the most severe forms of the disease.
- Non-immune pregnant women as malaria causes high rates of miscarriage and can lead to maternal death.
- Semi-immune pregnant women in areas of high transmission. Malaria can result in miscarriage and low birth weight, especially during first and second pregnancies.
- Semi-immune HIV-infected pregnant women in stable transmission areas, during all pregnancies. Women with malaria infection of the placenta also have a higher

risk of passing HIV infection to their newborns.

- People with HIV/AIDS (*Cohen et al.*, 2005).
- International travelers from non-endemic areas because they lack immunity.
- Immigrants from endemic areas and their children living in non-endemic areas and returning to their home countries to visit friends and relatives are similarly at risk because of waning or absent immunity.

Transmission of Malaria

Malaria is transmitted exclusively through the bites of *Anopheles* mosquitoes. The intensity of transmission depends on factors related to the parasite, the vector, the human host, and the environment. Transmission also depends on climatic conditions that may affect the number and survival of mosquitoes, such as rainfall patterns, temperature and humidity.

1.2 *Plasmodium*, the causative organism

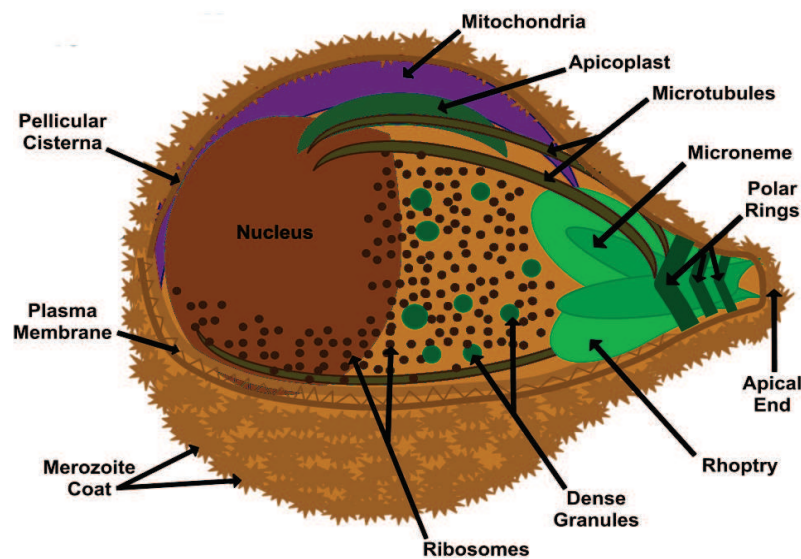


Figure 2: Diagram of *P.falciparum* with major organelles including the rhoptries, micronemes and polar rings near the apical end.

Malaria is caused by a protozoan parasite called *Plasmodium*, a genus of Apicomplexan parasite. It was described in 1885 by *Ettore Marchiafava* and *Angelo Celli*. Currently over 200 species of this genus are recognized and newspecies continue to be described (*Siddall and Barta*, 1992; *Chavatte et al.*, 2007; *Perkins*, 2008). *Plasmodium* is entirely an obligate intracellular parasite that grow and replicate only within the host cells. Four species of *Plasmodium* , *P.falciparum* , *P. vivax* , *P. ovale* and *P. malariae* commonly infect humans, and a fifth, *P.knowlesi* , has recently been identified as being responsible for a significant number of human cases in South-East Asia (*Cox-Singh et al.*, 2008; *Kantele and Jokiranta*, 2011).

1.2.1 Lifecycle of *Plasmodium falciparum*

Plasmodium falciparum is the causative agent of malaria. It causes most severe forms of human infectious diseases. The closest known relative of *P.falciparum* is *reichenowi* (*Rich et al.*, 2009). The life cycle of the *P. falciparum*, malaria parasite is complex and comprises two hosts: an intermediate vertebrate host (human) and a definitive invertebrate host (female *Anopheles* mosquito) where the asexual and sexual stages of the parasite occur respectively.

All these stages have their own unique shapes and structures and protein complements. The survival and development of the parasite is made possible by more than 5,000 genes and their specialized proteins which helps the parasite to invade and grow within multiple cell types and to evade host immune responses (*Greenwood et al.*, 2008; *Florens et al.*, 2002).

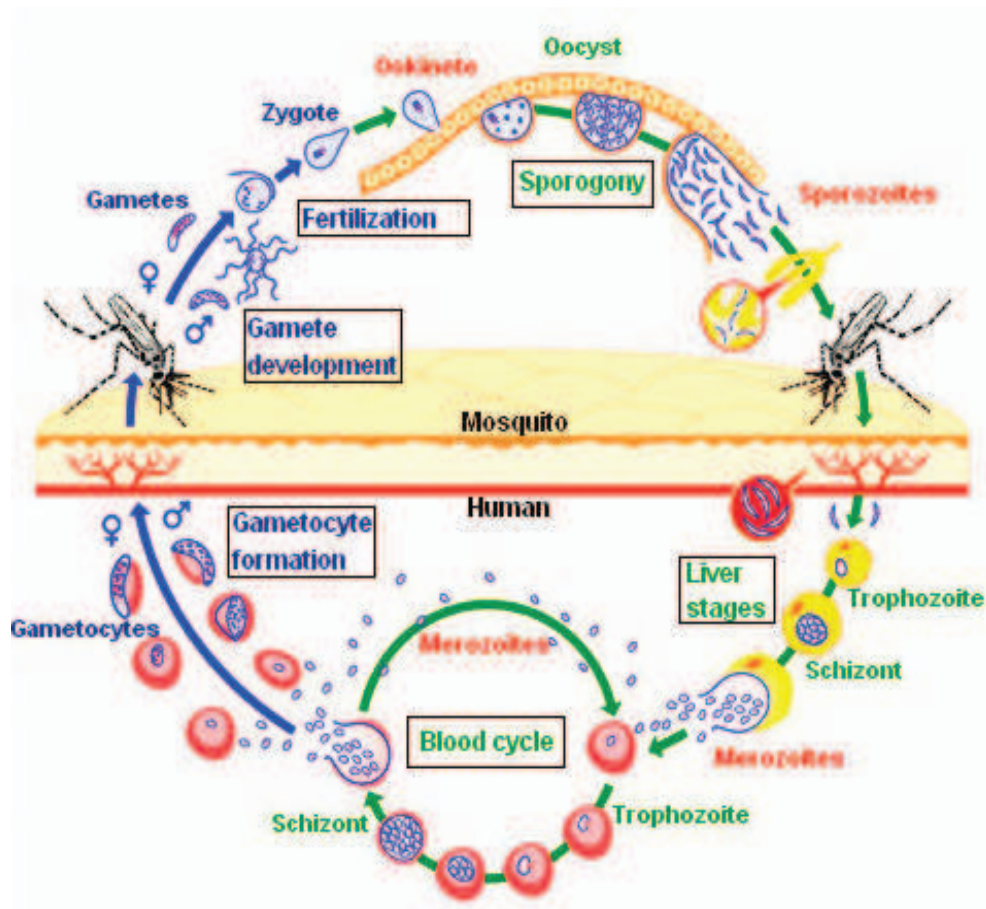


Figure 3: Several asexual and sexual stages of development of *P.falciparum* such as the sporozoites (Gr. *Sporos* = seeds; the infectious form injected by the mosquito), merozoites (Gr. *Meros* = piece; the stage invading the erythrocytes), trophozoites (Gr. *Trophes* = nourishment; the form multiplying in erythrocytes), schizonts are round to oval inclusions that contain the deeply staining merozoites and gametocytes (sexual stages).

1.2.1.1 The Asexual stages

Man is the intermediate host for malaria, wherein asexual phase of the life cycle occurs. This stage is further divided into two sub phases a) Pre-erythrocytic phase b) Erythrocytic phase. The sporozoites inoculated by the infested mosquito initiate this phase of cycle in the liver, and in the latter part it continues within the red blood cells.

a) Pre-erythrocytic phase

When the infected *Anopheles* mosquito takes a blood meal on mammalian host, tens to hundred invasive sporozoites are introduced into the skin (*Jin et al.*, 2007). Following the intradermal deposition, some sporozoites are destroyed by the local macrophages, some enter the lymphatics, while others find a blood vessel (*Yamauchi et al.*, 2007; *Vaughan et al.*, 2008; *Silvie et al.*, 2008). The sporozoites that enter a lymphatic vessel reach the draining lymph node wherein some of the sporozoites partially develop into exoerythrocytic stages (*Vaughan et al.*, 2008). The parasite might prime the T cells to mount a protective immune response (*Good and Doolan*, 2010). The sporozoites that enters a blood vessel reach the liver within a few hours.

It has been shown that the sporozoites travel by a continuous sequence of stick and slip motility, using the thrombospondin related anonymous protein (TRAP) family and an actin-myosin motor (*Baum et al.*, 2006; *Yamauchi et al.*, 2007; *Münter et al.*, 2009).

The sporozoites then negotiate through the liver sinusoids, and migrate into a few hepatocytes, where they multiply and grow within parasitophorous vacuoles. Each sporozoite develop into a schizont containing 10,000 – 30,000 merozoites (or more in case of *P.falciparum*) (*Amino et al.*, 2006; *Jones et al.*, 2006; *Kebaier et al.*, 2009).

The growth and development of the parasite in the liver cells is facilitated by a favorable environment created by the circumsporozoite protein of the parasite (*Prudêncio et al.*, 2006; *Singh et al.*, 2007). The entire pre-erythrocytic phase lasts about 5–16 days depending on the parasite species. It averages between 5 – 6 days for *P.falciparum*, 8 days for *P.vivax*, 9 days for *P.ovale*, 13 days for *P.malariae* and 8 – 9 days for *P.knowlesi*. The pre-erythrocytic phase remains a silent phase, with little pathology and no symptoms, as only a few hepatocytes are affected (*Vaughan et al.*, 2008).

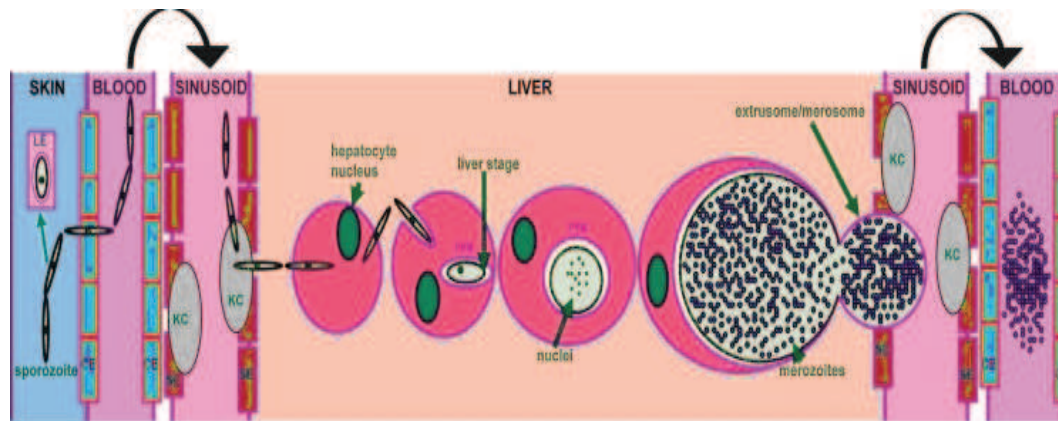


Figure 4: Courtesy: (Vaughan et al., 2008). The figure illustrates the sporozoite journey to the hepatocyte and subsequent liver stage development (Parasite/Host Interactions). The infectious sporozoite is deposited into the skin and subsequently enters the bloodstream through a capillary endothelial cell (CE). A number of sporozoites also enter draining lymph nodes and can partially develop within the lymphoid endothelium (LE). Once in the liver sinusoid, sporozoites glide along the fenestrated endothelia (SE) and cross the sinusoidal cell barrier by traversing a resident Kupffer cell (KC). The sporozoite then traverses a number of hepatocytes before invading a hepatocyte with the formation of a parasitophorous vacuole membrane (PVM). Massive replication and growth lead to the formation of erythrocyte-infectious merozoites that enter the sinusoid packaged in extrusomes/merosomes and are subsequently released in the pulmonary bloodstream. The parasite and host proteins known to be involved in the individual steps of this cascade are listed under the appropriate location, and a timeline for the whole process for rodent parasites and human parasites (postinfection, PI) is depicted at the base of the figure.

b) Erythrocytic phase

The merozoites released from the liver recognize, attach, and enter the red blood cells (RBCs) (see Figures. 3 & 4) by multiple receptor-ligand interactions in as little as 60 seconds. This quick disappearance from the circulation into the red cells minimizes the exposure of the antigens on the surface of the parasite, thereby protecting these parasite forms from the host immune response (Cowman and Crabb, 2006; Greenwood et al., 2008).

The invasion of the merozoites into the red cells is facilitated by molecular interactions between distinct ligands on the merozoite and host receptors on the erythrocyte membrane. *P.vivax* invades only "Duffy" blood group-positive red cells, using the Duffy-binding protein and the reticulocyte homology protein, found mostly on the reticulocytes. The more virulent *P.falciparum* uses several different receptor families and alternate invasion pathways that are highly redundant. Varieties of Duffy binding-like (DBL) homologous proteins and the reticulocyte binding-like homologous proteins of *P.falciparum* recognize different RBC receptors other than the Duffy blood group or the reticulocyte receptors. Such redundancy is helped by the fact that *P.falciparum* has four Duffy binding-like erythrocyte-binding protein genes, in comparison to only one gene in the DBL-EBP family as in the case of *P.vivax*, allowing *P.falciparum* to invade any red cell (Mayer *et al.*, 2009; Weatherall *et al.*, 2002).

The process of attachment, invasion, and establishment of the merozoite into the red cell is made possible by the specialized apical secretory organelles of the merozoite, called the micronemes, rhoptries, and dense granules. The initial interaction between the parasite and the red cell stimulates a rapid wave of deformation across the red cell membrane, leading to the formation of a stable parasite-host cell junction. Following this, the parasite pushes its way through the erythrocyte bilayer with the help of the actin-myosin motor, proteins of the thrombospondin-related anonymous protein family (TRAP) and aldolase. It thus creates a parasitophorous vacuole to seal itself from the host-cell cytoplasm, thus creating a hospitable environment for its development within the red cell. At this stage, the parasite appears as an intracellular ring (Cowman and Crabb, 2006; Haldar and Mohandas, 2007).

Within the red cells, the parasite numbers expand rapidly with a sustained cycling of the parasite population. Even though the red cells provide some immunological advantage to the growing parasite, the lack of standard biosynthetic pathways and intracellular organelles in the red cells tend to create obstacles for the fast growing intracellular parasites. These impediments are overcome by the growing ring stages by several mechanisms (a) restriction of the nutrient to the abundant hemoglobin, (b) dramatic expansion of the surface area through the formation of a tubovesicular

network, and (c) export of waste and range of remodeling and virulence factors into the red cell (*Silvie et al.*, 2008). Hemoglobin from the red cell, the principal nutrient for the growing parasite, is ingested into a food vacuole and degraded. The amino acids thus made available are utilized for protein biosynthesis and the remaining toxic heme is detoxified by heme polymerase and sequestered as hemozoin (malaria pigment). The parasite depends on anaerobic glycolysis for energy, utilizing enzymes such as pLDH, plasmodium aldolase etc. As the parasite grows and multiplies within the red cell, the membrane permeability and cytosolic composition of the host cell is modified (*Lew et al.*, 2003; *Kirk*, 2004). These new permeation pathways induced by the parasite in the host cell membrane help not only in the uptake of solutes from the extracellular medium but also in the disposal of metabolic wastes, and in the origin and maintenance of electrochemical ion.

The erythrocytic cycle occurs every 24 hours in case of *P.knowlesi*, 48 hours in cases of *P.falciparum*, *P.vivax* and *P.ovale* and 72 hours in case of *P.malariae*. During each cycle, each merozoite grows and divides within the vacuole into 8 – 32 (average 10) new merozoites, through the stages of ring, trophozoite, and schizont. At the end of the cycle, the infected red cells rupture, releasing the new merozoites that in turn infect more RBCs. With unbridled growth, the parasite numbers can rise rapidly to levels as high as 10^{13} per host (*Greenwood et al.*, 2008). A small proportion of asexual parasites do not undergo schizogony but differentiate into the sexual stage gametocytes. These male or female gametocytes are extracellular and nonpathogenic and help in transmission of the infection to others through the female anopheline mosquitoes, wherein they continue the sexual phase of the parasite's life cycle. Gametocytes of *P.vivax* develop soon after the release of merozoites from the liver, whereas in case of *P.falciparum*, the gametocytes develop much later with peak densities of the sexual stages typically occurring 1 week after peak asexual stage densities (*Pukrittayakamee et al.*, 2008).

1.2.1.2 The Sexual stages

Mosquitoes are the definitive hosts for the malaria parasites, wherein the sexual phase of the parasite's life cycle occurs. The sexual phase results in the development of innumerable infecting forms of the parasite within the mosquito that induce disease in the human host following their injection with the mosquito bite (see Figure.3).

Gametocytes are the only erythrocytic forms of the parasite that are capable of infecting *Anopheles* mosquito vectors (Talman *et al.*, 2004). When the female *Anopheles* draws a blood meal from an individual infected with malaria, the male and female gametocytes of the parasite find their way into the gut of the mosquito. The molecular and cellular changes in the gametocytes help the parasite to quickly adjust to the insect host from the warm-blooded human host and then to initiate the sporogonic cycle. The female gametocyte develops into a single female gamete, the male gametocyte undergoes exflagellation that gives rise to 8 thread-shaped motile male gametes (Rawlings *et al.*, 1992). In the mosquito midgut, the male gamete fuses with the female gamete resulting in a diploid zygote (see Figure.3). Within 20 – 24 hours following the blood meal, non-motile zygote undergoes morphological changes and develops into a diploid/tetraploid motile ookinete (Alano, 2007). Growth and division of each oocyst produces thousands of active haploid forms called sporozoites. After the sporogonic phase of 8 – 15 days, the oocyst bursts and releases sporozoites into the body cavity of the mosquito, from where they travel to and invade the mosquito salivary glands. When the mosquito thus loaded with sporozoites takes another blood meal, the sporozoites get injected from its salivary glands into the human bloodstream, causing malaria infection in the human host. The sporozoites along with the saliva are now ready to be injected into the vertebrate host during the next blood meal of the mosquito (Alano, 2007). It has been found that the infected mosquito and the parasite mutually benefit each other and thereby promote transmission of the infection. The *Plasmodium*-infected mosquitoes have a better survival and show an increased rate of blood feeding, particularly from an infected host (Barillas-Mury, 2007; Hill, 2006; Ferguson and Read, 2004).

1.3 Symptoms and pathology

Malaria typically begins after 8 – 25 days of infection. However, symptoms may occur later in those who have taken antimalarial medications as prevention (*Nadjm and Behrens, 2012*). Initial manifestations of the disease common to all malaria species are flu-like symptoms, (*Bartoloni and Zammarchi, 2012*) and can resemble other conditions such as septicemia, gastroenteritis, and viral diseases (*Nadjm and Behrens, 2012*).

The clinical symptoms of malaria are related to the development of asexual parasites in the blood. The disease can be broadly classified into two types, a) mild or uncomplicated malaria and b) severe or complicated malaria. The symptoms of mild or uncomplicated malaria are nonspecific, such as fever, shivering, chills, headache, musculoskeletal and abdominal pain, fatigue, vomiting and/or diarrhoea etc. These symptoms present a clinical picture that resembles the symptoms of many other childhood infectious diseases. These non-specific signs of malaria are believed to be caused by the release of a malarial toxin which induces macrophages to secrete tumour necrosis factor α (TNF α) and interleukin-1 (IL-1), common mediators induced by *Plasmodium* species. Although the nature of malarial toxin is controversial, it is generally agreed that it is released at the time of schizont rupture (*Miller et al., 2002*). Uncomplicated malaria is terminated either by host immunity or by drug treatment.

The classic symptom of malaria is paroxysm, a cyclical occurrence of sudden coldness followed by rigor and then fever and sweating, occurring every two days (tertian fever) in *P.vivax* and *P.ovale* infections, and every three days (quartan fever) for *P.malariae*. *P.falciparum* infection can cause recurrent fever every 36 – 48 hours or a less pronounced and almost continuous fever.

Symptoms of *P.falciparum* malaria arise 9 – 30 days after infection (*Bartoloni and Zammarchi, 2012*). Individuals with cerebral malaria frequently exhibit neurological symptoms, including abnormal posturing, nystagmus, conjugate gaze palsy (failure of the eyes to turn together in the same direction), opisthotonus, and seizures (*Bartoloni and Zammarchi, 2012*).

P.falciparum malaria indicate a complex syndrome, established by host and parasite factors. The main virulence phenotypes are related to cytoadherence, rosetting and antigenic variation. Cytoadherence or adhesion to the endothelium has an important role in the pathogenicity of the disease causing occlusion of small vessels and contributing to the failure of many organs. Rosetting signifies the formation of rosettes due to adhesion of uninfected erythrocytes with erythrocytes infected with mature forms of the parasite. In *P.falciparum* malaria, rosetting seems to increase microvascular obstruction of the blood flow and can hide the infected cell thereby protecting it from phagocytosis (Rowe *et al.*, 2009). In *P.falciparum*, various surface antigens mediate adhesion to several receptors of the host endothelium, preventing the infected erythrocytes from passing through the spleen, where they would be destroyed. In doing so however, the erythrocyte surface proteins make the parasite "visible" to the host immune system and thus the parasite needs to vary the proteins to avoid destruction (Scherf *et al.*, 2008). It is important to understand the role of host receptors and parasite ligands involved in the development of different clinical syndromes for developing new control methods to reduce the mortality rates of this disease.

Pathological disorders of *P.falciparum* malaria have shown severe complications. The obstruction of cerebral venules and capillaries with erythrocytes containing mature trophozoites and schizonts causes convulsions and coma. Acidosis and hypoglycemia are the most common metabolic complications in severe malaria. Acute pulmonary edema is also a common fatal complication, presenting interstitial edema with swollen endothelial cells and monocytes narrowing the capillary lumen. Acute renal failure is another important complication in severe malaria and is defined by an increase in the serum creatinine or an increase in blood urea (Greenwood *et al.*, 2008).

Some of the major pathological disorder caused by malaria are listed below : –

- Anaemia is the inevitable consequence of the infection of red cells with parasites, but other alterations of the infected red cell may lead to cell rigidity and to changes in cytoadherent properties.
- Sequestration of *P.falciparum* in the brain leads to cerebral malaria, the most dramatic complication of falciparum malaria.

- Enlargement of the spleen is the most constant clinical sign of malaria infections, but in some individuals this may lead to hyperreactive malarial splenomegaly.
- As in most infection, transient glomerulonephritis may occur in acute forms of the disease. Immune complex deposition may lead to fatal forms of "quartan malarial nephropathies".
- The intervillous spaces of the placenta offer a very favorable environment for parasite development which may lead to placental malaria, with its consequences on foetal growth.

1.4 Global malarial control strategy

Control, elimination and research are the 3 key strategies implemented to combat the disease. Control indicates controlling the disease in malaria-endemic countries. This makes a substantial impact on their malaria burden by controlling it with existing tools. Secondly, by reducing all locally-acquired infections within a country to zero will bring the world closer to the ambitious goal of global eradication. Together, malaria control and elimination efforts will require international research activities. This will help to discover new tools to combat malaria.

With a vision to eradicate the malaria; vector control, vaccination and chemotherapy are in prime focus amongst implemented strategies.

1.4.1 Vector control

Vector control is an important part of the global malaria control strategy. The idea behind vector control is to reduce the levels of mortality and morbidity by reducing transmission of the disease. Basically, there are many efforts focused on preventing man-vector contact by large-scale implementation of (i) Indoor Residual Spraying (IRS) which can be achieved by applying long-lasting chemical insecticides on the walls and the roofs of the houses and (ii) Insecticide Treated Nets (ITNs) which can be efficient at places where a large proportion of human-biting by local vectors takes place after

people have gone to sleep. In community-wide trials in several African settings, ITNs have been shown to reduce mortality rate by about 20%. Other measures includes larviciding, this is only used for vectors which tend to breed in permanent or semi-permanent water bodies that can be identified and treated.

1.4.2 Malarial Vaccine

Recombinant proteins, synthetic peptides, DNA vaccines, inactivated whole parasites, and vaccines (comprising mixtures of a large variety of potential antigens) are continuously evaluated against malaria.

Vaccine that are categorized specifically on the different stages of the parasite are as follows:-

- a). **Pre-erythrocytic Vaccine:** It aims to protect against the early stage of malaria infection. The first malaria vaccination trial against pre-erythrocytic stages was made with radiation attenuated sporozoites. Initial studies have shown that in humans, vaccination with radiation attenuated sporozoites provided about 90% protection when subsequently challenged by bite of infected mosquitoes (*Vanderberg, 2009*). Even though a high degree of protection could be achieved using irradiated sporozoites, it presents some challenges in extracting and purifying sporozoites from mosquito salivary glands. Nevertheless, there are some liver stage subunit vaccines in clinical trials which are based on immunogenic components of sporozoites or liver stage parasites. The most promising vaccine currently in phase III clinical trial is RTS,S which is directed against the CSP protein in the liver stage. Recent data from phase III clinical trials showed that RTS,S provided 50% reduction in incidence of malaria in young children (*Agnandji et al., 2011*).
- b). **Erythrocytic stage vaccine:** It targets the malaria parasite at its most destructive strategy rapid replication of the organism in human red blood cells. Vaccines targeting erythrocytic stages include antigens like PfMSP-1, PfMSP3 are in phase II clinical trials (*Pierce and Miller, 2009*).
- c). **Transmission-blocking Vaccine:** It interrupts with the life cycle of the par-

asite by inducing antibodies that prevent the parasite from maturing in the mosquito after it takes a blood meal from a vaccinated person. Most extensive studies have focused on sexual stagespecific antigens; Pfs48/45, Pfs230, Pfs25, Pfs28 of *P.falciparum* and orthologues in other *Plasmodium* species (Sutherland, 2009).

Although a safe and effective malaria vaccine would be the easiest way to control malaria, but even after decades of research, that vaccine is still elusive. The complex life cycle of the parasite involving human and vector mosquitoes as well as its allelic diversity, antigenic variations and difficulties in generating high levels of durable immunity continue to make the development and implementation of an effective vaccine problematic.

1.4.3 Chemotherapy

Successful malaria control depends greatly on treatment with efficacious anti-malarial drugs. To adequately treat malaria, drugs must be fast acting, highly potent against asexual blood stage infections, minimally toxic and affordable to residents of endemic regions. Correct use of such an antimalarial drug will not only shorten the duration of malaria illness but also reduce the incidence of complications and the risk of death. The state of the art knowledge on currently existing and developing antimalarial drugs has been reviewed in several recent articles (N Burrows *et al.*, 2011). A major problem leading to a decline in the efficacy of currently existing antimalarials is the growing emergence of drug resistance. Resistance to antimalarial drugs normally arises as a result of spontaneously-occurring mutations that affect the structure and activity of the drug target in the malaria parasite or affect the access of the drug to the target. Recent progress in understanding the mechanisms of parasite's resistance to antimalarials has been described by (Mita *et al.*, 2009; Sridaran *et al.*, 2010).

1.4.3.1 Pharmacology of antimalarials

Choloroquine which is a 4–Aminoquinolines derivative binds with toxic heme (released during haemoglobin catabolism in erythrocytic cycle) to prevent its crystallization to hemozoin. This allows heme concentration to rise and kill the parasite (*Bray et al.*, 1999). Chloroquine resistance has been associated to point mutation in Chloroquine Resistance Transporter (PfCRT), an integral membrane protein localized to the parasite's internal digestive vacuole. These mutations result in a marked reduction in the accumulation of chloroquine by the parasite (*Martin et al.*, 2009; *Sidhu et al.*, 2002).

Quinine, an aryl amino alcohol, is a naturally occurring compound obtained from the bark of American cinchona tree. It was the first antimalarial and its use dates back to 17th century. It is accumulated in the digestive vacuole of the erythrocytic parasites. It is less effective than chloroquine and has a narrow therapeutic range. Resistance to quinine has been developing in Southeast Asia (*White*, 1992). However, the short term efficacy of quinine plus antibiotics, notably quinine-clindamycin regimens, has been reported in the treatment of severe malaria in Africa (*Winstanley*, 2001).

Mefloquine, an amino alcohol, is also thought to work in much the same way as quinine. It is well absorbed from the gut and elimination is very slow (half-life ranging from 15–33 days). However, it is used only for uncomplicated malaria and is relatively expensive. Furthermore, in recent years, resistance to mefloquine has been reported in some parts of Southeast Asia (especially the Thai borders with Burma and Cambodia). Mefloquine can cause severe idiosyncratic adverse reactions, however these are rare. In contrast, dosedependent symptomatic reactions, most commonly gastrointestinal upset and dizziness are common. The most serious of these include psychoses, seizures, and acute encephalopathy (*Croft and Black*, 1999).

Halofantrine also seems to have a mechanism of action similar to that of chloroquine. Its parenteral formulation is under development. Like mefloquine, it is an expensive drug and is unaffordable for general use throughout tropical Africa. It is incompletely absorbed from the gut (*Amponsaa-Karikari et al.*, 2009).

Primaquine is a synthetic 8-Aminoquinoline compound and is mainly used to eradicate liver hypnozoites of *P.vivax* and *P.ovale* to prevent late relapses of malaria (Baird and Rieckmann, 2003). It is normally started when the course of chloroquine has been completed, and the patient is recovering. Primaquine is well absorbed from the gut after oral administration but has a short half-life (half-life 56 h) and needs to be administered daily. It may cause mild gastrointestinal adverse effects. One major problem of primaquine is that it can cause more serious toxicity in patients with glucose-6-phosphate dehydrogenase deficiency. Tafenoquine (WR238605) is a new synthetic analogue of primaquine which is currently in phase IIb clinical trials. It has a larger therapeutic index than primaquine and much slower elimination (half-life 14 days) (Brueckner et al., 1998).

Combination of antimalarials to overcome resistance

Pyrimethamine, a diamino pyrimidine, was always used in combination with sulfadoxine (Fansidar). The potential benefits of pyrimethamine combinations included synergistic effects resulting in improved efficacy and reduced exposure time of parasite populations (biomass) to drugs thus reducing occurrence of drugresistance mutations. Sulfadoxine-pyrimethamine combination was used only in uncomplicated cases of *P.falciparum* malaria because it produced clinical improvement too slowly in severe disease. Pyrimethamine inhibits the dihydrofolate reductase enzyme thereby blocking the synthesis of purines which are essential for DNA synthesis. Unfortunately, as a result of drug pressure, resistance to sulfadoxine + pyrimethamine combination has been reported which limits its use in many areas. The resistance is correlated to mutations in dihydrofolate reductase (DHFR) and dihydropteroate synthase (DHPS), the respective targets of pyrimethamine and sulfadoxine (Sridaran et al., 2010).

Artemisinin is sesquiterpene lactone peroxide that is extracted from the Chinese herb *Artemisia annua* that have been used since the late 1970s. They reduce the parasite load substantially earlier than other antimalarial drugs. Additionally, they can kill *Plasmodium* gametes and thus lower transmission rates. Their mechanism of action is unclear. Although highly effective, artemisinins are recommended for use in combi-

nation with the more long-lasting quinolines or antifolates due to their short half-life in vivo in order to ensure complete elimination of residual parasites. Hence, the rationale behind artemisinin-based combinations is that the rapid action of artemisinin compounds reduces parasite load, thereby leaving fewer parasites for the long-lasting combination drug to tackle and thus minimizing the chances of selecting drug-resistant organisms. Artemisinin derivatives commonly used include: (a) artemether, (b) artesunate and (c) dihydroartemisinin (*Adjuik et al., 2004*). The choice of the ACT is based on the efficacy of the combination drug in the country or area of intended use. In many African nations, ACTs in combination with vector control methods (like IRS and ITNs) have resulted in dramatic decrease in malaria associated morbidity and mortality (*Barnes et al., 2005; White, 1992*).

Albitiazolium, a new choline analogue

Our lab has identified a range of compounds that interfere with a "new" target, that is parasite phospholipid metabolism. One such compound which is a choline analog, albitiazolium that blocks the entry of choline into the parasite thereby disrupting phosphatidylcholine biosynthesis in the parasite and eventually inhibiting parasite growth in vitro as well as in vivo. Albitiazolium is accumulated inside the infected red blood cells. Its oral bioavailability is low and so it is now being investigated for parenteral formulation to treat severe and uncomplicated malaria (*Nicolas et al., 2005; Vial et al., 2004*). In an effort to seek for potential chemotherapeutic targets, our lab has been involved in unravelling the intricacies of phospholipid biosynthetic machinery. A detail report on albitiazolium could be found in chapter.2.

Chapter 2

Glycerophospholipid metabolism in *Plasmodium*

Lipid metabolism in *Plasmodium* has been covered in previous reports from a general perspective (*Holz Jr, 1977; Sherman and Greenan, 1984; Vial et al., 1989a, 1992; Vial H, 1998; Vial and Mamoun, 2005*) and via specific topics such as fatty acids (FAs) (*Mazumdar and Striepen, 2007; Tarun et al., 2009*), neutral lipids (*Coppens and Vielemeyer, 2005*), phospholipids (PLs) (*Vial et al., 2003; Vial and Mamoun, 2005*), sphingolipids (*Haldar, 1996; Vial and Mamoun, 2005; Pankova-Kholmiansky and Flescher, 2006*), phosphoinositide signalling (*Vial et al., 2003*), glycosylphosphatidylinositol (GPI) (*Channe Gowda, 2002; Boutlis et al., 2005; Debierre-Grockiego and Schwarz, 2010*), galactolipids (*Maréchal et al., 2002*), lipid rafts (*Murphy et al., 2006*) and haemozoin formation within lipids (*Egan, 2008; Pisciotta and Sullivan, 2008; Hoang et al., 2010*). A detailed scheme of lipid metabolic pathways could be found in, "the Malaria Parasite Metabolic Pathways database" (*Ginsburg, 2006*).

The chapter discusses about glycerophospholipid acquisition, metabolism and regulation in *Plasmodium species* (mainly in *P.falciparum, P.knowlesi*). It also focus on different metabolic pathways involved in the synthesis of these lipids and their roles in prokaryotes and other eukaryotes.

2.1 Introduction to Glycerophospholipids

The term 'glycerophospholipid' signifies any derivative of sn-glycero-3-phosphoric acid that contains at least one O-acyl, or O-alkyl, or O-alk-1'-enyl residue attached to the glycerol moiety and a polar head made of a nitrogenous base, a glycerol or an inositol unit. The alcohol here is glycerol, to which two fatty acids and a phosphoric acid are attached as esters. This basic structure is a phosphatidate which is an important intermediate for the synthesis of many phosphoglycerides. Examples of some glycerophospholipids and their structures as compared to cholesterol is shown in Figure.5.

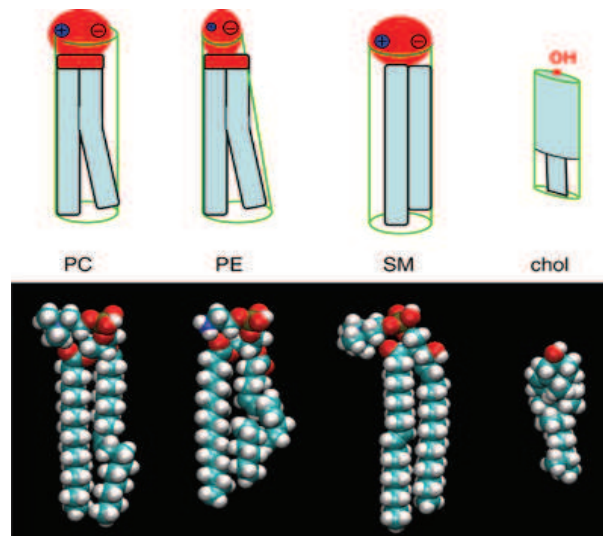


Figure 5: *The structure of the major membrane phospholipids. The more or less cylindrical glycerophospholipid phosphatidylcholine (PC) carries a zwitterionic phosphocholine headgroup on a glycerol with two fatty acyl chains (diacylglycerol), usually one unsaturated (bent). Phosphatidylethanolamine (PE) has a small headgroup and a conical shape and creates a stress in the bilayer: the PE-containing monolayer has a tendency to adopt a negative curvature. The phosphosphingolipid sphingomyelin (SM) tends to order membranes via its straight chains and its high affinity for the flat ring structure of cholesterol (chol). Courtesy (Fahy et al., 2005).*

Major roles of phospholipids

Phospholipids (PLs) are the most abundant class of biological lipids. They are found widely from prokaryotes to multicellular eukaryotes. Despite of similarity of their structures they have distinct roles both in constituting the membrane structure and in biological process. Phosphatidylcholine (PC) (also known as lecithin) is the most abundant phospholipid in animal and plant tissues. PC biosynthesis is required for normal secretion of very low density lipoproteins (VLDL) by liver (*Li and Vance, 2008*). Phosphatidylethanolamine (PE) (also known cephalin) is an abundant phospholipid in microbial, plant, and animal cells. PE plays a critical role during cell division by mediating co-ordinated movements between the contractile ring and the plasma membrane that are required for proper progression of cytokinesis (*Emoto et al., 2005*). PE also serves as a precursor of the ethanolamine moiety of glycosylphosphatidylinositol

anchors that are required for attachment of proteins on the cell surface (*Menon and Stevens, 1992*). Phosphatidylserine (PS) is involved in biological processes including apoptosis, blood coagulation, and activation of protein kinase C (signal transduction). PS expression on cell surface acts as a signal by which apoptotic cells are recognized and phagocytosed by macrophages (*Fadok et al., 2001*). A class of phospholipids with a high rate of metabolism is the phosphatidylinositols (PI) which have varying degrees of phosphorylation in the polar head group myo-inositol. The metabolic conversion of phosphatidylinositols to diacylglycerols and inositol phosphates is important in regulation of vital cellular functions such as differentiation, proliferation, and apoptosis, and in anchoring proteins via a glycosyl-bridge to the plasma membrane. Phosphatidylglycerol (PG) has important functions in bacterial membranes, chloroplasts and lung surfactants. It is a metabolic intermediate in the biosynthesis of cardiolipin.

2.1.1 Phospholipid (PL) acquisition in Prokaryotes and Eukaryotes

Phospholipid biosynthesis is a vital facet of cellular physiology that begins with the synthesis of the fatty acids which are grafted on lysophosphatidic acid by *fatty acid synthetase type I* (FAS I) or *fatty acid synthetase type II* (FAS II). Then, it assembles with phosphatidic acid (PA), a primary PL biosynthesized.

2.1.1.1 PL acquisition in Prokaryotes

The bacterial glycerol-phosphate acyltransferases utilize the complete fatty acid chains to form the first membrane phospholipid and thus plays a critical role in the regulation of membrane biogenesis (*Zhang and Rock, 2008*). Phospholipids in bacteria comprise about 10% of the dry weight of the cell, and each mole of lipid requires the FAS II (an assembly of series of distinct discrete protein) and about 32 mole of ATP for its synthesis. The enzymes of fatty acid synthesis are cytosolic, while those of membrane lipid synthesis are mainly integral inner membrane proteins (*Heath and Rock, 2004*).

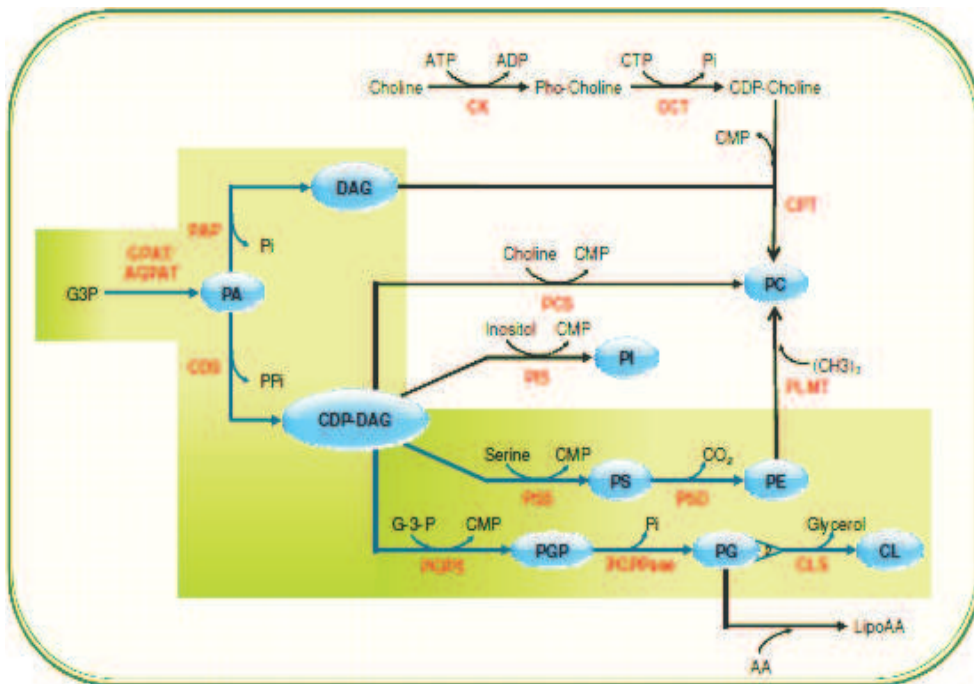


Figure 6: The scheme represents a model for prokaryotic phospholipid synthesis (from thesis of Dechamps, 2009). The pathways (in green shaded region) and the reactions (marked with arrows within this box) occurs in all prokaryotes. The lipid precursors and products are shown in ovals. The reactions/pathways outside this region are present in less than 10% of all prokaryotes

In most of bacteria (for example : *E.coli*), phosphatidylethanolamine (PE) forms major bulk (75%) of PLs with phosphatidylglycerol (PG) (15 – 20%), cardiolipin (CL), phosphatidylserine (PS) and phosphatidic acid (PA) comprises (5 – 10%) (*Kanfer and Kennedy, 1964; Heath and Rock, 2004*).

Cytidine diphosphate diacylglycerol (CDP-DAG) which comprise 0.05% (*Heath and Rock, 2004*) of total PLs bulk, is high energy lipid intermediate which is synthesized from PA and cytidine triphosphate (CTP) by the action of the enzyme CDP-DAG synthase (CDS)(EC 2.7.7.41).

CDP-DAG dependent pathways are source of the major PLs like PE,PG, PS and CL (*Kanfer and Kennedy, 1964*). PS is synthesized from CDP-DAG and L-serine by PS synthase (PSS). PS is then decarboxylated by PS decarboxylase (PSD) to PE (*Kanfer and Kennedy, 1964*). Phosphatidylglycerol (PG) is synthesized in two steps. In the first step, phosphatidylglycerolphosphate (PGP) is formed from CDP-DAG and G-3-P

by the action of the enzyme phosphatidylglycerolphosphate synthase (PGPS). In the second step, PGP is dephosphorylated by the enzyme PGP phosphatase (PGPPase), thereby leading to the formation of PG (Kanfer and Kennedy, 1964).

Phosphatidic acid (PA), is formed by the acylation of glycerol-3-phosphate (G-3-P) in two enzymatic steps. In the first step, PA is acylated to 1-acyl-G-3-P (or lyso PA) by the enzyme G-3-P acyltransferase (GPAT) and in the second step, 1-acyl-G-3-P is acylated by a distinct enzyme, 1-acyl-G-3-P acyltransferase (AGPAT) to form PA (Zhang and Rock, 2008).

Phosphatidylinositol (PI) is absent in majority of prokaryotes with a few exceptions like *Pseudomonas syringae*, *E.coli*, *Treponema pallidum* and *Mycobacterium smegmatis*. The synthesis of PI in these organisms is catalyzed by PI synthase (PIS) with inositol and CDP-DAG as substrates (Salman et al., 1999).

Apart from these PLs, phosphatidylcholine (PC) is also present in some bacteria that are photosynthetic or in close association with eukaryotes (Sohlenkamp et al., 2003). Synthesis of PC in such prokaryotes occurs via three pathways: (a) CDP-DAG dependent pathway in which an enzyme called PC synthase (PCS) condenses CDP-DAG and choline to PC (López-Lara and Geiger, 2001), (b) PE methylation pathway in which PE undergoes methylation to form PC by PL N-methyltransferase (PLMT) enzyme (this pathway is also present in yeast and mammalian liver) and (c) CDP-choline pathway or the *de novo* Kennedy pathway which is also a major pathway for PC synthesis in mammals (Sohlenkamp et al., 2003).

Transport of exogenous long chain fatty acids are utilized (example: *E.coli*) in two ways. Firstly, they can be incorporated into the membrane phospholipids by the acyltransferase system. Secondly, they can be used as the sole carbon source for growth, and are in fact an important source of energy (Clark and Cronan, 1996). Degradation of fatty acids proceeds via an inducible set of enzymes that catalyze the pathway of β -oxidation (Clark and Cronan, 1996).

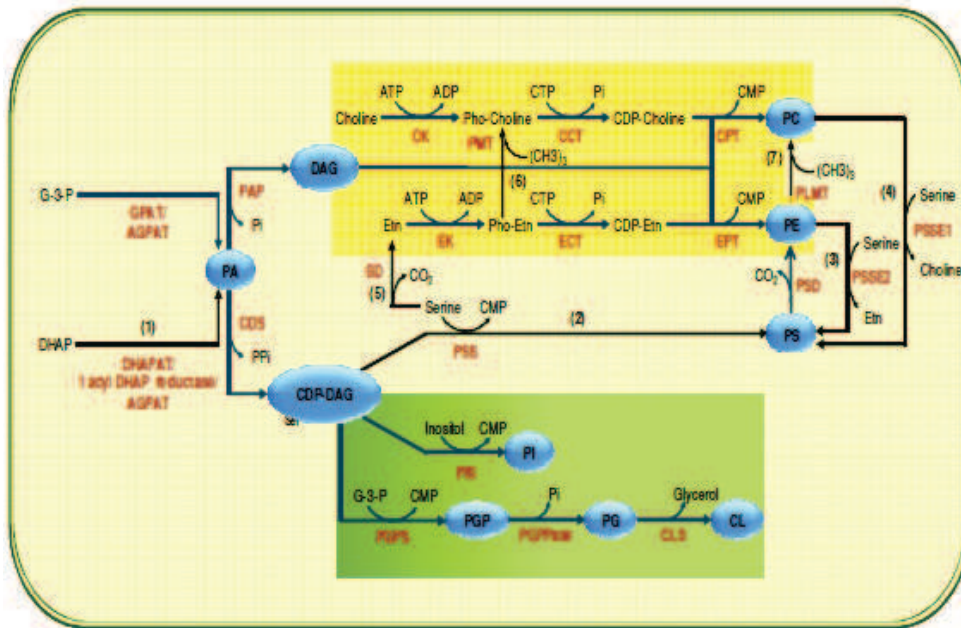


Figure 7: Scheme represents a model for eukaryotic phospholipid synthesis. This diagram represents a model for eukaryotic phospholipid synthesis (from thesis of Dechamps, 2009). The Kennedy and the CDP-DAG dependent pathways (in shaded yellow and dark green box respectively,) commonly occur in all eukaryotes. The lipid precursors and products are shown in ovals. The reactions/ pathways outside this shaded box with arrows are present only in yeast and mammals (1), yeast and plants (2), mammals and plants (3,4), Plasmodium and plants (5,6), yeast and mammalian liver cells (7).

2.1.1.2 PL acquisition in Eukaryotes

PL synthesis in eukaryotes is more complex and diversified. The major PLs in eukaryotes are PC (40 – 55%) and PE (20 – 40%) followed by smaller quantities of PI and PS (Vance and Steenbergen, 2005). PLs are known to be synthesized by two pathways in eukaryotes i) CDP-DAG dependent pathways, ii) the *de novo* Kennedy pathways.

In yeast, CDP-DAG dependent pathways of PS synthesis are the major source of the most abundant phospholipids like PC and PE, whereas *de novo* Kennedy pathways are the auxiliary pathways for the synthesis of PC and PE. In mammalian cell, CDP-DAG dependent PS synthesis is not present and the bulk of PE or PC are more biosynthesized.

In most eukaryotes, PA is synthesized from G-3-P by two successive acylation reactions in a quite similar way as seen in prokaryotes. In addition, in yeast and mammals, PA can also be synthesized from dihydroxyacetone phosphate (DHAP) which is the product of dehydrogenation of G-3-P by the enzyme G-3-P dehydrogenase. PA then enters PL biosynthetic pathways in two forms: CDP-DAG and DAG. Like in prokaryotes, CDP-DAG, precursor of CDP-DAG dependent pathways, arises as a result of transfer of PA to CTP catalyzed by enzyme CDS (*Carter and Kennedy, 1966*). Alternatively, DAG, a precursor for the Kennedy pathways, is synthesized by dephosphorylation of PA by PA phosphatase (PAP) (*Carman and Han, 2009*), which is then condensed and activated by CDP-Cho and CDP-Etn to produce PE and PC respectively.

PS, PI and PG are synthesized by CDP-DAG dependent pathways in a very similar way to the prokaryotic pathways. As in prokaryotes, PS in yeast and plants is also synthesized by transfer of phosphatidyl group from CDP-DAG to serine by the enzyme PSS (*Yamashita and Nikawa, 1997*).

In plants and mammalian cells, PS can also be synthesized by mammalian base-exchange mechanism. In yeast and mammalian mitochondria, PE is synthesized by decarboxylation of PS mediated by the enzyme PSD. PI is synthesized by transfer of phosphatidyl group from CDP-DAG to inositol in the presence of enzyme PI synthase (PIS) (*Cooke, 2009*). PG is synthesized in two steps, PGP is formed by G-3-P and CDP-DAG mediated by enzyme PGPS, thereafter PGP is dephosphorylated by the enzyme PGPase giving rise to PG.

In higher eukaryotes, PC and PE biosynthesis primarily takes place by the *de novo* routes, that is, CDP-choline and CDP-ethanolamine routes respectively (*Kennedy and Weiss, 1956*) while in yeast these pathways appear to be dispensable as long as PC and PE are supplied by CDP-DAG dependent pathways.

In plants along with Kennedy pathways, PE and PC are also synthesized by transversal pathway or serine decarboxylase phosphoethanolamine methylation (SDPM) pathway. In this pathway, serine is decarboxylated to form ethanolamine by an enzyme called serine decarboxylase (SD). This ethanolamine then enters the CDP-ethanolamine

pathway eventually leading to the formation of PE. On the other hand, phosphoethanolamine so formed as a result of *de novo* CDP-ethanolamine pathway can be converted into phosphocholine by a unique enzyme, phosphoethanolamine N-methyltransferase (PMT) which then enters the *de novo* CDP-choline pathway to form PC (*Bolognese and McGraw, 2000*). In mammals, the *de novo* Kennedy pathways are the major source of PC and PE. PS is synthesized only by base exchange mechanism wherein PS is formed at the expense of pre-existing phospholipids such as PC and PE and is mediated by the enzymes PS synthase I (PSSE1) and PS synthase II (PSSE2) respectively. While PSSE1 catalyzes the exchange of phospholipid head groups between serine and PC, PSSE2 catalyzes the exchange of phospholipid head groups between serine and PE (*Vance, 2008*).

In some other cases as in yeast, mammalian liver cells, PC can also be synthesized by triple methylation of PE. This reaction is S-adenosylmethionine (SAM) dependent which acts as a methyl group donor. In yeast, this reaction is mediated by the two classes of phospholipid N-methyltransferases (PLMT) while in mammalian liver, it is mediated by a single enzyme, phosphatidylethanolamine-N-methyltransferase (PEMT) (*Bell and Coleman, 1980*).

2.1.1.3 PL acquisition in *Plasmodium* species

Upon infection, the parasite multiplies within red blood cells leading to a production of 10-20 merozoites every 48 hours which rapidly invade further erythrocytes. This rate of production demands high metabolic activity in the parasite, particularly through increased requirement for novel membrane formation. Glycerophospholipids (PL) are the main *Plasmodium* membrane constituents, with a preponderance of PC and PE and with an increase in phosphatidylinositol (PI) involved in signaling. Phospholipids play a crucial role in the development of intracellular malaria parasite. Infected erythrocytes show a marked increase in PL content enhanced by approximately six-fold at the trophozoite stage. PC and PE together represent 75 – 85% of the parasite total PL composition after infection (*Vial et al., 1992*).

Origin of PL in *Plasmodium*

PL mostly originate from the parasite enzymatic machinery, which relies on the scavenging and downstream metabolism of polar heads and fatty acids serving as building units throughout a bewildering number of pathways. Besides, the lipid-derived signaling molecules phosphoinositide exert crucial function regulating parasite development and proliferation that are currently deciphered (*Raabe et al.*, 2011; *Tawk et al.*, 2010; *Vaid et al.*, 2010; *Bhattacharjee et al.*, 2012).

Composition of PLs in *Plasmodium*

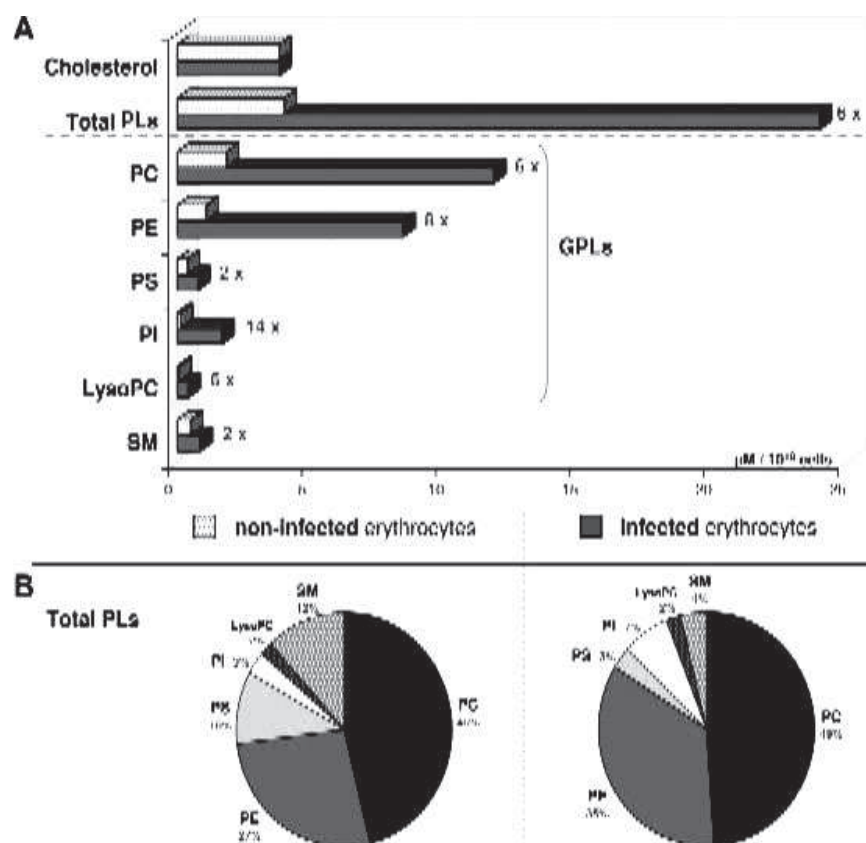


Figure 8: Cholesterol and phospholipid (PL) contents in non-infected and *P.falciparum*-infected (mature stage) human erythrocytes. Data have been obtained from previous studies (*Vial et al.*, 1992). (A) The increase in erythrocyte PL content upon infection is indicated at the right side of the grey bars (e.g. 6 means a 6-fold increase). (B) PL composition is expressed as the molar percentage of total PLs. For abbreviations (see Table.1), Courtesy: (*Déchamps et al.*, 2010c).

Little is known about the lipid composition of *Plasmodium* parasites at non erythrocytic stages. Among the phospholipids, PC comprises (40 – 50%), PE (35 – 45%), PI (4 – 11%), and SM and PS (= 5%). Interestingly, the PE content is unusually high compared with its level in other eukaryotes (*Vial et al.*, 1982a, 1992). A major increase in neutral lipids (DAG, TAG, FA) are also detected, but the final amount of these neutral PLs remain very low as compared to the total PLs (*Coppens and Vielemeyer*, 2005; *Vial et al.*, 1984a; *Demel et al.*, 1975).

Uptake of PL precursors in *Plasmodium*

Water soluble PL precursors are acquired mainly from the host. Normal or uninfected erythrocytes have a saturable carrier for choline uptake, but its maximal transport capacity is very minute. Choline (Cho) enters the infected red blood cell (RBC) via the erythrocytic Cho carrier and the New Permeation Pathway(s) (NPP) (*Anceletin et al.*, 1991; *Biagini et al.*, 2005; *Wein et al.*, 2012) at the erythrocyte plasma membrane and is then provided to the parasite by an Organic Cation Transporter (OCT)(PFE0825w) (*Biagini et al.*, 2004; *Lehane et al.*, 2004) or a choline-specific transporter-like protein (CTL)(PF14_0293) on the parasite membrane (*Biagini et al.*, 2004).

Ethanolamine enters erythrocytes mainly by passive diffusion (*Vial et al.*, 1994). Choline and ethanolamine are effectively trapped within the parasite by phosphorylation (*Anceletin and Vial*, 1986a,c). Serine is diverted from the erythrocyte and transported into the parasite (*Vial et al.*, 1982b, 1989b; *Déchamps et al.*, 2010a), or is obtained from haemoglobin degradation in the food vacuole (*Goldberg*, 2005). Myo-inositol can be scavenged from the host (*Vial et al.*, 1982b). It remains to be shown whether the parasite synthesizes myo-inositol from glucose through the sequential reactions of the single hexokinase (HK, PFF1155w) (*Olafsson et al.*, 1992), a putative inositol-3-phosphate synthase (IPS, PFE0585c) and a putative inositol-phosphate phosphatase (i.e. inositol monophosphatase, IMP, PF07_0024), which are all expressed at the blood stage (*Olafsson et al.*, 1992; and *PlasmoDB*). Fatty acids (FAs) are the basic units required to synthesize PLs. Historically, *Plasmodium* has been considered incapable of synthesizing FAs *de novo* and restricted to obtaining preformed FAs from the

host. It was not yet clear whether FAs enter the parasite by passive diffusion or energy dependent transport (Vial *et al.*, 1992). The activation of FAs to acyl-CoA thioesters by acyl CoA synthetase is required for incorporation of FAs into PLs.

FAS II system in *Plasmodium*

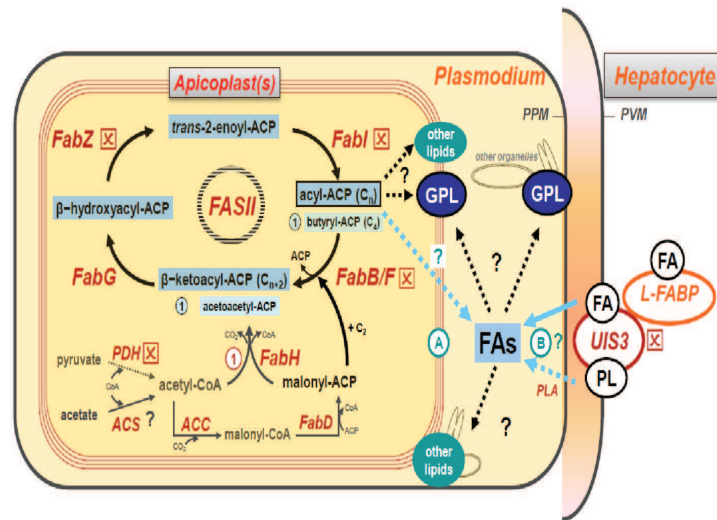


Figure 9: Schematic diagram of FAS II systems in *Plasmodium*, (Déchamps *et al.*, 2010c)

Recently, several enzymes associated with the type II fatty acid synthesis pathway (FAS II) have been identified in *Plasmodium* and appear to be located in the apicoplast, a plastid-like organelle (Gardner *et al.*, 2002a). This type II pathway is also found in plants and prokaryotes. Previously, FAS II system was thought to be essential in the blood stage of the parasite due to the inhibitory effect of triclosan, an antimicrobial biocide, on *P.falciparum* growth *in vitro* and on FabI enzyme (enzyme of FAS II pathway) (Surolia and Surolia, 2001). Recently, disruption of FabI gene in both *P.falciparum* and *P.berghei* parasites (Yu *et al.*, 2008) failed to impede blood stage growth as well as targeted deletion of FabB/F and FabZ (enzymes of FAS II pathway) in *P.yoelii* parasites failed to affect blood stage, mosquito stage and initial liver infection. However, FAS II deficient *P. yoelii* liver stages failed to generate exoerythrocytic merozoites (Vaughan *et al.*, 2009). These studies collectively suggested that FAS II system is not required in blood stage and mosquito stage development as

well as for initial infection of the liver. Rather FAS II system is crucial at only one specific life cycle transition point, that is, from liver to blood.

2.1.2 PL biogenesis in *Plasmodium*

Phospholipid biogenesis is crucial for the intracellular development of the parasite and constitutes a potential area for therapeutic intervention that has already been validated leading to a novel and promising pharmaceutical approach for the treatment of malaria (Vial *et al.*, 2004; Wein *et al.*, 2012). Phospholipid synthesis in *P.knowlesi* parasite at its blood stage is one of the most characterized metabolic network, due to the availability of infected erythrocyte collected from *Macaca mulatta* or *M. fascicularis* monkeys and several thorough fluxomics studies (Ancelin and Vial, 1989; Vial *et al.*, 1989b; Elabbadi *et al.*, 1997). Lipid metabolism in *P.knowlesi* takes place to a higher extent. This has been shown by experimental sensing of polar head and FA incorporation into PLs, in late trophozoite and early schizont stage of asexual (erythrocytic phase) (Elabbadi *et al.*, 1997; Vial *et al.*, 1989b). At the blood stage, *Plasmodium* species display a puzzling number of metabolic pathways that are rarely found together in a single organism (Déchamps *et al.*, 2010c), (a) the ancestral prokaryotic-type CDP- diacylglycerol dependent pathway (b) the eukaryotic-type *de novo* CDP-choline and CDP-ethanolamine (Kennedy) pathways (c) *P.falciparum* and *P.knowlesi* exhibit additional reactions that bridge some of these routes. A plant-like pathway that relies on serine to provide additional PC and PE, is named the serine decarboxylase-phosphoethanolamine methyltransferase (SDPM) pathway. This route is of great interest as it involves serine decarboxylase (SD) that has been characterized in plants and is distributed sporadically throughout animal genomes (Déchamps *et al.*, 2010c; Vial *et al.*, 2011b). In addition, base-exchange mechanisms are largely unexplored in *Plasmodium* but are currently explored in our laboratory.

2.1.2.1 Biochemical scheme of glycerophospholipid metabolism in *Plasmodium*

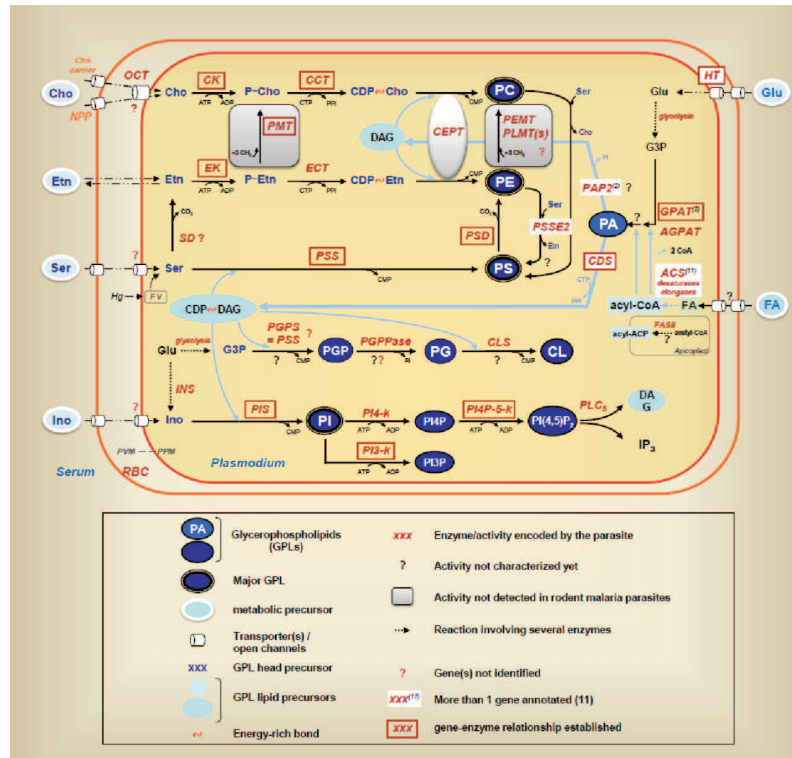


Figure 10: Scheme of glycerophospholipid (GPL) biosynthesis pathways in *Plasmodium*-infected red blood cells (RBCs). Precursor uptakes through the parasitophorous vacuole membrane (PVM) and the parasite plasma membrane (PPM) are not distinguished, but it is reported that the PVM is permeable to a wide range of nutrients (Desai et al., 1993). In *P. falciparum*, at least two acyl-CoA synthetase (ACS) isoforms are transported to the host cytoplasm where they interact with the host ankyrin protein, which binds itself to the cytoskeleton (Télliez et al., 2003). The type II fatty acid synthesis (FASII) pathway, generating acyl-acyl carrier protein (acyl-ACP) from acetyl-coenzyme A (acetyl-CoA), is not essential for parasite survival at the blood stage (Yuan et al., 2005; Vaughan et al., 2009), but in certain instances this de novo pathway might be recruited at this stage in vivo (Daily et al., 2007). Phospholipase C δ (PLC δ , putative gene: PF10_0132) activity has been reported at the blood stage and is correlated with microgametocyte exflagellation (Elabbadi et al., 1994; Martin et al., 1994). For abbreviations see Table.1. Courtesy (Déchamps et al., 2010c).

Difference in PL metabolism in *P.knowlesi* and *P.falciparum*

The major difference in the biochemical scheme of PL metabolism in *P.knowlesi* and *P.falciparum* is the enzyme PEMT that remains unidentified or its biochemical activity is not known in *P.falciparum* (Pessi *et al.*, 2005, 2004). However, the architecture of the network is rather conserved in *P.falciparum* and *P.knowlesi*. In other non-rodent species of *Plasmodium* (for example: *P.bergi*) PMT enzyme or its biochemical activity remains unidentified (Déchamps *et al.*, 2010c). This is discussed in the later part of this chapter.

2.1.2.2 Different pathways involve in PL metabolism

a). Kennedy pathways

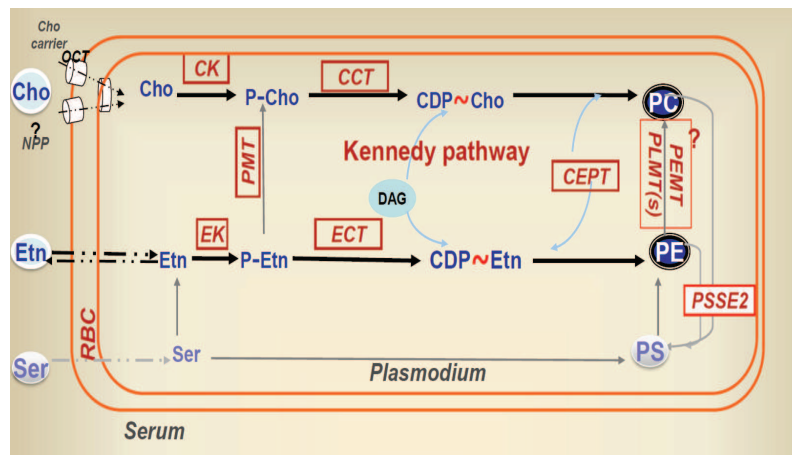


Figure 11: Kennedy pathway in *P.knowlesi*

Both PC and PE may be synthesized *de novo* by the CDP-Cho or CDP-Etn dependent Kennedy pathways. Choline is phosphorylated into phosphocholine (PCho), which is subsequently coupled to CTP, thus generating CDP-choline, which is further converted to PC by a parasite CDP-diacylglycerol-cholinephosphotransferase (CEPT). A similar *de novo* pathway allows the synthesis of PE from ethanolamine. The final stage of both branches of the Kennedy pathway involves the same CEPT enzyme, catalyzing the formation of PC and PE from CDP-Cho and CDP-Etn, respectively (Vial *et al.*, 2004; Déchamps *et al.*, 2010c; Wein *et al.*, 2012).

b). CDP-DAG pathways

Plasmodium also possesses the CDP-DAG-dependent ancestral pathway, which provides the anionic phospholipids PI, PG, cardiolipid and eventually PS (Vial and Mamoun, 2005). Biosynthesized PS is converted into PE via the activity of PS decarboxylase (PSD) (Baunaure et al., 2004).

c). SDPM plant-like horizontal pathways

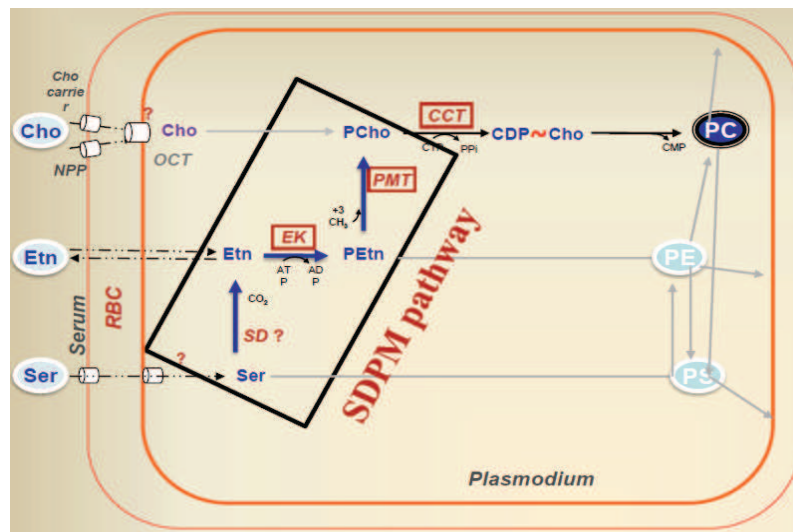


Figure 12: SDPM pathway in *Plasmodium*

P.knowlesi and *P.falciparum* possess a plant-like pathway that relies on serine to provide additional PC and PE, which is named the serine decarboxylase phosphoethanolamine methyltransferase (SDPM) pathway. Hereby, serine is first decarboxylated to form ethanolamine, which is then phosphorylated to lead to phosphoethanolamine (PEtn). Serine decarboxylase (SD) enzymatic activity was first described by Vial and group in *P.knowlesi* and *P.falciparum* (Elabbadi et al., 1997). The gene and related SD catalytic activities were subsequently identified in plants and algae (Rontein et al., 2001; Lykidis, 2007) while the corresponding plasmodial gene has not yet been identified. The resulting phosphoethanolamine is either incorporated into PE via the CDP-ethanolamine pathway or converted into phosphocholine by SAM-dependent triple methylation, which is carried out by a plant like

phosphoethanolamine-N-methyltransferase (PfPMT) (Pessi *et al.*, 2005, 2004). In the *Apicomplexa* phylum, the SDPM-pathway is only conserved in *Plasmodia* with the exception of rodent parasites, where the PMT activity is absent (Déchamps *et al.*, 2010c).

The SDPM pathway involves; decarboxylation of serine into ethanolamine which subsequently enters the CDP-Etn pathway leading to the formation of PE. This pathway was first demonstrated in our lab in *P.knowlesi* and *P.falciparum* (Elabbadi *et al.*, 1997).

In *P.falciparum*, phosphoethanolamine(PEtn), an intermediate of CDP-ethanolamine pathway for PE synthesis, can be converted to phosphocholine(PCho) by a triple methylation reaction and phosphocholine eventually synthesizes PC by CDP-choline pathway. The triple methylation is catalyzed by the enzyme PfPMT and uses S-adenosyl methionine as methyl donor (Pessi *et al.*, 2005).

d). Base-exchange reactions

The quantitative importance of base-exchange reaction was not distinctly measured in *Plasmodium spp.*, but they would be operational at the erythrocytic stage. In some plants species, in which both CDP-DAG-dependent and base-exchange PS synthesis take place, it has been shown that, these enzymatic reactions have different preferential molecular species as substrates (Vincent *et al.*, 2001).

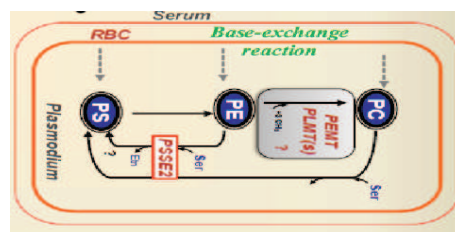


Figure 13: Base-exchange reactions in Plasmodium

2.1.2.3 Enzymes involved in PL metabolic pathways

a). Choline (CK) and ethanolamine kinases (EK)

EK and CK activities have been detected in *P.falciparum* and *P.knowlesi* infected erythrocyte extracts (Ancelin and Vial, 1986a). These are performed by PfCK and PfEK, that are expressed in all the erythrocytic stages of the parasite though higher in the mature stages and are localized in the parasite cytoplasm (Alberge *et al.*, 2010; Choubey *et al.*, 2006). On a first step these enzymes phosphorylates ethanolamine (Etn) and choline (Cho) diverted from the host into phosphoethanolamine (PEtn) and phosphocholine (PCho) respectively. It is an ATP dependent process (see Figure.10 & 11).

b). Choline (CCT) and ethanolamine (ECT)-phosphate cytidyltransferases

In the second step, PEtn and PCho are coupled to cytidine triphosphate (CTP) thus generating the high energy intermediates cytidine diphosphate ethanolamine (CDP-P-Etn) and cytidine diphosphate choline (CDP-Cho) respectively. These steps are considered to be the rate limiting steps of the Kennedy pathways and are catalyzed by the enzymes;CTP:phosphoethanolamine cytidyltransferase (ECT) and CTP:phosphocholine cytidyltransferase (CCT) respectively(see Figures.10 & 11).

ECT and CCT activities have been detected and characterized in *P.falciparum* and *P.knowlesi* (Elabbadi *et al.*, 1997; Vial *et al.*, 1989a); in *P.berghei* and also in *P.vinckeii* (Déchamps *et al.*, 2010c). Studies on choline incorporation in *P.knowlesi* infected RBCs demonstrated that increasing choline concentration led to an increase in phosphocholine levels but the pool of CDP-choline remained constant. This suggested that *P.knowlesi* CCT activity is rate-limiting (Ancelin and Vial, 1989). Radiolabeled serine and ethanolamine incorporation studies in *P.falciparum* and *P.knowlesi* infected erythrocytes have indicated the rate limiting role of ECT in PE biosynthesis (Elabbadi *et al.*, 1997).

c). Choline/ethanolamine phosphotransferase (CEPT)

The final step of the Kennedy pathways involves the transfer of CDP-Etn and CDP-Cho to DAG, thereby leading to the synthesis of PE and PC respectively. This reaction is catalyzed by a single enzyme named choline/ethanolamine phosphotransferase (CEPT) respectively (see Figures.10 & 11) (*Vial et al.*, 1984a). However in most eukaryotes, there are two genes coding for enzymes choline phosphotransferase (CPT) and ethanolamine phosphotransferase (EPT). In *P.berghei*, CEPT is reported to be localized in the endoplasmic reticulum (*Déchamps et al.*, 2010c).

d). PMT Vs PEMT

Other than CDP-choline pathway/Kennedy pathway there are two possible pathways which could furnish PC (see Figures.10 & 11). a) PMT, which transforms PEtn into PCho which in turn forms PC via CDP-choline pathway. This is a part of SDPM pathway by which host serine is incorporated into PC. The mechanism is S-adenosyl methionine (SAM)-dependent triple methylation carried out by a plant-like phosphoethanolamine N-methyltransferase (PMT or PEAMT) (EC.1.1.103). *P.falciparum* PMT (PfPMT), has been revealed by the *P.falciparum* genome sequencing program (*Gardner et al.*, 2002a). Subsequently, phosphoethanolamine methyltransferase (PMT) pathway has been characterized in *P.falciparum* (*Pessi et al.*, 2004). The orthologous gene (*PKH_121150*) has been identified in *P.knowlesi* (*Aurrecoechea et al.*, 2009). ii) PE transmethylase (PEMT or PLMT) pathway. The capacity of *P.knowlesi*-infected erythrocyte to methylate PE into PC has been documented in previous studies and clearly indicates PEMT activity (*Moll et al.*, 1988). However, the corresponding genes have not yet been found in any *Plasmodium* species.

Further, arguments for and against PEtn transmethylation in malaria parasites with biochemical evidences and genetic studies in different species (*Aktas and Narberhaus*, 2009; *Arondel et al.*, 1993; *Kanipes et al.*, 1998; *Keogh et al.*, 2009; *Nuccio et al.*, 2000a; *Vance et al.*, 2007) revealed the presence of PEtn methyltransferases (PMT). *In silico* analyses led to the identification of phosphoethanolamine-N-methyltransferase gene orthologs in primate and bird parasite genomes. However, the gene was not de-

tected in the rodent *P.berghei*, *P.yoelii*, and *P. chabaudi* species. To support this, biochemical experiments were done with labeled choline, ethanolamine, and serine. It showed marked differences in biosynthetic pathways when comparing rodent *P.berghei* and *P.vinckei*, and human *P.falciparum* species. Notably, in both rodent parasites, ethanolamine and serine were not significantly incorporated into PC, indicating the absence of phosphoethanolamine-N-methyltransferase activity (Déchamps *et al.*, 2010c). Furthermore, deletion of the PfPMT gene in *P.falciparum* parasites abolishes the incorporation of ethanolamine into PC (Le Roch *et al.*, 2008), suggesting that either PEtn transmethylation does not occur in *P.falciparum*, or that if such a reaction exists, it is catalyzed by PfPMT and requires a functional PfPMT enzyme. Thus far, biochemical and genetic analyses all appear to indicate that PfPMT does not catalyze the transmethylation of PE in *P.falciparum*. First, unlike yeast extracts, *P.falciparum* extracts used in a PE transmethylation reaction *in vitro* failed to catalyze such a reaction. Second, purified recombinant PfPMT was found to catalyze the methylation of phosphoethanolamine but not PE. Third, using yeast as a model system it was shown that PfPMT complementation of pem1, pem2 mutant growth defect in the absence of choline is ameliorated by ethanolamine supplementation and requires an active CDP-choline pathway. Thus, in *P.falciparum* available no data support the existence of a direct methylation of PE to form PC. However, study by (Moll *et al.*, 1988) indicates an extensive PE methylation when this PL was introduced into the *P.knowlesi* infected erythrocytes. Further biochemical and genetic studies in *P.knowlesi* are needed to determine whether the PMT ortholog can catalyze PE transmethylation and to identify a putative PEMT gene (Ben Mamoun *et al.*, 2010).

List of some of the enzymes involved in PL pathways and their corresponding ORFs

Substrates Products	Enzyme (EC number)	ORF(P.falciparum or P.knowlesi)	References for Biochemical activity or gene identification
SerE → Ser (Serine transport)	?	?	(Elabbadi <i>et al.</i> , 1997)
Ser → PS (Phosphatidylserine synthesis)	PSS	(MAL8P1.58) / (PKH.051100) <i>predicted</i>	Vial (unpublished data).
Ser → Etn (Serine decarboxylation)	SD 4.1.1	?	(Elabbadi <i>et al.</i> , 1997)
Etn → PEtn (Ethanamine phosphorylation)	EK 2.7.1.82	PfEK (PF11_0257) / (PKH.092210)	(Alberge <i>et al.</i> , 2010)
PEtn → PCho (Phosphoethanolamine methylation)	PMT 2.1.1.103	PfPMT (MAL13P1.214) / (PKH.121150)	(Pessi <i>et al.</i> , 2004, 2005)
PS → PE (Phosphatidylserine decarboxylation)	PSD 4.1.1.65	PfPSD (PF11370c) / (PKH.072580)	(Baunaure <i>et al.</i> , 2004)
PEtn → PE	ECT 2.7.7.14 CEPT/EPT 2.7.8.1	PfECT (PF13_0253) / (PKH.120620) PfCEPT (PFF1375c) / (PKH.112100)	(Vial <i>et al.</i> , 1984b; Elabbadi <i>et al.</i> , 1997)
PCho → PC	CCT 2.7.7.15 CEPT/CPT 2.7.8.2	PfCCT (MAL13P1.86) / (PKH.141580) PfCEPT (PFF1375c) / (PKH.112100)	(Yeo <i>et al.</i> , 1995, 1997) (Vial <i>et al.</i> , 1984b)
PE → PC (Methylation)	PEMT/PLMT 2.1.1.17/2.1.1.71	?	(Moll <i>et al.</i> , 1988; Elabbadi <i>et al.</i> , 1997) (Aurrecochea <i>et al.</i> , 2009)
PC → PS (base exchange)	PSSbe 2.7.8	(MAL13P1.335) / (PKH.110380)	
PE → PS (base exchange)	PSSbe 2.7.8	(MAL13P1.335) / (PKH.110380)	Berry and Vial (unpublished data)
PC → (Phosphatidylcholine efflux)	?	?	
PS → (Phosphatidylserine efflux)	?	?	
PE → (Phosphatidylethanolamine efflux)	?	?	
ChoE → Cho (Choline transport)	NPP/OCT/CTL	(PFE0825w) / (PKH.101630)	(Biagini <i>et al.</i> , 2004; Kirk <i>et al.</i> , 1991) (Goldberg <i>et al.</i> , 1990; Wein <i>et al.</i> , 2012)
Cho → PCho (Choline phosphorylation)	CK 2.7.1.32	PfCK	(Choubey <i>et al.</i> , 2006; Alberge <i>et al.</i> , 2010)
EtnE → Etn (Ethanamine diffusion)		?	

Table 2: The enzymes (shown in scheme/Figure.10), ?= enzyme not identified/characterized. For abbreviations see abbreviation Table.1

2.1.3 Pharmacology of choline uptake

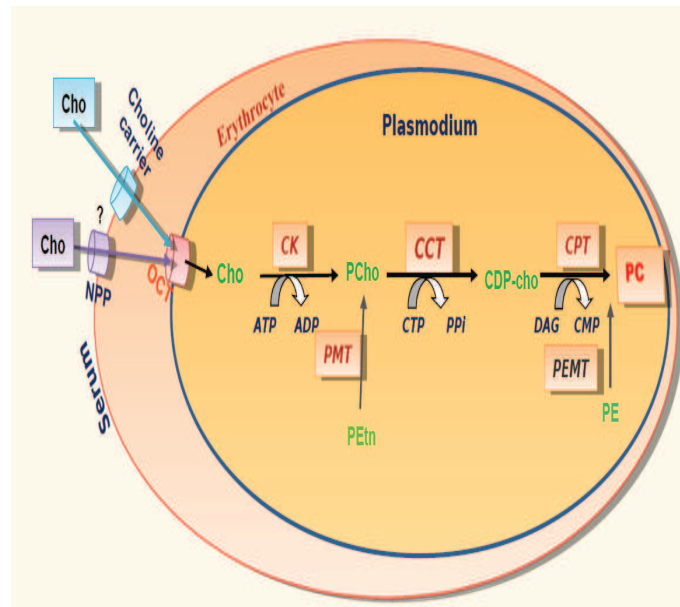


Figure 14: Scheme of choline transport in *P.knowlesi* and *P.falciparum*

Choline uptake has been well studied by (Ancelin *et al.*, 1991; Vial and Mamoun, 2005; Biagini *et al.*, 2005; Kirk and Saliba, 2007; Wein *et al.*, 2012). As, described earlier, normal or uninfected erythrocytes have a saturable carrier for choline uptake, but its maximal transport capacity is very minute. Choline (Cho) enters the infected red blood cell (RBC) by, a) the erythrocytic Cho carrier and b) an entirely passive furosemide-inhibited New Permeation Pathway(s)(NPP) (Ancelin *et al.*, 1991; Biagini *et al.*, 2005; Wein *et al.*, 2012) at the erythrocyte plasma membrane (see Figure.14). It is then provided to the parasite by an Organic Cation Transporter (OCT)(PFE0825w) (Biagini *et al.*, 2004; Lehane *et al.*, 2004) or a choline-specific transporter-like protein (CTL)(PF14.0293) on the parasite membrane (Biagini *et al.*, 2004).

(Desai *et al.*, 1993) proposed that precursor (for example: serine, choline, etc.) from host (erythrocytes) uptakes through the parasitophorous vacuole membrane (PVM) (not shown in Figure.14, see Figure.15). The parasite plasma membrane (PPM) were not distinguished, but it was reported to be permeable to wide range of nutrients.

(Ancelin and Vial, 1986b) further investigated uptake of choline from host (erythrocytes). It was found that choline reaches the PPM transporter through the PVM. There assumed to be no permeability barrier for choline. Within the parasite, the free choline concentration is rapidly reduced by kinase catalyzed choline phosphorylation, rate-limited by the choline supply through the PPM transporter. This arrangement operates like a choline sink presumably by maintaining a steady inward choline gradient. In this transport and sink chain, the most serious gap to the knowledge concerns the properties of the PPM choline transporter. The PPM choline transporter has attracted major interest as a possible transport route for a new class of potent antimalarials for which choline, a quaternary ammonium monovalent cation, served as lead compound: bisamidine and bis-quaternary ammonium compounds (Le Roch *et al.*, 2008; Stead *et al.*; Wengelnik *et al.*, 2002).

Tested both *in vitro* and *in vivo*, these compounds proved to have potent activity against *P.falciparum*, but their access pathway to the parasite was unknown. Biagini and colleagues provide a thorough functional and kinetic characterization of choline transport across the parasite PPM and show that bisamidine and bis-quaternary ammonium compounds gain access to the parasite cytoplasm via the PPM choline transporter.

Using a preparation of *P.falciparum* parasites freed from host permeability constraints by saponin permeabilization (Saliba *et al.*, 1998) showed that choline transport is carrier mediated, with a Michaelis constant $K_{1/2}$ of about 25 μM and a maximum velocity (V_{max}) of 4.6 pmol/ 10^6 cells/min. They compared the rates of choline transport through NPPs and through the PPM carrier at physiologic choline concentrations and demonstrate that choline entry through NPPs is rate limiting. They conclude that in steady-state, the host choline concentration will be depleted relative to the extracellular medium and describe the PPM transporter as a vacuum cleaner of choline entering the host cell.

Choline transport was inhibited competitively by pentamidine, a bis-cationic choline analog, but with a dissociation constant of an inhibitor (K_i) far above the antimalarial median effective concentration (EC_{50}), suggesting that inhibition of PPM choline

transport may not be a significant contributor to the antimalarial effects of these compounds.

Based on indirect evidence, (Biagini *et al.*, 2004) suggest that the PPM choline transporter is electrogenic, a conclusion firmly supported in recently published work by (Lehane *et al.*, 2004). These authors showed that the PPM membrane potential can energize choline accumulation within the parasite when the phosphorylation sink is blocked by adenosine triphosphate (ATP) depletion. It may appear puzzling that choline uptake needs energizing when the metabolic sink is expected to maintain a steady inward gradient. The answer may be to ensure the internalization of essentially all the choline made available to the parasite by the potential energized choline vacuum cleaner (Lew *et al.*, 2004).

A group based in Oxford (Elford *et al.*, 1990, 1995; Kirk *et al.*, 1991) found that the increased capacity for choline influx into *P.falciparum* infected erythrocytes has kinetic and pharmacological properties which are different from the endogenous erythrocyte transport system in that influx rate shows no tendency to saturate up to high external choline concentrations (0.5 mM). By contrast, (Ancelin *et al.*, 1991) found (in *P.knowlesi* infections *in vivo* in splenectomized monkeys) that the augmented choline influx in parasitized erythrocytes occurs via pathways with properties similar to the constitutive system but with a greatly increased V_{max} .

2.1.3.1 Albitiazolium (bis-thiazolium compound), an antimalarial drug candidate designed by Vial and group

Bis-thiazolium salts such as albitiazolium have been designed as choline analogues to inhibit malarial PC biosynthesis. It acts as a specific inhibitor of *de novo* PC biosynthesis. Further, it does not have simultaneous effect on PE or nucleic acid (NA) synthesis (Ancelin *et al.*, 1998).

Effect of albitiazolium was determined in three stages of the parasite blood cycle. The PC_{50} of albitiazolium, i.e. the drug concentration that reduces the amount of PC synthesized from choline by 50%, was found to be 2.8, 26 and 9.3 mM at ring,

trophozoite and schizont stages, respectively. It was found that albitiazolium specifically inhibits PC biosynthesis from choline at all blood stages. Under same conditions, Pentamidine (another bis-cationic compound which is not a choline analogue), supposed to interact with DNA. Thus, it primarily affects the synthesis of nucleic acids (NA). However, Pentamidine does not show an effect on PC synthesis (Wein *et al.*, 2012).

The antimalarial activity of albitiazolium was determined alone or in combination with choline, ethanolamine and serine (the polar heads of the three structural PL), the type of interaction exerted, using the isobologram method (Gupta *et al.*, 2002). Polar heads *per se* have a very weak antimalarial activity, with IC_{50} of 12, 0.32 and 65 mM for choline, ethanolamine and serine, respectively.

Choline supplementation to the culture medium antagonized the antimalarial activity of albitiazolium, indicating that its pharmacological activity occurs through interference with choline metabolism whose main end product is the newly synthesized PC (Wein *et al.*, 2012).

Albitiazolium transport was determined both in uninfected and infected erythrocytes at pharmacologically active concentrations (nM range) (Vial *et al.*, 2004) and at a concentration of 30 mM, which is beyond the plasma concentration observed in humans during phase I and II clinical trials. The addition of furosemide at 150 mM (STAINES and Kirk, 1998) reduced albitiazolium uptake by about 70%. Furosemide was unable to completely abolish drug entry, with 15% of albitiazolium uptake remaining even in the presence of 5 mM furosemide. Albitiazolium probably enters infected erythrocytes or RBC (IRBC) mainly through a furosemide sensitive route, which corresponds to NPPs while the residual non-saturable mechanism still remains unclarified.

Albitiazolium entry into isolated *P.falciparum* parasites was also measured. The entry appeared to occur through a saturable Michaelis-Menten process. The fate of albitiazolium and choline in the *P.falciparum*-infected erythrocyte and albitiazolium-induced inhibition of PC biosynthesis is shown in Figure.15.

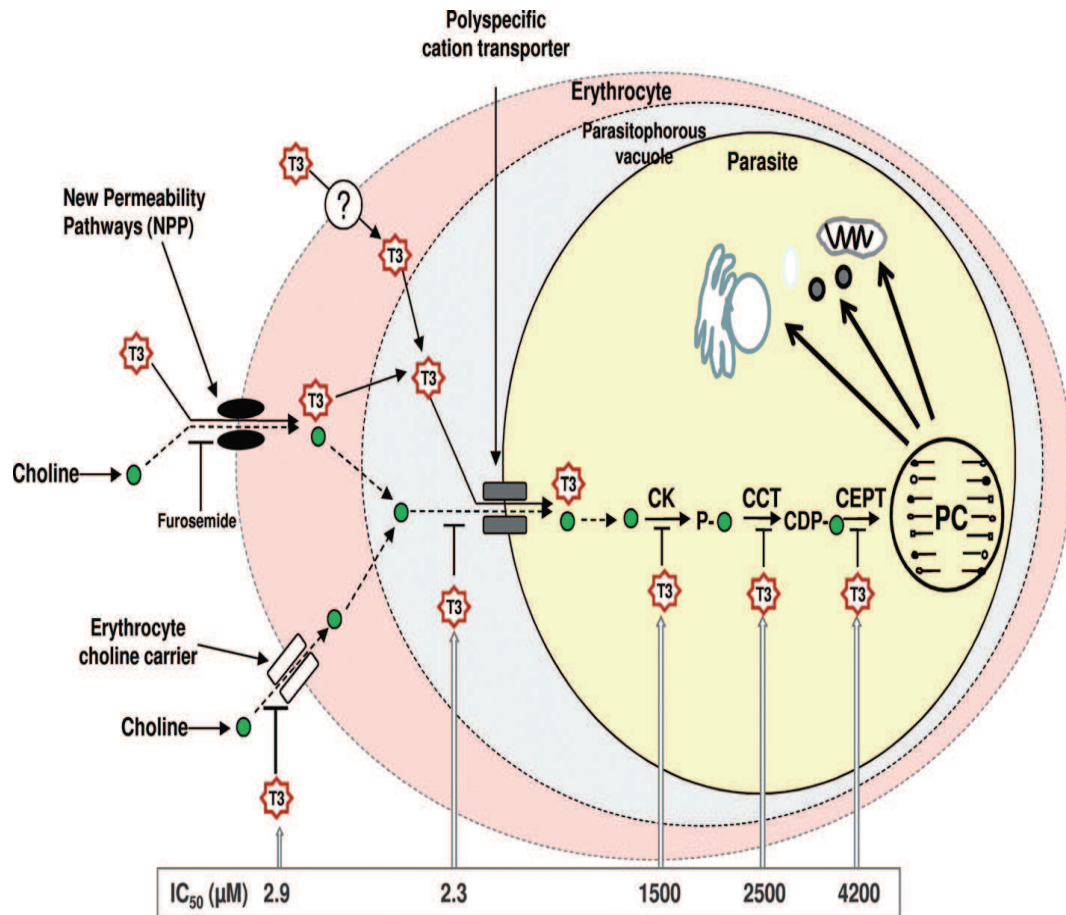


Figure 15: The fate of albitiazolium and choline in the *P. falciparum*-infected erythrocyte and albitiazolium-induced inhibition of PC biosynthesis. Choline enters the infected erythrocyte essentially through the erythrocyte choline carrier and a small amount via furosemide-sensitive NPPs. Choline is then transported into the parasite by the parasite choline carrier and used to synthesize PC via the Kennedy pathway. The choline analogue albitiazolium enters the infected erythrocyte via furosemide-sensitive NPPs and a furosemide-insensitive pathway. Albitiazolium inhibits choline transport by the erythrocyte choline carrier but is not transported by it. The choline analogue is taken up by the parasite via the parasite choline carrier, thus inhibiting choline transport. Albitiazolium is accumulated in the parasite and exerts its activity principally on the different steps of the de novo PC biosynthesis pathway. It should be noted that albitiazolium is abbreviated to T3 for convenience in this diagram. Courtesy: (Wein et al., 2012).

2.2 Regulation of PL metabolic pathways

Choline and ethanolamine polar head groups are phosphorylated by choline and ethanolamine kinases (CK and EK), respectively. These activities have been detected in *P.falciparum* and *P. knowlesi* (Ancelin and Vial, 1986a,c), *P.chabaudi* (Wunderlich et al., 1987), *P.berghei* and *P.vinckeii* (Déchamps et al., 2010a). Two distinct genes are annotated in different sequenced *Plasmodium* genomes. The predicted *Plasmodium* CK proteins possess the main classical CK features: the ATP-binding loop, the Brenners phosphotransferase motif and the CK motif, which are involved in choline, ATP and Mg²⁺ binding (Choubey et al., 2006; Déchamps et al., 2010d). The *P.falciparum* CK gene (PF14_0020) has been cloned and the recombinant protein exhibits CK activity and very weak EK activity (Alberge et al., 2010). CK activities of *P.knowlesi*-infected erythrocyte extracts and of the *P.falciparum* recombinant enzyme are inhibited by the phosphocholine product, but at non-physiological concentrations (Ancelin and Vial, 1986a; Choubey et al., 2006). PfCK is essentially expressed in trophozoites and schizonts, i.e. mature stages (Choubey et al., 2006; Alberge et al., 2010).

PfCK and *P.berghei* CK are localized in the parasite cytosol (Choubey et al., 2006; Alberge et al., 2010; Déchamps et al., 2010b). The *P.falciparum* EK counterpart (PF11_0257) exhibits the classical CK/EK motifs and is a cytosolic protein expressed mainly in mature blood stages (Alberge et al., 2010).

Two other enzymes are known to be rate-limiting and endure the regulation of Kennedy pathway for PE and PC production (see Figure.10). One such enzyme is CCT. It is the rate-limiting and regulatory enzyme of the CDP-Cho pathway for PC biosynthesis (Vance et al., 1980). A major mode of regulation of CCT activity was thus proposed, that is, reversible translocation of the inactive soluble CCT to active, membrane-bound form (Sleight and Kent, 1980). In *P.falciparum* the affinity of PfCCT enzyme for CTP increased and modulated by lipids (Yeo et al., 1997).

ECT is also an important rate-limiting and regulatory enzyme of the CDP-Etn pathway for the biosynthesis of PE (see Figure.10) (Houweling et al., 1992; Sundler, 1975; Sundler and Akesson, 1975; Tijburg et al., 1987). Initial studies of Sundler and

Akesson in rat hepatocytes demonstrated that increasing concentration of ethanolamine led to an increase in the phosphoethanolamine pool but the CDP-Etn levels remained constant. These observations suggested that the reaction catalyzed by ECT is involved in regulating the CDP-Etn pathway but only at physiological or higher ethanolamine concentrations (30-50 μM). However, at lower ethanolamine concentrations, the supply of ethanolamine limits PE synthesis by CDP-ethanolamine pathway (*Sundler and Akesson, 1975*). Further studies by *Tijburg* showed that treatment of rat hepatocytes with phorbol ester stimulated the incorporation of ethanolamine into PE, significantly at physiological ethanolamine concentrations. This was accompanied by reduction in PEtn and CDP-Etn pools as well as by increased conversion of CDP-Etn to PE. This effect was attributed to an enhanced activity of ECT and additionally to an increase in the levels of cellular DAG (*Tijburg et al., 1987*). In a nutshell, it can be stated that the regulation of PE synthesis can take place at more than one enzymatic step. Under most conditions, the supply of CDP-Etn, via the expression level of ECT, and the supply of DAG appear to be the principal factors controlling the rate of PE synthesis in the CDP-Etn pathway.

Regulation of the SDPM pathway unlike other organisms, has only started to be elucidated. Studies by *Elabbadi* and colleagues indicated that distinct pools of PEtn are synthesized by *P.falciparum* from different precursors and via the *de novo* pathway from ethanolamine or following PS decarboxylation, suggesting a possible compartmentalization of these metabolic pathways. However, it remains to be determined whether the genes encoding enzymes of the CDP-Etn pathway or the PS decarboxylase gene are regulated by their precursors. Evidence for the regulation of synthesis of PC by its precursors has been established using wild-type and transgenic *P.falciparum* parasites. It was shown that exogenous choline leads to repression of transcription of PfPMT as well as the induction of its proteasomal degradation (*Witola and Mamoun, 2007*). Addition of exogenous choline to cultures of wild-type parasites produced a dosedependent reduction in the amount of both PfPMT transcript and protein (*Witola and Mamoun, 2007*). The choline-mediated transcriptional response was not evident in transgenic parasites expressing PfPMT under the transcriptional control of a heterologous pro-

moter, whereas PfPMT protein degradation persisted in these parasites. These findings suggest that the promoter of PfPMT may contain elements important for transcriptional regulation by choline (or its phosphorylated form), and that this substrate may also regulate PfPMT.

PfPMT plays an important role in *P.falciparum* development and multiplication. To determine the functional role of PfPMT in intact parasites, the PfPMT locus was disrupted to create a *pfpmt* Δ null mutant lacking PfPMT activity. Parasites lacking PfPMT display delay growth, altered DNA replication, reduced multiplication rate, and increased cell death (*Witola et al.*, 2008). The viability of *pfpmt* Δ knockout parasites is most likely due to the availability of residual choline in human red blood cells, which allows synthesis of phosphatidylcholine via the parasite *de novo* pathway from choline. Interestingly, choline is important for the survival of *pfpmt* Δ . Addition of choline up to 10-times its physiological concentration did not complement the growth, replication, and multiplication defects of these knockout parasites (*Witola et al.*, 2008). This suggests that the SDPM and CDP-Cho pathways produces the initial precursor (phosphocholine, PCho) for the synthesis of phosphatidylcholine (PC). These studies also suggest that inhibition of the initial steps of phosphatidylcholine biosynthesis would require compounds that inhibit both PfPMT activity and choline transport or phosphorylation.

Enzyme kinetics and PL metabolism

The enzymes of the glycerophospholipid pathway mostly obeys Michaelis-Menton kinetics (*Henri, 1902*). K_m (affinity constants of enzymes for the substrate) and V_m (maximum velocity) of some of the enzymes involved in PL metabolism of *P. falciparum* are listed in Table.3.

List of the K_m and V_m of some of the enzymes involved in phospholipid metabolism of *P. falciparum*

Reactions	Enzyme	K_m	V_m	References
SerE → Ser	?	?	?	(Elabbadi et al., 1997)
Ser → PS	PSS	?	?	Vial (unpublished data).
Ser → Etn	SD	?	?	(Elabbadi et al., 1997)
Etn → PEtn	PEEK	475.7 +/- 80.2 μM	1.3 +/- 0.1 $\mu mol/min/mg$	(Alberge et al., 2010)
PEtn → PCho	PFPMT	79 μM	1.2 $nmol/mg/min$	(Pessi et al., 2004, 2005)
PS → PE	PFPSD	63 +/- 19 μM	680 +/- 49 $nmol/mg/min$	(Baunaure et al., 2004)
PEtn → PE	PEECT	465 +/- 70 μM	4.3 +/- 3 $pmol/min/10^7 cells$	(Vial et al., 1984b; Elabbadi et al., 1997)
	CEPT/EPT	13.2 0.7 μM	?	
PCho → PC	PCCT	511.0 24.8 μM	?	(Yeo et al., 1995, 1997)
	CEPT/CPT	13.2 0.7 μM	?	(Vial et al., 1984b)
PE → PC	PEMT/PLMT	?	?	(Moll et al., 1988)
PE → PS	PSSbe	?	?	Berry and Vial (unpublished data)
ChoE → Cho	NPP/OCT/CTL	25.0 3.5 μM	4.6 0.2 $pmol/10^6 cells/min$	(Biagini et al., 2004; Kirk et al., 1991)
				(Goldberg et al., 1990; Wein et al., 2012)
Cho → PCho	PFCK	135.3 +/- 15.5 μM	10.8 +/- 2.8 $\mu mol/min/mg$	(Choubey et al., 2006; Alberge et al., 2010)

Table 3: "?" means K_m or V_m values not found. For abbreviations see abbreviation Table.1

2.3 Future scope

The enzymes comprising PL pathways are either absent from humans, or markedly different from their human counterparts. With the advances made during the past few years in the genetic manipulation of different *Plasmodium* species, it is becoming possible to validate specific steps and networks in these metabolic pathways as targets for the development of new antimalarial therapeutic strategies. The success of the chemical approach that led to the synthesis of potent antimalarial quaternary ammonium compounds highlights the importance of these pathways as drug targets. Thus far, only a few genes encoding lipid metabolism enzymes have been genetically ablated to validate their role in parasite growth and survival. Secondly, the metabolic machineries for the synthesis of phospholipids have stimulated great interest as potential targets for the development of novel antimalarial drugs, largely due to their importance for the growth, proliferation, and pathogenesis of *Plasmodium* parasites.

Quantitative modelling of glycerophospholipid metabolism in *Plasmodium* would help to understand the dynamics of lipid precursors. These studies could be extended to understand the mode of regulation of the metabolic precursors. This would also focus

on the critical steps/pathway(s) involved in phospholipid metabolism. The key enzymes of this step could act as potential drug targets. Thus, it provides scope to design new antimalarials.

Chapter 3

Kinetic modelling of Phospholipid synthesis in *P.knowlesi*

In this chapter we introduce a fully parametrized kinetic model for the multiple phospholipid synthetic pathways in *P.knowlesi*. This model has been used to clarify the relative importance of the various reactions in these metabolic pathways. Future work extensions of this modelling strategy will serve to elucidate the regulatory mechanisms governing the development of *Plasmodium* during its blood stages, as well as the mechanisms of action of drugs on membrane biosynthetic pathways and eventual mechanisms of resistance.

3.1 Introduction and Background

In the last decades, isotope labelling became a major tool for studying metabolic activity of many organisms from bacteria to human (*Chance et al.*, 1983; *de Mas et al.*, 2011). Such experimental techniques have as primary aim the quantification of intracellular metabolic fluxes. The mathematical analysis of the data can be intricate and depends on the technique (radioactive precursor incorporation, isotopomers distribution) and on the type of experimental measurement (steady state, transient data), therefore there is no unique equation or algorithm allowing to extract information from any fluxomic data.

We have based our modelling work on a series of experimental studies designed to elucidate the synthetic pathways of phospholipids in the malaria parasite (*Vial and Ancelin*, 1998). The experimental protocol in these studies uses incorporation of PL radiolabelled precursors and measurement of concentration of end products and intermediate labelled metabolites in the metabolic network (see Figure.10 & 19). Most of the available data consist of concentrations of metabolites after a relatively long incorporation time, for various external concentrations of the precursors.

3.2 The Model description

In order to model the incorporation of precursors we have used a kinetic metabolic network model. The time dependent variables of this model are the concentrations of various metabolites inside the parasite. We gather these concentrations in a column vector $\bar{c}^{in} = (c_1^{in}, c_2^{in}, \dots, c_n^{in})^T$, where c_i^{in} , $i \in [1, n]$ denotes the concentrations of i^{th} metabolite. Some metabolites, namely the scavenged precursors, are considered to be kept at constant concentrations outside the parasites. The corresponding concentration vector is $\bar{c}^{ext} = (c_1^{ext}, c_2^{ext}, \dots, c_m^{ext})^T$, where c_i^{ext} , $i \in [1, m]$ are the fixed, external concentrations of the i^{th} metabolite. In a typical experiment, concentrations \bar{c}^{in} are measured after a given time, for several values of \bar{c}^{ext} . The list of metabolites for our PL metabolic network is given in Table.2.

There are three types of external precursors (serine, ethanolamine, and choline), therefore for the study presented here, $m = 3$. The model is a network of biochemical reactions. To simplify, all the reactions of the network are modelled as single substrate enzymatic reactions. By doing this, we implicitly assume that co-factors are either not limiting or not time dependent. This constraint could be released in more realistic models, for instance when studying the crosstalk between several pathways. We also consider that all the enzymatic reactions have *Henri-Michaelis-Menten* kinetics (*Henri*, 1902; *Michaelis and Menten*, 1913b):

$$R(c) = \frac{V_{max}c}{K_m + c} \quad (3.1)$$

where R is the reaction rate, V_{max} is the maximum reaction rate, K_m is the Michaelis constant, and c is the concentration of the substrate.

The only exception from this kinetics law, is the passive transport of ethanolamine across the parasite membrane. This process has been modelled as a first order mass action law reaction as follows:

$$R(c^{ext}, c^{in}) = K_f c^{ext} - K_b c^{in} \quad (3.2)$$

where R is the ethanolamine influx, K_f , K_b are first order kinetic constants and c^{ext} , c^{in} , are the external and internal concentrations of ethanolamine, respectively.

The topology of the metabolic network is summarized by the stoichiometric matrix $[S]$. The columns of $[S]$ are the stoichiometric vectors, and the elements S_{ij} are integers representing the numbers of molecules of the species i that are consumed (in which case $S_{ij} < 0$) or produced (in which case $S_{ij} > 0$) by the reaction j . The ordinary differential equations describing the kinetics of the model read :

$$\frac{d(\vec{c}^{in})}{dt} = [S]\vec{R}(\vec{c}^{in}, \vec{c}^{ext}) \quad (3.3)$$

where $\vec{R} = (R_1, R_2, \dots, R_r)^T$ is the column vector of reaction rates, in other words the vector of fluxes.

3.3 The hybrid method of optimization.

Given the external concentrations of precursors, \vec{c}^{ext} , the model can predict the intracellular distribution of fluxes, and the concentrations of metabolites, \vec{c}^{in} , as functions of time. These predictions are solutions of the Eq. (3.3) and depend on the kinetic parameters $\vec{k} = (K_{m1}, V_{max1}, \dots, K_{mr}, V_{maxr}, k_d)$ and on the external concentrations \vec{c}^{ext} . Rather generally, parameter fitting is a least-square optimisation problem. In our situation, the least-square objective function is

$$\Phi(\vec{k}) = \sum_{j=1}^d \|\vec{F}(\vec{k}, \vec{c}_j^{ext}) - \vec{c}_j^{in}\|^2, \quad (3.4)$$

where the index $j \in [1, d]$ denotes several external concentration values \vec{c}_j^{ext} of the precursors, \vec{c}_j^{in} are the measured concentrations of metabolites after a long incorporation time (at steady state) and the vector function \vec{F} gives the predicted metabolite concentrations. Here $\|\vec{x}\|$ stands for the Euclidean norm of the vector \vec{x} . Of course, steady state data do not uniquely determine steady state parameters. Indeed, multiplying all the flux parameters (V_{max} in *Michaelis-Menten kinetics*) by the same constant, does not change the steady state and preserves the value of the objective function Φ . In order to fix this multiplicative constant, we used the values of the influxes, that were estimated by dividing the cumulated quantity of end products by the time needed for their accumulation.

Another, more difficult, problem is how to avoid local minima of Φ . In order to solve this problem we use a hybrid method combining discrete sampling of flux values, inversion of the smooth flux-concentration relation, and a final smooth local optimization. The main idea of this method can be summarized as follows. If for each reaction, we can determine the flux for various substrate concentrations, then we can invert the flux-concentration relation for the *Michaelis-Menten's* mechanism and obtain V_{max} and K_m . The optimisation of V_{max} and K_m has an unique solution, as can be shown by the well-known *Lineweaver-Burk* plot (*Cornish-Bowden and Cornish-Bowden, 1995*). However, even though the substrate concentrations are readily available from the data, the flux profiles are unknown. A global optimum will be found by sampling the discretized space of admissible flux profiles. From (3.3) we find that the steady state fluxes satisfy the equation

$$[S]\vec{R} = 0. \quad (3.5)$$

where $[S]$ is the stoichiometric matrix and \vec{R} is the flux vector.

Although it constrains the flux values, Eq. (3.5) has not an unique solution. The number of independent steady state flux profiles is equal to the dimension of the kernel $Ker(S)$ of the stoichiometric matrix S . The rank-nullity theorem provides the number of independent steady state flux profiles, $dim(Ker(S)) = n - rank(S)$, where n is the number of reactions in the network, and $rank(S)$ is the rank of the matrix $rank(S)$, i.e. the number of reactions that have linearly independent stoichiometries. According to the rank-nullity theorem, if there are n reactions in the network, there are $n - rank(S)$ linearly independent, distinct flux profiles, compatible with the constraints. We call admissible fluxes, the solutions of Eq.(3.5) such that $R_i \geq 0$, for any irreversible reaction.

In order to sample the set of admissible fluxes, we need a convenient parametrization of the admissible flux values. For simplicity, we present such a parametrisation for the case when the network contains only monomolecular reactions, i.e. each reaction has only one substrate and only one product. Our kinetic model satisfies this condition, because we chose not to represent cofactors. We also consider that all reactions are irreversible and impose $R_i \geq 0$ for all fluxes. This condition is fulfilled by all

reactions in our model, with the exception of the passive ethanolamine influx that is reversible. The latter does not represent a problem, because in our data there is no ethanolamine incorporation and the corresponding reaction functions unidirectionally evacuate internal ethanolamine excess.

The generalization of the method to networks with reversible reactions is straightforward. In this case a bidirectional reaction can be replaced by two unidirectional reactions, each one having positive rate. $\{R_j^{in}\}_{j \in [1, n_1]}$ denotes the influxes, the fluxes that enter the network (in our case $n_1 = 3$, there are three different PL precursors). Similarly, $\{R_j^{out}\}_{j \in [1, n_2]}$ denotes the effluxes, namely the fluxes that leave the network (in our case $n_2 = 3$, the model produces three main PLs, namely PC, PE and PS). Given the influxes, the steady state flux distribution depends on a number of branching parameters α_i^j , satisfying the relations $\sum_i \alpha_i^j = 1, 0 \leq \alpha_i^j \leq 1$ and defined as follows. For each metabolite j , let us denote by $\{R_i^{out,j}\}_{i \in [1, n_j^{out}]}$ the fluxes that consume the metabolite and by $\{R_i^{in,j}\}_{i \in [1, n_j^{in}]}$ the fluxes that produce the metabolite. The corresponding stoichiometries (the numbers of molecules of metabolite j produced or consumed by the reaction i) are denoted by $\nu_i^{in,j} > 0, \nu_i^{out,j} > 0$, respectively. The positive integers n_j^{out}, n_j^{in} will be called flux outdegree and indegree, respectively. For each metabolite j whose flux outdegree satisfies $n_j^{out} > 1$, we define the positive parameters α_i^j such that $\sum_i \alpha_i^j = 1$. Then, any admissible solution can be computed from the influxes by the following relations (see *Appendix.A* for proof):

$$R_i^{out,j} = \left[\sum_{k=1}^{n_j^{in}} R_k^{in,j} \nu_k^{in,j} / \nu_i^{out,j} \right] \alpha_i^j \quad (3.6)$$

This reasoning also leads to the following formula for the nullity of a monomolecular network, which is the number of independent admissible flux profiles:

$$\dim(Ker(S)) = n_1 + \sum_j (n_j^{out} - 1), \quad (3.7)$$

where n_1 is the number of influxes. Eqs.(3.6), (3.7) show that in a network without branching (when all $n_j^{out} = 1$), all the fluxes can be uniquely calculated from the influxes. Relations (3.6) are also applicable to non-monomolecular networks. However, the nullity formula (3.7) should be modified in general. Indeed, the same flux can

consume several metabolites, which introduce further constraints in the system (3.6); the result will be a decrease of the nullity with respect to the monomolecular value (3.7).

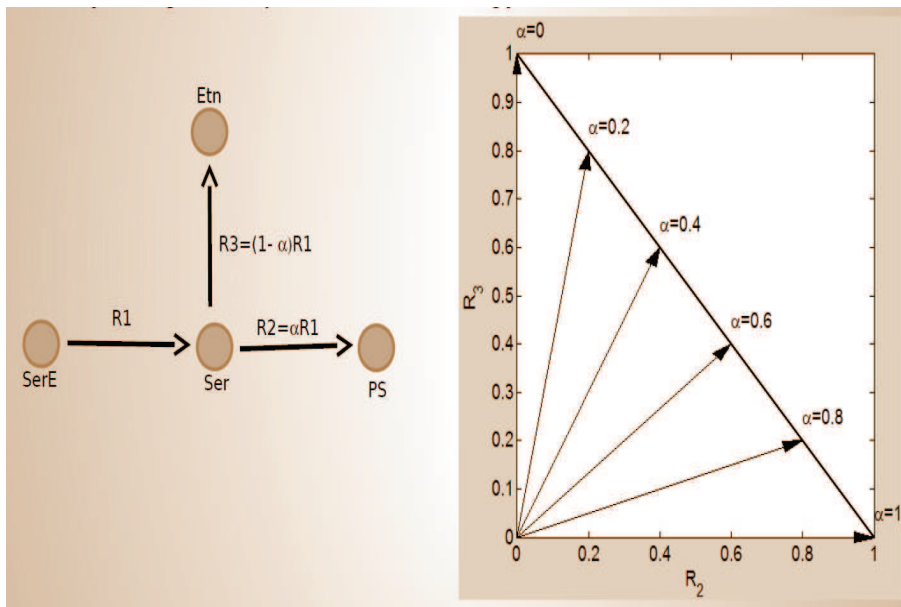


Figure 16: The figure shows discretization of the cone of admissible fluxes

For networks with branching, the parametrization (3.6) is used to sample admissible fluxes by choosing values of the branching parameters $\alpha_i^j = p_i^j/N$, where p_i^j, N are positive integers satisfying $\sum_i p_i^j = N, 0 \leq p_i^j < N$.

For each choice of branching parameters α_i^j , the reaction fluxes are computed for all the available concentrations, resulting from changing the external concentrations of the incorporated precursors. Then, the *Michaelis-Menten* flux-concentration relations are inverted for all the reactions independently, providing kinetic parameters (see Figure.17).

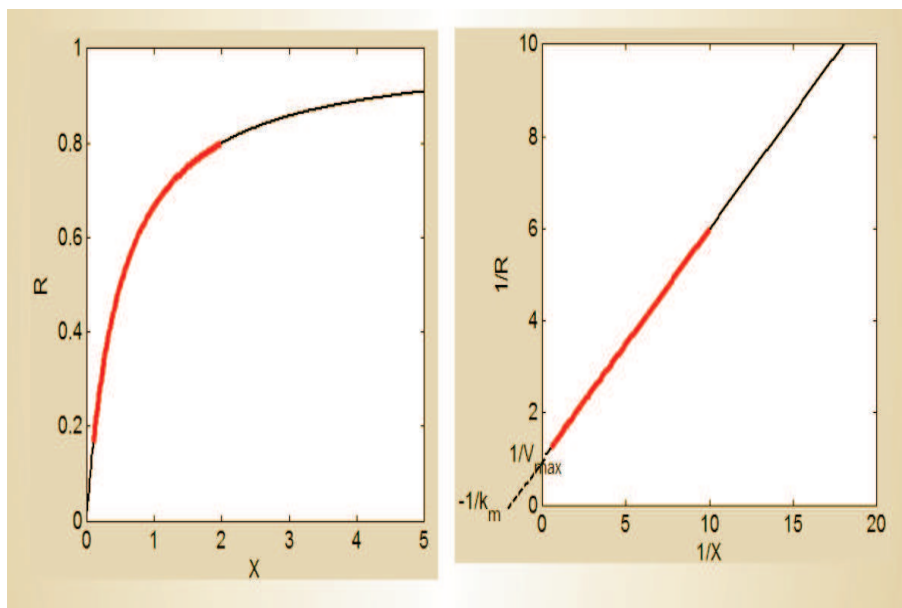


Figure 17: The figure shows inversion of the Michaelis-Menten relation.

Because of the fitting errors, admissibility of the predicted fluxes is only approximate. Therefore, a second optimization step is needed, this time for all the reactions together. The kinetic parameters resulting from the inversion of *Michaelis-Menten* relations are used as initial guesses for a Levenberg-Marquardt local optimizer, minimizing the objective function Φ (3.4). This algorithm outputs optimal values of the kinetic parameters, for each initial choice of the branching parameters α_i^j . Each of the resulting kinetic parameters \vec{k} is a local minimum of the objective function Φ . By comparing these values of Φ one can find the global minimum.

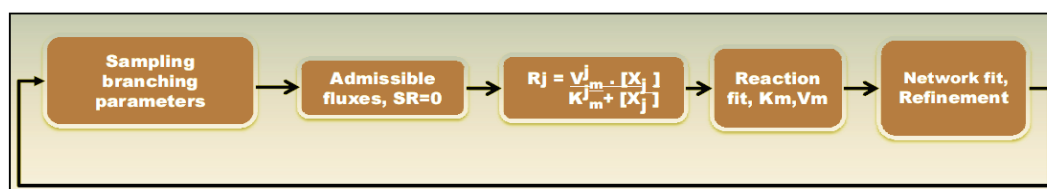


Figure 18: Flowchart illustrating the hybrid optimisation method used for modeling. Branching parameters are discretized and sampled to calculate admissible fluxes. For each individual reaction, Michaelis-Menten formula is inverted to obtain the parameters K_m, V_{max} . A final optimisation step leads to refined parameters for the full network.

In our method, the sampling of admissible fluxes can be exhaustive (for simple networks this is doable), or stochastic, using, for instance, simulated annealing in the discretized simplex of branching parameters. The flowchart of our optimisation procedure is represented in Figure.18.

Multi-objective optimization.

In order to analyse complex metabolic networks with a large number of parallel pathways one needs several types of fluxomic datasets, obtained in various conditions. We use two types of data corresponding each to incorporating only one PL precursor, either serine or choline. This leads to two datasets and least-squares objective functions. For simplicity of the calculations we combine the two objective functions by summing them. Because of the small overlap of the two datasets, more sophisticated analysis using Pareto optimality would lead to similar results.

Limiting-step determination.

Although very popular among biochemists, the limiting step concept surprisingly lacks a clear definition (*Gorban and Radulescu, 2008*). Citing IUPAC Compendium of Chemical Terminology, rate-controlling, or rate-determining, or rate-limiting step in a reaction mechanism is an elementary reaction which exerts a strong effect - stronger than any rate constant - on the overall rate. The quantitative expression of this effect could be given by a sensitivity coefficient, defined as the derivative of the logarithm of the flux F with respect to the logarithm of the rate constant k :

$$C_F^k = \frac{\partial \log(F)}{\partial \log k}. \quad (3.8)$$

In our study, the parameter k can be either V_{max} or K_m . Also the flux value can be the steady state value, or, if steady state conditions can not be reached, the value at a given time, suggested by experiment. Let us notice that our sensitivity coefficients become the flux control coefficients from metabolic control theory, only when $k = V_{max}$ and F is the steady state flux. In this case only, F is homogeneous in

the parameters and the corresponding control coefficients satisfy the usual summation theorems (Reder, 1988). As discussed by Ray (Ray Jr, 1983), the use of sensitivity analysis in this context can lead to existence of many important reactions instead of just one limiting step. In other words, one can speak of limiting steps when sensitivities are concentrated (there is one or a few important reactions) instead of dispersed (all the reactions are equally important) (Fell et al., 1997).

The concept of limiting step is often assimilated to a slow step or narrow place in a chain of transformations. This choice has a meaning for linear pathways, but has to be revised for pathways with branching and cycles (Gorban and Radulescu, 2008). Furthermore, in a simple chain of transformations, the steady state flux, common to all the reactions in the chain, is controlled by the rate constant of the first reaction and does not depend on parameters of other reactions. Metabolic control leads to a trivial result in this case : irrespectively of the presence or not of a narrow place, the flux control coefficients are all zero, excepting for the first step that has control coefficient one. However, a narrow place in a chain of transformations is limiting in the sense that it provides an upper bound to the steady state flux. One gets unlimited accumulation of downstream metabolites, if the narrow place is not the first step of the chain and if the conduction capacity of the narrow place is exceeded.

3.4 Flux Balance Analysis.

Flux Balance analysis (FBA) is an alternate method to compute fluxes, given the reaction network and the biomass definition. It is based on the steady state constraint (3.5) and optimality of biomass production (Klamt et al., 2003). Throughout this chapter we have used the following equation for the Biomass rate: 45% efflux PE + 50% efflux PC + 5% efflux PS is maximal (Vial et al., 1992; Déchamps et al., 2010c). FBA does not determine influxes, that can be arbitrarily normalized by multiplication with a constant. In order to compare FBA fluxes and values resulting from another method, the multiplicative constant should be chosen such that the influx, or, in the case of several influxes, the average input flux is the same in both methods.

3.5 Results and Discussion

Phospholipid synthesis in *P. knowlesi* parasite at its blood stage is one of the most characterized metabolic network, due to the availability of infected erythrocyte collected from *Macaca mulatta* or *M. fascicularis* monkeys and several thorough fluxomic studies (Vial *et al.*, 1989b; Elabbadi *et al.*, 1997; Ancelin and Vial, 1989). Figure.19 represents the network of reactions that are supported by biochemical findings. It provides a global overview of the pathways present in *P.knowlesi*. The availability of the genome sequence of *P.knowlesi* and the subsequent genomic annotations brought a considerable amount of information for the existence of biological processes and existing biochemical pathways, offering a global view of the parasite biology.

Lipid metabolism in *P.knowlesi* takes place to a higher extent in late trophozoite and early schizont stage of asexual (erythrocytic) phase (Vial *et al.*, 1989b; Elabbadi *et al.*, 1997).

The intra-erythrocytic proliferation of *P.knowlesi* requires large amount of PC and PE that together constitute the bulk of the malaria membrane lipids (Vial *et al.*, 1992). The very high biosynthetic capacity of *Plasmodium* operates at the expense of the fatty acids mainly originating from the plasma and polar heads building units. Choline entry into infected red blood cells (IRBC) involves the erythrocytic choline-carrier (Biagini *et al.*, 2004; Ancelin *et al.*, 1991) and parasite-induced new permeation pathways (NPP) (Biagini *et al.*, 2004; Kirk *et al.*, 1991; Wein *et al.*, 2012; Goldberg *et al.*, 1990). Choline is provided to the parasite by a characterized and very efficient organic-cation transporter (OCT/CTL) (Biagini *et al.*, 2004; Kirk *et al.*, 1991; Wein *et al.*, 2012; Goldberg *et al.*, 1990).

Ethanolamine can be supplied from the poorly available plasmatic ethanolamine, which can cross the membrane by passive diffusion, and from serine. Serine is diverted from the serum, host RBC or from hemoglobin degradation in food vacuoles (Goldberg *et al.*, 1990).

Glycerophospholipid model (PL model) shown in Figure.19 represents a rather exhaustive scheme encompassing the phospholipid synthesis and metabolic reactions in

Plasmodium, including 17 reactions and enzymes. Biochemical experimental data and quantification experiments, supports that this parasite machinery can provide the bulk of PL composing the *P.knowlesi* membranes. Genomic studies have confirmed that malaria parasites possess most of the panoply of corresponding genes (see Table.2). Some of the genes, such as those coding for the base exchange and for PS synthase (PSS) enzymes, remain hypothetical in *Plasmodium*. One of the aims of our quantitative modelling is to test the relative importance of various reactions in the model and, eventually, the absence for activity of some of them.

3.5.1 Model simplification

In CDP-choline pathway, PC is produced from PCho in two steps (see Figure.10). First, PCho gives CDP-choline and then CDP-choline transforms to PC. The intermediate CDP-choline was produced in minute quantity which was difficult to measure experimentally (*Déchamps et al.*, 2010b; *Elabbadi et al.*, 1997). Again the yield of labelled PCho was found to be 35 times more as compared to CDP-choline. Thus, the formation of PC from CDP-Choline is very rapid relative to the formation of CDP-choline from PCho (*Elabbadi et al.*, 1997) and CDP-choline is a quasi-steady state species. So, we have ignored this fast intermediate and combined the 2 reactions into a single reaction (labelled R8 in the model, see Figure.19).

Similarly, in CDP-ethanolamine pathway formation of PE from PEtn takes place in two steps. PEtn forms CDP-ethanolamine and in turn produces PE. Again CDP-ethanolamine is produced in minute quantity which is not possible to quantify experimentally. Formation of PE from CDP-ethanolamine is very rapid with respect to the rate limiting formation of CDP-ethanolamine from PCho (*Ancelin and Vial*, 1989). So, we have combined these two reactions into a single reaction (labelled R7, see Figure.19).

This model was deposited in BioModels Database (*Li et al.*, 2010) and assigned the identifier 'MODEL1310130000'.

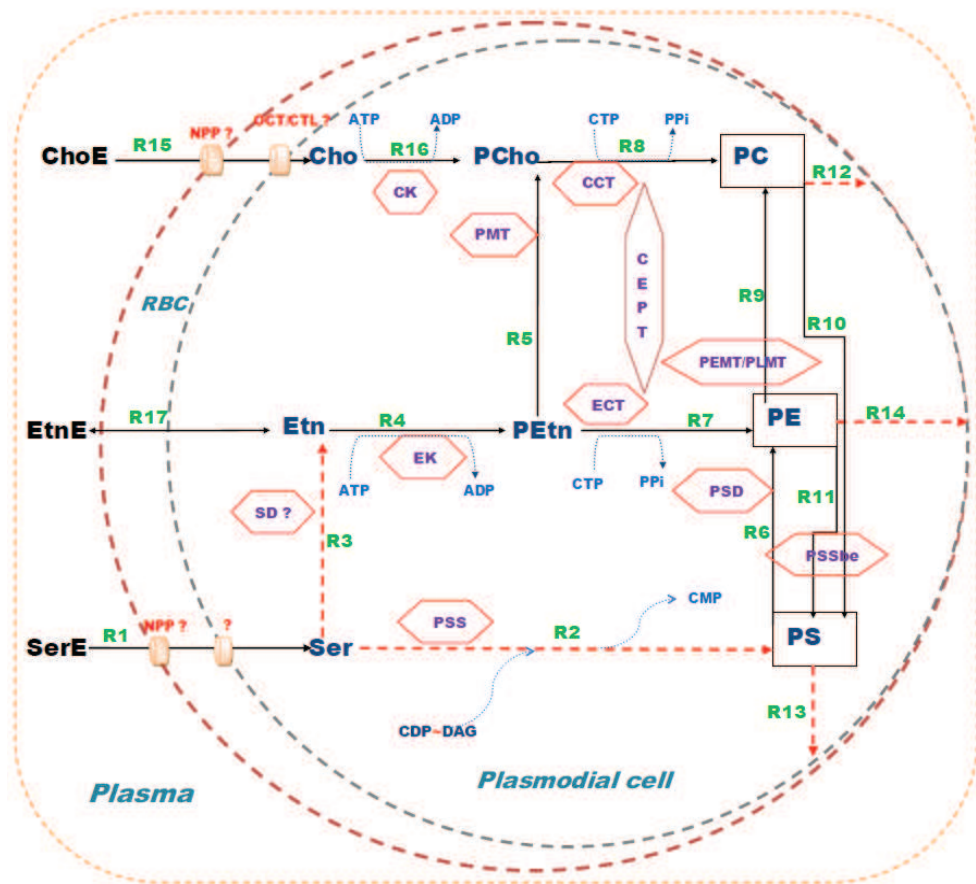


Figure 19: Schematic overview of *P.knowlesi* reactions in structural phospholipid biosynthesis as demonstrated by experimental work. Solid lines correspond to metabolite transport or biochemical reactions with an identified enzyme whereas dotted line correspond to reaction identified with unidentified enzyme. Squares represent the phospholipid end products. Hexagons represent the enzymes. R1 to R17 denote the reaction rates/fluxes. For abbreviations see Table.1

3.5.2 Training the PL model

The glycerophospholipid model (PL model) was trained with two datasets, (i) incorporation of serine (Elabbadi *et al.*, 1997)(ii) incorporation of choline (Ancelin and Vial, 1989) to their different metabolites (PS, PE, PC) in the phospholipid metabolism pathway. The experimental datasets includes the steady state concentrations of the radiolabelled precursors (serine and choline) with respect to their exogenous concentrations.

PL model trained with serine and choline incorporation datasets

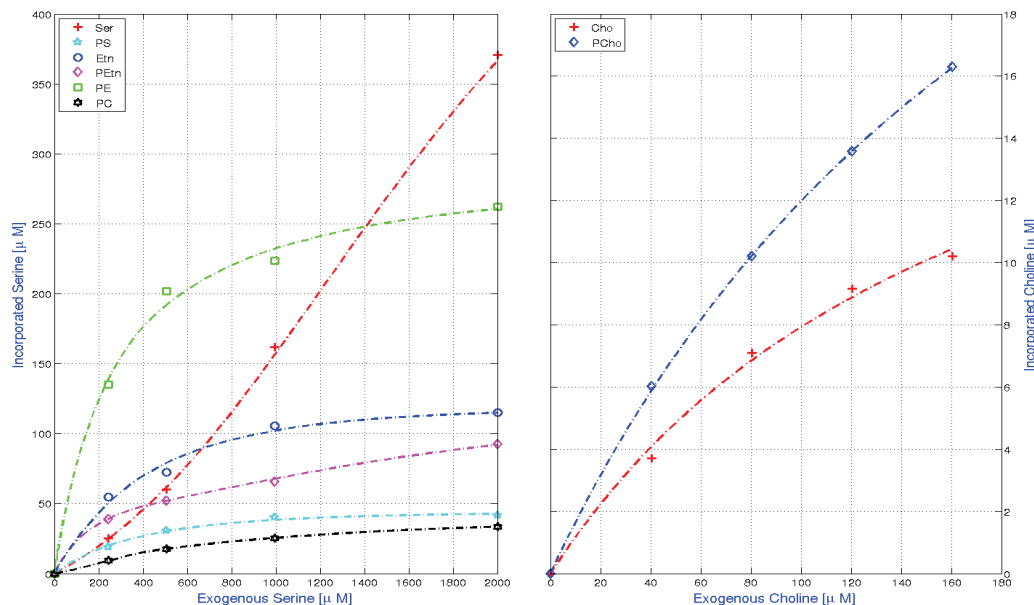


Figure 20: The plot illustrates the fit between the steady state concentration of serine and choline incorporated metabolites with the extracellular serine (0 – 2000 μM)(left panel) and choline (0 – 160 μM)(right panel) from experimental studies and from simulation respectively. The points(or markers) represent the steady state concentration of serine incorporated metabolites with varying extracellular serine measured in the experiment. The dash-lines represent the concentration of metabolites with varying concentration of extracellular serine, as calculated from (PL) Model(ODE). Similarly, in the right panel, points (or markers) represent the steady state concentration of choline incorporated metabolites with varying extracellular choline measured in the experiment. The dash-lines represent the concentration of metabolites with varying concentration of extracellular choline, as calculated from (PL) Model(ODE).

In the experiment (Elabbadi *et al.*, 1997), variable amounts from 0 – 2000 μM of radiolabelled serine were subjected exogenously to the cell and were incorporated into various metabolites (see Figures.19 & 20).These data was used to train the model. The steady state concentration of all the serine derived metabolites were predicted and used to fit the experimental data by the procedure discussed before. For each extracellular serine concentration, the influx of serine was calculated by dividing the total amount of accumulated end products (PC + PE + PS) by the characteristic accumulation time

(2 h).

The characteristic accumulation time correspond to the cross-over between accumulation that is approximately linear in time and corresponds to constant net fluxes, and saturation, corresponding to proximity of steady state (when the net fluxes vanish). For serine incorporation, this time is approximately two hours (*Elabbadi et al.*, 1997).

Radiolabelled experiments were also performed with choline as metabolic precursors. Choline produces different metabolic compounds (see Figures.19 & 20) with PC as the major end product in (*Ancelin and Vial*, 1989). This dataset was also used to train the model, with a unique set of parameters for both experiments. In order to reproduce the experimental protocol, extracellular concentration of choline (ChoE) was taken for several values from 0 – 160 μM , whereas concentrations of extracellular serine (SerE) and ethanolamine (EtnE) were kept very low. Like for the previous data sets, the influx of precursor was calculated by dividing the total amount of accumulated end product (PC) by the accumulation time (1 hour). Though used for influx estimates, the phosphatidylcholine does not reach steady state in this experiment (see Fig.1 of (*Ancelin and Vial*, 1989), also the model analysis section) and PC profile has not been taken into account for the calculation of the objective function Φ , defined by Eq.(3.4). A model prediction with the experimental results is shown in Figure.20.

Parameter values for the ODE (PL) Model

All the reactions have mass action kinetics, with the exception of the reaction 17 that has first order mass action law kinetics (the forward and the backward rate constants are denoted K_f and K_b , respectively). For those reactions whose regime is linear (L), only the ratio V_{max}/K_m has a meaning.

Reaction ID	Reactions	Enzymes	Estimated $V_m(\mu M/min)$	Estimated $K_m(\mu M)$	Regime
R1	SerE \rightarrow Ser	..	$3.41 \in [3.08, 3.95]$	$363 \in [326, 410]$	
R2	Ser \rightarrow PS	PSS	$1.31 \in [0.517, 1.65]$	$797 \in [352, 1.25 \cdot 10^3]$	
R3	Ser \rightarrow Etn	SD	$2.62 \in [2.33, 3.11]$	$24 \in [22.7, 29.5]$	
R4	Etn \rightarrow PEtn	EK	$8.62 \in [6.19, 13.3]$	$109 \in [75.6, 193]$	
R5	PEtn \rightarrow PCho	PMT	$1.08 \in [0.725, 13.9]$	$122 \in [78.5, 2650]$	
R6	PS \rightarrow PE	PSD	$2.25 \in [0.747, 2.94]$	$204 \in [152, 413]$	
R7	PEtn \rightarrow PE	ECT/CEPT	$5.61 \in [4.19, 7.65]$	$227 \in [175, 353]$	
R8	PCho \rightarrow PC	CCT/CEPT	$0.413 \in [0.315, 0.599]$	$31 \in [26.2, 34.9]$	
R9	PE \rightarrow PC	PEMT/PLMT	$1.42 \cdot 10^3 \in [59.2, 1.33 \cdot 10^4]$	$3.21 \cdot 10^5 \in [2.73 \cdot 10^4, 1.92 \cdot 10^6]$	L
R10	PC \rightarrow PS	PSSbe	$0.697 \in [0.318, 0.944]$	$3.76 \in [0.06, 3.88]$	
R11	PE \rightarrow PS	PSSbe	$89.9 \in [9.16, 527]$	$1.71 \cdot 10^5 \in [1.58 \cdot 10^4, 9.14 \cdot 10^5]$	L
R12	PC \rightarrow	..	$1.57 \in [0.75, 3.84]$	$24.1 \in [16.5, 35.8]$	
R13	PS \rightarrow	..	$1.54 \in [0.013, 3.28]$	$204 \in [41.1, 1020]$	
R14	PE \rightarrow	..	$774 \in [9.44, 1.08 \cdot 10^4]$	$1.55 \cdot 10^5 \in [2.52 \cdot 10^4, 1.65 \cdot 10^6]$	L
R15	ChoE \rightarrow Cho	OCT/NPP	$0.232 \in [0.182, 0.323]$	$102 \in [91.9, 109]$	
R16	Cho \rightarrow PCho	CK	$0.556 \in [0.384, 0.882]$	$30.4 \in [22.8, 36.7]$	
R17	EtnE \rightarrow Etn	..	$K_f = 5.10^{-4} min^{-1} \in [10^{-4}, 2.5 \cdot 10^{-3}]$	$K_b = 1.33 \cdot 10^{-4} min^{-1} \in [4.45 \cdot 10^{-15}, 1.4 \cdot 10^{-3}]$	

Table 4: Parameter values for the ODE (PL) Model.

For the calculation of the confidence intervals see *Appendix.A* (the allowed objective function values were less than 1.5 times the global minimum).

3.5.3 Model predictions and analysis

Calculations of Fluxes from the model (ODE method) and comparison with Flux Balance Analysis (FBA)

Using the parametrized ODE model we can compute the steady state concentrations of the metabolites, as well as the steady state values of the fluxes through all reactions. Steady state fluxes can also be calculated using the FBA method. We compare the results from two methods. Because FBA does not fix the time scale, in this method fluxes are determined up to multiplication by a constant. In order to compare the two methods, we renormalized the FBA fluxes such that the input fluxes (the average when there are several) coincide in the two methods. Although there is no reason to expect that the FBA method provides an absolute reference, this comparison

is informative. Agreement will confirm the relevance of the optimal biomass production concept, whereas disagreement will indicate the limitations of the FBA method. We have performed different *in silico* experiments with the incorporation of different metabolic precursors.

Serine incorporation

At physiological concentration of exogenous serine (SerE) ($0 - 100 \mu M$), fluxes were calculated using the FBA method (Klamt *et al.*, 2003) and the ODE kinetic model (with fitted parameters). The fluxes from these two different methods were compared. The concentration of extracellular choline (ChoE) and ethanolamine (EtnE) was kept very low. Distribution of fluxes with five different concentration of SerE ($0 - 100 \mu M$) is shown in Figure.21.

Fluxes from FBA (represented with blue bars) are independent of the concentration of the metabolites but they depend on the assigned biomass and on the influxes. The biomass 'M' was defined to be, $M = 50\%PC + 5\%PS + 45\%PE$ (Vial *et al.*, 1992; Déchamps *et al.*, 2010c).

Relative to the influx, the distribution of fluxes from FBA method (blue bars, Figure.21) does not change with the concentration of exogenous serine (SerE). On the other hand, the relative distribution of fluxes calculated by the ODE method, changes slightly for some reactions with change in concentration of SerE. The fluxes from both the methods were compared to each other and to previously reported biochemical findings.

Fluxes from ODE (green bars, Figure.21) marks the major part of serine derived PE, formed via serine decarboxylation (SD)(R3 in Figure.19 & Figure.21). PS decarboxylation (PSD)(R6 in Figure.19 & Figure.21) which also can form PE, has less contribution.

Indeed, the flux R7 is much higher than R6 and it does not increase much with increase in concentration of exogenous serine (SerE, Figure.19 & Figure.21). Again, R3 is much greater than R2. A very low flux R2 indicates low, possibly vanishing, activity

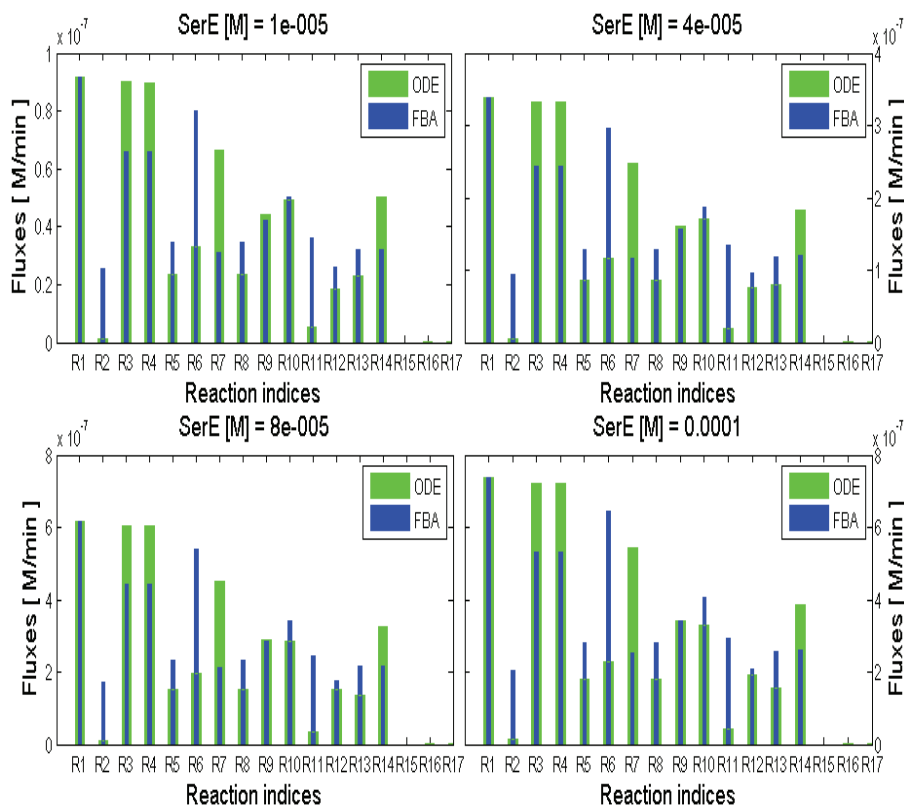


Figure 21: The bar plots shows the distribution of fluxes in the network with four different concentrations of SerE, 0 – 100 μM . In each subplot the reaction rates/fluxes are denoted by (R1 to R16). The blue bar color represent fluxes from the FBA method and green bars represent fluxes from ODE.

of phosphatidylserine synthase (PSS) during blood stages of *P.knowlesi* in presence of exogenous serine.

These findings suggest that, direct decarboxylation of serine and CDP-ethanolamine pathway (R3, R4, R7) (see Figure.19) is the preferred pathway for the formation of PE from serine in agreement with (Elabbadi *et al.*, 1997).

On the contrary, fluxes from FBA method (blue bars, Figure.21) suggest that R6 is greater than R7. So, the FBA results contradict the experimental findings (Elabbadi *et al.*, 1997). Further more, the branching parameters resulting from FBA method that are bound to the values of the objective function which is much higher than the global optimum. This again contradicts with the experimental data. This contradiction may be due to the lack of relevance of the biomass optimisation in the situation when serine

only is incorporated and emphasizes the utility of kinetic modeling.

Base-exchange reactions (PSSbe) between serine and PE or PC were initially not detected in *Plasmodium*. However, recent biochemical studies revealed calcium-dependent base exchanges between serine and PLs in *P.falciparum* (Berry and Vial, unpublished data). This is an area which remains unexplored in *Plasmodium*. PS could be formed directly from serine via PS synthase (R2), or by transformation of PC and PE via (PSSbe), R10 and R11 respectively (Figure.19). In order to understand the relative importance of these pathways, we compared the fluxes R2, R10 and R11 in both the methods.

Fluxes from ODE suggest that, very less quantity of PS was produced from serine via R2 (PSS) but considerable amount from PC (R10) and PE (R11). The flux values of R2 from FBA (blue bars) was much higher than the ODE (green bars), though remained significantly smaller than R3. It means considerable amount of PS was formed from serine via R2 (PSS), which quantitatively contradicts the biochemical findings (*Elabbadi et al., 1997*). However, the flux R10 (PSSbe) from both the methods suggests an exchange of PC and PS in presence of SerE.

3.5.4 Source of PC production in absence of CDP-choline pathway.

The major source of PC is thought to be provided by CDP-choline or Kennedy's pathway (*Lew, 2004; Ancelin and Vial, 1989*). Thus, the *denovo* CDP-choline pathway has been proposed to be the primary route for synthesis of PC in *Plasmodium* (*Vial et al., 1982b; Ancelin and Vial, 1989*). However, *in vitro* growth assays using dialyzed serum indicated that CDP-choline pathway was not essential for parasite intra-erythrocytic development and survival (*Divo et al., 1985a; Mitamura et al., 2000*). There are two possible pathways which could furnish PC synthesis other than CDP-choline pathway/Kennedy pathway (see Figure.19) :

- PMT, which transforms PEtn into PCho, which in turn forms PC via CDP-choline pathway. This is a part of SDPM pathway by which host serine is incorporated into PC. The mechanism is S-adenosyl methionine (SAM)-dependent triple methylation carried out by a plant-like phosphoethanolamine N-methyltransferase (PMT or PEAMT) (EC 2.1.1.103). *P.falciparum* PMT (PfPMT), has been revealed by the *P.falciparum* genome sequencing program (Gardner *et al.*, 2002b). Subsequently, the role of phosphoethanolamine methyltransferase (PMT) pathway has been identified in *Plasmodium falciparum* (Pessi *et al.*, 2004). The orthologous gene (*PKH_121150*) has been identified in *P. knowlesi* (Aurrecochea *et al.*, 2009).
- PE transmethylase (PEMT or PLMT) pathway. The capacity of *P.knowlesi*-infected erythrocyte to methylate PE into PC has been documented in previous studies and clearly indicates PEMT activity (Moll *et al.*, 1988). However, the corresponding genes have not yet been found in any *Plasmodium* species.

It is thus necessary to understand the kinetics of SDPM and PE transmethylase pathway which diverts host serine and ethanolamine (via PE) into PC. For this, we compared the fluxes R5 (PMT) and R9 (PEMT/PLMT) from ODE and FBA methods (see Figure.21). We found that behavior of the fluxes in both the methods is coherent. Flux R9 (PEMT/PLMT) is slightly more as compared to R5 (PMT) in both FBA and ODE methods. These suggests that both R5 and R9 could act as a source for the production of PC. In order to gain further understanding into the relevance of R5 (PMT) or R9 (PEMT/PLMT) *in silico* knockout experiments were performed.

***In silico* knockout of R5 (PMT)**

The PL Model was simulated for two hours with the knockout of R5(PMT). The exogenous serine (SerE) was kept at 100 μM , whereas the concentrations of choline and ethanolamine were kept very low. The PC efflux (R12), PS efflux (R13) and PE efflux (R14) were estimated before knockout or wild-type (BKO) and after knockout or mutant (AKO) as shown in Figure.22.

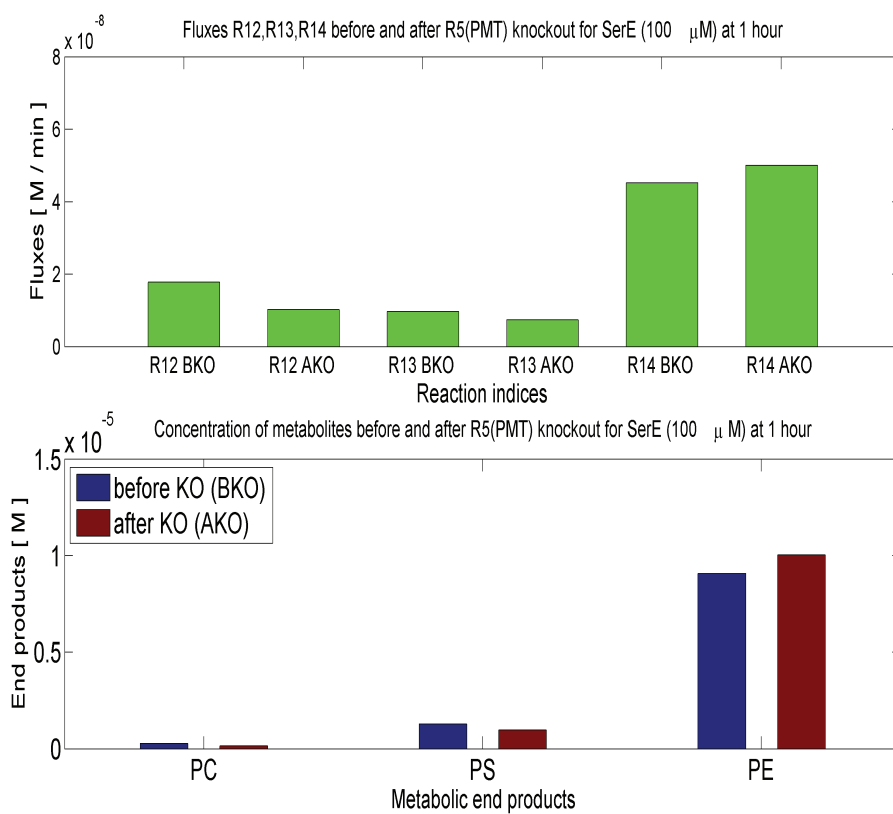


Figure 22: The bar plots illustrate the results of *in silico* knock-out of PMT in presence of SerE (100 μ M) and in absence of ChoE, EtnE. 'BKO' denotes before knockout and 'AKO' denotes after knockout. The upper panel shows the effect on effluxes, whereas the lower panel shows the effect on concentrations of end products. The fluxes and concentrations were calculated by simulating the ODE (PL) model for two hours starting from zero initial metabolite concentrations.

The result is a two fold decrease in the efflux R12 and PC concentration (see Figure.22). Thus, when R5 (PMT) was knocked out, the rate of incorporation of PC into the membrane decreased in the absence of exogenous choline (ChoE). However, there was a small increase in the rate of PE efflux.

***In silico* knockout of R9 (PEMT/PLMT)**

Similarly, the PL Model was simulated for two hours with the knockout of R9 (PEMT/PLMT). The fluxes before knockout (BKO) and after knockout (AKO) are shown in Figure.23.

There was a marked decrease in PC efflux (R12) and concentration. Thus, when R9 (PEMT/PLMT) was knocked out, the rate of incorporation of PC into the membrane decreased in the absence of exogenous choline (ChoE).

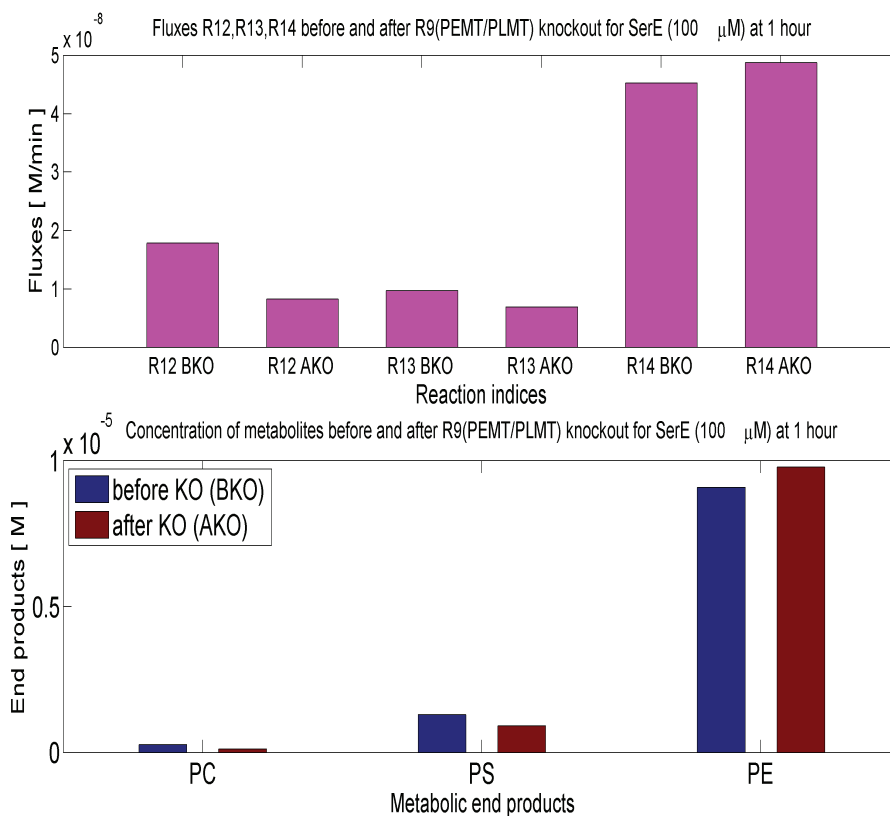


Figure 23: The bar plots illustrate the results of *in silico* knock-out of PEMT/PLMT in presence of SerE (100 μM) and in absence of ChoE, EtnE. 'BKO' denotes before knockout and 'AKO' denotes after knockout. The upper panel shows the effect on effluxes, whereas the lower panel shows the effect on concentrations of end products. The fluxes and concentrations were calculated by simulating the ODE (PL) model for two hours starting from zero initial metabolite concentrations.

The behavior of fluxes with R5 (PMT) or R9 (PEMT/PLMT) knockout followed the same pattern. There was a significant decrease in PC efflux (R12), and a small increase in the PE efflux (R14). A marked R9 (PEMT/PLMT) reaction denotes the capacity of the parasite to convert PE to PC.

From the knockout studies (see Figures.22 & 23) it was found that, part of PC was produced by the even contribution of R5(PMT) and R9(PEMT/PLMT). Looking

to the results of (Witola *et al.*, 2008; Pessi *et al.*, 2004, 2005), knockout of PMT pathway in *P.falciparum* produces a severely affected phenotype. This suggests that PC biosynthesis from SPDM pathway cannot be compensated by the CDP-choline pathway. This is only partially in agreement with our predictions and could mean that PMT might also have PEMT activity *in vivo* in particular conditions. Because the corresponding genes coding for PEMT have not been found in any *Plasmodium* species, deletion of PMT gene in *P.falciparum* could be equivalent to a double knockout of PMT and PEMT in our model, that completely abolishes the incorporation of ethanolamine into PC.

3.5.5 Rate-limiting steps for PC synthesis

We are interested here in detecting rate limiting steps for the major PC synthesis pathway, namely the CDP-choline pathway. The analysis is based on experiments that have been done with choline as unique metabolic precursor (Ancelin and Vial, 1989). This experimental setting was designed to probe the *denovo* synthesis of PC via CDP-choline pathway. In this experiments the extracellular concentration of choline (ChoE) was changed from 0 – 100 μM *in silico*.

Concentrations of extracellular serine (SerE) and ethanolamine (EtnE) were kept very low. As shown in Fig1. of (Ancelin and Vial, 1989), the parasite choline and phosphocholine reach steady state concentrations after two hours of incorporation. However, the phosphatidylcholine concentration is linearly growing with time even after three hours of incorporation and does not reach steady state. The incorporation data correspond to concentration of choline derived metabolites after 1 hour of incubation of infected erythrocytes in the presence of radiolabelled choline. It explains the dynamics of the pathways to provide PC which is readily incorporated into *P.knowlesi* membrane or structural phospholipids.

We have simulated the ODE model for 1 h starting with vanishing initial metabolite concentrations and computed the resulting fluxes. The kinetic parameters (K_m, V_{max}) are the ones obtained from model training and common both to serine and to choline incorporation.

In order to find limiting steps we use a sensitivity based approach. Parameters K_m , V_{max} are perturbed with respect to the nominal values. We compute sensitivity coefficients defined as the derivatives of the fluxes with respect to all parameters of the model (see Limiting-step determination section). As seen in Figure.24, for choline incorporation via the CDP-choline (Kennedy) pathway, sensitivity coefficients have similar orders of magnitude for fluxes and concentrations. These coefficients have even, rather than concentrated distributions.

Consequently, and contrary to our former study (*Ancelin and Vial, 1989*), the model cannot identify *stricto sensu* rate limiting steps. As expected, rate constants of reaction 15 (the choline influx) controls all the non-vanishing fluxes and concentrations. In order of importance, follows reaction R8 (CCT: phosphocholine cytidyltransferase) and to a lesser extent, R16 (CK: choline kinase).

Our former experimental work (*Ancelin and Vial, 1989*) which finds CCT as rate-limiting step should be interpreted in different terms. Indeed, the relatively slow step CCT produces the quasi-steady state CDP-choline that is rapidly consumed and hence present in minute quantities compared to the CCT substrate PCho. This means that CDP-choline is a fast intermediate that can be depleted from the model, which we actually did from the very beginning when we reduced the model. The sensitivity coefficients of the remaining reactions, although different, do not differ by orders of magnitude.

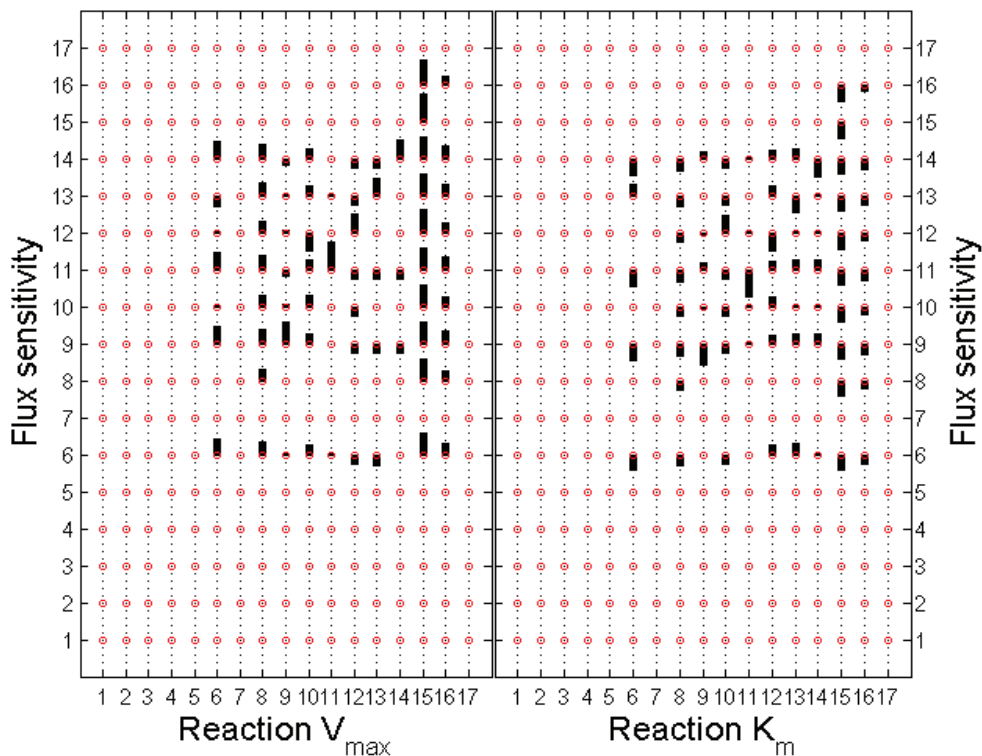


Figure 24: The plots represent the result of the sensitivity analysis. We have computed the sensitivity coefficients matrix for the fluxes (panel a) and for the metabolite concentrations (panel b) with respect to parameters V_{max} and K_m . We have considered choline incorporation via Kennedy pathway, namely $ChoE = 50\mu M$, $SerE = 0$, $EtnE = 0$. Fluxes and parameters are numbered from 1 to 17 that correspond to reaction labels from Figure.19. Metabolites are numbered from 1 to 8, which corresponds to species represented in Figure.19. Each bar has a size proportional to the value of the control coefficient (when this coefficient is negative the bars are oriented downwards). We can notice that the strongest effect on both the PC production (flux 8, panel a) and PC concentrations (species 6, panel b) is produced by changes of parameters of reactions 15 and 8, in this order. However, all the reactions in the CDP-choline pathway (with the exception of the fast, non-represented one, transforming CDP-choline into PC) have comparable sensitivity coefficients, meaning that this pathway has not an unique limiting step. The PC concentrations are also sensitive to the base exchange reaction R10 (panel b), which is normal, because this reaction consumes PC.

3.6 Conclusion

Precise quantitative models for essential metabolic functions of pathogens can be used to understand their intricate set of biological process and their regulation. It guides us to determine the specificities of their physiology, improve the action of known drugs and discover new treatments directed against them. Even when the full genome is available, as in the case of *Plasmodium*, the reconstruction of metabolic pathways can be particularly challenging. Generic pathways databases provide incomplete or unverified metabolic pathways for *Plasmodium*. For instance, Kegg database (*Kanehisa and Goto, 2000*) proposes the similar glycerophospholipid metabolism map for *P.knowlesi*, *P.berghei*, and *Bacillus subtilis*, in fact based on evidence coming mainly from *S. cerevisiae* and *E. coli*. Hagai Ginsburg's Malaria Parasite Metabolic Pathways (<http://priweb.cc.huji.ac.il/malaria/>) is more specific because based on data from *Plasmodium* species (without interspecies distinction), but is still incomplete and not quantitative. We have proposed here, for the first time, a complete quantitative model for the glycerophospholipid synthesis in *P.knowlesi*. This model is based on several fluxomic experiments of incorporation of radiolabelled phospholipid precursors.

In order to learn the metabolic network from data we have developed a new hybrid optimisation scheme, which is based on the discretization of the simplex that parametrizes the set of directions in the cone of admissible fluxes. The main interest of this method is that it facilitates the global search in the parameter space and can be combined with other global optimization algorithms, such as genetic algorithms or simulated annealing. Our method was specifically designed to understand glycerophospholipid metabolism in *Plasmodium* from radiolabelled precursor fluxomic data. It provides an effective sampling of the parameter space. This method can be generally applied to metabolic networks with *Michaelis Menten* reactions, functioning at steady state. It can be therefore used for other studies of the same kind, for rate constant identification in isotope labelling experiments.

The metabolic network model has been used to elucidate the functioning of the multiple phospholipid synthetic pathways in *P.knowlesi*. The main source of PC is

the CDP-choline Kennedy pathway, however, SDPM and PE transmethylase pathways could provide part of PC. The values of the fluxes as well as *in silico* knock-out experiments showed comparable importance of PMT and PEMT/PLMT for PC synthesis in *P.knowlesi*.

These findings confirm earlier hypotheses about the existence of both PMT and PEMT activity in *P.falciparum* and *P.knowlesi* (Moll *et al.*, 1988). Our *in silico* knock-out experiments prove partial dependence of PC production on both PMT and PEMT, meaning that single knock-out of any of these enzymes will reduce but not completely eliminate PC production from serine in *P. knowlesi*. This prediction can not explain the result of (Witola *et al.*, 2008) that deletion of pfPMT gene in *P.falciparum* abolish the incorporation of ethanolamine into PC. Because the corresponding genes coding for PEMT have not been found in any *Plasmodium* species, altogether these findings could suggest that PfPMT might also have PEMT activity *in vivo* in particular conditions (which are not met *in vitro* or in yeast) (Déchamps *et al.*, 2010b; Ben Mamoun *et al.*, 2010).

Our model also indicate that the major part of serine derived PE is formed by serine decarboxylation. PS is predominantly formed by base-exchange reactions and not by the direct CDP-DAG phosphatidyl-synthase (PSS) mechanism.

Sensitivity analysis of CDP-choline pathway in our model, does not identify limiting steps. However, it shows that the carrier-mediated choline entry into the parasite and the phosphocholine cytidylyltransferase (CCT) reaction have, in order, the largest sensitivity coefficients in this pathway. This finding is in agreement with previous knowledge, and has been partially exploited in the search for antimalarial drugs. Indeed, choline entry is targeted by a new the class of potent antimalarial drugs (Wengelnik *et al.*, 2002; Vial *et al.*, 2011a, 2004). It would be interesting to combine this action with simultaneous inhibition of the CCT reaction.

Chapter 4

Insights of *Plasmodium* omics from High-throughput analysis

The chapter focus on recent advances in Functional genomics of *P. falciparum*. It also elaborates about different methodologies used for processing, quantification and analysis of high throughput omics data in *P. falciparum*. Some of these techniques are used to understand and draw inferences from transcriptome and metabolome of *P. falciparum*, across the cell cycle which is discussed in chapter.5.

4.1 An overview of *Plasmodium* genome

The first complete draft of the human malaria parasite genome was released in 2002 (*Gardner et al.*, 2002a). The size of the genome was initially estimated to be 30 Mb (but confirmed later to be 25 Mb (*Lai et al.*, 1999; *Gardner et al.*, 2002a)). In addition to its nuclear genome, the parasite contains 6 and 35 kb circular DNA found in its mitochondria and apicoplast, respectively. The genome segregated into 14 chromosomes and 5300 protein-encoding predicted genes. *P. falciparum* genome is (A+T) rich. The overall (A+T) composition is 80.6% and can rise to 95% in introns and intergenic regions (in case of centromeric sequences identified on chromosome 2 and 3 (*Bowman et al.*, 1999)). Whereas, (G+C) content is 19% that is the lowest of any genome sequenced till date.

Major discoveries during genome sequencing are listed below:-

- a. Two new gene families that were predicted to encode potentially variant surface antigens rifins and STEVORS (*Chen et al.*, 1998, 2000; *Gardner et al.*, 2002a; *Kyes et al.*, 2003).
- b. A cluster of four genes of unknown function repeated on one end of chromosomes 2 and 3 and putative centromeres (*Bowman et al.*, 1999).
- c. Genes encoding enzymes of the type II fatty acid biosynthetic pathway that was thought to be restricted to plants and bacteria (*Gardner et al.*, 2002a; *Waller et al.*, 1998).

After almost 7 years of sequencing (using the Sanger method and chromosome shotgun strategy) and 9 years of co-ordinated efforts of genome curation, the com-

plete genome was determined. The haploid genome is 23.26 Mb in size which comprise 6372 genes. Out of these, 5524 are protein-coding (genome version: 06-01-2010) (<http://plasmodb.org/plasmo/>). Approximately half of these genes (49.6%) have no detected sequence homology with any other model organism (GeneDB). *P. falciparum* genome has a large number of hypothetical proteins (nearly 60%) (with limited homology to genes with known functions). However, the functions of these proteins are still unknown.

4.2 Functional genomics in *Plasmodium*

The advancement of functional genomics and its application to *Plasmodium* biology opened new arena of malarial research. Genome-wide analyses delivered a refined annotation of the parasite genome. Now, there is better knowledge of RNA, proteins and metabolites. However, recent access to next-generation sequencing technologies, along with an increased number of genome-wide applications, is expanding the impact of the parasite genome on biomedical research, contributing to a paradigm shift in research activities that may possibly lead to new optimized diagnosis and treatments (*Le Roch et al.*, 2012). Genetic mapping, comparative genomic analysis, and combination of transcriptomic, epigenomic and proteomic approaches can play important roles in understanding gene functions in *P. falciparum* (*Mu et al.*, 2010).

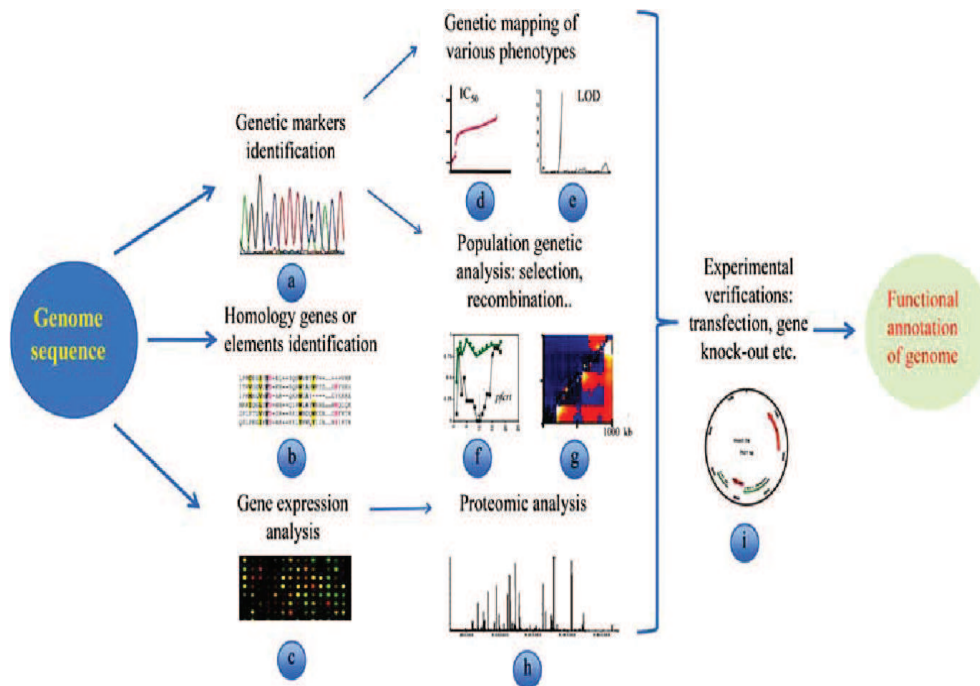


Figure 25: A schematic representation of contribution of Functional genomics with various aspects a) Sequence based analysis to identify genetic polymorphisms b) sequence comparison to search for homolog genes or elements c) microarray chips to evaluate the gene expression at mRNA level d), e) analysis of different phenotype and genotype data to locate candidate genes/loci associated with drug resistance and other traits f), g) population genetic analysis to detect genetic loci under selection or with elevated recombination frequency h) protein expression analysis and association with developmental stages and i) predicated functions of candidate genes can be studied using genetic knock-out and other methods (Courtesy: (Mu et al., 2010)).

4.2.1 Genome diversity and genetic polymorphism

Genetic diversity is considered to contribute to the majority of phenotype differences, therefore the function of a gene can be inferred either from the linkage or association of genetic polymorphisms to differences in phenotypes (Anderson et al., 1993). Genetic variation allows the malaria parasite *P. falciparum* to overcome chemotherapeutic agents, vaccines and vector control strategies and remain a leading cause of global morbidity and mortality. Extensive sequencing of 16 geographically diverse parasites identified 46,937 SNPs, demonstrating rich diversity among *P. falciparum*

parasites with a strong correlation with gene function. Figure.26 represents an initial map of genetic diversity in *P. falciparum*. It demonstrate the potential utility in identifying genes subject to recent natural selection and in understanding the population genetics of this parasite (Volkman *et al.*, 2006).

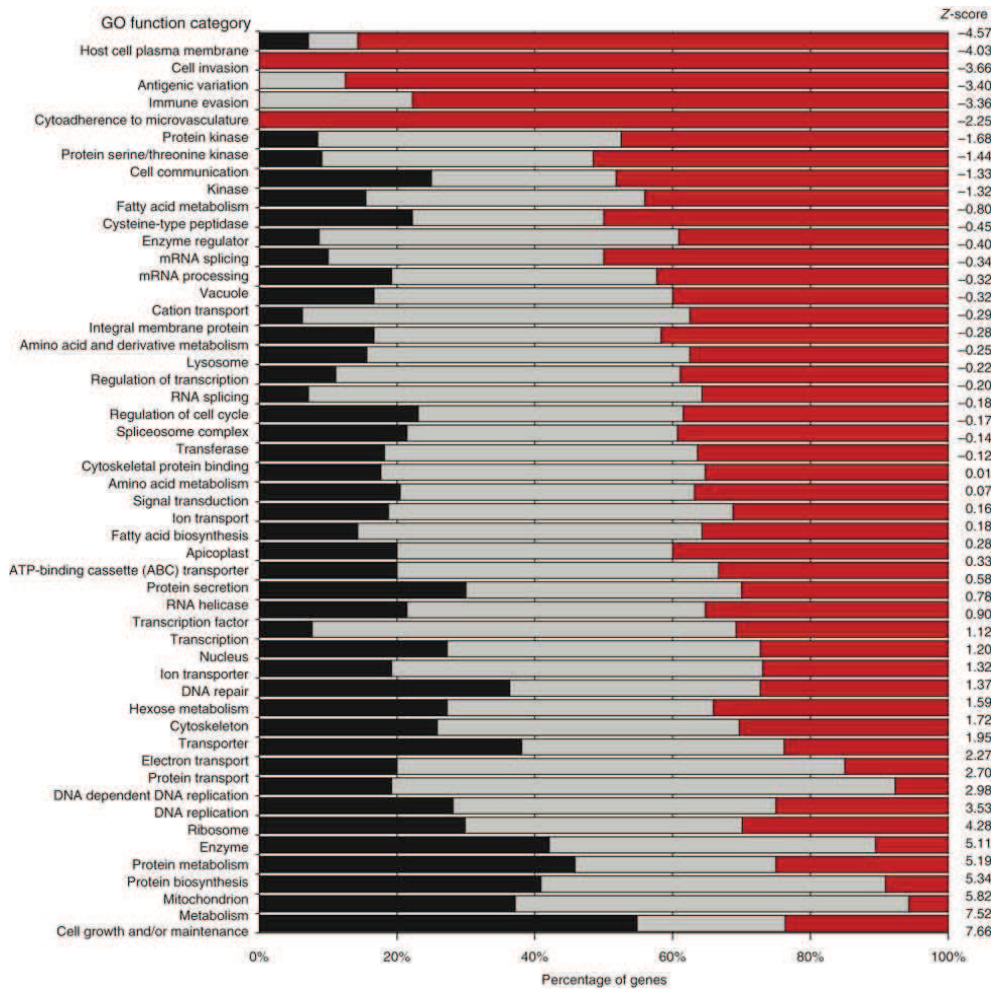


Figure 26: Genetic diversity within Gene Ontology (GO) classified on functional categories. Red colour represents high diversity of genes within a functional class, grey is intermediate and black is low or neglected diversity. The majority of genes in GO categories for molecules found at the cell membrane have high levels of nucleotide diversity, whereas most of the genes classified into GO categories for functionally conserved molecules lack nucleotide diversity (Courtesy, (Volkman *et al.*, 2006)).

With the advancement in multiple technological advances, particularly development of high-throughput genotyping, the genetic markers used for mapping purposes in *P. falciparum* have shifted from the microsatellite (MS) to single nucleotide polymorphism

(SNPs). Currently, approximately 1.8 million SNPs have been identified from 18 full or partially sequenced *P. falciparum* strains.

In addition to the resequencing approach, high-density tiling arrays have also been developed to study gene expression and genome diversity in malaria parasites (*Kidgell et al.*, 2006; *Jiang et al.*, 2008). Approximately 20,000 single-feature polymorphisms (SFPs) from 14 field isolates and laboratory lines were identified using an Affymetrix array containing 2.9 million oligonucleotide probes (*Kidgell et al.*, 2006; *Jiang et al.*, 2008). A similar study using a higher-density array (PFSANGER array) containing 2.5 million probes also detected more than 40,000 SFPs from five *P. falciparum* isolates (*Jiang et al.*, 2008). Moreover, high-throughput SNP typing arrays have been developed for studying parasite population and genetic mapping.

4.2.2 Epigenetics and epigenomics of *P. falciparum*

Epigenetic mechanisms are one of the major factors that determines the dynamics of gene expression in the human malaria parasite, *P. falciparum*. Recently, it was also shown that epigenetic factors affect clonally variant transcription in *P. falciparum* (*Rovira-Graells et al.*, 2012) likely via switching between hetero and euchromatic structures at several genetic loci that mainly encode factors involved in host-parasite interactions. A total of 44 different post-translational covalent modifications on *P. falciparum* histones including acetylations and methylations have been recently identified (*Trelle et al.*, 2009). There are insights from temporal relationship between post-translational modifications and their effect on global transcriptional regulation associated with the complex intra developmental cycle (*Gupta et al.*, 2013).

Epigenomics of *P. falciparum* focus on genome-wide distribution of various euchromatic or heterochromatic histone marks. (*Lopez-Rubio et al.*, 2009) used high-resolution ChIP-on-chip to show that H3K9me3, a silencing mark. It has an atypical distribution in the *P. falciparum* genome. They also found that H3K9me3 is indeed confined within the subtelomeric and limited chromosome internal regions that are closely associated with genes involved in antigenic variation.

ChIP-on-chip profiling of histones H3K4me3, H3K9me3 and H3K9ac confirmed that heterochromatin is restricted to the regions of the genome which contains the variant surface antigen families in *P. falciparum* (Salcedo-Amaya *et al.*, 2009). Colocalization of the heterochromatin protein 1 to H3K9me3, along with their association with regions of the genome that code for *Plasmodium* virulence factors was also discovered (Flueck *et al.*, 2009). Global histone mass spectrometry analysis also confirmed the prevalence of active acetylated histone marks compared with inhibitory methylated ones (Trelle *et al.*, 2009).

All together, these results suggest an atypical euchromatin or heterochromatin structure in the malaria parasite; active chromatin is prevalent genome-wide, whereas silencing marks are less frequent although they seem to play a significant role in transcriptional control of genes involved in phenotypic variation and pathogenesis.

4.2.3 Comparative genomics of *P. falciparum* isolates

Comparative genetics has also been important in locating genetic regulatory elements, particularly the apicomplexan AP2 (ApiAP2), in the *P. falciparum* genome (Balaji *et al.*, 2005; De Silva *et al.*, 2008). These discoveries have drastically changed the landscape of transcriptional regulation in *P. falciparum*. More than 20 ApiAP2 genes have been identified on different chromosomes, all of which were previously annotated as hypothetical proteins (Aurrecoechea *et al.*, 2009). Detailed investigation of two members of this family, PF14_0063 and PFF0200c, suggests an essential role in regulating parasite development (De Silva *et al.*, 2008). These data, combined with large catalogs of potential cis-acting sequences obtained from *in silico* discovery of transcription regulatory elements (Young *et al.*, 2008), have enhanced the understanding of transcriptional regulation in *P. falciparum*.

Comparative genomics has opened doors for other newly emerging fields to secretome and epigenome research in *P. falciparum*. Through close examination of known exported proteins in *P. falciparum*, conserved motifs termed *Plasmodium* export element (PEXEL) and vacuolar transport signal (VTS) have been identified from the

parasite genome (Hiller *et al.*, 2004; Marti *et al.*, 2004). These elements are necessary for export of hundreds of proteins from the parasites that serve to remodel the host erythrocyte (Marti *et al.*, 2004; Maier *et al.*, 2008; van Ooij *et al.*, 2008). The role of these unique modifications on the infected erythrocyte has already been examined by genetic knockout and functional screens (Maier *et al.*, 2008). Molecules with secretion signals might be evaluated for antivirulence targets, as some of these genes are important in knob formation or involved in the increased rigidity of the infected erythrocytes (Maier *et al.*, 2008). A central portal through which most or all of these exported proteins are transported through the erythrocyte has been recently characterized (de Koning-Ward *et al.*, 2009). Further investigations into the functions of these exported proteins are needed to gain additional insight into the *P. falciparum* secretome.

4.2.4 Transcriptomics

Gene expression could be measured by several methods. One such method is microarray-based technology. The large-scale analyses of *P. falciparum* transcripts led to the discovery of expressed genes, their functional association with the various stages of the parasite life cycle and their involvement in particular biological processes with a high degree of accuracy (Le Roch *et al.*, 2003; Llinas *et al.*, 2006; Bozdech *et al.*, 2008). More recent sequencing-based studies such as RNA-seq confirmed these initial microarray experiments and showed promising results on the prediction of new splicing events.

Several findings from recent transcriptional (RNA-seq) analysis

- a) Identification of new open reading frames with their untranslated flanking regions (Dimon *et al.*, 2010).
- b) Moreover, transcriptome analyses in *P. falciparum* field isolates identified previously unknown factors involved in pathogenesis and immune evasion (Siau *et al.*, 2007; Mackinnon *et al.*, 2009; Petter *et al.*, 2008).
- c) Analyses of transcription profiles of variant surface antigens identified patterns

List of transcript count during the Intra-developement cycle (IDC) of *P. falciparum*

Stages in <i>P. falciparum</i>	Transcripts counts <i>(Bozdech Z and Leroch KG)</i>
Late Schizont to Ring	300
Ring Trophozoites	950
Trophozoites to early-Schizont	1050
Mid late Schizonts	550

Table 5: Transcript counts in during development stage of *P. falciparum*

that are specific to the parasite sexual stages and could be relevant for new vaccine interventions (*Petter et al., 2008; Wang et al., 2010*)

- d) In addition to mRNA-related transcriptomics, noncoding protein RNA (ncpRNA) transcriptome has been analysed (*Raabe et al., 2010*). In eukaryotes, structural ncpRNA is known to participate in the regulation of diverse biochemical pathways, e.g. transcription, translation, epigenetic regulations, cell differentiation and proliferation. In *P. falciparum*, 604 putative ncpRNAs were detected (*Li et al., 2008a; Mourier et al., 2008*) and were showed to form a complex regulatory network.
- e) All together, these latest analyses suggest that *P. falciparum* ncpRNAs may play a critical role in determining antigenic variation and virulence mechanisms (*Raabe et al., 2010*).

4.2.5 Proteomics

Functional annotations of the genes could be proposed by proteomic profiling, previous proteomics (*Florens et al., 2002; Lasonder et al., 2002*) and interactomics (*LaCount et al., 2005*) studies have confirmed these. A complete understanding of their function and regulation will therefore be critical to disrupt one of the most pathological effects of *Plasmodium* infections.

Important findings from proteomic analysis : –

- a) Proteomics analyses surveyed stage-specific proteins and investigated them as potential drug targets. Parasite surface proteins (parasite proteins that are exported to the surface of the infected red blood cells) also represent new potential antigens for rational vaccine development (*Florens et al.*, 2002; *Lasonder et al.*, 2002; *Le Roch et al.*, 2004; *Sam-Yellowe et al.*, 2004).
- b) In order to investigate the role of post-transcriptional controls in the regulation of protein expression for the malaria parasite, *P. falciparum*, (*Le Roch et al.*, 2004) have compared mRNA transcript and protein abundance levels for seven different stages of the parasite life cycle. A moderately high positive relationship between mRNA and protein abundance was observed for these stages; the most common discrepancy was a delay between mRNA and protein accumulation. Potentially post-transcriptionally regulated genes are identified, and families of functionally related genes were observed to share similar patterns of mRNA and protein accumulation.
- c) (*Foth et al.*, 2011) studied the dynamics of protein profiles in *P. falciparum* and human host cells. From their study it was found that mRNA and protein abundance profiles exhibit a cyclic pattern with one peak during the intra-developmental cycle (IDC). The presence of functionally related proteins are highly correlated. Again, the abundance of most parasite proteins peaks significantly later (median 11 h) than the corresponding transcripts and often decreases slowly in the second half of the IDC. Computational modeling indicates that the considerable and varied incongruence between transcript and protein abundance may largely be caused by the dynamics of translation and protein degradation. Furthermore, they confirmed the presence of five human proteins with a potential role in antioxidant defense within the parasites.
- d) Together, genomics, cell biology and proteomics studies identified a conserved protein export motif, the *PEXEL* motif, which has been reported in as many as 400 proteins. Most of these proteins are expressed during the erythrocytic stages.

List of Peptide spectral count during the Intra-developement cycle (IDC) of *P. falciparum*

Stages in <i>P. falciparum</i>	Transcripts counts <i>(Lasonder E and Florens S)</i>
Sporozoites	1049
Merozoites	839
Trophozoites	1036
Gametocytes	1147

Table 6: Peptide spectral count during the Intra-developement cycle (IDC) of *P. falciparum*

Comparative proteomics throughout the lifecycle of *P. falciparum* reveals that the sporozoite proteome appeared markedly different from the other stages. Almost half (49%) of the sporozoite proteins were unique to this stage, which shared an average of 25% of its proteins with any other stage. On the other hand, trophozoites, merozoites and gametocytes had between 20% and 33% unique proteins, and they shared between 39% and 56% of their proteins. Consequently, only 152 proteins (6%) were common to all four stages. Those common proteins were mostly housekeeping proteins such as ribosomal proteins, transcription factors, histones and cytoskeletal proteins (*Florens et al.*, 2002).

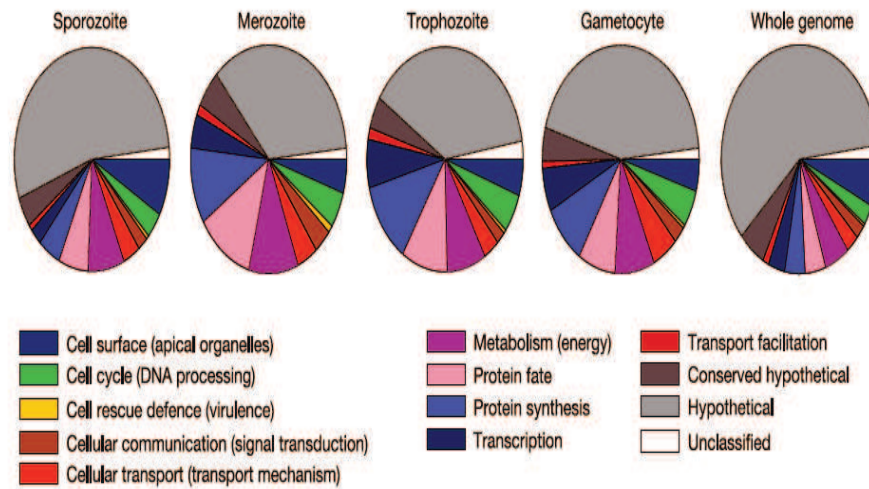


Figure 27: Functional profiles of the expressed proteins. Proteins identified in each stage are plotted as a function of its functional class (Florens et al., 2002).

4.2.6 Regulation of gene expression in *P. falciparum*

Gene expression is a process by which information from a gene is used in the synthesis of functional gene product. It is mainly comprised of two stage process, transcription and translation. These two process involve series of intermediate steps. Gene expression must be strictly regulated, this enable the cell to produce proteins/enzymes that drives the cellular metabolism. Cell exerts fine control of gene expression at transcriptional (Spellman et al., 1998) (in yeast), (Mamoun et al., 2001) (in *Plasmodium*) and translational level (Ghazalpour et al., 2011; Ghaemmaghami et al., 2003) (in yeast)).

Genome-wide transcriptomic and proteomic approaches have been extensively utilized to identify regulatory elements that control gene expression in the parasite genome. The mechanism of gene expression variation has been linked not only to DNA sequence alterations but also to epigenetic modifications and other mechanism in *P. falciparum* (Deitsch et al., 2009). The most extensively studied gene family is the *var* gene family, which encodes hyper-variable surface antigens and displays mutually exclusive expression in infected red blood cells (Su et al., 1995). Switching of gene expression states from active to silent or vice versa may be associated with chromatin modifications

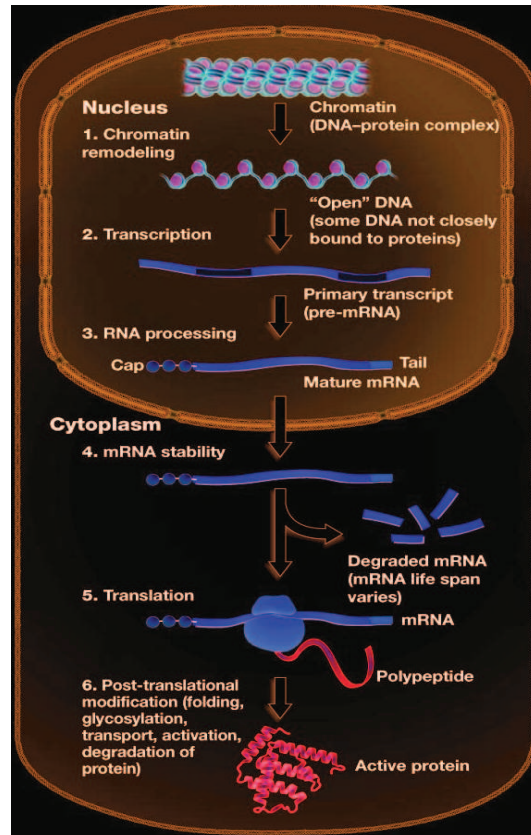


Figure 28: Schematic overview of process of translation in *Plasmodium*

(*Deitsch et al.*, 2009), locations of active genes in the nucleus (*Duraisingh et al.*, 2005) and presence of regulatory introns (*Deitsch et al.*, 2009).

4.2.6.1 Mechanism of transcriptional and post-transcriptional regulation

The core transcriptional machinery that drives RNA polymerase II dependent transcription (*Coulson et al.*, 2004) and 27 Apicomplexan AP2 (ApiAP2) plant-related transcription factors (*Balaji et al.*, 2005; *Painter et al.*, 2007) have been identified as major regulators of parasite gene expression. All together, the proteins involved in the transcriptional machinery represents less than 2% of the total genome. Considering the *P. falciparum* genome size, twice this amount is required for a classical transcription factor-mediated model of gene regulation (*Coulson et al.*, 2004; *Templeton*, 2009; *Aravind et al.*, 2003). Thus, either more atypical and elusive regulators remain to be discovered, or gene regulation in *Plasmodium* is not so classically based on the co-

ordinated action (Mamoun *et al.*, 2001; Bachmann *et al.*, 2011) of specific positive or negative regulators only.

The initial characterization of the ApiAP2 transcription factor family was a major step forward understanding key regulators in *Plasmodium* (Campbell *et al.*, 2010). However, their exact role in the parasite biology is still obscure. Furthermore, recent studies have started to underline that the malaria parasite may have adapted and optimized its mechanisms of transcriptional regulation for its lifestyle. Indeed, in contrast to what is observed in other eukaryotes, environmental perturbations and small molecule inhibitors do not cause specific transcriptional changes in *P. falciparum*, as revealed by genome-wide analyses of parasite expression profiles in response to stress (Ganesan *et al.*, 2008; Le Roch *et al.*, 2008).

The concept of transcriptional rigidity has been proposed and characterized in *Plasmodium* (Ganesan *et al.*, 2008). Parasites subjected to chemical or environmental stresses do not specifically compensate for the stress-targeted pathways at the transcriptional level, they exhibit a strong cell cycle arrest and an induction of genes involved in general (nonspecific) stress responses and sexual differentiation. Taken together, these studies highlight an unusual method of transcriptional regulation with a limited capacity for positive or negative feedback mechanisms. Correlation analyses of mRNA vs. protein profiles showed significant varying time shifts between transcript and protein levels. An extensive post-transcriptional mechanisms of gene regulation may have important roles during parasite development (Le Roch *et al.*, 2004, 2008; Foth *et al.*, 2003). Characterization of protein complexes involved in translational repression (Maier *et al.*, 2008) and whole-genome analysis of mRNA decay rates strongly supports the idea that post-transcriptional regulation may be an important mechanism for gene regulation in *P. falciparum* (Shock *et al.*, 2007).

4.2.6.2 Mechanism of translational and post-translational regulation

Translation refers to the process of synthesis of protein from mRNA, and involves three major steps—initiation, elongation and termination. This is the last step of gene expression.

The mechanism of translational regulation in *Plasmodium* is highly dissimilar to the human host (*Marintchev and Wagner, 2004*). In *P. falciparum*, several studies have been carried out to understand the mechanisms of translational regulation but very few is known till date. A review by (*Jackson et al., 2011*) provides a fairly comprehensive view of translation in the parasite. The parasite possesses three distinct intracellular compartments believed to be the hub of functional protein-translation machinery, namely, the apicoplast, mitochondrion and cytosol. The former are organelles thought to be acquired by endosymbiosis events, and they are nestled in the cytosol (*Ralph et al., 2004*). These organelles are the hub for prokaryotic mRNA translation, whereas the cytosol possesses the eukaryotic counterparts of the same (*Foth et al., 2003; Van Dooren et al., 2006*). The translation machinery in the parasite comprises tRNAs, tRNA synthetases, tRNA ligases and translation factors, which together control the initiation, elongation and termination steps.

Interesting facts about translation in *P. falciparum* : –

- Only nuclear and apicoplast genomes code for tRNAs and translation factors (*Chaubey et al., 2005*). Furthermore, *P. falciparum* has only 46 nuclear and 35 apicoplast tRNA genes, and only one gene copy per tRNA isoacceptor, which makes it the poorer known organism in terms of total tRNA gene copy numbers (*Jackson et al., 2011*). This peculiarity should lead to important slow-down of translation rate for the most used codons.
- Another interesting feature of the parasite is its translation machinery, which is very efficient to translate the AT-rich genome. *P. falciparum* mRNA have longer untranslated regions (UTRs) than other eukaryotes, with an average length of 350 bases (*Watanabe et al., 2002*). Due to these two exceptional features, the frequency of AUG in the 5' UTRs of *P. falciparum* mRNAs is 6 per 500 bases. Comparatively, in most eukaryotes, half of the mRNAs have no AUG in the 5' UTRs. Thus, in the parasite, the choice of a translation initiation site (TIS) by the ribosomal machinery is a critical step in translation.

Translation factors

Translation factors required for protein synthesis in the apicoplast and mitochondrion have been reported in *P. falciparum*. These translation factors include initiation, elongation and termination factors which all are coded by the nuclear genome, with elongation factor Tu (EF-Tu) being the only exception, as it is coded by the apicoplast genome (*Chaubey et al.*, 2005). The cytosolic factors that have been cloned from *P. falciparum* cDNA include eIF4E, eIF4A, eIF4F and poly-A binding protein PABP (*Tuteja and Pradhan*, 2010). Unlike the nuclear genome, the apicoplast genome is equipped with genes coding only for rRNAs, tRNAs, ribosomal proteins and the elongation factor EF-Tu, while the nuclear encoded tRNA synthetases and other essential factors required for translation are imported (*Bhatt et al.*, 2009; *Istvan and Goldberg*, 2005). The identification of polysomes carrying plastid-specific mRNA and rRNAs, and the confirmed localization of plastid-origin EF-Tu to the apicoplast (*Chaubey et al.*, 2005) support the hypothesis of a translationally active apicoplast. Another site of translation is the mitochondrion, which has the smallest genome known yet (6 kb) that encodes only three proteins - cytochrome c oxidase subunits I, III, cytochrome b92 and some fragmented rRNA genes (*Feagin*, 1992).

Translation inhibitors lead to delayed death. Treatment with a series of prokaryotic translation inhibitors, such as clindamycin and tetracyclines, highlighted a very unique trend. This phenomenon, now universally referred to as 'delayed death' (*Divo et al.*, 1985b).

4.2.7 Metabolomics

Metabolomics is the study of the entire repertoire of metabolites, i.e. small molecules such as amino acids, sugars and fatty acids that are known to perform critical functions in various biological processes.

Plasmodium is an obligate intracellular protozoan parasite. For proliferation, differentiation and survival, it relies on its own protein-encoding genes, as well as its host cells for nutrient sources. Nutrients and subsequent metabolites are required by

the parasites to support their high rate of growth and replication, particularly in the intra-erythrocytic stages of the parasite that are responsible for the clinical symptoms of the disease. Advances in mass spectrometry have improved the analysis of endogenous metabolites and enabled a global approach to identify the parasite's metabolites by metabolomic analyses. Metabolomics along with genomic, transcriptomic and proteomic allows the identification of novel metabolites, original pathways and networks of regulatory interactions within the parasite, and between the parasite and its hosts.

Functional annotation of genes by metabolic profiling have been leveraging biochemical and metabolomics strategies (*Lakshmanan et al.*, 2011). It has already uncovered important biological insights with possible implications in terms of adaptation, evolution and host-pathogen interactions (*Lian et al.*, 2009; *Olszewski et al.*, 2009; *Teng et al.*, 2009).

Some metabolites like phospholipids (PL) constitute a major class of lipids in *P. falciparum*. These PLs are important for membrane biogenesis during parasite proliferation. Phospholipid biogenesis and its role in *Plasmodium* is elaborated with a dedicated chapter in the later part of the thesis.

Other comprise of polyamines that makes upto 14% of the total metabolome of isolated parasites (*Teng et al.*, 2009). A study using ¹³C-glucose-supplemented media enabled the detection of all the by-products of glucose metabolism in *P. falciparum* (*Lian et al.*, 2009). Carbon-13 NMR was used to confirm the generation of the expected end-products of glucose metabolism including lactate, pyruvate, and alanine (*Lian et al.*, 2009). Interestingly, the study also found that parasites generated glycerol and glycerol-3-phosphate from glucose, a metabolic conversion that had previously not been known to exist. These metabolites were thought to be produced due to the operation of a glycerol-3-phosphate shuttle in the parasite in response to growth under limited O₂ and elevated CO₂ (*Lian et al.*, 2009). HPLC or GC-MS/MS and LC-MS/MS could not detect glycerol because of its poor ionization potential (*Lian et al.*, 2009). A combinatorial approach is critical to achieving the most comprehensive analysis of small molecules in a biological sample. Tracking the metabolism of ¹³C-labeled precursors using LC-MS led to the discovery that the malaria parasite employs the TCA-cycle

in an unconventional manner with important biological implications (Olszewski *et al.*, 2010). Glutamate and glutamine were the major metabolites that entered the parasites tricarboxylic acid cycle to generate acetyl-CoA moieties for histone acetylation, whereas glucosederived acetyl-CoA was used to acetylate amino sugars (Olszewski *et al.*, 2010). For an in-depth account of carbon metabolism in malaria, we refer the reader to a recent comprehensive review (Olszewski *et al.*, 2010).

4.2.8 Fluxomics

Fluxomics is largely unexplored in malaria research, while for other experimentally amenable species it is well established and rapidly developing (Teng *et al.*, 2009). The fluxomics study that took place in *Plasmodium* includes, a) assessment of influx of glucose (Mehta *et al.*, 2006), b) isoleucine (Martin and Kirk, 2007), c) inorganic phosphate (Saliba *et al.*, 2006). The other studies includes, metabolic profiling by Mass spectroscopy with infected and uninfected parasites (Olszewski *et al.*, 2009). In this study they have monitored the relative changes of 90 molecules over a cycle of 48 hours (Olszewski *et al.*, 2009).

4.3 Methodology for identification, quantification and integration of OMICS

With the avalanches of High-throughput data, it is necessary to handle, process and relate data effectively to extract useful information. Semi-quantitative studies are well developed for identification of cellular species, where as quantitative studies are still in its stage of infancy. Quantitative omics studies (How much or many ?) are used to determine the amount or change of expression of target(s) (protein, transcript, metabolite, fluxes) in two or more samples. In quantitative studies, samples are obtained from healthy or disease patients sampled in different consecutive times. The targets are quantified by relative or absolute methods. Some of the methods that have been applied to quantify *Plasmodium* omics data are discussed below.

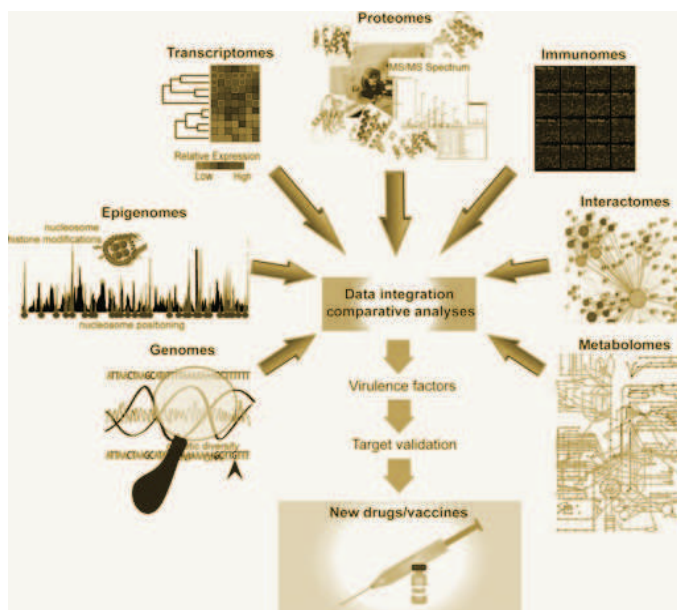


Figure 29: Schematic overview and the scope of identification, quantification and integration of *Plasmodium* 'OMICS'

4.3.1 Processing and quantification of transcripts or gene expression.

There are different methodology to measure mRNA expressions or gene expression. Some of the methods are, a). DNA-Microarray b). RNA-seq (Next-Generation sequencing) c). qPCR d). Chip-seq.

4.3.1.1 DNA-Microarray

One of the widely used method for studying transcriptional changes across a genome is DNA-microarray hybridization. DNA microarrays consist of nucleic acid, either amplified DNA or more recently synthesized oligonucleotides, printed onto a derivitized glass surface. The surface is either 96 or 384 well plates. The identity of the gene on the glass slide is determined from its plate well address and its location on the slide. Complementary DNA is synthesized from total or messenger RNA from two different biological samples (i. e. a drug-treated (test) sample and a control). Each sample is quoted with one of two fluorescent nucleotides (Cy3- or Cy5-dNTP (deoxynucleotide

triphosphate)) into the first strand cDNA synthesis. These two cDNAs (one control and one test sample) are so called differentially labelled sample. These samples are allowed to hybridize to the surface of the DNA microarray. After washing the slide, a scanning dual-channel confocal laser is used to measure the relative fluorescence intensities at each spot address, giving the relative amounts of each labelled cDNA and therefore the relative amounts of each initial RNA transcript from the two samples.

DNA microarrays created using either pre-existing EST or GST (glutathione S-transferase) libraries as templates for amplification, *de novo* gene-specific amplification by PCR or printed synthesized oligonucleotides have their relative advantages. *P. falciparum* DNA microarrays based on pre-existing libraries (Hayward *et al.*, 2000; Mamoun *et al.*, 2001) from oligomers (Bozdech *et al.*, 2003) chromosome-specific PCR products (Sacci Jr *et al.*, 2005) have been constructed.

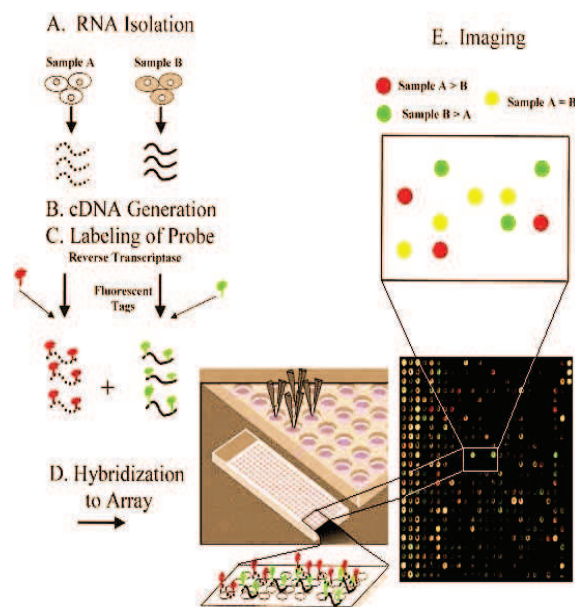


Figure 30: Illustration of DNA Microarray, a general protocol

Since only the blood stages of *P. falciparum* can be cultivated *in vitro*, this stage of parasite development has been the most amenable to study by DNA microarrays. These arrays are being used to study changes in gene expression that occur with *in vitro* cultivation, the effects of drugs on parasite growth *in vitro*, the mechanisms of drug action and resistance and others. In general, significant levels of change are

typically reported when one sample is over or under expressed by two-fold or more. A method of quantification of differential expression of DNA microarray could be found in *Appendix. B*

4.3.1.2 Next-Generation sequencing (NGS)

Recent advances in high-throughput sequencing present a new opportunity to deeply probe an organism's transcriptome. Illumina-based massively parallel sequencing to gain insight into the transcriptome of the human malaria parasite *P. falciparum*. The methodology of Next-Generation sequencing data processing and quantification is discussed below.

There are several of strata's of sequencing methods namely;

- a) **First-generation sequencing** (Or The Sanger sequencing): Sanger sequencing is limited in its ability to detect multiple parasite types in a mixed infection, because this method depends on reading major and minor peaks on a chromatogram to determine allele presence or absence in a sample. The proportion of these peaks may not correlate well with the actual proportion of parasite DNA in a sample, because incorporation of dye-labeled dideoxynucleotide can vary within a sample and be influenced by flanking sequence. Complete haplotypes for each unique parasite clone that is in a sample cannot be determined by Sanger sequencing. It is also impossible to resolve diversity with respect to repetitive DNA sequences in mixed infections using this sequencing method (*Gandhi et al.*, 2012). This method was used to sequence *P. falciparum* genome (*Gardner et al.*, 2002a).
- b) **Second-generation sequencing** (Or NextGeneration sequencing or NGS methods): After 30 years of dominance of first-generation, Sanger dideoxy sequencing, there is a boom of NGS methods since past 5 years. Unlike Sanger sequencing, NGS avoids the need for cloning and therefore bypasses associated biases. Three main NGS platforms have been commercialized over the past 5 years, i)The Roche 454 (Roche Life Sciences, Branford, CT, USA), ii) The Applied Biosystems SOLiD (Applied Biosystems , Carlsbad, CA, USA) , iii) Finally the Illumina (formally known as Solexa) Genome Analyzer and Hi-Seq platforms.

The Illumina sequencers are currently capable of producing up to 2 billion reads per run this value is continually increasing as a result of constant improvements of reagents and consumables with a recommended read length of 35-100 bp (<http://www.illumina.com>). This technique is by far the most successful NGS method to sequence the *P. falciparum* genome.

- c) **Third generation sequencing (TGS methods)**: Going further, third-generation sequencing (TGS) technologies propose to use single molecules as direct templates for sequencing (techniques so far under development at Helicos Biosciences and Pacific Biosciences). These TGS technologies should simplify the sample preparation procedure, avoid the bias introduced by DNA amplification and library preparation and be even more affordable than their predecessors. Nevertheless, the power of high-throughput sequencing also represents one of the major pitfalls for the analysts.

RNA Sequencing or RNA-seq

RNA-seq is also known as Whole Transcriptome Shotgun Sequencing (WTSS). It is a technology that utilizes the capabilities of next-generation sequencing to reveal a snapshot of RNA presence and quantity from a genome at a given moment in time (*Chu and Corey, 2012*). The NGS using RNA-seq is used to identify DNA transcripts (mRNA) in a cell, providing the ability to look at alternative gene spliced transcripts, post-transcriptional changes, gene fusion, mutations/SNPs and changes in gene expression (*Maher et al., 2009*). In addition to mRNA transcripts, RNA-Seq can look at different populations of RNA to include total RNA, small RNA (such as miRNA), tRNA. RNA-Seq can also be used to determine exon/intron boundaries and verify or amend previously annotated 5' and 3' gene boundaries. Prior to NGS, transcriptomics and gene expression studies were previously done with expression microarrays, which contain thousands of DNA sequences that probe for a match in the target sequence, making available a profile of all transcripts being expressed. This was later done with Serial Analysis of Gene Expression (SAGE).

List of post infection RNA-seq evidences in *P. falciparum* is given in the table below :-

Evidences	Author (Source: PlasmoDB)
Time series data	Stunnenberg and group
IE Cycle	Newbold et al. , Linas et al.
7 stages	Su et al. ,
Pregnant woman and children	Duffy et al.
Splicing analysis	K. Sober et al. , Derisi et al.

Table 7: RNAseq evidences in *P. falciparum*, source:PlasmoDB

Polysome-seq

Definition of Polysome :- mRNA strand bound by 2 or more ribosome. This is a sign of active translation.

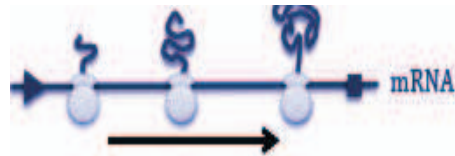


Figure 31: Translating ribosome bound mRNA

Polysome-seq is a technique that uses messenger RNA (mRNA) to determine what proteins are being translated. It produces a global snapshot of all the active ribosomes in a cell at a particular moment. Consequently, this enables to identify the location of translation start sites, their distribution, and the speed of the translating ribosomes (Ingolia et al., 2012; Weiss and Atkins, 2011).

Ribosomal profiling - a generalized protocol:

Ribosome profiling was formed from the old discovery that the mRNA within a ribosome can be isolated through the use of nucleases that degrade unprotected mRNA regions. This technique analyzes the ratio of multiple specific mRNA to proteins being synthesized, to provide insight into global gene expression. Prior to its development, efforts to measure this ratio included microarray analysis on the RNA isolated from polysomes, as well as translational profiling through the affinity purification of epitope

tagged ribosomes. However, neither of these techniques provides the positional and quantitative information of ribosome profiling (*Ingolia et al.*, 2012; *Weiss and Atkins*, 2011).

The mRNA bound ribosomal complexes are immobilized (commonly with cycloheximide but other chemicals can be employed, isolated using Trizol (*LeRoch et al.*, unpublished) and generate cross-linking using formaldehyde. Infected cells are lysed and mRNA-ribosome (Polysome) complexes are isolated using sucrose gradient (15-16%) density by centrifugation. The complex is subjected to PCIA purifications. Using nucleases, all of the RNA not directly bound to the ribosome are cut away. Further purification by phenol/chloroform are undertaken to remove proteins. Preparation of library are done by reverse transcription (using reverse transcriptase) where cDNA strand are sequenced.

The reads (strands) from the library are made to compare with genomic sequence to determine translational profile (*Ingolia et al.*, 2012). There are different methods that maps the single/paired-end reads to a reference genome. Some of these are Tophat2 (*Kim et al.*, 2013), SSAHA2 (*Ning et al.*, 2001), MAQ (*Li et al.*, 2008b), BWA (*Li et al.*, 2009) and ELAND (<http://www.illumina.com/>).

Quantification of RNA-seq and Polysome-seq data:-

There are many ways to estimate the relative abundances of the transcripts from RNA-seq and Polysome-seq data. One of such is discussed below.

In paired-end RNA-Seq experiments, fragments are sequenced from both ends, providing two reads for each fragment. To estimate isoform-level abundances, one must assign fragments to individual transcripts, which may be difficult because a read may align to multiple isoforms of the same gene. Cufflinks (*Trapnell et al.*, 2012) uses a statistical model of paired-end sequencing experiments to derive a likelihood for the abundances of a set of transcripts given a set of fragments. This likelihood function can be shown to have a unique maximum, which Cufflinks finds using a numerical optimization algorithm. The program then multiplies these probabilities to compute

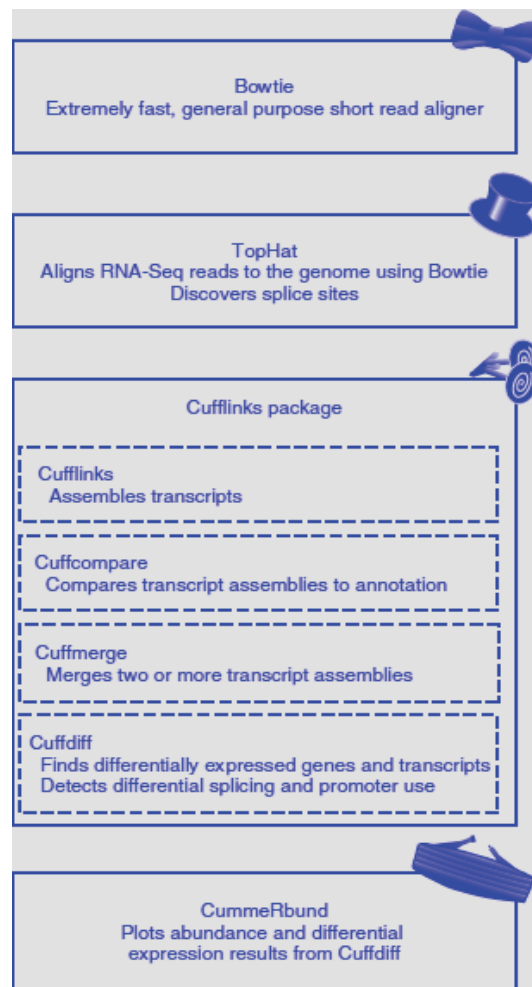


Figure 32: Step by step flow of quantification of NGS data demonstrated by (Trapnell et al., 2012)

the overall likelihood that one would observe the fragments in the experiment, given the proposed abundances on the transcripts. Because Cufflinks statistical model is linear, the likelihood function has a unique maximum value, and Cufflinks finds it with a numerical optimization algorithm. Using this statistical method, Cufflinks estimates the abundances of the isoforms present in the sample, either using a known 'reference' annotation, or after an ab-initio assembly of the transcripts using only the reference genome. FPKM (Trapnell et al., 2010, 2012) that denotes the Fragments (pair end reads)-per-kilobase-per-million exon mapped is the measure of quantification of transcript expression. Similarly, RPKM (Mortazavi et al., 2008) could be used as another measure when single end reads are used to build the sequencing library. FPKM could be calculated for each assembled transcripts of the sample. Again, each gene could

have several transcripts. In order to obtain the gene expression, the FPKM's of the corresponding transcripts/mRNA of a gene could be averaged or median value could be considered as estimate for gene expression. The dormant genes i. e the gene with FPKM value equals to zero are discarded from the analysis.

Microarray Vs RNA-seq in *P. falciparum*

(*Otto et al.*, 2010) has generated sequencing-based transcriptome data during the IDC, these data were compare and validated with the sequencing results with microarray data generated in parallel using the same RNA samples. Previous studies have found variable correlations when measuring gene expression with different technologies. (*Bloom et al.*, 2009), suggesting that both methods have their biases when compared with quantitative PCR. When plotted according to the phase of gene expression, as previously determined by (*Llinas et al.*, 2006), the well-established cascade of gene expression were reproduced.

4.3.1.3 qPCR

Quantitative polymerase chain reaction (qPCR), also called real-time polymerase chain reaction, is a laboratory technique of molecular biology based on the polymerase chain reaction (PCR). This is used to amplify and simultaneously quantify a targeted DNA molecule. For one or more specific sequences in a DNA sample, quantitative PCR enables both detection and quantification. The quantity can be either an absolute number of copies or a relative amount when normalized to DNA input or additional normalizing genes.

Quantification of gene expression by qPCR Quantitative PCR can be used to quantify nucleic acids by two common methods: absolute and relative quantification (*Dhanasekaran et al.*, 2010).

Absolute quantification gives the number of target DNA molecules by comparison with DNA standards using a calibration curve. It is therefore essential that the PCR of the sample and the standard have the same amplification efficiency.

Relative quantification is based on internal reference genes to determine fold-differences in expression of the target gene. The quantification is expressed as the change in expression levels of mRNA interpreted as complementary DNA (cDNA, generated by reverse transcription of mRNA). Relative quantification is easier to carry out as it does not require a calibration curve as the amount of the studied gene is compared to the amount of a control housekeeping gene.

As the units used to express the results of relative quantification are unimportant the results can be compared across a number of different RT-QPCR. The reason for using one or more housekeeping genes is to correct non-specific variation, such as the differences in the quantity and quality of RNA used, which can affect the efficiency of reverse transcription and therefore that of the whole PCR process. However, the most crucial aspect of the process is that the reference gene must be stable (*Brunner et al.*, 2004).

4.3.2 Processing and quantification of protein expression

Quantitative proteomics is used to obtain quantitative information about all proteins in a sample (*Ong and Mann, 2005; Bantscheff et al., 2007; Nikolov et al., 2012*). Other than providing lists of proteins identified in a certain sample. Quantitative proteomics yields information about differences between samples. For example, this approach can be used to compare samples from healthy and diseased patients. Quantitative proteomics mainly uses the technology of mass spectrometry (MS) to detect the changes of the protein.

Discovery Vs Targeted

Discovery proteomics optimizes protein identification by spending more time and effort per sample and reducing the number of samples analyzed. In contrast, targeted proteomics strategies limit the number of features that will be monitored and then optimize the chromatography, instrument tuning and acquisition methods to achieve

Evidences of post-infection quantitative proteomics in *P. falciparum*

Evidences	Author
Time series data	kluss and Bozdech et al. 2012.
Quatitaitve proteomics data	Nirmalan et al. , 2004
7 stages	Su et al. ,
Protomics on drug treatment	Judith et al, 2008
time-course profiling of parasite and host cell proteins	Forth et al. , 2011

Table 8: Evidences of post-infection quantitative proteomics in *P. falciparum*

the highest sensitivity and throughput for hundreds or thousands of samples.

Relative Vs Absolute

Mass spectrometry is not inherently quantitative because of differences in the ionization efficiency and/or detectability of the many peptides in a given sample, which has sparked the development of methods to determine relative and absolute abundance of proteins in samples (*Nikolov et al.*, 2012). The intensity of a peak in a mass spectrum is not a established indicator of the amount of the analyte in the sample, although differences in peak intensity of the same analyte between multiple samples accurately reflect relative differences in its abundance. One approach for relative quantitation is to separately analyze samples by MS and compare the spectra to determine peptide abundance in one sample relative to another, as in label-free quantitation strategies. An approach for relative quantitation that is more costly and time-consuming, though less sensitive to experimental bias than label-free quantitation, entails labeling the samples with stable isotope labels that allow the mass spectrometer to distinguish between identical proteins in separate samples. One type of label, isotopic tags, consist of stable isotopes incorporated into protein cross-linkers that causes a known mass shift of the labeled protein or peptide in the mass spectrum. Differentially labeled samples are combined and analyzed together, and the differences in the peak intensities of the isotope pairs accurately reflect difference in the abundance of the corresponding proteins.

Absolute proteomic quantitation using isotopic peptides entails spiking known concentrations of synthetic, heavy isotopologues of target peptides into an experimental sample and then performing LC-MS/MS. Absolute quantitation is performed using, Selected Reaction Monitoring (SRM). As with relative quantitation using isotopic labels, peptides of equal chemistry co-elute and are analyzed by MS simultaneously. Unlike relative quantitation, though, the abundance of the target peptide in the experimental sample is compared to that of the heavy peptide and back-calculated to the initial concentration of the standard using a pre-determined standard curve to yield the absolute quantitation of the target peptide. Some of the relative quantitation methods include: i) Isotope-coded affinity tags (ICAT), ii) Isobaric labeling, iii) Tandem mass tags (TMT), iv) Isobaric tags for relative and absolute quantitation (iTRAQ), v) Label-free quantification, vi) Metal-coded tags (MeCATs), vii) N-terminal labelling, viii) Stable isotope labeling with amino acids in cell culture (SILAC).

Transcriptome-Proteome of *P. falciparum*

Studies of the *P. falciparum* transcriptome have shown that the tightly controlled progression of the parasite through the intra-erythrocytic developmental cycle (IDC) that is accompanied by a continuous gene expression cascade in which most expressed genes exhibit a single transcriptional peak. Because the biochemical and cellular functions of most genes are mediated by the encoded proteins, understanding the relationship between mRNA and protein levels is crucial for inferring biological activity from transcriptional gene expression data. Although studies on other organisms show that less than 50% of protein abundance variation may be attributable to corresponding mRNA levels, the situation in *Plasmodium* is further complicated by the dynamic nature of the cyclic gene expression cascade.

Quantitative analyses of mRNA levels measured at nine time-points (life cycle (six asexual intraerythrocytic, merozoite, late gametocyte, and salivary gland sporozoite)) of *P. falciparum* using a short oligonucleotide array (*Le Roch et al.*, 2003), and semi-quantitative analyses of protein levels measured at seven stages (ring, trophozoite, schizont, merozoite, gametocyte, gamete, and salivary gland sporozoite) detected by

multidimensional protein identification technology (MudPIT) (Florens *et al.*, 2002; Friedman *et al.*, 2005) provide abundance profiles for thousands of parasite transcripts and proteins, with abundance correlated to specific stages and time points in the parasite life cycle.

(Le Roch *et al.*, 2004) have compared mRNA transcript and protein abundance levels for seven different stages of the parasite life cycle. A moderately high positive relationship between mRNA and protein abundance was observed for these stages; the most common discrepancy was a delay between mRNA and protein accumulation. Potentially post-transcriptionally regulated genes are identified, and families of functionally related genes were observed to share similar patterns of mRNA and protein accumulation. (Foth *et al.*, 2011) by comparing mRNA and protein abundance profiles for parasites (*P. falciparum*) during the IDC at 2 hour resolution based on oligonucleotide microarrays and two-dimensional differential gel electrophoresis protein gels. It was found that most proteins are represented by more than one isoform, presumably because of post-translational modifications. Like transcripts, most proteins exhibit cyclic abundance profiles with one peak during the IDC, whereas the presence of functionally related proteins is highly correlated. In contrast, the abundance of most parasite proteins peaks significantly later (median 11 h) than the corresponding transcripts and often decreases slowly in the second half of the IDC. Computational modeling indicates that the considerable and varied incongruence between transcript and protein abundance may largely be caused by the dynamics of translation and protein degradation.

4.3.3 Quantification and analysis of metabolic response.

Metabonomics is defined as "*the quantitative measurement of the dynamic multi-parametric metabolic response of living systems to pathophysiological stimuli or genetic modification*" (Nicholson *et al.*, 1999).

Gas chromatography, especially when interfaced with mass spectrometry (GC-MS), is one of the most widely used and powerful metabonomic quantitative methods. It

offers very high chromatographic resolution, but requires chemical derivatization for many biomolecules: only volatile chemicals can be analysed without derivatization. Compared to GC, HPLC has lower chromatographic resolution, but it does have the advantage that a much wider range of analytes can potentially be measured (*Gika HG et al. , 2007*). Capillary electrophoresis (CE) has a higher theoretical separation efficiency than HPLC, and is suitable for use with a wider range of metabolite classes than is GC. As for all electrophoretic techniques, it is most appropriate for charged analytes (*Soga T et al., 2003*).

Mass spectrometry (MS) is used to identify and to quantify metabolites after separation by GC, HPLC (LC-MS), or CE. GC-MS is the most 'natural' combination of the three, and was the first to be developed. In addition, mass spectral fingerprint libraries exist or can be developed that allow identification of a metabolite according to its fragmentation pattern. MS is both sensitive (although, particularly for HPLC-MS, sensitivity is more of an issue as it is affected by the charge on the metabolite, and can be subject to ion suppression artifacts) and can be very specific. There are also a number of studies which use MS as a stand-alone technology: the sample is infused directly into the mass spectrometer with no prior separation, and the MS serves to both separate and to detect metabolites. The target analysis follows the same protocol as described in proteomics section.

In *P. falciparum* the challenge was to extract the water soluble metabolites. The difficulty of this task results from the fact that metabolite pools in the host cell cytosol and parasite compartments are mixed during the metabolite extraction. To specifically profile parasite-specific metabolites, it is necessary to isolate the parasite from the host cell material. One example of parasite purification is saponin lysis. The obvious disadvantage of saponin lysis is that it subjects the parasite to non-physiological conditions for relatively long periods of time, which may result in alterations of metabolic pools, fluxes or labeling patterns. However, saponin lysis and other related techniques provide a powerful mechanism for differentiating between host and parasite metabolism and quantifying the flow of metabolites between various sub-cellular compartments. Another biological consideration is sample preparation protocol. The other is accurate

quantifications and reproducibility of results. (Olszewski and Llinás, 2013), proposed a method for extraction and quantification of water soluble metabolites in *P. falciparum* infected erythrocytes.

Nuclear magnetic resonance (NMR) spectroscopy is the only detection technique which does not rely on separation of the analytes, and the sample can thus be recovered for further analyses. All kinds of small molecule metabolites can be measured simultaneously - in this sense, NMR is close to being a universal detector. The main advantages of NMR are high analytical reproducibility and simplicity of sample preparation. Practically, however, it is relatively insensitive compared to mass spectrometry-based techniques (Griffin *et al.* , 2003). NMR spectroscopy was used to identify and quantify compounds in extracts prepared from mature trophozoite-stage *P. falciparum* parasites isolated by saponin-permeabilisation of the host erythrocyte (Teng *R et al.* , 2009). One dimensional (1) H-NMR spectroscopy and four two-dimensional NMR techniques were used to identify more than 50 metabolites.

Isotopic labeling (or isotopic labelling) is a technique used to track the passage of an isotope, or an atom with a variation, through a reaction, metabolic pathway, or cell. The reactant is 'labeled' by replacing specific atoms by their isotope. The reactant is then allowed to undergo the reaction. The position of the isotopes in the products is measured to determine the sequence the isotopic atom followed in the reaction or the cell's metabolic pathway. Radioisotopic labeling is a technique for tracking the passage of a sample of substance through a system. The substance is "labeled" by including radionuclides in its chemical composition. When these decay, their presence can be determined by detecting the radiation emitted by them. Radioisotopic labeling is a special case of isotopic labeling.

Different techniques are used to measure stable isotopes; MS and NMR has been used to measure difference between isotopomers in a stable isotope labelling. Isotope labelling techniques are used to understand glycerophospholipid metabolism in *P. knowlesi* and *P. falciparum* (Elabaddi *et al.* , 1998). A detail of the output of this method was elaborated in the chapter.3 of this thesis.

Data Analysis and Quantification

The data generated in metabolomics usually consist of measurements performed on subjects under various conditions. These measurements may be digitized spectra, or a list of metabolite levels. For mass spectrometry data, different softwares are available to identify molecules that vary in subject groups on the basis of mass and sometimes retention time depending on the experimental design. The first comprehensive software to analyze global mass spectrometry-based metabolomics datasets was developed by the Siuzdak laboratory at The Scripps Research Institute in 2006. This software, called XCMS (*Smith et al.*, 2006). Other popular metabolomics programs for mass spectral analysis are MZmine (*Katayama et al.*, 2013), MetAlign (*Lommen et al.*, 2009), MathDAMP (*Baran et al.*, 2006), which also compensate for retention time deviation during sample analysis. LCMStats is another R package for detailed analysis of liquid chromatography mass spectrometry (LCMS) data and is helpful in identification of co-eluting ions especially isotopologues from a complicated metabolic profile. After identification, the relative (fold change) or absolute abundances of the metabolite expression are estimated by the formulae described in above proteomics section.

4.3.4 Quantification of Fluxes in the Metabolic network.

Metabolic flux analysis (MFA) using stable isotope labeling is an important tool to figure out the metabolic pathways and reactions that occur within a cell. An isotopic label is fed to the cell, then the cell is allowed to grow utilizing the labeled feed. For stationary metabolic flux analysis the cell must reach a steady state (the isotopes entering and leaving the cell remain constant with time) or a quasi-steady state (steady state is reached for a given period of time) (*Wiechert et al.*, 2001). The isotope pattern of the output metabolite is determined. The output isotope pattern provides valuable information, which can be used to find the magnitude of flux, rate of conversion from reactants to products, through each reaction (*Lee et al.*, 2011). By measuring the isotopomer distribution of the differently labeled metabolites, the flux through each reaction can be determined (*Stephanopoulos et al.*, 1998).

MFA combines the data harvested from isotope labeling with the stoichiometry of each reaction, constraints, and an optimization procedure resolves the flux map. The irreversible reactions provide the thermodynamic constraints needed to find the fluxes. A matrix is constructed that contains the stoichiometry of the reactions. The intracellular fluxes are estimated by using an iterative method in which simulated fluxes are plugged into the stoichiometric model.

4.3.4.1 Modelling approaches to metabolism of *P. falciparum*

Annotation studies of the full genome lead to comprehensive, genome scale, reconstruction of metabolic networks of *P. falciparum*. Large metabolic networks were studied using graph theoretical methods and flux balance analysis.

Graph theoretical methods compute various indices such as centrality, betweenness, to identify important nodes such as chokepoints, whose elimination from the network critically affect connectivity. These important nodes are then proposed as potential drug targets. A few studies use this approach for *P. falciparum* (Fatumo et al., 2009; Yeh et al., 2004).

Flux balance analysis (FBA) is a mathematical method for predicting the distribution of fluxes within metabolic networks. FBA formalizes the functioning of a metabolic network in steady state conditions, as a problem in linear programming. First, the steady state constraints are expressed as a set of linear equations for the fluxes :

$$\mathbf{S} \cdot \mathbf{v} = 0 \quad (4.1)$$

where S is the stoichiometric matrix (defined in chapter.3) and \mathbf{v} is the vector of unsolved fluxes.

Supplementary constraints are imposed on the values of some fluxes. For instance, the fluxes of all irreversible reactions are positive :

$$v_i \geq 0, \quad i^{th} \text{ reaction irreversible.} \quad (4.2)$$

FBA uses as input the proportion of different metabolites in the total biomass production rate, needed for growth of the given organism. Mathematically, this can be

represented as a column vector \mathbf{B} whose entries represent experimentally measured, dry weight proportions of cellular components. Then, the scalar dot product $\mathbf{B}^T \cdot \mathbf{v}$ represents the biomass production rate. Linear programming is then used to calculate the distribution of steady state fluxes maximising the biomass production rate $\mathbf{B}^T \cdot \mathbf{v}$ under the constraints (4.1), (4.2).

The flux distribution can be recalculated after some reactions being taken off the network, therefore FBA can be used for *in silico* studies of enzyme knock outs and essentiality of the genes coding for these enzymes.

FBA is appealing as apparently does not involve parameters. However, this is not entirely true, because the predicted flux distribution depends on the parameters entering the definition of the biomass. Therefore, the accuracy of experimental measurements plays an essential role in the correct definition of the biomass function.

FBA analysis after metabolic network reconstruction of *P. falciparum* was performed by (Plata *et al.*, 2010). The compartmentalized metabolic network accounts for 1001 reactions and 616 metabolites. Enzyme-gene associations were established for 366 genes and 75% of all enzymatic reactions. Compared with other microbes, the *P. falciparum* metabolic network contains a relatively high number of essential genes, suggesting little redundancy of the parasite metabolism. The model was able to reproduce phenotypes of experimental gene knockout and drug inhibition assays with up to 90% accuracy. Using FBA of the reconstructed network, they have identified 40 enzymatic drug targets (i.e. *in silico* essential genes), with no or very low sequence identity to human proteins. Similar studies are reviewed in (Tymoshenko *et al.*, 2013).

4.3.5 Conclusion and future perspectives for functional genomics of *Plasmodium*

Functional genomics suffers from the lack of tools to analyze the malaria parasite genome. For instance, gene silencing using RNAi cannot be used in *Plasmodium* because the machinery does not exist in the parasite. Furthermore, gene knockout experiments are very limited because of the haploid nature of the genome and the

essentiality of most of the genes.

However, a promising alternative are the inducible knock-outs, also called knock-downs. These incomplete inactivations are generally not lethal and can be studied experimentally. The generation of knock-down parasites is a rapidly evolving field. The current methods are based on either transcriptional or post-transcriptional regulation. The first uses of small-molecule inducible promoters like the tetracycline system that has very recently been confirmed for the rodent malaria parasite *P. berghei* (Pino *et al.*, 2012) and is expected to be available soon for *P. falciparum*. On the other hand posttranscriptional regulation takes advantage of the generation of a fusion of the protein of interest to a so-called destabilisation domain that will lead to rapid degradation of the fusion protein by the parasites proteasome. However, proteolysis can be inhibited by addition of a ligand that by binding to the destabilisation domain leads to a conformational change that stabilises the protein preventing it from degradation (Armstrong and Goldberg, 2007; Muralidharan *et al.*, 2011).

The high-throughput (HTS) and depth of quantitative measurements produced by NGS and TGS technologies come at the cost of producing sophisticated algorithms and software tools capable of accurately examining millions to billions of reads. The data generated by these methods are complex, novel and abundant. The computational and statistical analysis of raw outputs are critical steps where incorrect normalization and processing can yield misleading conclusions. Integrating these data with mathematical models is an important, but insufficiently investigated avenue.

However, novel methods of quantitative analysis are constantly under development and testing. There is yet no consensus on which analytical approach is the most accurate, particularly for the *Plasmodium* genome. The avalanche of whole-genome data over the past few years generated an immense source of knowledge still requires maturing and processing. Considering all these facts with proper understanding and manipulations, Functional genomic approaches will certainly catalyze the transformation of this biological knowledge into viable therapeutic strategies.

Systems biology provides promising future perspectives for functional genomics of malaria. Up to now, data depositary banks and the Web-based databases such as

PLASMODB (<http://plasmodb.org/plasmo/>) have greatly facilitated the access, the comprehensive visualization and the analysis of large data sets. Gene predictions and annotations, new drug target identifications and discoveries of vaccine candidates all resulted from various genome-wide analyses. Indeed, a systemic view of the malaria parasite biology can only be achieved with the successful integration and accessibility of the data from various origins. An integration of transcriptomics, proteomics and metabolomics data are a powerful way to identify new metabolic pathways as well as genes that encode for specific enzymatic functions (*Friedman et al.*, 2005). Some progress has been done in modelling metabolic pathways of *Plasmodium* using annotated genome, metabolomics and transcriptomics (*Olszewski et al.*, 2009). Several directions remain to be investigated in order to get a clear picture of the transcriptome associated to its metabolome. In particular, one would like to have a dynamical view of the regulation of genes and metabolites that will help to formulate new molecular mechanisms. To this end, models based on differential equations, capturing the temporal regulation of the transcriptome, proteome and of the metabolome, will be valuable tools. Other questions are related to the still unknown mechanisms of the transcriptomic clock modulating gene expression during the intra-erythrocytic cycle of *Plasmodium* as well as of the translational and post-translational interactions responsible of various transitions along this cycle.

Chapter 5

Integrating transcriptome,
proteome and metabolome in blood
stages of *P falciparum*

The chapter discusses about the genes, proteins and metabolites regulations in *P. falciparum*. It includes a modelling strategy, that was deployed to understand translational control on the genes and their subsequent delays in producing proteins. An important event in the regulated expression of genes, namely the lift of translation repression, has been identified during ring-trophozoite transition of the *Plasmodial* cell. The later part of the chapter focus on the experimental approaches undergone to understand the gene and metabolite expression throughout the cell cycle of *P. falciparum*. Together, modelling (gene–protein expression) and experiment (gene–metabolite expression) helped to understand the state of the parasite’s cell throughout its life-cycle. We have assembled these findings together to understand the regulation of phospholipid pathways along the 48 hours cell cycle.

5.1 Introduction and background

Studies of the gene expression in *P. falciparum* emphasized the tightly controlled progression of the parasite through the intra-erythrocytic developmental cycle. The most salient manifestation of this control is the continuous gene expression cascade in which most expressed genes exhibit a single transcriptional peak (*Llinas et al.*, 2006).

The mechanisms and even the nature of the gene regulatory processes in *P. falciparum* are largely unknown. Several findings indicated translational regulation of genes during sexual stage development (in gametocytes) (*Mair et al.*, 2006; *Hall et al.*, 2005), of liver stage-specific transcripts in salivary gland sporozoites (*Zhang et al.*, 2010), and of genes involved in antigenic variation of the asexual blood forms of the parasites (the *var* gene family) (*Mok et al.*, 2008). In addition, the enzyme DHFR-TS has been shown to be up-regulated on a translational but not on a transcriptional level following drug treatment (*Nirmalan et al.*, 2004b). Other studies have evaluated the links between transcription and translation during the *Plasmodium* life cycle progression in more general terms by employing different types of large scale proteomics assays (*Hall et al.*, 2005; *Le Roch et al.*, 2004; *Nirmalan et al.*, 2004a; *Foth et al.*, 2008; *Gilson et al.*, 2006; *Florens et al.*, 2002; *Lasonder et al.*, 2002; *Gelhaus et al.*, 2005; *Briolant*

et al., 2010; *Tarun et al.*, 2008).

The results from all of these studies implied a complex relationship between transcripts and corresponding proteins in *Plasmodium*, with the prevailing trend being a time delay between the maximal concentrations of mRNA transcripts and the corresponding peaks of protein products. It was therefore proposed that *Plasmodium* cells employ an intricate system of post-transcriptional regulation that modulates the overall gene expression pattern associated with the parasite life cycle.

(*Foth et al.*, 2011) established quantitative relationship of transcript–proteins along the cell-cycle of *P.falciparum*. They found that most of the proteins are represented by more than one isoform, presumably because of transcriptional modifications by alternative splicing. Like transcripts, most proteins exhibit cyclic abundance profiles with one peak during the IDC, whereas the presence of functionally related proteins is highly correlated. In contrast, the abundance of most parasite proteins peaks significantly later (median 11 h) than the corresponding transcripts and often decreases slowly in the second half of the IDC.

The field of *P. falciparum* metabolomics is still in its infancy (*Le Roch et al.*, 2012), and most studies so far focus on relative quantitation by comparing cells in two different metabolic states, rather than performing absolute quantitation.

The first mass spectrometry-based metabolomic analysis of the parasite throughout its 48 hours intraerythrocytic developmental cycle was attempted by (*Olszewski et al.*, 2009). They have shown general modulation of metabolite levels by the parasite, with numerous metabolites varying in phase with the developmental cycle. The phase of the metabolites also differed from uninfected cells, irrespective of the developmental stage.

(*Duy et al.*, 2012) proposed a comprehensive method of identifying and quantifying metabolites of this intracellular parasite. These methods (shown in Figure.33) were based on liquid chromatography tandem mass spectrometry for reliable measurement of water-soluble metabolites involved in phospholipid biosynthesis, as well as several other metabolites that reflect the metabolic status of the parasite including amino acids, carboxylic acids, energy-related carbohydrates, and nucleotides. A total of 35

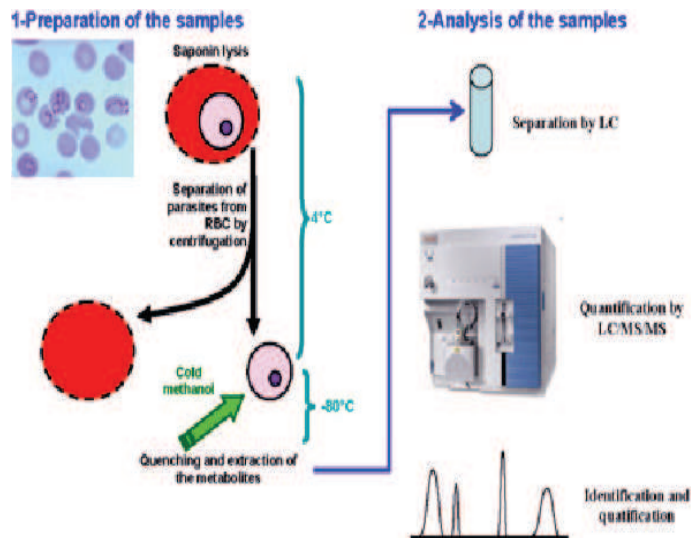


Figure 33: Illustration of identification and quantification of metabolites, Courtesy: (Duy et al., 2012)

compounds was quantified. These methods were validated and successfully applied to determine intracellular concentrations of metabolites from uninfected host RBCs and isolated *Plasmodium* parasites.

Combined studies were performed to establish relationship between transcripts and metabolites. It was found that these interactions are complex. In plants, intermediate steps between transcription and metabolite production such as post-transcriptional and translational modification (Carrari et al., 2006), regulation or buffering expression by metabolite levels (Gibon et al., 2006) have been found to seriously affect any simple relationship. Simpler interpretations such as direct coordination between metabolite and expression where either locally restricted (Fendt et al., 2010), around specific reporter reactions (Cakir et al., 2006), or highly specific to environmental stress conditions (Bradley et al., 2009). Further, It is known that metabolic gene expression is highly coordinated along pathways (Ihmels et al., 2003; Takigawa and Mamitsuka, 2008).

Clearly this regulated coordination of gene expression along metabolic pathways is intended to effect the protein and finally metabolite profiles. Enzymes are the key players that drive the metabolic forces. Following an environmental stress, the en-

zymes alters the metabolic concentrations through specific reaction kinetics and redirect metabolic fluxes.

5.2 A model for translation control during ring to trophozoite transition.

5.2.1 Dynamical equations relating transcriptome and proteome

The simplest translation model is to consider that the translation rate is proportional to the concentration of mRNA. This corresponds to a linear ordinary differential equation:

$$\frac{dP}{dt} = \alpha R(t) - \beta P, \quad (5.1)$$

where $P(t)$, $R(t)$ are the concentrations of mRNA and protein at time t , respectively. α , β are parameters representing the translation efficiency and the protein degradation/dilution rate, respectively.

If protein degradation can be neglected with respect to the dilution effect produced by volume growth, β is the logarithmic growth rate:

$$\beta = \frac{d \log V}{dt}, \quad (5.2)$$

where V is the volume of the parasites inside the blood cell. The doubling time, defined as the time needed to double the volume of the parasite is related to β by the formula,

$$T_2 = \frac{\log(2)}{\beta}. \quad (5.3)$$

Generally, the logarithmic growth rate provides a lower bound for the parameter β . As a matter of fact, degradation regulation by proteolytic processes can increase the value β , but there is no way to compensate the dilution effect.

The solution of (5.1) reads:

$$P(t; C, \beta, \alpha) = C \exp(-\beta t) + \alpha \int_0^t R(s) \exp(\beta(s - t)) ds, \quad (5.4)$$

where C is a parameter ($C = P(0)$).

The parameters C, α, β can be determined for all the genes for which we have transcriptome and proteome profiles. $R(t)$ is obtained from the transcriptome data, then (5.4) calculates $P(t)$ that can be compared to the observed proteomic profiles. Then, we search for parameters C, α, β that minimise the objective function $\sum_i (P(t_i; C, \beta, \alpha) - P_{exp}(t_i))^2$, where t_i are experimental times and $P_{exp}(t_i)$ is the experimental protein quantity at time t_i .

The simple model (5.1) considers that the translation efficiency does not change in time, therefore does not cope with translation regulation. A model including translation control is to consider that the translation efficiency is reduced r times during the interval $[0, t_0]$ and has a nominal value α at times larger than t_0 . This model corresponds to a translational switch, and can be described by the following piecewise-linear differential equation:

$$\frac{dP}{dt} = \alpha R(t) \theta(t - t_0) + \frac{\alpha}{r} R(t) (1 - \theta(t - t_0)) - \beta P, \quad (5.5)$$

where $\theta(t)$ is the Heaviside function, $\theta = \begin{cases} 1 & \text{if } t > 0 \\ 0 & \text{if } t < 0 \end{cases}$.

Let us define

$$f(t; t_0, r) = \begin{cases} R(t) & \text{if } t > t_0 \\ R(t)/r & \text{if } t < t_0 \end{cases}$$

Then the time dependent protein level for a translational switch is given by:

$$P(t; C, \beta, \alpha, t_0, r) = C \exp(-\beta t) + \alpha \int_0^t f(s; t_0, r) \exp(\beta(s - t)) ds \quad (5.6)$$

5.2.2 Ranking transcriptome and proteome according to phase

A large proportion of the protein coding genes of *P. falciparum* have periodic transcriptome profile. This means that the gene expression level at the beginning of the ring stage is the same as at the end of schizont stage, that allows reinvasion. Blood

stage transcriptome functions as a clock that sends signal to different genes to be active at different times.

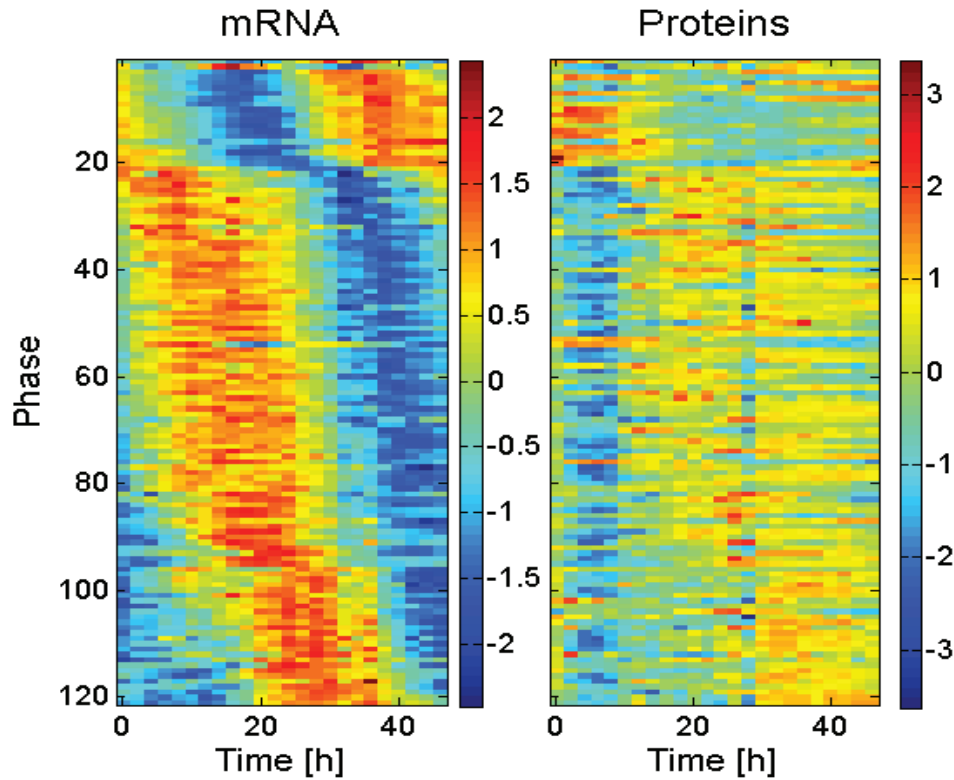


Figure 34: *Transcriptome and proteome data for 121 oscillatory genes during intra-erythrocytic stage of P. falciparum. Genes are ranked according to the phase of their transcriptome oscillation. In this picture orange means up-regulation, and blue down-regulation.*

Transcriptome and proteome data (matrices of time dependent profiles) were processed according to the same protocol:

- i). Each profile (line in data) is mean centered and normalized by dividing it to the standard deviation.
- ii). The normalized profile is Fourier transformed by using the fast Fourier transform algorithm.
- iii). The maximum absolute value of the Fourier transform amplitude is identified for each gene and the phase (argument of the maximum complex amplitude) rendered.

iv). Genes are sorted according to their phase in the transcriptome.

After ranking the genes according to the phase of their transcriptome oscillation, we colour code the transcriptome and proteome profiles and stack them as lines in images. In Figure. 34, generated with data obtained in (Foth *et al.*, 2011), one can notice the wave-like behaviour of the transcriptome: different genes are not synchronous oscillators, the position of the maximum expression is distributed continuously from early ring to schizont stage. For many genes, the protein level is delayed with respect to the mRNA level, for instance genes having maximum of transcripts in ring stage can be not expressed in this stage and have their maximum of protein expression in trophozoite stage.

A delay in translation with respect to transcription can be explained in at least two ways. One possible explanation is that the protein response time is slow. Thus, the simple model (5.1) can explain the delay. In this model, the response time is the doubling time of the protein T_2 . Slow response means large protein half life but also very slow growth.

The second explanation is translation control, and consists in considering that genes are translationally repressed and thus protein levels are insensitive to mRNA level before the trophozoite stage, and translation is allowed starting with the trophozoite stage. This model corresponds to a translation switch and is described by (5.5). (Foth *et al.*, 2011) used the first model (no switch) to fit his data. We argue here that there are several arguments in favour of the second model.

Figure.35 represent the volume of the parasite inside the cell as a function of time. We notice that growth starts with trophozoite stage and from this stage on the average volume doubling time is $T_2 \approx 5.7h$.

As stated in (Foth *et al.*, 2011), we have used the linear model (5.1) to explain the delay in the protein expression. This model depends on three parameters α, β, C that were fitted from the transcriptome and proteome data. Both transcriptome and proteome data were provided as \log_2 relative abundances ratios (supplemental files of (Foth *et al.*, 2011)). In order to transform them into abundances, we applied the exponential function to all these values. The value of the parameter β was used

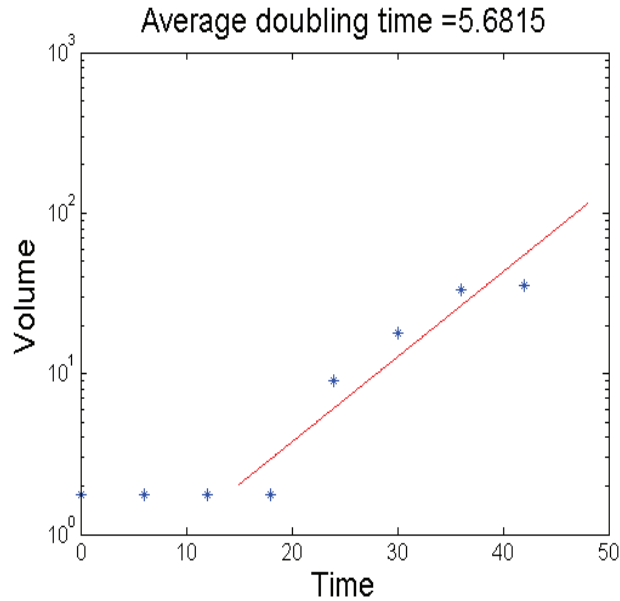


Figure 35: Volume of the parasite during intra-erythrocytic stage of *P. falciparum* as a function of time. Growth starts with the trophozoite stage ($t_0 \approx 20h$) and the average growth rate corresponds to a volume doubling time $T_2 \approx 5.7h$.

to compute the volume doubling time according to the formula (5.3). In order to explain the delays, the doubling time for the linear model (averaged on all genes) was approximately, $70h$ which is about 10 times higher than the one given by the observed growth rates.

We have also used our second model (translation switch (5.5)) to fit the data. This model contains five parameters α, β, C, t_0, r , that were estimated by least squares optimisation. The value of β was again used to compute the volume doubling time according to the formula (5.3). Under the translation switch hypothesis, we found an average volume doubling time of approximately $8h$, that is very close to value resulting from the experimental logarithmic growth rate. Although a linear model can also fit the data, one needs growth rates that are ten times smaller than the observed ones in order to explain the delays. The piecewise linear model (5.5) is thus more appropriate to explain the delays, as it leads to degradation/dilution constants compatible with the observed growth rates.

The transition corresponding to a change in the translation efficiency parameter

α is illustrated in Figure.36. The position of the transition (parameter t_0 in (5.5)) is illustrated in Figure.36. Our modelling suffers from a collinearity effect, as parameters t_0 and β are not entirely independent. As a matter of fact, we have seen that using small values of β allow to use the linear model, which is equivalent to a piecewise linear model with $t_0 = 0$. More generally, correlated variations of t_0 and β could preserve the goodness of fit. For these reasons, the lack of precise localization of the transition can be simply due to the small sensitivity of our model and data to position of t_0 . More precise measurements of the gene expression are needed in order to accurately locate the transition time.

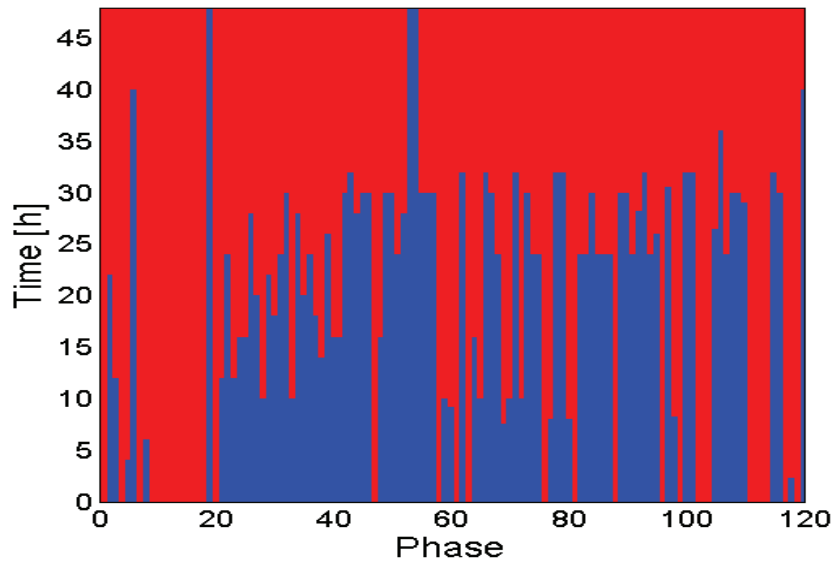


Figure 36: *Genes numbered from 1 to 121, are sorted according to the phase of the mRNA transcript. For each gene we have indicated as a red vertical segment, the interval during which translation is active, and as a blue vertical segment, the interval during which translation is reduced. In the average we notice a transition at approximately 20 h from the start of invasion, indicating the ring to trophozoite transition. The first 20 profiles, corresponding to genes with transcription activity in early ring and schizont phases are not submitted to the transition and the delay between mRNA and protein expression is much less pronounced.*

5.3 The experimental study of the relation between transcriptome and metabolome

To investigate the relationship between levels of gene expression and metabolite profiles we have used an experimental approach. A combined metabolomic and transcriptomic analyses was performed. LC–MS/MS and qPCR techniques are simultaneously used to measure changes in metabolite concentrations and gene expression respectively. This study mainly focuses on the regulation of genes (that encodes PL enzymes) and metabolites along PL metabolic pathways of *P. falciparum*.

5.3.1 Materials and Methods

Preparation of cultures

Three independent cultures were prepared and synchronized at 2 hours. Complete medium was used to culture the parasites. Sampling is done every 6 hours throughout 48 hours (one life cycle of the parasite). For each time points samples were divided into two and subjected to a) Metabolomic (LC–MS/MS) b) qRT-PCR analysis.

Data analysis

5.3.2 Processing and quantification of metabolomics data

In this study, the high sensitivity and specificity of LC–MS/MS was used to perform a comprehensive metabolomic profiling, both in *Plasmodium* and the host cell (RBC), of selected metabolites important for the growth of parasite.

During asexual development the volume of the parasite reaches about 50% of the uninfected erythrocyte volume but the infected erythrocyte volume remains relatively constant. The total hemoglobin content gradually decreases during the 48 hour cycle but its concentration remains constant until early trophozoite stage, decreases by 25%, then remains constant again until just prior to rupture. During early sexual develop-

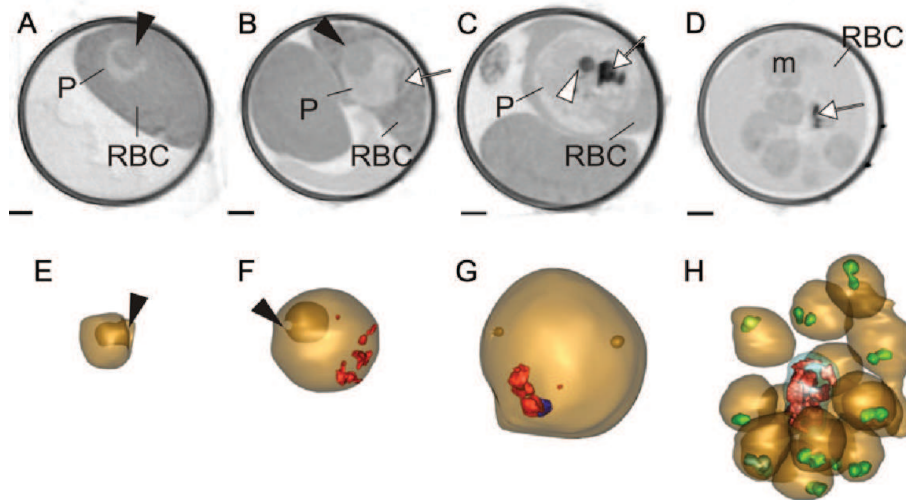


Figure 37: *Transmission X-ray tomography of asexual stages of P. falciparum.* (AD) Individual virtual z-sections (66 nm) of RBCs infected with ring, early and late trophozoites and a segmented schizont. The parasites (P) are indicated. (EH) Rendered models generated by segmentation of the tomograms. In the models the parasite surface is depicted in gold and the hemozoin crystals in red. Invaginations of the parasite surface are depicted in deeper gold. In the segmenting schizont the rhoptry pairs in each of the nascent daughter cells are rendered in green and the digestive vacuole in blue. The ring stage parasite (A and E) is invaginated (black arrowheads) to form a cup shape. The invagination persists, with a smaller opening, (black arrowheads) in the early trophozoite (B and F), and the first evidence of hemozoin (white arrow) is visible (B and F). An early schizont (C and G) has 8 nuclei, an accumulation of hemozoin (white arrow) and an X-ray dense lipid body (white arrowhead). A segmented schizont (D and H) has 16 daughter cells, and shows a decrease in hemoglobin density. Hemozoin (D, white arrow; H, red crystals) accumulates in the digestive vacuole in a central remnant body courtesy: (Hanssen et al., 2012).

ment the gametocyte has a similar morphology to a trophozoite but then undergoes a dramatic shape change.

Cryo X-ray tomography analysis (shown in Figure.37) reveals that about 70% of the host cell hemoglobin is taken up and digested during gametocyte development and the parasite eventually occupies about 50% of the uninfected erythrocyte volume (Hanssen et al., 2012).

5.3 The experimental study of the relation between transcriptome and metabolome127

Factors for volume corrections along the cell cycle

Time series	Volume factors
RBC	86.00
T1 = 6 hr, T2 = 12 hr, T3 = 18 hr	1.75
T4 = 24 hr	9.00
T5 = 30 hr	18.00
T6 = 36 hr	33.00
T7 = 42 hr	35.50

Table 9: Factors for volume corrections that corresponds to T1...T7, seven different time-points. Volume of *Plasmodial* cell varies from 3–40 femto liters.

Coutsey: (*Hanssen et al.*, 2012)

The water soluble metabolites were identified and quantified (pmol/10⁷ parasites) by the protocol (*Duy et al.*, 2012). The absolute concentration of these metabolites is converted to $\mu\text{M}/\text{L}/10^7$ parasites. The concentration of each profile (time series of the metabolites) is normalized with volume factors shown in Table. 9. Each profile of metabolite expressed in $\mu\text{M}/\text{L}/10^7$ parasites are re-normalized with its maximum expression along the cell cycle. This is called as 'Fold change' of the metabolites with respect to its maximum expression along the cell cycle.

5.3.3 Processing and quantification of qPCR data

Quantitative qPCR are done and the relative expression of the genes were obtained by normalizing the expression of each profile with respect to expression of *tRNA-synthase* gene. Then the profiles were re-normalize with their maximum expression along the cell-cycle. This is named as 'Fold change' of the genes with respect to its maximum expression along the cell cycle.

5.3.4 Results and Discussions

5.3.4.1 Metabolomics of Host erythrocyte/RBC

There are only a few recently published analyses of the RBCs metabolome (*Darghouth et al.*, 2011; *Nishino et al.*, 2009). However, several biochemical and proteomic

studies have been performed and have identified the enzymatic activities and the metabolic pathways present in RBCs (*Nishino et al.*, 2009; *Roux-Dalvai et al.*, 2008). RBC metabolism is thought to be mostly restricted to glycolysis, nucleotide catabolism, and glutathione metabolism. For instance, mature human RBCs have lost their mitochondria and are entirely dependent on glycolysis to generate ATP. Thus, it is not surprising that the two most abundant products we measured in RBC extracts are glucose and lactate (the end product of glycolysis).

Glycerophospholipid metabolism in *P. falciparum*

The lipid metabolism in *Plasmodium* has been thoroughly covered in chapter.2.

It is known that during the active replication phase, the parasites are in high demands for metabolic intermediates necessary for growth. Lipids are among the most critical components required during development of the *Plasmodium* malaria parasite since they are involved in numerous cellular functions.

Biochemical Scheme of glycerophospholipid metabolism in *P. falciparum*

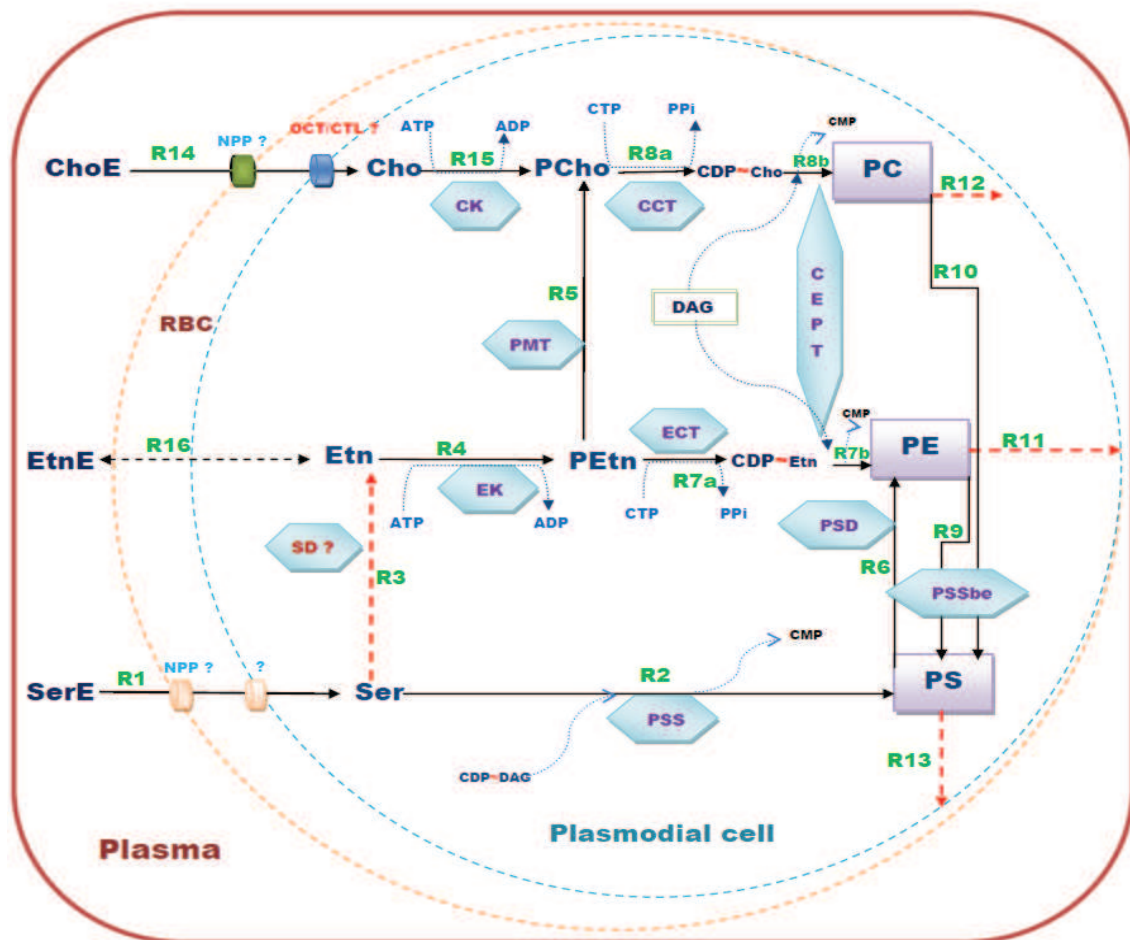


Figure 38: Biochemical scheme showing glycerophospholipid metabolism in *P. falciparum*, for abbreviations see Table.1. For reactions details see Table.10

Reaction ID	Enzyme/ORF	References
R1_(SerE-Ser)	?	(Elabbadi et al., 1997)
R2_(Ser-PS)	PSS0/PGPS	Vial (unpublished data)
R3_(Ser-Etn)	SD	(Elabbadi et al., 1997)
R4_(Etn - PEtn)	PfEK / PF11.0257	(Alberge et al., 2010)
R5_(PEtn-PCho)	PfPMT /MAL13P1.214	(Pessi et al., 2004, 2005)
R6_(PS-PE)	PfPSD /PF11370c	(Baunaure et al., 2004)
R7a_(PEtn-CDP_PETn)	PfECT/PF13.0253	(Vial et al., 1984b; Elabbadi et al., 1997)
R7b_(CDP_PETn-PE)	CEPT/PFF1375c	(Vial et al., 1984b; Elabbadi et al., 1997)
R8a_(PCho-CDP_PCho)	PfCCT/MAL13P1.86	(Yeo et al., 1995, 1997)
R8b_(CDP_PCho-PC)	CEPT/PFF1375c	(Vial et al., 1984b; Elabbadi et al., 1997)
PE-PC ?	PEMT/PLMT ?	–
R9_(PE-PS)	PSSbe/Mal13P1.335	Berry and Vial (unpublished data)
R10_(PC-PS)	PSSbe/Mal13P1.335	Berry and Vial (unpublished data)
R11_PE-efflux	?	–
R12_PC-efflux	?	–
R13_PE-efflux	?	–
R14_ChoE-Cho	NPP/OCT/CTL/PFE0825w	(Biagini et al., 2004; Kirk et al., 1991) (Goldberg et al., 1990; Wein et al., 2012)
R15_Cho-PCho	PfCK	(Choubey et al., 2006; Alberge et al., 2010)
R16_EtnE-Etn	Passive diffusion/facilitated diffusion	

Table 10: List of enzymes and ORF indicated in *P. falciparum*

5.3.5 Regulation of LP genes and metabolites along cell-cycle

The fold change of expression of genes and metabolites were analyzed stage by stage along the 48 hours the cell-cycle . The fold change in the expression of some PL genes and metabolites are shown in Figure.40.

Nearly, 75% of genes gained their maximum expression during late trophozoite or schizogony stage (T = 42 hours). This is the stage where the cell requires lipid to synthesize new membranes for daughter cells.

About 70% of metabolites peaked up to their maximum expression around 20 hours of the cell-cycle (i.e in early trophozoite stage). Most of the metabolites were abruptly down- regulation after this stage. The data shown in Figure.40 illustrates a phase shift in the expression of metabolites during ring–trophozoite transition. Some PL metabolites like Serine and Choline are under this transitions. Other PL metabolites

5.3 The experimental study of the relation between transcriptome and metabolome131

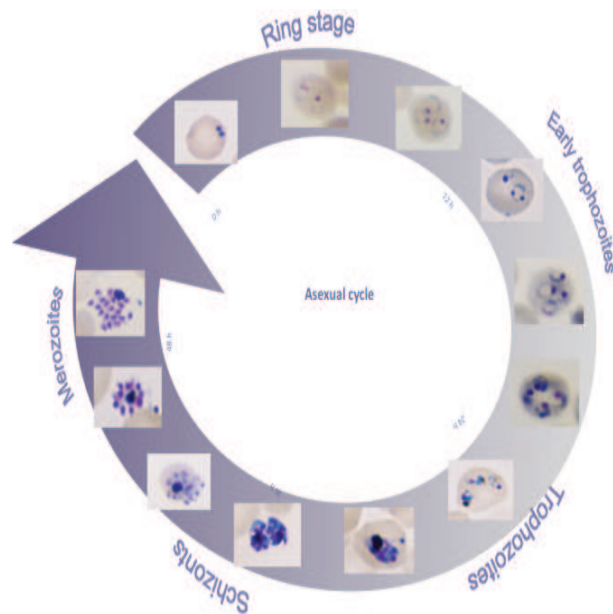


Figure 39: The 48 hours cell cycle of *P. falciparum*

like CDP-etha, CDP-chol, EthaP, ChoP gains its maximum expression during late phase of the cell-cycle. It also marks the requirement of the cell for PC and PE i.e produced from CDP-Choline and CDP-ethanolamine intermediates respectively.

The regulations of these genes and metabolites involved in different PL metabolic pathways are discussed below.

5.3.5.1 Regulation of CDP-choline and CDP-ethanolmaine pathway

a). Post Invasion and early ring stage (T1=6 hr)

A substantial expression of gene encoding OCT (PfOCT) (see Figure.41, left panel) was marked with high expression of intracellular choline (labelled, Chol). The expression of genes encoding CK (PfCK) was quite low. These suggest that choline is accumulating, which can be seen in (Figure.41 left panel).

PfCCT has low expression and correlates with the expression of PfCK (see Figure.41, left & middle panel). Furthermore, PfPMT (see Figure.42, left panel) is expressed. All together, these suggest that the major portion of CholP (PCho) comes from the PMT pathway, leading to a moderate accumulation of PCho during this stage.

Interestingly, the expression of PfCEPT (gene encoding CEPT) is quite high. Be-

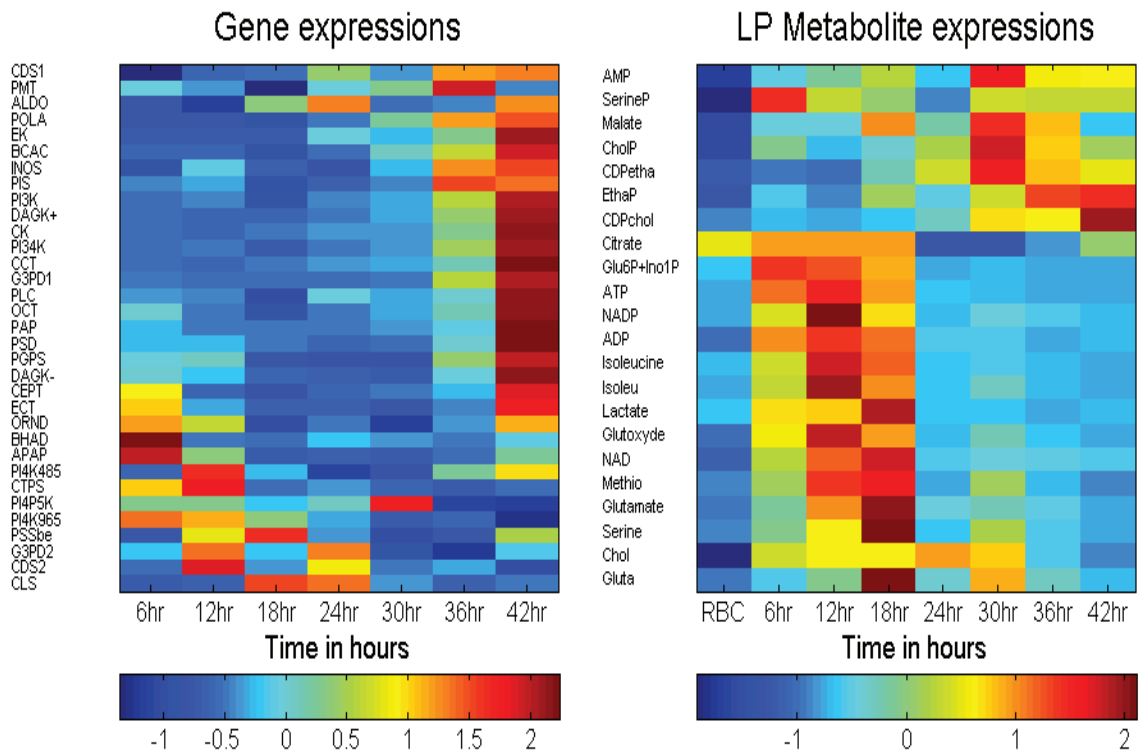


Figure 40: The left panel of the plot illustrates the fold change in expression of PL genes obtained by qPCR and the right panel shows the fold change in expression of PL metabolites obtained by LC/MS–MS with a resolution of 6 hours along the 48 hours cell cycle in *P. falciparum* 3D7. Each line represents a profile (gene or metabolite)

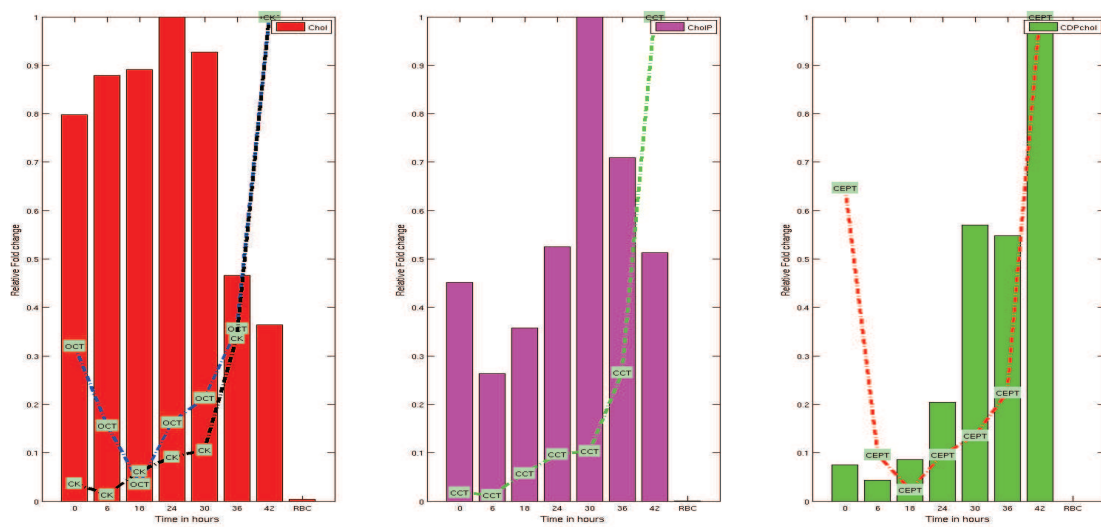


Figure 41: Regulation of genes and metabolites of CDP-choline pathway along the cell cycle

5.3 The experimental study of the relation between transcriptome and metabolome133

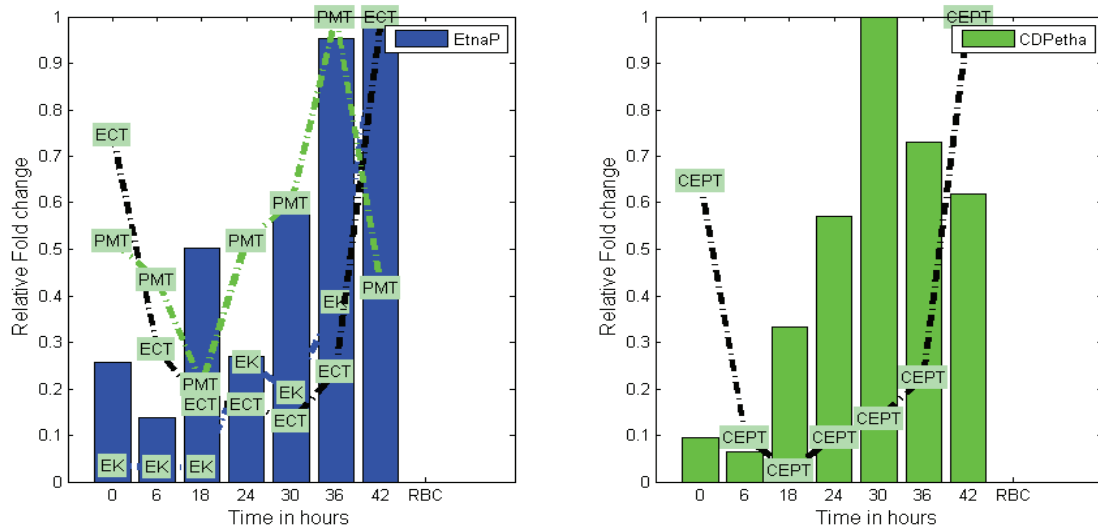


Figure 42: Regulation of genes and metabolites of CDP-ethanolamine pathway along the cell cycle

cause the CDP-chol and CDP-etha influxes are weak at this time, this implies that the substrates CDP-chol and CDP-etha (see Figures.41 & 42, right panel) are very low compared to later stages. This may be a consequence of the rigid transcriptional control of *Plasmodium* genes during the IE cycle. PfCEPT belongs to the group of genes expressed during early ring and schizont stages. Although not needed during the early ring stage, the corresponding enzyme is strongly demanded in the schizont stage, which justifies the control. As shown in the previous section, the majority of the genes in this group are not submitted to translation repression during the ring stage. However, the question remains open whether this generic property of early ring genes applies also to PfCEPT, that could be translationally repressed during the ring stage, being thus fully expressed only during schizogony.

Ethanolamine enters the cell by passive diffusion. The expression of PfEK (gene encoding EK) is low (see Figure.41, right panel). This explains the decrease of Petn during the early ring stage. The relatively higher value of Petn at the beginning of the cycle could be a re-invasion condition resulting from much larger concentrations in late schizont stage. Thus, at post-invasion stage, the Kennedy pathways are less used by the *Plasmodial* cell for the formation of biomass (lipids). The transverse pathways contribute to preparing the pool of PCho.

b). Ring stage (T2=12 hr)

At this stage PfOCT, was down regulated as compared to T1 stage. The expression of intracellular choline (Chol) does not change. PfCEPT was abruptly down regulated. As the concentrations of CDP-Cho (see Figure.41, right panel) and CDP-etha (see Figure.42, right panel) are as well at their lowest values, this means that the outfluxes of the Kennedy pathways should be at the lowest. PfCK and PfCCT maintain low expressions and were well correlated. Interestingly, the decrease in expression of PfPMT in presence of ChoP, reflects the findings of (*Pessi et al.,2004*). It was shown that PfPMT activity was down regulated and inhibited by its product PCho and by the phosphocholine analog, miltefosine.

In summary, the low level of expressions of PL genes and metabolites depicts the cell in its resting or preparatory state.

c). Late Ring stage (T3=18 hr)

The effect of CholP on PfPMT was more pronounced. There was increase of CholP expression with a marked decrease in PfPMT that attains its minimal expression across the cell-cycle. The expression of PfPMT, PfCEPT and PfOCT are minimum across the cell-cycle.

A raise in EthaP is not accompanied by a raise in PfEK. There could be two possibilities, a) The expression of EthaP was over estimated in the sample, b) There could be an alternate mechanism for the production of EthaP. From Figure.43, there was a high expression of Serine found during the late Ring stage, this is the stage where Serine gained its maximum expression across the cell cycle. This could indicate a possibility of formation of PEtn from intracellular Serine directly without going into serine decarboxylase (SD) pathway.

d). Early Trophozoite stage (T4=24 hr)

Intracellular choline (Chol) peaked up to its maximum value. The expression of PfOCT, PfCK, PfCEPT and PfCCT are increasing. Interestingly, expression of PfPMT

5.3 The experimental study of the relation between transcriptome and metabolome¹³⁵

increased with increasing ChoP and decreasing EthaP. This means that the inhibition of PfPMT by its product PCho could be reversible. Most probably, PfPMT also belongs to the group of early ring/schizogony genes that are under the control of the transcriptional clock.

At this stage there was an accumulation of PCho as compared to CDP-chol while the concentration of PfCCT remained low. This suggests that reaction R8a (see Figure.41) is the slowest step and CCT is limiting. This agrees with the findings of (*Vance et al., 1980*) where CCT was shown to be a rate-limiting and regulatory enzyme of *de novo* CDP-choline pathway for PC biosynthesis. Major mode of regulation of CCT activity is known to be reversible translocation of the inactive soluble CCT to active, membrane-bound form (*Sleight and Kent, 1980*).

Again considering the concentration of Chol and CholP, it was also found that Chol accumulated in the cell as compared to its product CholP. PfCK maintained a low expression and was correlated with PfCCT. This also indicates the limiting nature of CK at this stage.

e). Mid Trophozoite stage (T5=30 hr)

The expression of genes and metabolites peaked up. CholP gained to its maximum concentration across the cell-cycle (see Figure.42). The rising PfCEPT also correlated well with the expression of CDP-cho. All this findings together showed the necessity in production of PC predominantly via CDP-choline pathway. Interestingly, the expression of PfCK remained low when Chol accumulated in the cell. Surprising, expression of PfPMT was quite high. Moreover, the expression of PfoCT remained low. So, it is still to understand if the major part of CholP was formed by CK via R15 or by PMT via (R5) (see Figure.38) at mid trophozoite stage. Probably, this is the stage where the *de novo* CDP-choline pathway is more proactive than the transversal, SDPM pathway.

f). Late Trophozoite/Early Schizont (T6=36 hr)

PfPMT gained its maximum expression across the cell cycle, with down-regulation of CholP and up-regulation of EthaP (see Figures.41 & 42). PfPMT expression is well correlated with the expression of EthaP (substrate for PMT) but uncorrelated to the expression of CholP. This suggests a strong regulation of PMT. Increase in expression of PfoCT with decrease in expression of Chol and increase in level of PCho as compared to CholP indicates conversion of Cho to PCho. This also suggests a marked increase in activity of CDP-Cho pathway.

The expression of PfEK tends to peak up with the accumulation of EthaP (see Figure.42). The expression of PfECT did not changed much, the expression of CDPetha was low as compared to EthaP but it correlated well with PfCEPT. All together it indicates that, ECT is limiting (*Houweling et al., 1992; Sundler, 1975; Sundler and Akesson, 1975; Tijburg et al., 1987*) for the biosynthesis of PE.

g). Late Schizont stage or merozoite stage (T7=42 hr)

PfCK, PfCCT, PfCEPT and PfoCT gained their maximum expression along the cell-cycle (see Figure.41). CDP-cho also peaked up to its maximum expression. There was abrupt down regulation of PfPMT with increased EthaP (substrate for PMT) but with decreased ChoP. All these findings pointed towards enhanced PC biosynthesis. Down regulation of PfPMT also suggested the effective use of *de novo* CDP-choline pathway for the production of PC.

Moreover, from Figure.41, it is shown that CholP (substrate of CCT) gained its maximum expression at mid-trophozoite stage and CDP-cho (product of CCT) at late-schizont stage. In other words, there is a delay of 12 hours between the maximum expression of CholP and CDP-cho. PfCCT peaked up to its maximum at late-schizont stage (T7) stage. These observations points towards the regulatory nature of PfCCT which boosts PL synthesis in late schizont stage.

The expression of genes and metabolites peaked up until EthaP attains its maximum level across the cell-cycle. The fold change in expression of EthaP correlated well with

5.3 The experimental study of the relation between transcriptome and metabolome¹³⁷

the expression of PfEK. Further, expression of PfPMT was minimal across the cell cycle. All these findings together suggest that *de novo* CDP-etha is essentially used by the cell for PE biosynthesis.

5.3.5.2 Regulation of serine and base-exchange reactions

PSSbe and PGPS/PSS0 are the two genes that are currently deciphered in our lab. PSSbe tends to participate in base-exchanges of PC/PE to PS. PGPS/PSS0 is involved in synthesis of PS from Serine. The expression of PSSbe peaked up and gained to its maximum level during late ring stage (see Figures.43). Expression of PGPS correlated well with the expression of PfPSD, PfCK, PfECT and PfCCT. Further, investigation is needed to ascertain the roles and underlying mechanisms of PGPS and PSSbe in the production of PS and base-exchange mechanisms respectively.

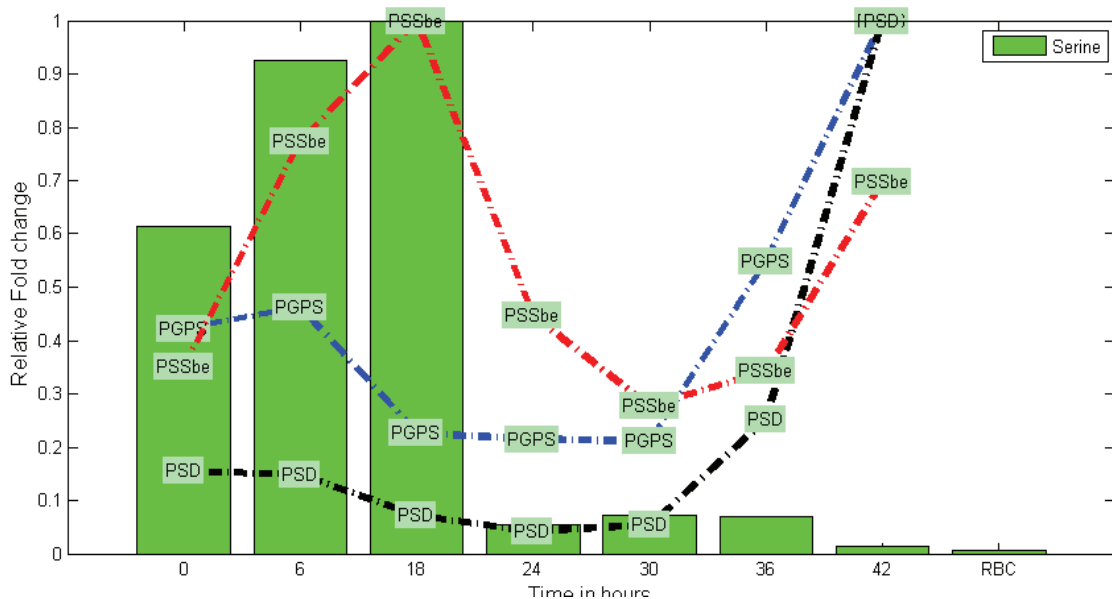


Figure 43: Regulation of serine

5.3.5.3 Regulation of LP genes and metabolites in Serine decarboxylation pathway

The expression of PfPSD did not correlated with the high expression of serine. This behavior was marked throughout the cell-cycle (see Figure.43). The genes encoding

serine decarboxylase has not been characterized in *P. falciparum*. It seems that serine is preferentially decarboxylated to Etn (Elabaddi, 1997) via R3 (see Figure.38) or directly to EthaP.

5.4 Conclusion

We have used a combined modelling and experimental approaches to understand regulation of genes, proteins and metabolites expressions in *P. falciparum*. Two models (a linear model and a piecewise-linear model with translational switch) were introduced to understand the translational control on the genes and subsequent delays in protein production during the 48 hours cell cycle. The models were made to fit with the experimental data and average volume doubling time that stands for growth rate was computed. Although a linear model fitted the experimental data, it needed a growth rate 10 times smaller than the measured one in order to explain the delays. Again the piecewise linear model (the second model) was thus found to be more appropriate to explain these delays. This model considered volume doubling time which was compatible with the observed growth rates. The piecewise linear model predicts a translational switch which operates around 20 hours, during ring-trophozoite transition of the cell cycle. After this period the mRNAs that were under translational repression can be used for protein production. The translation repression affects genes whose expression peaks in ring and trophozoite stages. Genes having maximum expression in early ring and schizogony stages seem to be much less affected by this regulatory mechanism.

Combined transcriptomic and metabolomic experiments were undertaken to understand the regulation of genes and metabolites throughout the cell cycle. Interestingly, the delayed expression observed and modelled for genes was also observed for metabolites in the phospholipid synthetic pathways. Such a phase shift characterized the concentrations of metabolites at or around 20 hours (ring-trophozoite transition) of the cell cycle, corresponding also to the onset of growth. Some of the metabolites accumulated before this stage and were down-regulated in the subsequent stages. We investigated this behaviour in expression of the PL metabolites. Serine and Choline

were found to exhibit this behaviour. Metabolites like CDP-etha, CDP-cho, EthaP, CholP peaked up only during the late phases (late trophozoite or schizogony) of the cell cycle. At this stage most of the PL genes showed their maximum expression.

The experimental data was further used to investigate the regulation of genes and metabolites of PL metabolic pathways along the 48 h cell cycle. It was found that the cell effectively uses the Kennedy synthetic pathways (CDP-choline and CDP-ethanolamine) for production of PC and PE during the later part of the cell cycle, whereas the transversal pathways operate during the early stages. The experimental data was able to reproduce the findings of (*Pessi et al. , 2005*), which showed the down regulation of PfPMT by its product CholP.

Chapter 6

General Conclusion

Antimalarial chemotherapy is challenged by the emergence of drug resistance. Therefore, several efforts are made to identify new targets that are druggable and pathways that are specific to the parasite. Among different complex pathways, glycerophospholipid metabolic pathways stands out. The parasite effectively utilizes these pathways to produce PLs which are primarily used for membrane neogenesis. On infection there was 6 fold increase in glycerophospholipids among which PC, PE, PS were the major components. Interestingly, the parasite has its own machinery to produce PLs by incorporating precursors from the host RBCs. Moreover, some of the enzymes of this pathway is specific to the parasite (for instance, PMT), in other words they were not identified in host RBCs. All these findings enhanced our interest to understand and explore phospholipid metabolism and acquisition in *Plasmodium*.

We have reconstructed the glycerophospholipid metabolic network in *P. falciparum* and *P. knowlesi*. In order to determine the kinetics of the PL enzymes, we have developed a new hybrid optimisation scheme. This scheme is based on the discretization of the simplex that parametrizes the set of directions in the cone of admissible fluxes. The method was trained with the radiolabelled fluxomic data of the metabolic precursors from *P. knowlesi*. The predicted fluxes and estimated steady state concentrations of different intracellular PL metabolites were subjected to further analysis. On investigating the dynamics of these PL metabolites, it was found that major part of serine was preferentially decarboxylated into ethanolamine. There was minor contribution of serine for the direct formation of PS. In fact, the major part of PS was base exchanged from PC and PE. The metabolic network model was used to elucidate the contribution of different phospholipid synthetic pathways in PC biosynthesis. It was found that in absence of choline precursor there was a balanced contribution of PMT and PEMT that facilitates PC biosynthesis. However, the PC produced by this pathways contribute very less to the total bulk of PC. The CDP-choline Kennedy pathway is the primary source for PC biosynthesis. Sensitivity analysis of CDP-choline pathway in our model, does not identify limiting steps. However, it shows that the carrier-mediated choline entry into the parasite and the phosphocholine cytidylyltransferase (CCT) reaction have, in order, the largest sensitivity coefficients in this pathway. This finding is in agreement

with the biochemical findings.

The transcriptome of *P. falciparum* is known to exhibit a highly coordinated behaviour. About 75% of genes peak up once during the 48 hours cell cycle. The combined study of the transcriptome and of the proteome shows a time delay in the production of proteins from the expressed mRNA. This delay was found by (Foth *et al.*, 2011) to be of 11 hours (median value). We have used a modelling approach to identify the origin of the delays and distinguish between two hypothesis, namely a large protein response time or a translationally controlled transition. Two models (a linear model and a piecewise-linear model with translational switch) were developed to understand the translational control on genes and the subsequent delays in protein production. The models were made to fit with the experimental data and an average volume doubling time was computed and compared with the measured one. Although the linear model fitted the experimental data, it needed a growth rate 10 times smaller than the one observed from experiments in order to explain the delays. The piecewise linear model (the translational switch model) was thus found to be more appropriate to explain these delays. This model predicts a translational switch that operates around 25 hours (ring–trophozoite transition) of the cell cycle. After this period the mRNAs that were subjected to translational repression can be used for protein production. The mRNAs were subjected to translational control up to 25 hours, thus there was a delayed production of proteins. The control was released after this period when proteins levels become sensitive to the mRNAs. These findings provide a first quantitative understanding of translational regulation in *P. falciparum*.

To get a deeper insight of the regulation of PL metabolites and genes throughout the cell cycle of *P. falciparum* we have measured the expressions of the PL metabolites and genes by an assay with combined experimental techniques LC/MS–MS and qPCR respectively. These experiments were designed to identify, isolate and quantify water soluble PL metabolites. The temporal behaviour PL metabolites and genes were compared one to another and with the literature. These datasets was able to confirm previous experimental findings, but many new observations stood out.

Most of the PL genes had a synchronous transcriptomic behaviour and were well correlated with each other. Some of these correlated genes are PfCK, PfCCT, PfEK, PfECT that peak at early ring and/or schizogony stage, whereas PfPMT and PSSbe peak at late ring and trophozoite stages. This type of behavior correlated to the transcriptional clock and allows to utilize various metabolic pathways when they are needed. Thus, PL metabolites have been shown to accumulate up to late ring stage and consumed thereafter. The expression of PL intermediates like CDP-chol and CDP-etha correlated strongly with PfCEPT expression which marks the requirement of the cell for the production of PC and PE from these intermediates at late trophozoite or schizont stages. From the integrated analysis of PL transcriptomics and metabolomics data we understood that CDP-chol and CDP-etha *de novo* pathways were effectively used by the cell during the late trophozoite or schizont stages. The transversal pathways (SDPM) pathways were more proactive during the early stages of the cell cycle. This also explains the dichotomous behaviour of PL metabolic network.

PMT is known to be down regulated by its product PCho (CholP) (*Pessi et al., 2004*). This behaviour was explained with our dataset. The effect was more pronounced in late ring stages.

We were also able to explain our early findings that showed the limiting nature of CCT, CK and ECT during the early stages of the cell cycle. The low expression of PGPS gene during the early stages and the high expression of PSSbe marks the formation of PS by base-exchange reactions from PE or PC. However, in very late stages (schizont) the expression of PSSbe decreases while there is a small increase in PGPS expression. This elucidates that, PC and PE biosynthesized during the late stages are effectively used by the cell for membrane neogenesis and a very less amount would be exchanged to PS. Further investigation is required to understand the underlying mechanisms of base-exchange reactions and their participation in the PL metabolism along the cell-cycle.

The model of lipid metabolism in *Plasmodium* emphasizes a panoply of various complex metabolic pathways that are rarely found in a single organism. The dynamics of the PL precursors unravelled the functioning of different metabolic pathways towards

PL synthesis and acquisition. The integrated analysis of transcriptome, proteome and metabolome has focused on the temporal regulation of the PL targets (genes, proteins and metabolites). Some enzyme like PfCCT and PfECT that are known to be rate-limiting in *de novo* pathways could be targeted with inhibitors. The future scope, would be to adapt a target-based strategy to design new inhibitors against these targets. This strategy has been developed in our lab by designing several inhibitors (compound class bis-thiazolium salts) to target the choline transport in *P. falciparum*, (Wein *et al.*, 2012) and is currently extended to the inhibition of synthesis. The quantitative modelling approaches developed in this thesis could be extended to include the control of enzyme expression, as well as the regulatory mechanisms of translation and transcription. Including metabolites, enzyme genes and proteins into larger network models containing their regulators is a middle-out, multiscale modelling strategy that provides precious insight into essential functions of the lifecycle of *Plasmodium*.

Bibliography

- World malaria report, world health organization, 2010. URL http://www.who.int/malaria/world_malaria_report_2010/en/index.html.
- M. Adjuk, A. Babiker, P. Garner, P. Olliaro, W. Taylor, and N. White. Artesunate combinations for treatment of malaria: meta-analysis. *Lancet*, 363(9402):9–17, 2004.
- S. T. Agnandji, B. Lell, S. S. Soulanoudjingar, J. F. Fernandes, B. P. Abossolo, C. Conzelmann, B. Methogo, Y. Doucka, A. Flamen, B. Mordmüller, et al. First results of phase 3 trial of rts, s/as01 malaria vaccine in african children. *The New England journal of medicine*, 365(20):1863, 2011.
- P. Alano. Plasmodium falciparum gametocytes: still many secrets of a hidden life. *Molecular microbiology*, 66(2):291–302, 2007.
- B. Alberge, L. Gannoun-Zaki, C. Bascunana, v. B. C. Tran, H. Vial, and R. Cerdan. Comparison of the cellular and biochemical properties of plasmodium falciparum choline and ethanolamine kinases. *Biochem. J*, 425:149–158, 2010.
- D. B. Allison, X. Cui, G. P. Page, and M. Sabripour. Microarray data analysis: from disarray to consolidation and consensus. *Nature Reviews Genetics*, 7(1):55–65, 2006.
- R. Amino, S. Thiberge, B. Martin, S. Celli, S. Shorte, F. Frischknecht, and R. Ménard. Quantitative imaging of plasmodium transmission from mosquito to mammal. *Nature medicine*, 12(2):220–224, 2006.
- A. Amponsaa-Karikari, N. Kishikawa, K. Ohyama, K. Nakashima, and N. Kuroda. Determination of halofantrine and its main metabolite desbutylhalofantrine in rat plasma by high-performance liquid chromatography with on-line uv irradiation and peroxyoxalate chemiluminescence detection. *Biomedical Chromatography*, 23(1):101–106, 2009.
- M. Ancelin, M. Calas, J. Bompart, G. Cordina, D. Martin, M. Bari, T. Jei, P. Druilhe, and H. Vial. Antimalarial activity of 77 phospholipid polar head analogs: close correlation between inhibition

- of phospholipid metabolism and in vitro plasmodium falciparum growth. *Blood*, 91(4):1426–1437, 1998.
- M. L. Ancelin and H. J. Vial. Choline kinase activity in plasmodium-infected erythrocytes: characterization and utilization as a parasite-specific marker in malarial fractionation studies. *Biochimica et Biophysica Acta (BBA)-Lipids and Lipid Metabolism*, 875(1):52–58, 1986a.
- M. L. Ancelin and H. J. Vial. Quaternary ammonium compounds efficiently inhibit plasmodium falciparum growth in vitro by impairment of choline transport. *Antimicrobial agents and chemotherapy*, 29(5):814–820, 1986b.
- M. L. Ancelin and H. J. Vial. Several lines of evidence demonstrating that plasmodium falciparum, a parasitic organism, has distinct enzymes for the phosphorylation of choline and ethanolamine. *FEBS letters*, 202(2):217–223, 1986c.
- M. L. Ancelin and H. J. Vial. Regulation of phosphatidylcholine biosynthesis in plasmodium-infected erythrocytes. *Biochimica et Biophysica Acta (BBA)-Lipids and Lipid Metabolism*, 1001(1):82–89, 1989.
- M. L. Ancelin, M. Parant, M. J. Thuet, J. R. Philippot, and H. J. Vial. Increased permeability to choline in simian erythrocytes after plasmodium knowlesi infection. *Biochem. J*, 273:701–709, 1991.
- J. Anderson, G. Churchill, J. Autrique, S. Tanksley, and M. Sorrells. Optimizing parental selection for genetic linkage maps. *Genome*, 36(1):181–186, 1993.
- L. Aravind, L. M. Iyer, T. E. Wellems, and L. H. Miller. Plasmodium biology: Genomic gleanings. *Cell*, 115(7):771–785, 2003.
- C. Armstrong and D. Goldberg. An fkbp destabilization domain modulates protein levels in plasmodium falciparum. *Nature methods*, 4(12):1007–1009, 2007.
- C. Aurrecochea, J. Brestelli, B. P. Brunk, J. Dommer, S. Fischer, B. Gajria, X. Gao, A. Gingle, G. Grant, O. S. Harb, et al. Plasmodb: a functional genomic database for malaria parasites. *Nucleic acids research*, 37(suppl 1):D539–D543, 2009.
- A. Bachmann, S. Predehl, J. May, S. Harder, G. D. Burchard, T.-W. Gilberger, E. Tannich, and I. Bruchhaus. Highly co-ordinated var gene expression and switching in clinical plasmodium falciparum isolates from non-immune malaria patients. *Cellular microbiology*, 13(9):1397–1409, 2011.
- J. K. Baird and K. H. Rieckmann. Can primaquine therapy for vivax malaria be improved? *Trends in parasitology*, 19(3):115–120, 2003.

- S. Balaji, M. M. Babu, L. M. Iyer, and L. Aravind. Discovery of the principal specific transcription factors of apicomplexa and their implication for the evolution of the ap2-integrase dna binding domains. *Nucleic acids research*, 33(13):3994–4006, 2005.
- M. Bantscheff, M. Schirle, G. Sweetman, J. Rick, and B. Kuster. Quantitative mass spectrometry in proteomics: a critical review. *Analytical and bioanalytical chemistry*, 389(4):1017–1031, 2007.
- C. Barillas-Mury. Clip proteases and plasmodium melanization in *Anopheles gambiae*. *Trends in parasitology*, 23(7):297–299, 2007.
- K. I. Barnes, D. N. Durrheim, F. Little, A. Jackson, U. Mehta, E. Allen, S. S. Dlamini, J. Tsoka, B. Bredenkamp, D. J. Mthembu, et al. Effect of artemether-lumefantrine policy and improved vector control on malaria burden in kwazulu–natal, south africa. *PLoS Medicine*, 2(11):e330, 2005.
- A. Bartoloni and L. Zammarchi. Clinical aspects of uncomplicated and severe malaria. *Mediterranean journal of hematology and infectious diseases*, 4(1), 2012.
- J. Baum, A. T. Papenfuss, B. Baum, T. P. Speed, and A. F. Cowman. Regulation of apicomplexan actin-based motility. *Nature Reviews Microbiology*, 4(8):621–628, 2006.
- F. Baunaure, P. Eldin, A. Cathiard, and H. Vial. Characterization of a non-mitochondrial type i phosphatidylserine decarboxylase in plasmodium falciparum. *Molecular microbiology*, 51(1):33–46, 2004.
- R. M. Bell and R. A. Coleman. Enzymes of glycerolipid synthesis in eukaryotes. *Annual review of biochemistry*, 49(1):459–487, 1980.
- C. Ben Mamoun, S. T. Prigge, and H. Vial. Targeting the lipid metabolic pathways for the treatment of malaria. *Drug development research*, 71(1):44–55, 2010.
- T. Bhatt, C. Kapil, S. Khan, M. Jairajpuri, V. Sharma, D. Santoni, F. Silvestrini, E. Pizzi, and A. Sharma. A genomic glimpse of aminoacyl-trna synthetases in malaria parasite plasmodium falciparum. *BMC genomics*, 10(1):644, 2009.
- S. Bhattacharjee, R. Stahelin, K. Speicher, D. Speicher, and K. Haldar. Endoplasmic reticulum pi (3) p lipid binding targets malaria proteins to the host cell. *Cell*, 148(1):201–212, 2012.
- G. A. Biagini, E. M. Pasini, R. Hughes, H. P. De Koning, H. J. Vial, P. M. O’Neill, S. A. Ward, and P. G. Bray. Characterization of the choline carrier of plasmodium falciparum: a route for the selective delivery of novel antimalarial drugs. *Blood*, 104(10):3372–3377, 2004.
- G. A. Biagini, S. A. Ward, and P. G. Bray. Malaria parasite transporters as a drug-delivery strategy. *Trends in parasitology*, 21(7):299–301, 2005.

- J. S. Bloom, Z. Khan, L. Kruglyak, M. Singh, and A. A. Caudy. Measuring differential gene expression by short read sequencing: quantitative comparison to 2-channel gene expression microarrays. *BMC genomics*, 10(1):221, 2009.
- C. P. Bolognese and P. McGraw. The isolation and characterization in yeast of a gene for arabidopsis s-adenosylmethionine: Phospho-ethanolamine-methyltransferase. *Plant Physiology*, 124(4):1800–1813, 2000.
- C. Boutlis, E. Riley, N. Anstey, and J. De Souza. Glycosylphosphatidylinositols in malaria pathogenesis and immunity: potential for therapeutic inhibition and vaccination. In *Immunology and Immunopathogenesis of Malaria*, pages 145–185. Springer, 2005.
- S. Bowman, D. Lawson, D. Basham, D. Brown, T. Chillingworth, C. Churcher, A. Craig, R. Davies, K. Devlin, T. Feltwell, et al. The complete nucleotide sequence of chromosome 3 of plasmodium falciparum. *Nature*, 400(6744):532–538, 1999.
- Z. Bozdech, M. Llinás, B. L. Pulliam, E. D. Wong, J. Zhu, and J. L. DeRisi. The transcriptome of the intraerythrocytic developmental cycle of plasmodium falciparum. *PLoS biology*, 1(1):e5, 2003.
- Z. Bozdech, S. Mok, G. Hu, M. Imwong, A. Jaidee, B. Russell, H. Ginsburg, F. Nosten, N. P. Day, N. J. White, et al. The transcriptome of plasmodium vivax reveals divergence and diversity of transcriptional regulation in malaria parasites. *Proceedings of the National Academy of Sciences*, 105(42):16290–16295, 2008.
- P. H. Bradley, M. J. Brauer, J. D. Rabinowitz, and O. G. Troyanskaya. Coordinated concentration changes of transcripts and metabolites in saccharomyces cerevisiae. *PLoS computational biology*, 5(1):e1000270, 2009.
- P. G. Bray, O. Janneh, K. J. Raynes, M. Mungthin, H. Ginsburg, and S. A. Ward. Cellular uptake of chloroquine is dependent on binding to ferriprotoporphyrin ix and is independent of nhe activity in plasmodium falciparum. *The Journal of cell biology*, 145(2):363–376, 1999.
- S. Briolant, L. Almeras, M. Belghazi, E. Boucomont-Chapeaublanc, N. Wurtz, A. Fontaine, S. Granjeaud, T. Fusaï, C. Rogier, and B. Pradines. Research plasmodium falciparum proteome changes in response to doxycycline treatment. 2010.
- R. P. Brueckner, K. C. Lasseter, E. T. Lin, and B. G. Schuster. First-time-in-humans safety and pharmacokinetics of wr 238605, a new antimalarial. *The American journal of tropical medicine and hygiene*, 58(5):645–649, 1998.
- A. Brunner, I. Yakovlev, and S. Strauss. Validating internal controls for quantitative plant gene expression studies. *BMC plant biology*, 4(1):14, 2004.

- T. Cakir, K. R. Patil, Z. I. Önsan, K. Ö. Ülgen, B. Kirdar, and J. Nielsen. Integration of metabolome data with metabolic networks reveals reporter reactions. *Molecular systems biology*, 2(1), 2006.
- T. L. Campbell, E. K. De Silva, K. L. Olszewski, O. Elemento, and M. Llinás. Identification and genome-wide prediction of dna binding specificities for the apiap2 family of regulators from the malaria parasite. *PLoS pathogens*, 6(10):e1001165, 2010.
- G. M. Carman and G.-S. Han. Regulation of phospholipid synthesis in yeast. *Journal of lipid research*, 50(Supplement):S69–S73, 2009.
- F. Carrari, C. Baxter, B. Usadel, E. Urbanczyk-Wochniak, M.-I. Zanon, A. Nunes-Nesi, V. Nikiforova, D. Centero, A. Ratzka, M. Pauly, et al. Integrated analysis of metabolite and transcript levels reveals the metabolic shifts that underlie tomato fruit development and highlight regulatory aspects of metabolic network behavior. *Plant Physiology*, 142(4):1380–1396, 2006.
- J. R. Carter and E. P. Kennedy. Enzymatic synthesis of cytidine diphosphate diglyceride. *Journal of lipid research*, 7(5):678–683, 1966.
- E. Chance, S. Seeholzer, K. Kobayashi, and J. Williamson. Mathematical analysis of isotope labeling in the citric acid cycle with applications to ^{13}C nmr studies in perfused rat hearts. *Journal of Biological Chemistry*, 258(22):13785–13794, 1983.
- D. Channe Gowda. Structure and activity of glycosylphosphatidylinositol anchors of plasmodium falciparum. *Microbes and infection*, 4(9):983–990, 2002.
- S. Chaubey, A. Kumar, D. Singh, and S. Habib. The apicoplast of plasmodium falciparum is translationally active. *Molecular microbiology*, 56(1):81–89, 2005.
- J. Chavatte, F. Chiron, A. Chabaud, and I. Landau. Probable speciations by” host-vector’fidelity”’: 14 species of plasmodium from magpies]. *Parasite (Paris, France)*, 14(1):21, 2007.
- Q. Chen, V. Fernandez, A. Sundström, M. Schlichtherle, S. Datta, P. Hagblom, and M. Wahlgren. Developmental selection of var gene expression in plasmodium falciparum. *Nature*, 394(6691):392–395, 1998.
- Q. Chen, A. Heddini, A. Barragan, V. Fernandez, S. F. A. Pearce, and M. Wahlgren. The semiconserved head structure of plasmodium falciparum erythrocyte membrane protein 1 mediates binding to multiple independent host receptors. *The Journal of experimental medicine*, 192(1):1–10, 2000.
- V. Choubey, M. Guha, P. Maity, S. Kumar, R. Raghunandan, P. R. Maulik, K. Mitra, U. C. Halder, and U. Bandyopadhyay. Molecular characterization and localization of plasmodium falciparum choline kinase. *Biochimica et Biophysica Acta (BBA)-General Subjects*, 1760(7):1027–1038, 2006.

- Y. Chu and D. R. Corey. Rna sequencing: Platform selection, experimental design, and data interpretation. *nucleic acid therapeutics*, 22(4):271–274, 2012.
- D. Clark and J. Cronan. Two-carbon compounds and fatty acids as carbon sources. *Escherichia coli and Salmonella: cellular and molecular biology, 2nd ed. ASM Press, Washington, DC*, pages 343–357, 1996.
- C. Cohen, A. Karstaedt, J. Frean, J. Thomas, N. Govender, E. Prentice, L. Dini, J. Galpin, and H. Crewe-Brown. Increased prevalence of severe malaria in hiv-infected adults in south africa. *Clinical infectious diseases*, 41(11):1631–1637, 2005.
- F. T. Cooke. Measurement of polyphosphoinositides in cultured mammalian cells. In *Lipid Signaling Protocols*, pages 1–16. Springer, 2009.
- I. Coppens and O. Vielemeyer. Insights into unique physiological features of neutral lipids in apicomplexa: from storage to potential mediation in parasite metabolic activities. *International journal for parasitology*, 35(6):597–615, 2005.
- A. Cornish-Bowden and A. Cornish-Bowden. *Fundamentals of enzyme kinetics*, volume 3. Portland Press London, 1995.
- R. M. Coulson, N. Hall, and C. A. Ouzounis. Comparative genomics of transcriptional control in the human malaria parasite plasmodium falciparum. *Genome research*, 14(8):1548–1554, 2004.
- A. F. Cowman and B. S. Crabb. Invasion of red blood cells by malaria parasites. *Cell*, 124(4):755–766, 2006.
- J. Cox-Singh, T. M. Davis, K.-S. Lee, S. S. Shamsul, A. Matusop, S. Ratnam, H. A. Rahman, D. J. Conway, and B. Singh. Plasmodium knowlesi malaria in humans is widely distributed and potentially life threatening. *Clinical infectious diseases*, 46(2):165–171, 2008.
- H. S. A. Croft and M. Black. Dermatological adverse effects with the antimalarial drug mefloquine: a review of 74 published case reports. 1999.
- J. Daily, D. Scanfeld, N. Pochet, K. Le Roch, D. Plouffe, M. Kamal, O. Sarr, S. Mboup, O. Ndir, D. Wypij, et al. Distinct physiological states of plasmodium falciparum in malaria-infected patients. *Nature*, 450(7172):1091–1095, 2007.
- D. Darghouth, B. Koehl, G. Madalinski, J.-F. Heilier, P. Bovee, Y. Xu, M.-F. Olivier, P. Bartolucci, M. Benkerrou, S. Pissard, et al. Pathophysiology of sickle cell disease is mirrored by the red blood cell metabolome. *Blood*, 117(6):e57–e66, 2011.

- T. F. de Koning-Ward, P. R. Gilson, J. A. Boddey, M. Rug, B. J. Smith, A. T. Papenfuss, P. R. Sanders, R. J. Lundie, A. G. Maier, A. F. Cowman, et al. A newly discovered protein export machine in malaria parasites. *Nature*, 459(7249):945–949, 2009.
- I. de Mas, V. Selivanov, S. Marin, J. Roca, M. Orešič, L. Agius, and M. Cascante. Compartmentation of glycogen metabolism revealed from ^{13}C isotopologue distributions. *BMC Systems Biology*, 5(1):175, 2011.
- E. K. De Silva, A. R. Gehrke, K. Olszewski, I. León, J. S. Chahal, M. L. Bulyk, and M. Llinás. Specific dna-binding by apicomplexan ap2 transcription factors. *Proceedings of the National Academy of Sciences*, 105(24):8393–8398, 2008.
- F. Debierre-Grockiego and R. T. Schwarz. Immunological reactions in response to apicomplexan glycosylphosphatidylinositols. *Glycobiology*, 20(7):801–811, 2010.
- S. Déchamps, M. Maynadier, S. Wein, L. Gannoun-Zaki, E. Maréchal, and H. J. Vial. Rodent and non-rodent malaria parasites differ in their phospholipid metabolic pathways. *Journal of lipid research*, 51(1):81–96, 2010a.
- S. Déchamps, M. Maynadier, S. Wein, L. Gannoun-Zaki, E. Maréchal, and H. J. Vial. Rodent and nonrodent malaria parasites differ in their phospholipid metabolic pathways. *Science Signaling*, 51(1):81, 2010b.
- S. Déchamps, S. Shastri, K. Wengelnik, and H. J. Vial. Glycerophospholipid acquisition in plasmodium –a puzzling assembly of biosynthetic pathways. *International journal for parasitology*, 40(12):1347–1365, 2010c.
- S. Déchamps, K. Wengelnik, L. Berry-Sterkers, R. Cerdan, H. J. Vial, and L. Gannoun-Zaki. The kennedy phospholipid biosynthesis pathways are refractory to genetic disruption in plasmodium berghei and therefore appear essential in blood stages. *Molecular and biochemical parasitology*, 173(2):69–80, 2010d.
- K. W. Deitsch, S. A. Lukehart, and J. R. Stringer. Common strategies for antigenic variation by bacterial, fungal and protozoan pathogens. *Nature Reviews Microbiology*, 7(7):493–503, 2009.
- R. Demel, W. Geurts van Kessel, R. Zwaal, B. Roelofsen, and L. Van Deenen. Relation between various phospholipase actions on human red cell membranes and the interfacial phospholipid pressure in monolayers. *Biochimica et Biophysica Acta (BBA)-Biomembranes*, 406(1):97–107, 1975.
- S. A. Desai, D. J. Krogstad, and E. W. McCleskey. A nutrient-permeable channel on the intraerythrocytic malaria parasite. 1993.

- S. Dhanasekaran, T. M. Doherty, and J. Kenneth. Comparison of different standards for real-time pcr-based absolute quantification. *Journal of immunological methods*, 354(1):34–39, 2010.
- M. T. Dimon, K. Sorber, and J. L. DeRisi. Hmmsplicer: a tool for efficient and sensitive discovery of known and novel splice junctions in rna-seq data. *PLoS One*, 5(11):e13875, 2010.
- A. Divo, T. Geary, N. Davis, and J. Jensen. Nutritional requirements of plasmodium falciparum in culture. i. exogenously supplied dialyzable components necessary for continuous growth. *Journal of Eukaryotic Microbiology*, 32(1):59–64, 1985a.
- A. A. Divo, T. G. Geary, and J. B. Jensen. Oxygen-and time-dependent effects of antibiotics and selected mitochondrial inhibitors on plasmodium falciparum in culture. *Antimicrobial agents and chemotherapy*, 27(1):21–27, 1985b.
- M. T. Duraisingh, T. S. Voss, A. J. Marty, M. F. Duffy, R. T. Good, J. K. Thompson, L. H. Freitas-Junior, A. Scherf, B. S. Crabb, and A. F. Cowman. Heterochromatin silencing and locus repositioning linked to regulation of virulence genes in plasmodium falciparum. *Cell*, 121(1):13–24, 2005.
- S. V. Duy, S. Besteiro, L. Berry, C. Perigaud, F. Bressolle, H. Vial, and I. Lefebvre-Tournier. A quantitative liquid chromatography tandem mass spectrometry method for metabolomic analysis of plasmodium falciparum lipid related metabolites. *Analytica Chimica Acta*, 739(0):47 – 55, 2012.
- T. J. Egan. Recent advances in understanding the mechanism of hemozoin (malaria pigment) formation. *Journal of inorganic biochemistry*, 102(5):1288–1299, 2008.
- N. Elabbadi, M. L. Ancelin, and H. J. Vial. Characterization of phosphatidylinositol synthase and evidence of a polyphosphoinositide cycle in plasmodium-infected erythrocytes. *Molecular and biochemical parasitology*, 63(2):179–192, 1994.
- N. Elabbadi, M. ANCELIN, and H. Vial. Phospholipid metabolism of serine in plasmodium-infected erythrocytes involves phosphatidylserine and direct serine decarboxylation. *Biochem. J*, 324:435–445, 1997.
- B. Elford, R. Pinches, C. Newbold, and J. Ellory. Heterogeneous and substrate-specific membrane transport pathways induced in malaria-infected erythrocytes. *Blood cells*, 16(2-3):433, 1990.
- B. C. Elford, G. Cowan, and D. Ferguson. Parasite-regulated membrane transport processes and metabolic control in malaria-infected erythrocytes. *Biochemical Journal*, 308(Pt 2):361, 1995.

- K. Emoto, H. Inadome, Y. Kanaho, S. Narumiya, and M. Umeda. Local change in phospholipid composition at the cleavage furrow is essential for completion of cytokinesis. *Journal of Biological Chemistry*, 280(45):37901–37907, 2005.
- V. A. Fadok, A. de Cathelineau, D. L. Daleke, P. M. Henson, and D. L. Bratton. Loss of phospholipid asymmetry and surface exposure of phosphatidylserine is required for phagocytosis of apoptotic cells by macrophages and fibroblasts. *Journal of Biological Chemistry*, 276(2):1071–1077, 2001.
- E. Fahy, S. Subramaniam, H. A. Brown, C. K. Glass, A. H. Merrill, R. C. Murphy, C. R. Raetz, D. W. Russell, Y. Seyama, W. Shaw, et al. A comprehensive classification system for lipids. *Journal of lipid research*, 46(5):839–862, 2005.
- S. Fatumo, K. Plaimas, J.-P. Mallm, G. Schramm, E. Adebisi, M. Oswald, R. Eils, and R. König. Estimating novel potential drug targets of plasmodium falciparum by analysing the metabolic network of knock-out strains in silico. *Infection, Genetics and Evolution*, 9(3):351–358, 2009.
- J. E. Feagin. The 6-kb element of plasmodium falciparum encodes mitochondrial cytochrome genes. *Molecular and biochemical parasitology*, 52(1):145–148, 1992.
- D. Fell et al. *Understanding the control of metabolism*. Portland Press Ltd., 1997.
- S.-M. Fendt, J. M. Buescher, F. Rudroff, P. Picotti, N. Zamboni, and U. Sauer. Tradeoff between enzyme and metabolite efficiency maintains metabolic homeostasis upon perturbations in enzyme capacity. *Molecular systems biology*, 6(1), 2010.
- H. M. Ferguson and A. F. Read. Mosquito appetite for blood is stimulated by plasmodium chabaudi infections in themselves and their vertebrate hosts. *Malaria journal*, 3(1):12, 2004.
- L. Florens, M. P. Washburn, J. D. Raine, R. M. Anthony, M. Grainger, J. D. Haynes, J. K. Moch, N. Muster, J. B. Sacci, D. L. Tabb, et al. A proteomic view of the plasmodium falciparum life cycle. *Nature*, 419(6906):520–526, 2002.
- C. Flueck, R. Bartfai, J. Volz, I. Niederwieser, A. M. Salcedo-Amaya, B. T. Alako, F. Ehlgen, S. A. Ralph, A. F. Cowman, Z. Bozdech, et al. Plasmodium falciparum heterochromatin protein 1 marks genomic loci linked to phenotypic variation of exported virulence factors. *PLoS pathogens*, 5(9):e1000569, 2009.
- B. J. Foth, S. A. Ralph, C. J. Tonkin, N. S. Struck, M. Fraunholz, D. S. Roos, A. F. Cowman, and G. I. McFadden. Dissecting apicoplast targeting in the malaria parasite plasmodium falciparum. *Science*, 299(5607):705–708, 2003.

- B. J. Foth, N. Zhang, S. Mok, P. R. Preiser, Z. Bozdech, et al. Quantitative protein expression profiling reveals extensive post-transcriptional regulation and post-translational modifications in schizont-stage malaria parasites. *Genome Biol*, 9(12):R177, 2008.
- B. J. Foth, N. Zhang, B. K. Chaal, S. K. Sze, P. R. Preiser, and Z. Bozdech. Quantitative time-course profiling of parasite and host cell proteins in the human malaria parasite *Plasmodium falciparum*. *Molecular & Cellular Proteomics*, 10(8), 2011.
- J. F. Friedman, A. M. Kwena, L. B. Mirel, S. K. Kariuki, D. J. Terlouw, P. A. Phillips-Howard, W. A. Hawley, B. L. Nahlen, Y. P. Shi, and F. O. Ter Kuile. Malaria and nutritional status among pre-school children: results from cross-sectional surveys in western Kenya. *The American journal of tropical medicine and hygiene*, 73(4):698–704, 2005.
- K. Gandhi, M. A. Thera, D. Coulibaly, K. Traoré, A. B. Guindo, O. K. Doumbo, S. Takala-Harrison, and C. V. Plowe. Next generation sequencing to detect variation in the *Plasmodium falciparum* circumsporozoite protein. *The American journal of tropical medicine and hygiene*, 86(5):775, 2012.
- K. Ganesan, N. Ponmee, L. Jiang, J. W. Fowble, J. White, S. Kamchonwongpaisan, Y. Yuthavong, P. Wilairat, and P. K. Rathod. A genetically hard-wired metabolic transcriptome in *Plasmodium falciparum* fails to mount protective responses to lethal antifolates. *PLoS pathogens*, 4(11):e1000214, 2008.
- M. J. Gardner, N. Hall, E. Fung, O. White, M. Berriman, R. W. Hyman, J. M. Carlton, A. Pain, K. E. Nelson, S. Bowman, et al. Genome sequence of the human malaria parasite *Plasmodium falciparum*. *Nature*, 419(6906):498–511, 2002a.
- M. J. Gardner, S. J. Shallom, J. M. Carlton, S. L. Salzberg, V. Nene, A. Shoaibi, A. Ciecko, J. Lynn, M. Rizzo, B. Weaver, et al. Sequence of *Plasmodium falciparum* chromosomes 2, 10, 11 and 14. *Nature*, 419(6906):531–534, 2002b.
- C. Gelhaus, J. Fritsch, E. Krause, and M. Leippe. Fractionation and identification of proteins by 2-de and ms: towards a proteomic analysis of *Plasmodium falciparum*. *Proteomics*, 5(16):4213–4222, 2005.
- S. Ghaemmaghami, W.-K. Huh, K. Bower, R. W. Howson, A. Belle, N. Dephoure, E. K. O’Shea, and J. S. Weissman. Global analysis of protein expression in yeast. *Nature*, 425(6959):737–741, 2003.
- A. Ghazalpour, B. Bennett, V. A. Petyuk, L. Orozco, R. Hagopian, I. N. Mungrue, C. R. Farber, J. Sinsheimer, H. M. Kang, N. Furlotte, et al. Comparative analysis of proteome and transcriptome variation in mouse. *PLoS genetics*, 7(6):e1001393, 2011.

- Y. Gibon, B. Usadel, O. E. Blaesing, B. Kamlage, M. Hoehne, R. Trethewey, and M. Stitt. Integration of metabolite with transcript and enzyme activity profiling during diurnal cycles in arabidopsis rosettes. *Genome biology*, 7(8):R76, 2006.
- P. R. Gilson, T. Nebl, D. Vukcevic, R. L. Moritz, T. Sargeant, T. P. Speed, L. Schofield, and B. S. Crabb. Identification and stoichiometry of glycosylphosphatidylinositol-anchored membrane proteins of the human malaria parasite plasmodium falciparum. *Molecular & Cellular Proteomics*, 5(7):1286–1299, 2006.
- H. Ginsburg. Progress in in silico functional genomics: the malaria metabolic pathways database. *Trends in parasitology*, 22(6):238–240, 2006.
- D. Goldberg. Hemoglobin degradation. In *Malaria: Drugs, Disease and Post-genomic Biology*, pages 275–291. Springer, 2005.
- D. Goldberg, A. Slater, A. Cerami, and G. Henderson. Hemoglobin degradation in the malaria parasite plasmodium falciparum: an ordered process in a unique organelle. *Proceedings of the National Academy of Sciences*, 87(8):2931, 1990.
- M. F. Good and D. L. Doolan. Malaria vaccine design: immunological considerations. *Immunity*, 33(4):555–566, 2010.
- A. Gorban and O. Radulescu. Dynamic and static limitation in reaction networks, revisited . In D. W. Guy B. Marin and G. S. Yablonsky, editors, *Advances in Chemical Engineering - Mathematics in Chemical Kinetics and Engineering*, volume 34 of *Advances in Chemical Engineering*, pages 103–173. Elsevier, 2008. doi: 10.1016/S0065-2377(08)00002-1.
- B. M. Greenwood, D. A. Fidock, D. E. Kyle, S. H. Kappe, P. L. Alonso, F. H. Collins, and P. E. Duffy. Malaria: progress, perils, and prospects for eradication. *The Journal of clinical investigation*, 118(4):1266, 2008.
- A. P. Gupta, W. H. Chin, L. Zhu, S. Mok, Y.-H. Luah, E.-H. Lim, and Z. Bozdech. Dynamic epigenetic regulation of gene expression during the life cycle of malaria parasite plasmodium falciparum. *PLoS pathogens*, 9(2):e1003170, 2013.
- S. Gupta, M. Thapar, W. Wernsdorfer, and A. Björkman. In vitro interactions of artemisinin with atovaquone, quinine, and mefloquine against plasmodium falciparum. *Antimicrobial agents and chemotherapy*, 46(5):1510–1515, 2002.
- K. Haldar. Sphingolipid synthesis and membrane formation by plasmodium. *Trends in Cell Biology*, 6(10):398–405, 1996.

- K. Haldar and N. Mohandas. Erythrocyte remodeling by malaria parasites. *Current opinion in hematology*, 14(3):203–209, 2007.
- N. Hall, M. Karras, J. D. Raine, J. M. Carlton, T. W. Kooij, M. Berriman, L. Florens, C. S. Janssen, A. Pain, G. K. Christophides, et al. A comprehensive survey of the plasmodium life cycle by genomic, transcriptomic, and proteomic analyses. *Science*, 307(5706):82–86, 2005.
- E. Hanssen, C. Knoechel, M. Dearnley, M. W. Dixon, M. Le Gros, C. Larabell, and L. Tilley. Soft x-ray microscopy analysis of cell volume and hemoglobin content in erythrocytes infected with asexual and sexual stages of *Plasmodium falciparum*. *Journal of structural biology*, 177(2):224–232, 2012.
- R. E. Hayward, J. L. DeRisi, S. Alfadhli, D. C. Kaslow, P. O. Brown, and P. K. Rathod. Shotgun dna microarrays and stage-specific gene expression in *Plasmodium falciparum* malaria. *Molecular Microbiology*, 35(1):6–14, 2000.
- R. J. Heath and C. O. Rock. Fatty acid biosynthesis as a target for novel antibacterials. *Current opinion in investigational drugs (London, England: 2000)*, 5(2):146, 2004.
- V. Henri. Théorie générale de l'action de quelques diastases. *CR Acad. Sci. Paris*, 135:916–919, 1902.
- A. V. Hill. Aspects of genetic susceptibility to human infectious diseases. *Annu. Rev. Genet.*, 40:469–486, 2006.
- N. L. Hiller, S. Bhattacharjee, C. van Ooij, K. Liolios, T. Harrison, C. Lopez-Estrano, and K. Haldar. A host-targeting signal in virulence proteins reveals a secretome in malarial infection. *Science*, 306(5703):1934–1937, 2004.
- A. N. Hoang, K. K. Ncokazi, K. A. de Villiers, D. W. Wright, and T. J. Egan. Crystallization of synthetic haemozoin ([small beta]-haematin) nucleated at the surface of lipid particles. *Dalton Trans.*, 39:1235–1244, 2010.
- G. Holz Jr. Lipids and the malarial parasite. *Bulletin of the World Health Organization*, 55(2-3):237, 1977.
- J. Ihmels, R. Levy, and N. Barkai. Principles of transcriptional control in the metabolic network of *Saccharomyces cerevisiae*. *Nature biotechnology*, 22(1):86–92, 2003.
- N. T. Ingolia, G. A. Brar, S. Rouskin, A. M. McGeachy, and J. S. Weissman. The ribosome profiling strategy for monitoring translation in vivo by deep sequencing of ribosome-protected mrna fragments. *nature protocols*, 7(8):1534–1550, 2012.

- E. S. Istvan and D. E. Goldberg. Distal substrate interactions enhance plasmepsin activity. *Journal of Biological Chemistry*, 280(8):6890–6896, 2005.
- K. E. Jackson, S. Habib, M. Frugier, R. Hoen, S. Khan, J. S. Pham, L. R. d. Pouplana, M. Royo, M. A. Santos, A. Sharma, et al. Protein translation in plasmodium parasites. *Trends in parasitology*, 27(10):467–476, 2011.
- H. Jiang, M. Yi, J. Mu, L. Zhang, A. Ivens, L. J. Klimczak, Y. Huyen, R. M. Stephens, and X.-z. Su. Detection of genome-wide polymorphisms in the at-rich plasmodium falciparum genome using a high-density microarray. *Bmc Genomics*, 9(1):398, 2008.
- Y. Jin, C. Kebaier, and J. Vanderberg. Direct microscopic quantification of dynamics of plasmodium berghei sporozoite transmission from mosquitoes to mice. *Infection and immunity*, 75(11):5532–5539, 2007.
- M. L. Jones, E. L. Kitson, and J. C. Rayner. Plasmodium falciparum erythrocyte invasion: A conserved myosin associated complex. *Molecular and biochemical parasitology*, 147(1):74–84, 2006.
- M. Kanehisa and S. Goto. Kegg: kyoto encyclopedia of genes and genomes. *Nucleic acids research*, 28(1):27–30, 2000.
- J. Kanfer and E. P. Kennedy. Metabolism and function of bacterial lipids ii. biosynthesis of phospholipids in escherichia coli. *Journal of Biological Chemistry*, 239(6):1720–1726, 1964.
- A. Kantele and T. S. Jokiranta. Review of cases with the emerging fifth human malaria parasite, plasmodium knowlesi. *Clinical infectious diseases*, 52(11):1356–1362, 2011.
- K. Katayama, T. Sato, T. Arai, H. Amao, Y. Ohta, T. Ozawa, P. Kenyon, R. Hickson, and H. Tazaki. Non-targeted analyses of animal plasma: betaine and choline represent the nutritional and metabolic status. *Journal of animal physiology and animal nutrition*, 97(1):119–125, 2013.
- C. Kebaier, T. Voza, and J. Vanderberg. Kinetics of mosquito-injected plasmodium sporozoites in mice: fewer sporozoites are injected into sporozoite-immunized mice. *PLoS pathogens*, 5(4):e1000399, 2009.
- E. P. Kennedy and S. B. Weiss. The function of cytidine coenzymes in the biosynthesis of phospholipides. *Journal of Biological Chemistry*, 222(1):193–214, 1956.
- C. Kidgell, S. K. Volkman, J. Daily, J. O. Borevitz, D. Plouffe, Y. Zhou, J. R. Johnson, K. G. Le Roch, O. Sarr, O. Ndir, et al. A systematic map of genetic variation in plasmodium falciparum. *PLoS pathogens*, 2(6):e57, 2006.

- D. Kim, G. Pertea, C. Trapnell, H. Pimentel, R. Kelley, and S. L. Salzberg. Tophat2: accurate alignment of transcriptomes in the presence of insertions, deletions and gene fusions. *Genome biology*, 14(4):R36, 2013.
- K. Kirk. Channels and transporters as drug targets in the plasmodium-infected erythrocyte. *Acta tropica*, 89(3):285–298, 2004.
- K. Kirk and K. J. Saliba. Targeting nutrient uptake mechanisms in plasmodium. *Current drug targets*, 8(1):75–88, 2007.
- K. Kirk, H. Wong, B. Elford, C. Newbold, and J. Ellory. Enhanced choline and rb+ transport in human erythrocytes infected with the malaria parasite plasmodium falciparum. *Biochemical Journal*, 278 (Pt 2):521, 1991.
- S. Klant, J. Stelling, M. Ginkel, and E. D. Gilles. Fluxanalyzer: exploring structure, pathways, and flux distributions in metabolic networks on interactive flux maps. *Bioinformatics*, 19(2):261–269, 2003.
- S. A. Kyes, Z. Christodoulou, A. Raza, P. Horrocks, R. Pinches, J. A. Rowe, and C. I. Newbold. A well-conserved plasmodium falciparum var gene shows an unusual stage-specific transcript pattern. *Molecular microbiology*, 48(5):1339–1348, 2003.
- D. J. LaCount, M. Vignali, R. Chettier, A. Phansalkar, R. Bell, J. R. Hesselberth, L. W. Schoenfeld, I. Ota, S. Sahasrabudhe, C. Kurschner, et al. A protein interaction network of the malaria parasite plasmodium falciparum. *Nature*, 438(7064):103–107, 2005.
- Z. Lai, J. Jing, C. Aston, V. Clarke, J. Apodaca, E. T. Dimalanta, D. J. Carucci, M. J. Gardner, B. Mishra, T. S. Anantharaman, et al. A shotgun optical map of the entire plasmodium falciparum genome. *nature genetics*, 23(3):309–313, 1999.
- V. Lakshmanan, K. Y. Rhee, and J. P. Daily. Metabolomics and malaria biology. *Molecular and biochemical parasitology*, 175(2):104–111, 2011.
- E. Lasonder, Y. Ishihama, J. S. Andersen, A. M. Vermunt, A. Pain, R. W. Sauerwein, W. M. Eling, N. Hall, A. P. Waters, H. G. Stunnenberg, et al. Analysis of the plasmodium falciparum proteome by high-accuracy mass spectrometry. *Nature*, 419(6906):537–542, 2002.
- K. G. Le Roch, Y. Zhou, P. L. Blair, M. Grainger, J. K. Moch, J. D. Haynes, P. De la Vega, A. A. Holder, S. Batalov, D. J. Carucci, et al. Discovery of gene function by expression profiling of the malaria parasite life cycle. *Science*, 301(5639):1503–1508, 2003.

- K. G. Le Roch, J. R. Johnson, L. Florens, Y. Zhou, A. Santrosyan, M. Grainger, S. F. Yan, K. C. Williamson, A. A. Holder, D. J. Carucci, et al. Global analysis of transcript and protein levels across the plasmodium falciparum life cycle. *Genome research*, 14(11):2308–2318, 2004.
- K. G. Le Roch, J. R. Johnson, H. Ahiboh, D.-W. D. Chung, J. Prudhomme, D. Plouffe, K. Henson, Y. Zhou, W. Witola, J. R. Yates, et al. A systematic approach to understand the mechanism of action of the bisthiazolium compound t4 on the human malaria parasite, plasmodium falciparum. *BMC genomics*, 9(1):513, 2008.
- K. G. Le Roch, D.-W. CHUNG, and N. Ponts. Genomics and integrated systems biology in plasmodium falciparum: a path to malaria control and eradication. *Parasite immunology*, 34(2-3):50–60, 2012.
- A. M. Lehane, K. J. Saliba, R. J. Allen, and K. Kirk. Choline uptake into the malaria parasite is energized by the membrane potential. *Biochemical and biophysical research communications*, 320(2):311–317, 2004.
- V. Lew. A choline “vacuum cleaner”. *Blood*, 104(10):3006–3007, 2004.
- V. L. Lew, T. Tiffert, and H. Ginsburg. Excess hemoglobin digestion and the osmotic stability of plasmodium falciparum-infected red blood cells. *Blood*, 101(10):4189–4194, 2003.
- V. L. Lew, L. Macdonald, H. Ginsburg, M. Krugliak, and T. Tiffert. Excess haemoglobin digestion by malaria parasites: a strategy to prevent premature host cell lysis. *Blood Cells, Molecules, and Diseases*, 32(3):353–359, 2004.
- C. Li, M. Donizelli, N. Rodriguez, H. Dharuri, L. Endler, V. Chelliah, L. Li, E. He, A. Henry, M. I. Stefan, et al. Biomodels database: An enhanced, curated and annotated resource for published quantitative kinetic models. *BMC systems biology*, 4(1):92, 2010.
- F. Li, L. Sonbuchner, S. A. Kyes, C. Epp, and K. W. Deitsch. Nuclear non-coding rnas are transcribed from the centromeres of plasmodium falciparum and are associated with centromeric chromatin. *Journal of Biological Chemistry*, 283(9):5692–5698, 2008a.
- R. Li, Y. Li, K. Kristiansen, and J. Wang. Soap: short oligonucleotide alignment program. *Bioinformatics*, 24(5):713–714, 2008b.
- R. Li, C. Yu, Y. Li, T.-W. Lam, S.-M. Yiu, K. Kristiansen, and J. Wang. Soap2: an improved ultrafast tool for short read alignment. *Bioinformatics*, 25(15):1966–1967, 2009.
- Z. Li and D. E. Vance. Thematic review series: glycerolipids. phosphatidylcholine and choline homeostasis. *Journal of lipid research*, 49(6):1187–1194, 2008.

- L.-Y. Lian, M. Al-Helal, A. M. Roslainsi, N. Fisher, P. G. Bray, S. A. Ward, G. A. Biagini, et al. Glycerol: an unexpected major metabolite of energy metabolism by the human malaria parasite. *Malar J*, 8(38):1–4, 2009.
- M. Llinas, Z. Bozdech, E. D. Wong, A. T. Adai, and J. L. DeRisi. Comparative whole genome transcriptome analysis of three plasmodium falciparum strains. *Nucleic acids research*, 34(4):1166–1173, 2006.
- I. M. López-Lara and O. Geiger. Novel pathway for phosphatidylcholine biosynthesis in bacteria associated with eukaryotes. *Journal of biotechnology*, 91(2):211–221, 2001.
- J.-J. Lopez-Rubio, L. Mancio-Silva, and A. Scherf. Genome-wide analysis of heterochromatin associates clonally variant gene regulation with perinuclear repressive centers in malaria parasites. *Cell host & microbe*, 5(2):179–190, 2009.
- A. Lykidis. Comparative genomics and evolution of eukaryotic phospholipid biosynthesis. *Progress in lipid research*, 46(3):171–199, 2007.
- M. J. Mackinnon, J. Li, S. Mok, M. M. Kortok, K. Marsh, P. R. Preiser, and Z. Bozdech. Comparative transcriptional and genomic analysis of plasmodium falciparum field isolates. *PLoS pathogens*, 5(10):e1000644, 2009.
- C. A. Maher, N. Palanisamy, J. C. Brenner, X. Cao, S. Kalyana-Sundaram, S. Luo, I. Khrebtukova, T. R. Barrette, C. Grasso, J. Yu, et al. Chimeric transcript discovery by paired-end transcriptome sequencing. *Proceedings of the National Academy of Sciences*, 106(30):12353–12358, 2009.
- A. G. Maier, M. Rug, M. T. O’Neill, M. Brown, S. Chakravorty, T. Szeszak, J. Chesson, Y. Wu, K. Hughes, R. L. Coppel, et al. Exported proteins required for virulence and rigidity of plasmodium falciparum-infected human erythrocytes. *Cell*, 134(1):48–61, 2008.
- G. R. Mair, J. A. Braks, L. S. Garver, J. C. Wiegant, N. Hall, R. W. Dirks, S. M. Khan, G. Dimopoulos, C. J. Janse, and A. P. Waters. Regulation of sexual development of plasmodium by translational repression. *Science*, 313(5787):667–669, 2006.
- C. B. Mamoun, I. Y. Gluzman, C. Hott, S. K. MacMillan, A. S. Amarakone, D. L. Anderson, J. M.-R. Carlton, J. B. Dame, D. Chakrabarti, R. K. Martin, et al. Co-ordinated programme of gene expression during asexual intraerythrocytic development of the human malaria parasite plasmodium falciparum revealed by microarray analysis. *Molecular microbiology*, 39(1):26–36, 2001.
- E. Maréchal, N. Azzouz, C. S. de Macedo, M. A. Block, J. E. Feagin, R. T. Schwarz, and J. Joyard. Synthesis of chloroplast galactolipids in apicomplexan parasites. *Eukaryotic cell*, 1(4):653–656, 2002.

- A. Marintchev and G. Wagner. Translation initiation: structures, mechanisms and evolution. *Quarterly reviews of biophysics*, 37(3):197–284, 2004.
- M. Marti, R. T. Good, M. Rug, E. Knuepfer, and A. F. Cowman. Targeting malaria virulence and remodeling proteins to the host erythrocyte. *Science*, 306(5703):1930–1933, 2004.
- R. E. Martin and K. Kirk. Transport of the essential nutrient isoleucine in human erythrocytes infected with the malaria parasite plasmodium falciparum. *Blood*, 109(5):2217–2224, 2007.
- R. E. Martin, R. V. Marchetti, A. I. Cowan, S. M. Howitt, S. Bröer, and K. Kirk. Chloroquine transport via the malaria parasites chloroquine resistance transporter. *science*, 325(5948):1680–1682, 2009.
- S. K. Martin, M. Jett, and I. Schneider. Correlation of phosphoinositide hydrolysis with exflagellation in the malaria microgametocyte. *The Journal of parasitology*, pages 371–378, 1994.
- D. G. Mayer, J. Cofie, L. Jiang, D. L. Hartl, E. Tracy, J. Kabat, L. H. Mendoza, and L. H. Miller. Glycophorin b is the erythrocyte receptor of plasmodium falciparum erythrocyte-binding ligand, ebl-1. *Proceedings of the National Academy of Sciences*, 106(13):5348–5352, 2009.
- J. Mazumdar and B. Striepen. Make it or take it: fatty acid metabolism of apicomplexan parasites. *Eukaryotic cell*, 6(10):1727–1735, 2007.
- M. Mehta, H. M. Sonawat, and S. Sharma. Glycolysis in plasmodium falciparum results in modulation of host enzyme activities. *Journal of vector borne diseases*, 43(3):95, 2006.
- A. Menon and V. Stevens. Phosphatidylethanolamine is the donor of the ethanolamine residue linking a glycosylphosphatidylinositol anchor to protein. *Journal of Biological Chemistry*, 267(22):15277–15280, 1992.
- L. Michaelis and M. L. Menten. The kinetics of the inversion effect. *Biochem. Z*, 49:333–369, 1913a.
- L. Michaelis and M. L. Menten. Die kinetik der invertinwirkung. *Biochem. z*, 49(333-369):352, 1913b.
- L. H. Miller, D. I. Baruch, K. Marsh, and O. K. Doumbo. The pathogenic basis of malaria. *Nature*, 415(6872):673–679, 2002.
- T. Mita, K. Tanabe, and K. Kita. Spread and evolution of plasmodium falciparum drug resistance. *Parasitology international*, 58(3):201–209, 2009.
- T. Mitamura, K. Hanada, E. Ko-Mitamura, M. Nishijima, and T. Horii. Serum factors governing intraerythrocytic development and cell cycle progression of plasmodium falciparum. *Parasitology international*, 49(3):219–229, 2000.

- B. W. Mok, U. Ribacke, N. Rasti, F. Kironde, Q. Chen, P. Nilsson, and M. Wahlgren. Default pathway of var2csa switching and translational repression in plasmodium falciparum. *PLoS One*, 3(4):e1982, 2008.
- G. Moll, H. Vial, M. Ancelin, J. Op den Kamp, B. Roelofsen, and L. Van Deenen. Phospholipid uptake by plasmodium knowlesi infected erythrocytes. *FEBS letters*, 232(2):341–346, 1988.
- A. Mortazavi, B. A. Williams, K. McCue, L. Schaeffer, and B. Wold. Mapping and quantifying mammalian transcriptomes by rna-seq. *Nature methods*, 5(7):621–628, 2008.
- T. Mourier, C. Carret, S. Kyes, Z. Christodoulou, P. P. Gardner, D. C. Jeffares, R. Pinches, B. Barrell, M. Berriman, S. Griffiths-Jones, et al. Genome-wide discovery and verification of novel structured rnas in plasmodium falciparum. *Genome research*, 18(2):281–292, 2008.
- J. Mu, K. B. Seydel, A. Bates, and X.-Z. Su. Recent progress in functional genomic research in plasmodium falciparum. *Current genomics*, 11(4):279, 2010.
- S. Münter, B. Sabass, C. Selhuber-Unkel, M. Kudryashev, S. Hegge, U. Engel, J. P. Spatz, K. Matuschewski, U. S. Schwarz, and F. Frischknecht. Plasmodium sporozoite motility is modulated by the turnover of discrete adhesion sites. *Cell host & microbe*, 6(6):551–562, 2009.
- V. Muralidharan, A. Oksman, M. Iwamoto, T. Wandless, and D. Goldberg. Asparagine repeat function in a plasmodium falciparum protein assessed via a regulatable fluorescent affinity tag. *Proceedings of the National Academy of Sciences*, 108(11):4411–4416, 2011.
- S. C. Murphy, N. Luisa Hiller, T. Harrison, J. W. Lomasney, N. Mohandas, and K. Haldar. Lipid rafts and malaria parasite infection of erythrocytes (review). *Molecular membrane biology*, 23(1):81–88, 2006.
- J. N Burrows, K. Chibale, and T. NC Wells. The state of the art in anti-malarial drug discovery and development. *Current topics in medicinal chemistry*, 11(10):1226–1254, 2011.
- B. Nadjm and R. H. Behrens. Malaria:: An update for physicians. *Infectious disease clinics of North America*, 26(2):243–259, 2012.
- J. K. Nicholson, J. C. Lindon, and E. Holmes. 'metabonomics': understanding the metabolic responses of living systems to pathophysiological stimuli via multivariate statistical analysis of biological nmr spectroscopic data. *Xenobiotica*, 29(11):1181–1189, 1999.
- O. Nicolas, D. Margout, N. Taudon, S. Wein, M. Calas, H. J. Vial, and F. M. Bressolle. Pharmacological properties of a new antimalarial bithiazolium salt, t3, and a corresponding prodrug, te3. *Antimicrobial agents and chemotherapy*, 49(9):3631–3639, 2005.

- M. Nikolov, C. Schmidt, and H. Urlaub. Quantitative mass spectrometry-based proteomics: An overview. In *Quantitative Methods in Proteomics*, pages 85–100. Springer, 2012.
- Z. Ning, A. J. Cox, and J. C. Mullikin. Ssaha: a fast search method for large dna databases. *Genome research*, 11(10):1725–1729, 2001.
- N. Nirmalan, P. F. Sims, and J. E. Hyde. Quantitative proteomics of the human malaria parasite plasmodium falciparum and its application to studies of development and inhibition. *Molecular microbiology*, 52(4):1187–1199, 2004a.
- N. Nirmalan, P. F. Sims, and J. E. Hyde. Translational up-regulation of antifolate drug targets in the human malaria parasite *Plasmodium falciparum* upon challenge with inhibitors. *Molecular and biochemical parasitology*, 136(1):63–70, 2004b.
- T. Nishino, A. Yachie-Kinoshita, A. Hirayama, T. Soga, M. Suematsu, and M. Tomita. In silico modeling and metabolome analysis of long-stored erythrocytes to improve blood storage methods. *Journal of biotechnology*, 144(3):212–223, 2009.
- K. L. Olszewski and M. Llinás. Extraction of hydrophilic metabolites from plasmodium falciparum-infected erythrocytes for metabolomic analysis. In *Malaria*, pages 259–266. Springer, 2013.
- K. L. Olszewski, J. M. Morrissey, D. Wilinski, J. M. Burns, A. B. Vaidya, J. D. Rabinowitz, and M. Llinás. Host-parasite interactions revealed by plasmodium falciparum metabolomics. *Cell host & microbe*, 5(2):191–199, 2009.
- K. L. Olszewski, M. W. Mather, J. M. Morrissey, B. A. Garcia, A. B. Vaidya, J. D. Rabinowitz, and M. Llinás. Branched tricarboxylic acid metabolism in plasmodium falciparum. *Nature*, 466(7307):774–778, 2010.
- S.-E. Ong and M. Mann. Mass spectrometry-based proteomics turns quantitative. *Nature chemical biology*, 1(5):252–262, 2005.
- T. D. Otto, D. Wilinski, S. Assefa, T. M. Keane, L. R. Sarry, U. Böhme, J. Lemieux, B. Barrell, A. Pain, M. Berriman, et al. New insights into the blood-stage transcriptome of plasmodium falciparum using rna-seq. *Molecular microbiology*, 76(1):12–24, 2010.
- H. J. Painter, J. M. Morrissey, M. W. Mather, and A. B. Vaidya. Specific role of mitochondrial electron transport in blood-stage plasmodium falciparum. *Nature*, 446(7131):88–91, 2007.
- I. Pankova-Kholmyansky and E. Flescher. Potential new antimalarial chemotherapeutics based on sphingolipid metabolism. *Chemotherapy*, 52(4):205–209, 2006.

- S. L. Perkins. Molecular systematics of the three mitochondrial protein-coding genes of malaria parasites: Corroborative and new evidence for the origins of human malaria: Full-length research article. *Mitochondrial DNA*, 19(6):471–478, 2008.
- G. Pessi, G. Kociubinski, and C. Mamoun. A pathway for phosphatidylcholine biosynthesis in plasmodium falciparum involving phosphoethanolamine methylation. *Proceedings of the National Academy of Sciences of the United States of America*, 101(16):6206, 2004.
- G. Pessi, J. Choi, J. Reynolds, D. Voelker, and C. Mamoun. In vivo evidence for the specificity of plasmodium falciparum phosphoethanolamine methyltransferase and its coupling to the kennedy pathway. *Journal of Biological Chemistry*, 280(13):12461, 2005.
- M. Petter, I. Bonow, and M.-Q. Klinkert. Diverse expression patterns of subgroups of the rif multigene family during plasmodium falciparum gametocytogenesis. *PLoS One*, 3(11):e3779, 2008.
- S. K. Pierce and L. H. Miller. World malaria day 2009: what malaria knows about the immune system that immunologists still do not. *The Journal of Immunology*, 182(9):5171–5177, 2009.
- P. Pino, S. Sebastian, E. Kim, E. Bush, M. Brochet, K. Volkman, E. Kozlowski, M. Llinás, O. Billker, and D. Soldati-Favre. A tetracycline-repressible transactivator system to study essential genes in malaria parasites. *Cell Host & Microbe*, 12(6):824–834, 2012.
- J. M. Pisciotta and D. Sullivan. Hemozoin: oil versus water. *Parasitology international*, 57(2):89–96, 2008.
- G. Plata, T.-L. Hsiao, K. L. Olszewski, M. Llinás, and D. Vitkup. Reconstruction and flux-balance analysis of the plasmodium falciparum metabolic network. *Molecular systems biology*, 6(1), 2010.
- M. Prudêncio, A. Rodriguez, and M. M. Mota. The silent path to thousands of merozoites: the plasmodium liver stage. *Nature Reviews Microbiology*, 4(11):849–856, 2006.
- S. Pukrittayakamee, M. Imwong, P. Singhasivanon, K. Stepniewska, N. J. Day, and N. J. White. Effects of different antimalarial drugs on gametocyte carriage in p. vivax malaria. *The American journal of tropical medicine and hygiene*, 79(3):378–384, 2008.
- A. Raabe, K. Wengelnik, O. Billker, and H. Vial. Multiple roles for plasmodium berghei phosphoinositide-specific phospholipase c in regulating gametocyte activation and differentiation. *Cellular microbiology*, 2011.
- C. A. Raabe, C. P. Sanchez, G. Randau, T. Robeck, B. V. Skryabin, S. V. Chinni, M. Kube, R. Reinhardt, G. H. Ng, R. Manickam, et al. A global view of the nonprotein-coding transcriptome in plasmodium falciparum. *Nucleic acids research*, 38(2):608–617, 2010.

- S. A. Ralph, G. G. van Dooren, R. F. Waller, M. J. Crawford, M. J. Fraunholz, B. J. Foth, C. J. Tonkin, D. S. Roos, and G. I. McFadden. Tropical infectious diseases: metabolic maps and functions of the plasmodium falciparum apicoplast. *Nature Reviews Microbiology*, 2(3):203–216, 2004.
- D. J. Rawlings, H. Fujioka, M. Fried, D. B. Keister, M. Aikawa, and D. C. Kaslow. α -tubulin ii is a male-specific protein in plasmodium falciparum. *Molecular and biochemical parasitology*, 56(2):239–250, 1992.
- W. J. Ray Jr. Rate-limiting step: a quantitative definition. application to steady-state enzymic systems. *Biochemistry*, 22(20):4625–4637, 1983.
- C. Reder. Metabolic control theory: a structural approach. *Journal of Theoretical Biology*, 135(2):175–201, 1988.
- S. M. Rich, F. H. Leendertz, G. Xu, M. LeBreton, C. F. Djoko, M. N. Aminake, E. E. Takang, J. L. Diffo, B. L. Pike, B. M. Rosenthal, et al. The origin of malignant malaria. *Proceedings of the National Academy of Sciences*, 106(35):14902–14907, 2009.
- D. Rontein, I. Nishida, G. Tashiro, K. Yoshioka, W. Wu, D. Voelker, G. Basset, and A. Hanson. Plants synthesize ethanolamine by direct decarboxylation of serine using a pyridoxal phosphate enzyme. *Journal of Biological Chemistry*, 276(38):35523, 2001.
- F. Roux-Dalvai, A. G. de Peredo, C. Simó, L. Guerrier, D. Bouyssié, A. Zanella, A. Citterio, O. Burlet-Schiltz, E. Boschetti, P. G. Righetti, et al. Extensive analysis of the cytoplasmic proteome of human erythrocytes using the peptide ligand library technology and advanced mass spectrometry. *Molecular & Cellular Proteomics*, 7(11):2254–2269, 2008.
- N. Rovira-Graells, A. P. Gupta, E. Planet, V. M. Crowley, S. Mok, L. R. de Poupiana, P. R. Preiser, Z. Bozdech, and A. Cortés. Transcriptional variation in the malaria parasite plasmodium falciparum. *Genome research*, 22(5):925–938, 2012.
- J. A. Rowe, A. Claessens, R. A. Corrigan, and M. Arman. falciparum-infected erythrocytes to human cells: molecular mechanisms and therapeutic implications. 2009.
- J. B. Sacci Jr, J. Ribeiro, F. Huang, U. Alam, J. A. Russell, P. L. Blair, A. Witney, D. J. Carucci, A. F. Azad, and J. C. Aguiar. Transcriptional analysis of in vivo plasmodium yoelii liver stage gene expression. *Molecular and biochemical parasitology*, 142(2):177–183, 2005.
- A. M. Salcedo-Amaya, M. A. van Driel, B. T. Alako, M. B. Trelle, A. M. van den Elzen, A. M. Cohen, E. M. Janssen-Megens, M. van de Vegte-Bolmer, R. R. Selzer, A. L. Iniguez, et al. Dynamic histone h3 epigenome marking during the intraerythrocytic cycle of plasmodium falciparum. *Proceedings of the National Academy of Sciences*, 106(24):9655–9660, 2009.

- K. J. Saliba, P. I. Folb, and P. J. Smith. Role for the plasmodium falciparum digestive vacuole in chloroquine resistance. *Biochemical pharmacology*, 56(3):313–320, 1998.
- K. J. Saliba, R. E. Martin, A. Bröer, R. I. Henry, C. S. McCarthy, M. J. Downie, R. J. Allen, K. A. Mullin, G. I. McFadden, S. Bröer, et al. Sodium-dependent uptake of inorganic phosphate by the intracellular malaria parasite. *Nature*, 443(7111):582–585, 2006.
- M. Salman, J. T. Lonsdale, G. S. Besra, and P. J. Brennan. Phosphatidylinositol synthesis in mycobacteria. *Biochimica et Biophysica Acta (BBA)-Molecular and Cell Biology of Lipids*, 1436(3):437–450, 1999.
- T. Y. Sam-Yellowe, L. Florens, J. R. Johnson, T. Wang, J. A. Drazba, K. G. Le Roch, Y. Zhou, S. Batalov, D. J. Carucci, E. A. Winzeler, et al. A plasmodium gene family encoding maurel’s cleft membrane proteins: structural properties and expression profiling. *Genome research*, 14(6):1052–1059, 2004.
- A. Scherf, J. J. Lopez-Rubio, and L. Riviere. Antigenic variation in plasmodium falciparum. *Annu. Rev. Microbiol.*, 62:445–470, 2008.
- I. W. Sherman and J. R. Greenan. Altered red cell membrane fluidity during schizogonic development of malarial parasites (plasmodium falciparum and p. lophurae). *Transactions of the Royal Society of Tropical Medicine and Hygiene*, 78(5):641–644, 1984.
- L. Shi, L. H. Reid, W. D. Jones, R. Shippy, J. A. Warrington, S. C. Baker, P. J. Collins, F. De Longueville, E. S. Kawasaki, K. Y. Lee, et al. The microarray quality control (maq) project shows inter-and intraplatform reproducibility of gene expression measurements. *Nature biotechnology*, 24(9):1151–1161, 2006.
- J. L. Shock, K. F. Fischer, and J. L. DeRisi. Whole-genome analysis of mrna decay in plasmodium falciparum reveals a global lengthening of mrna half-life during the intra-erythrocytic development cycle. *Genome Biol*, 8(7):R134, 2007.
- A. Siau, F. S. Touré, O. Ouwe-Missi-Oukem-Boyer, L. Cicéron, N. Mahmoudi, C. Vaquero, P. Froidsard, U. Bisvigou, S. Bisser, J.-Y. Coppée, et al. Whole-transcriptome analysis of plasmodium falciparum field isolates: identification of new pathogenicity factors. *Journal of Infectious Diseases*, 196(11):1603–1612, 2007.
- M. E. Siddall and J. R. Barta. Phylogeny of plasmodium species: Estimation and inference. *The Journal of parasitology*, 78(3):567–568, 1992.
- A. B. S. Sidhu, D. Verdier-Pinard, and D. A. Fidock. Chloroquine resistance in plasmodium falciparum malaria parasites conferred by pfcr mutations. *Science*, 298(5591):210–213, 2002.

- O. Silvie, K. Goetz, and K. Matuschewski. A sporozoite asparagine-rich protein controls initiation of plasmodium liver stage development. *PLoS pathogens*, 4(6):e1000086, 2008.
- A. P. Singh, C. A. Buscaglia, Q. Wang, A. Levay, D. R. Nussenzweig, J. R. Walker, E. A. Winzeler, H. Fujii, B. Fontoura, and V. Nussenzweig. Plasmodium circumsporozoite protein promotes the development of the liver stages of the parasite. *Cell*, 131(3):492–504, 2007.
- R. Sleight and C. Kent. Regulation of phosphatidylcholine biosynthesis in cultured chick embryonic muscle treated with phospholipase c. *Journal of Biological Chemistry*, 255(22):10644–10650, 1980.
- C. A. Smith, E. J. Want, G. O’Maille, R. Abagyan, and G. Siuzdak. Xcms: processing mass spectrometry data for metabolite profiling using nonlinear peak alignment, matching, and identification. *Analytical chemistry*, 78(3):779–787, 2006.
- C. Sohlenkamp, I. M. López-Lara, and O. Geiger. Biosynthesis of phosphatidylcholine in bacteria. *Progress in lipid research*, 42(2):115–162, 2003.
- P. T. Spellman, G. Sherlock, M. Q. Zhang, V. R. Iyer, K. Anders, M. B. Eisen, P. O. Brown, D. Botstein, and B. Futcher. Comprehensive identification of cell cycle-regulated genes of the yeast *saccharomyces cerevisiae* by microarray hybridization. *Molecular biology of the cell*, 9(12):3273–3297, 1998.
- S. Sridaran, S. K. McClintock, L. M. Syphard, K. M. Herman, J. W. Barnwell, and V. Udhayakumar. Anti-folate drug resistance in africa: meta-analysis of reported dihydrofolate reductase (dhfr) and dihydropteroate synthase (dhps) mutant genotype frequencies in african plasmodium falciparum parasite populations. *Malaria journal*, 9(1):247, 2010.
- H. STAINES and K. Kirk. Increased choline transport in erythrocytes from mice infected with the malaria parasite plasmodium vinckei vinckei. *Biochem. J*, 334:525–530, 1998.
- A. Stead, P. Bray, I. Edwards, H. DeKoning, B. Elford, and P. Stocks. S. 32 a. ward. 2001. diamidine compounds: selective uptake and targeting in plasmodium 33 falciparum. *Mol. Pharmacol*, 59: 1298–1306.
- G. Stephanopoulos, A. A. Aristidou, and J. Nielsen. *Metabolic engineering: principles and methodologies*. Academic Press, 1998.
- X.-z. Su, V. M. Heatwole, S. P. Wertheimer, F. Guinet, J. A. Herrfeldt, D. S. Peterson, J. A. Ravetch, and T. E. Wellems. The large diverse gene family var encodes proteins involved in cytoadherence and antigenic variation of plasmodium falciparum-infected erythrocytes. *Cell*, 82(1):89–100, 1995.

- R. Sundler and B. Akesson. Regulation of phospholipid biosynthesis in isolated rat hepatocytes. effect of different substrates. *Journal of Biological Chemistry*, 250(9):3359–3367, 1975.
- N. Surolia and A. Surolia. Triclosan offers protection against blood stages of malaria by inhibiting enoyl-acyl reductase of plasmodium falciparum. *Nature medicine*, 7(2):167–173, 2001.
- C. J. Sutherland. Surface antigens of plasmodium falciparum gametocytes: a new class of transmission-blocking vaccine targets? *Molecular and biochemical parasitology*, 166(2):93–98, 2009.
- I. Takigawa and H. Mamitsuka. Probabilistic path ranking based on adjacent pairwise coexpression for metabolic transcripts analysis. *Bioinformatics*, 24(2):250–257, 2008.
- A. M. Talman, O. Domarle, F. E. McKenzie, F. Ariey, and V. Robert. Gametocytogenesis: the puberty of plasmodium falciparum. *Malaria Journal*, 3(1):24, 2004.
- A. S. Tarun, X. Peng, R. F. Dumpit, Y. Ogata, H. Silva-Rivera, N. Camargo, T. M. Daly, L. W. Bergman, and S. H. Kappe. A combined transcriptome and proteome survey of malaria parasite liver stages. *Proceedings of the National Academy of Sciences*, 105(1):305–310, 2008.
- A. S. Tarun, A. M. Vaughan, and S. H. Kappe. Redefining the role of de novo fatty acid synthesis in plasmodium parasites. *Trends in parasitology*, 25(12):545–550, 2009.
- L. Tawk, G. Chicanne, J. Dubremetz, V. Richard, B. Payrastre, H. Vial, C. Roy, and K. Wengelnik. Phosphatidylinositol 3-phosphate, an essential lipid in plasmodium, localizes to the food vacuole membrane and the apicoplast. *Eukaryotic Cell*, 9(10):1519–1530, 2010.
- M.-d.-M. Téllez, F. Matesanz, and A. Alcina. The c-terminal domain of the plasmodium falciparum acyl-coa synthetases pfacs1 and pfacs3 functions as ligand for ankyrin. *Molecular and biochemical parasitology*, 129(2):191–198, 2003.
- T. J. Templeton. The varieties of gene amplification, diversification and hypervariability in the human malaria parasite, plasmodium falciparum. *Molecular and biochemical parasitology*, 166(2):109–116, 2009.
- R. Teng, P. R. Junankar, W. A. Bubb, C. Rae, P. Mercier, and K. Kirk. Metabolite profiling of the intraerythrocytic malaria parasite plasmodium falciparum by 1h nmr spectroscopy. *NMR in Biomedicine*, 22(3):292–302, 2009.
- C. Trapnell, B. A. Williams, G. Pertea, A. Mortazavi, G. Kwan, M. J. van Baren, S. L. Salzberg, B. J. Wold, and L. Pachter. Transcript assembly and quantification by rna-seq reveals unannotated transcripts and isoform switching during cell differentiation. *Nature biotechnology*, 28(5):511–515, 2010.

- C. Trapnell, A. Roberts, L. Goff, G. Pertea, D. Kim, D. R. Kelley, H. Pimentel, S. L. Salzberg, J. L. Rinn, and L. Pachter. Differential gene and transcript expression analysis of rna-seq experiments with tophat and cufflinks. *Nature protocols*, 7(3):562–578, 2012.
- M. B. Trelle, A. M. Salcedo-Amaya, A. M. Cohen, H. G. Stunnenberg, and O. N. Jensen. Global histone analysis by mass spectrometry reveals a high content of acetylated lysine residues in the malaria parasite plasmodium falciparum. *Journal of proteome research*, 8(7):3439–3450, 2009.
- V. G. Tusher, R. Tibshirani, and G. Chu. Significance analysis of microarrays applied to the ionizing radiation response. *Proceedings of the National Academy of Sciences*, 98(9):5116–5121, 2001.
- R. Tuteja and A. Pradhan. Pfeif4e and pfeif4a colocalize and their double-stranded rna inhibits plasmodium falciparum proliferation. *Communicative & integrative biology*, 3(6):611–613, 2010.
- S. Tymoshenko, R. D. Oppenheim, D. Soldati-Favre, and V. Hatzimanikatis. Functional genomics of plasmodium falciparum using metabolic modelling and analysis. *Briefings in functional genomics*, 12(4):316–327, 2013.
- A. Vaid, R. Ranjan, W. Smythe, H. Hoppe, and P. Sharma. Pfpi3k, a phosphatidylinositol-3 kinase from plasmodium falciparum, is exported to the host erythrocyte and is involved in hemoglobin trafficking. *Blood*, 115(12):2500, 2010.
- G. G. Van Dooren, L. M. Stimmler, and G. I. McFadden. Metabolic maps and functions of the plasmodium mitochondrion. *FEMS microbiology reviews*, 30(4):596–630, 2006.
- C. van Ooij, P. Tamez, S. Bhattacharjee, N. L. Hiller, T. Harrison, K. Liolios, T. Kooij, J. Ramesar, B. Balu, J. Adams, et al. The malaria secretome: from algorithms to essential function in blood stage infection. *PLoS pathogens*, 4(6):e1000084, 2008.
- D. Vance, E. Trip, and H. Paddon. Poliovirus increases phosphatidylcholine biosynthesis in hela cells by stimulation of the rate-limiting reaction catalyzed by ctp: phosphocholine cytidyltransferase. *Journal of Biological Chemistry*, 255(3):1064–1069, 1980.
- J. E. Vance. Thematic review series: Glycerolipids. phosphatidylserine and phosphatidylethanolamine in mammalian cells: two metabolically related aminophospholipids. *Journal of lipid research*, 49(7):1377–1387, 2008.
- J. E. Vance and R. Steenbergen. Metabolism and functions of phosphatidylserine. *Progress in lipid research*, 44(4):207–234, 2005.
- J. P. Vanderberg. Reflections on early malaria vaccine studies, the first successful human malaria vaccination, and beyond. *Vaccine*, 27(1):2–9, 2009.

- A. M. Vaughan, A. S. Aly, and S. H. Kappe. Malaria parasite pre-erythrocytic stage infection: gliding and hiding. *Cell host & microbe*, 4(3):209–218, 2008.
- A. M. Vaughan, M. T. O’Neill, A. S. Tarun, N. Camargo, T. M. Phuong, A. S. Aly, A. F. Cowman, and S. H. Kappe. Type ii fatty acid synthesis is essential only for malaria parasite late liver stage development. *Cellular microbiology*, 11(3):506–520, 2009.
- H. Vial and M. Ancelin. Malarial lipids. *Malaria: parasite biology, pathogenesis, and protection*. ASM Press, Washington, DC, pages 159–175, 1998.
- H. Vial and C. Mamoun. Plasmodium lipids: metabolism and function. *Molecular Approach to Malaria*, pages 327–352, 2005.
- H. Vial, M. Ancelin, J. Philippot, and M. Thuet. Biosynthesis and dynamics of lipids in plasmodium-infected mature mammalian erythrocytes. *Blood cells*, 16(2-3):531–55, 1989a.
- H. Vial, M. Ancelin, M. Thuet, J. Philippot, et al. Phospholipid metabolism in plasmodium-infected erythrocytes: guidelines for further studies using radioactive precursor incorporation. *Parasitology*, 98(03):351–357, 1989b.
- H. Vial, M. Ancelin, J. Avila, J. Harris, et al. Malarial lipids: an overview. *Subcellular biochemistry, volume 18: Intracellular parasites.*, pages 259–306, 1992.
- H. Vial, S. Wein, C. Farenc, C. Kocken, O. Nicolas, M. Ancelin, F. Bressolle, A. Thomas, and M. Calas. Prodrugs of bisthiazolium salts are orally potent antimalarials. *Proceedings of the National Academy of Sciences of the United States of America*, 101(43):15458–15463, 2004.
- H. Vial, D. Penarete, S. Wein, S. Caldarelli, L. Fraisse, and S. Peyrottes. Lipids as drug targets for malaria therapy. In P. Selzer and K. Becker, editors, *Apicomplexan Parasites: Molecular Approaches Toward Targeted Drug Development*, page 23. Wiley-VCH Press, 2011a.
- H. Vial, D. Penarete, S. Wein, S. Caldarelli, L. Fraisse, and S. Peyrottes. Lipids as drug targets for malaria therapy. *Apicomplexan Parasites*, pages 137–162, 2011b.
- H. J. Vial, M. J. Thuet, J. L. Broussal, and J. R. Philippot. Phospholipid biosynthesis by plasmodium knowlesi-infected erythrocytes: the incorporation of phospholipid precursors and the identification of previously undetected metabolic pathways. *The Journal of parasitology*, pages 379–391, 1982a.
- H. J. Vial, M. J. THUET, and J. R. PHILIPPOT. Phospholipid biosynthesis in synchronous plasmodium falciparum cultures¹. *Journal of Eukaryotic Microbiology*, 29(2):258–263, 1982b.

- H. J. Vial, J. R. Philippot, and D. F. Wallach. A reevaluation of the status of cholesterol in erythrocytes infected by plasmodium knowlesi and p. falciparum. *Molecular and biochemical parasitology*, 13(1): 53–65, 1984a.
- H. J. Vial, M. J. Thuet, and J. R. Philippot. Cholinephosphotransferase and ethanolaminephosphotransferase activities in plasmodium knowlesi-infected erythrocytes: Their use as parasite-specific markers. *Biochimica et Biophysica Acta (BBA)-Lipids and Lipid Metabolism*, 795(2):372–383, 1984b.
- H. J. Vial, M. L. Ancelin, N. Elabbadi, H. Orcel, H.-J. Yeo, and C. Gumila. Infected erythrocyte choline carrier inhibitors: exploring some potentialities inside plasmodium phospholipid metabolism for eventual resistance acquisition. *Memórias do Instituto Oswaldo Cruz*, 89:91–97, 1994.
- H. J. Vial, P. Eldin, A. G. Tielens, and J. J. van Hellemond. Phospholipids in parasitic protozoa. *Molecular and biochemical parasitology*, 126(2):143–154, 2003.
- A. M. Vial H. Malarial lipids. *Sherman, I. (Ed.), Malaria: Parasite Biology, Biogenesis, Protection*, pages 159–175, 1998.
- P. Vincent, L. Maneta-Peyret, C. Cassagne, and P. Moreau. Phosphatidylserine delivery to endoplasmic reticulum-derived vesicles of plant cells depends on two biosynthetic pathways. *FEBS letters*, 498(1):32–36, 2001.
- S. K. Volkman, P. C. Sabeti, D. DeCaprio, D. E. Neafsey, S. F. Schaffner, D. A. Milner, J. P. Daily, O. Sarr, D. Ndiaye, O. Ndir, et al. A genome-wide map of diversity in plasmodium falciparum. *Nature genetics*, 39(1):113–119, 2006.
- R. F. Waller, P. J. Keeling, R. G. Donald, B. Striepen, E. Handman, N. Lang-Unnasch, A. F. Cowman, G. S. Besra, D. S. Roos, and G. I. McFadden. Nuclear-encoded proteins target to the plastid in toxoplasma gondii and plasmodium falciparum. *Proceedings of the National Academy of Sciences*, 95(21):12352–12357, 1998.
- C. W. Wang, S. B. Mwakalinga, C. J. Sutherland, S. Schwank, S. Sharp, C. C. Hermsen, R. W. Sauerwein, T. G. Theander, and T. Lavstsen. Identification of a major rif transcript common to gametocytes and sporozoites of plasmodium falciparum. *Malaria journal*, 9(1):147, 2010.
- J. Watanabe, M. Sasaki, Y. Suzuki, and S. Sugano. Analysis of transcriptomes of human malaria parasite plasmodium falciparum using full-length enriched library: identification of novel genes and diverse transcription start sites of messenger rnas. *Gene*, 291(1):105–113, 2002.
- D. J. Weatherall, L. H. Miller, D. I. Baruch, K. Marsh, O. K. Doumbo, C. Casals-Pascual, and D. J. Roberts. Malaria and the red cell. *ASH Education Program Book*, 2002(1):35–57, 2002.

- S. Wein, M. Maynadier, Y. Bordat, J. Perez, S. Maheshwari, P. Bette-Bobillo, C. Tran Van Ba, D. Penarete-Vargas, L. Fraisse, R. Cerdan, et al. Transport and pharmacodynamics of albitazolium, a candidate antimalarial drug. *British journal of pharmacology*, (166):2263–2276, 2012.
- R. B. Weiss and J. F. Atkins. Translation goes global. *Science*, 334(6062):1509–1510, 2011.
- K. Wengelnik, V. Vidal, M. Ancelin, A. Cathiard, J. Morgat, C. Kocken, M. Calas, S. Herrera, A. Thomas, and H. Vial. A class of potent antimalarials and their specific accumulation in infected erythrocytes. *Science*, 295(5558):1311–1314, 2002.
- N. White. Antimalarial drug resistance: the pace quickens. *Journal of Antimicrobial Chemotherapy*, 30(5):571–585, 1992.
- P. Winstanley. Modern chemotherapeutic options for malaria. *The Lancet infectious diseases*, 1(4):242–250, 2001.
- W. H. Witola and C. B. Mamoun. Choline induces transcriptional repression and proteasomal degradation of the malarial phosphoethanolamine methyltransferase. *Eukaryotic cell*, 6(9):1618–1624, 2007.
- W. H. Witola, K. El Bissati, G. Pessi, C. Xie, P. D. Roepe, and C. B. Mamoun. Disruption of the plasmodium falciparum pfpmt gene results in a complete loss of phosphatidylcholine biosynthesis via the serine-decarboxylase-phosphoethanolamine-methyltransferase pathway and severe growth and survival defects. *Journal of Biological Chemistry*, 283(41):27636–27643, 2008.
- L. M. Yamauchi, A. Coppi, G. Snounou, and P. Sinnis. Plasmodium sporozoites trickle out of the injection site. *Cellular microbiology*, 9(5):1215–1222, 2007.
- I. Yeh, T. Hanekamp, S. Tsoka, P. D. Karp, and R. B. Altman. Computational analysis of plasmodium falciparum metabolism: organizing genomic information to facilitate drug discovery. *Genome research*, 14(5):917–924, 2004.
- H. Yeo, M. LARVOR, M. ANCELIN, and H. Vial. Plasmodium falciparum ctp: phosphocholine cytidyltransferase expressed in escherichia coli: purification, characterization and lipid regulation. *Biochem. J*, 324:903–910, 1997.
- H.-J. Yeo, J. S. Widada, O. Mercereau-Puijalon, and H. J. Vial. Molecular cloning of ctp: phosphocholine cytidyltransferase from plasmodium falciparum. *European Journal of Biochemistry*, 233(1):62–72, 1995.

- J. A. Young, J. R. Johnson, C. Benner, S. F. Yan, K. Chen, K. G. Le Roch, Y. Zhou, and E. A. Winzeler. In silico discovery of transcription regulatory elements in plasmodium falciparum. *BMC genomics*, 9(1):70, 2008.
- M. Yu, T. Kumar, L. J. Nkrumah, A. Coppi, S. Retzlaff, C. D. Li, B. J. Kelly, P. A. Moura, V. Lakshmanan, J. S. Freundlich, et al. The fatty acid biosynthesis enzyme fabi plays a key role in the development of liver-stage malarial parasites. *Cell host & microbe*, 4(6):567–578, 2008.
- P. Yuan, E. F. Hendriks, H. R. Fernandez, W. J. O’Sullivan, and T. S. Stewart. Functional expression of the gene encoding cytidine triphosphate synthetase from plasmodium falciparum which contains two novel sequences that are potential antimalarial targets. *Molecular and biochemical parasitology*, 143(2):200–208, 2005.
- M. Zhang, C. Fennell, L. Ranford-Cartwright, R. Sakthivel, P. Gueirard, S. Meister, A. Caspi, C. Dorig, R. S. Nussenzweig, R. Tuteja, et al. The plasmodium eukaryotic initiation factor-2 α kinase ik2 controls the latency of sporozoites in the mosquito salivary glands. *The Journal of experimental medicine*, 207(7):1465–1474, 2010.
- Y.-M. Zhang and C. O. Rock. Membrane lipid homeostasis in bacteria. *Nature Reviews Microbiology*, 6(3):222–233, 2008.

Article published/submitted

Article:I

Kinetic modelling of Phospholipid synthesis in Plasmodium knowlesi unravels crucial steps and relative importance of multiple pathways, **Partho Sen, Henri J.Vial** and **Ovidiu Radulescu**, published in *BMC systems biology*, (<http://www.biomedcentral.com/1752-0509/7/123#B1>).

Appendix A

Proofs of mathematical results, parameter confidence intervals, sensitivity analysis

Derivation of Eq.(3.6) found in Chapter.3

Let us consider a monomolecular reaction network. If some reactions are reversible, we split these reactions into two by using distinct indices for the forward and for the backward directions, in such a way that $R_i \geq 0$, for all i . Then, we show that the steady state condition defining admissible fluxes

$$S\vec{R} = 0, \tag{S1}$$

is equivalent to the branching parametrisation relation

$$R_i^{out,j} = \left[\sum_{k=1}^{n_j^{in}} R_k^{in,j} \nu_k^{in,j} / \nu_i^{out,j} \right] \alpha_i^j, \tag{S2}$$

where $\sum_i \alpha_i^j = 1, 0 \leq \alpha_i^j \leq 1$.

Indeed, let us notice that $\nu_i^{out,j} = -S_{ji}$ and $R_i = R_i^{out,j}$, if $S_{ji} < 0$. Similarly, $\nu_i^{in,j} = S_{ji}$ and $R_i = R_i^{in,j}$, if $S_{ji} > 0$. Relation (S1) is equivalent to

$$\sum_{i, S_{ji} > 0} S_{ji} R_i + \sum_{i, S_{ji} < 0} S_{ji} R_i = 0,$$

that reads

$$\sum_{k=1}^{n_j^{in}} \nu_k^{in,j} R_k^{in,j} - \sum_{i=1}^{n_j^{out}} \nu_i^{out,j} R_i^{out,j} = 0 \tag{S3}$$

The fluxes $R_i^{out,j}$ can always be expressed as in (S2), for some positive parameters α_i^j . However, if (S3) is satisfied, then $\sum_i \alpha_i^j = 1$ follows. Conversely, if (S2) is satisfied with $\sum_i \alpha_i^j = 1$, then (S3) follows.

Parameter confidence intervals

The available data constrain the values of many parameters. However, not all parameters are identifiable with the same precision. We describe here a simple post-processing procedure that allows to quantify the parametric uncertainty.

Our optimization method generates a set of values of parameters, that are local minima of the objective function. The lowest of such minima is the global optimum. To take into account possible experimental errors, and because several local minima can fit the experimental data reasonably well, we have considered not only the globally best fit, but also several local optima closest to the global optimum. Among these sets of parameters we considered as representative the one that is closest in the Euclidean distance to the median parameter value. The spread of parameter values around the median value provides a first estimate of the parameter range. Then, we have performed a local sensitivity analysis around each of the selected local minima of the objective function. To this aim, we multiply each parameter by factors that are independent, and log-uniformly distributed, namely $k_i = k_{0i} \exp((2U_i - 1)a)$, where U_i are independent, uniformly distributed in the interval $[0, 1]$, $a > 0$, and k_{0i} , k_i are the local optimum and the perturbed parameter values, respectively. The parameter range is defined in this case by all the perturbed parameters values k such that $|\log(\Phi(\vec{k})) - \log(\Phi(\vec{k}_0))| < \epsilon$, where ϵ is a small positive value. We call this perturbation scheme *uncorrelated, multiplicative*.

For further insight into the parametric uncertainty we have investigated, for each Michaelis-Menten reaction, the dynamical range of substrate concentrations. These ranges should ideally include concentration values both below and above the Michaelis constant K_m . In this case, both V_{max} and K_m are accurately determined. If the substrate concentration range lies below K_m , then the enzymatic reaction performs in its linear regime. In this case, one gets the ratio V_{max}/K_m , but V_{max} and K_m can not

be independently determined. If the concentration range is above K_m , then V_{max} is well determined, but for K_m one has only upper bounds. The situations corresponding to various parameters in this model are presented in Figure.S1.

For Michaelis-Menten reactions functioning in the linear regime, the range of the V_{max} and K_m values can be extended with no change in the objective function, if both V_{max} and K_m are multiplied by the same positive constant. We have therefore considered a *correlated, multiplicative* perturbation scheme in which the parameters of the same reaction are multiplied by the same factor, namely $V_{maxi} = V_{max0i} \exp((2U_i - 1)a)$ $K_{mi} = K_{m0i} \exp((2U_i - 1)a)$, where V_{max0i} , K_{m0i} are the unperturbed parameters and U_i are independent, uniformly distributed in the interval $[0, 1]$.

For the data hereby presented, we have selected 10 sets of parameters corresponding to the 10 lowest values of the objective function. The corresponding unperturbed values of the parameters are represented as lines in the Figure S1. We have applied random perturbations (1000 samples for each parameter and for each parameter set) and chose an ϵ value such that the perturbed objective function is not larger than the largest objective function in the unperturbed set. Then, we represented the minimum and maximum perturbed values of the parameters as error bars superimposed on the unperturbed values profiles. The resulting plot gives an idea of the parameter uncertainty. Some confidence intervals are large, as expected. The confidence intervals transcribed in the Table.4 of the chapter.3, are much larger, as they correspond to the minimum and maximum values of the perturbed parameters, all parameter sets confounded. For Table.4, we have chosen the correlated multiplicative perturbation scheme leading to the largest confidence ranges.

Of course, this does not mean that choosing a parameter value at random in the ranges provided will provide a good objective function, because the represented confidence intervals are the projections onto the parameters directions of a complicated domain in the parameter space.

Figure S1

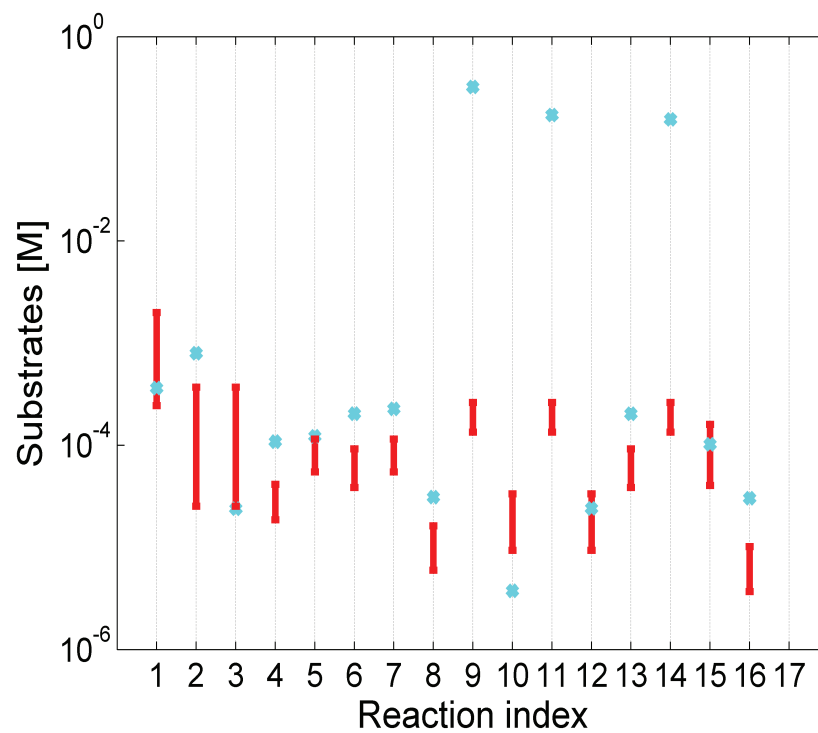


Figure 44: *Dynamic ranges of substrate concentrations.*

The interval of substrate concentrations are presented in red and the magenta dots represent the positions of K_m . The reaction 17 is not of Michaelis-Menten type and has not been represented in this plot. The dynamical concentration ranges could be supplemented by the zero concentrations (when it is supposed that the reactions rates are zero) and extended to $-\infty$ in logarithmic scale, but in this plot we have only considered non-vanishing concentrations, corresponding to effective measurements.

Figure S2

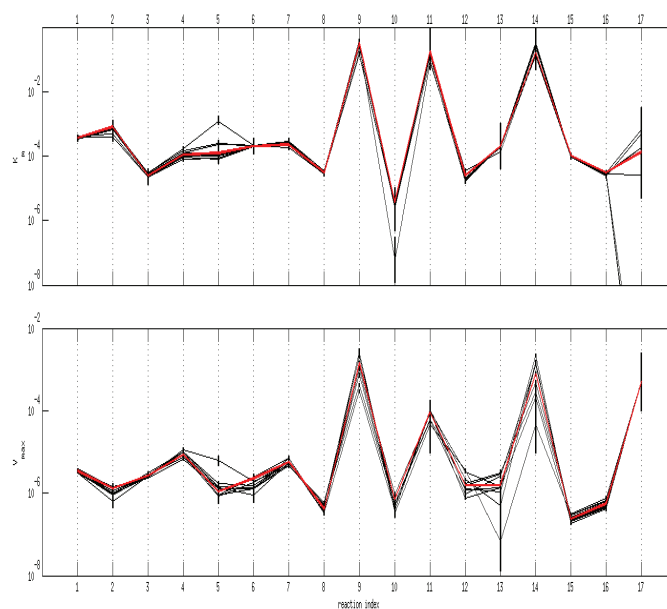


Figure 45: *Parameter profiles and confidence intervals for a uncorrelated, multiplicative perturbation scheme*

Parameter profiles and confidence intervals for a uncorrelated, multiplicative perturbation scheme. The lines connect parameter values corresponding to local minima of the objective function and therefore inform on the parameter correlation.

Figure S3

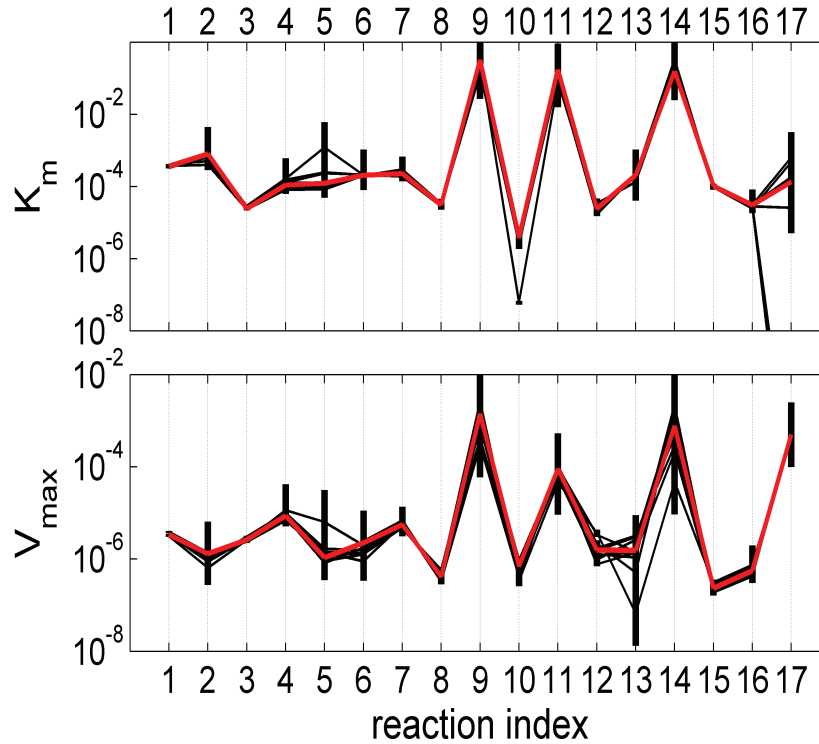


Figure 46: *Parameter profiles and confidence intervals for a correlated, multiplicative perturbation scheme*

Parameter profiles and confidence intervals for a correlated, multiplicative perturbation scheme. Notice the larger confidence intervals, corresponding to correlated variations of V_{max} and K_m . The lines connect parameter values corresponding to local minima of the objective function, also inform on the parameter correlation.

Sensitivity coefficients

The kinetic model was simulated for one hour, starting with $ChoE = 50\mu M$, $SerE = 0$, $EtnE = 0$, for optimal parameters and also for perturbed values of the parameters. Partial derivatives of the fluxes and concentrations were numerically estimated using the two point symmetric finite difference scheme, ensuring second order error in the variation of the argument. The results of this calculations are given in Tables S1-S4.

Table.S1

Flux sensitivity vs. V_{max}

	V_{max1}	V_{max2}	V_{max3}	V_{max4}	V_{max5}	V_{max6}	V_{max7}	V_{max8}	V_{max9}	V_{max10}	V_{max11}	V_{max12}	V_{max13}	V_{max14}	V_{max15}	V_{max16}	V_{max17}
R_1	0	0	0	0	0	0	0	0	0	0	0	0	0	0	0	0	0
R_2	0	0	0	0	0	0	0	0	0	0	0	0	0	0	0	0	0
R_3	0	0	0	0	0	0	0	0	0	0	0	0	0	0	0	0	0
R_4	0	0	0	0	0	0	0	0	0	0	0	0	0	0	0	0	0
R_5	0	0	0	0	0	0	0	0	0	0	0	0	0	0	0	0	0
R_6	0	0	0	0	0	0.58	0	0.44	0.05	0.37	0.02	-	-	-	0.77	0.39	0
R_7	0	0	0	0	0	0	0	0	0	0	0	0	0	0	0	0	0
R_8	0	0	0	0	0	0	0	0.40	0	0	0	0	0	0	0.78	0.34	0
R_9	0	0	0	0	0	0.61	0	0.50	0.75	0.37	-	-	-	-	0.78	0.44	0
R_{10}	0	0	0	0	0	0.04	0	0.41	0.06	0.37	-	-	-	-	0.76	0.35	0
R_{11}	0	0	0	0	0	0.61	0	0.50	-	0.37	0.96	-	-	-	0.78	0.44	0
R_{12}	0	0	0	0	0	0.04	0	0.42	0.07	-	-	0.65	-	-	0.82	0.36	0
R_{13}	0	0	0	0	0	-	0	0.44	0.05	0.37	0.02	-	0.62	-	0.77	0.39	0
R_{14}	0	0	0	0	0	0.61	0	0.50	-	0.37	-	-	-	0.67	0.78	0.44	0
R_{15}	0	0	0	0	0	0	0	0	0	0	0	0	0	1	0	0	0
R_{16}	0	0	0	0	0	0	0	0	0	0	0	0	0	0	0.88	0.30	0
R_{17}	0	0	0	0	0	0	0	0	0	0	0	0	0	0	0	0	0

Table.S2

Flux sensitivity vs. K_m

	K_{m1}	K_{m2}	K_{m3}	K_{m4}	K_{m5}	K_{m6}	K_{m7}	K_{m8}	K_{m9}	K_{m10}	K_{m11}	K_{m12}	K_{m13}	K_{m14}	K_{m15}	K_{m16}	K_{m17}
R_1	0	0	0	0	0	0	0	0	0	0	0	0	0	0	0	0	0
R_2	0	0	0	0	0	0	0	0	0	0	0	0	0	0	0	0	0
R_3	0	0	0	0	0	0	0	0	0	0	0	0	0	0	0	0	0
R_4	0	0	0	0	0	0	0	0	0	0	0	0	0	0	0	0	0
R_5	0	0	0	0	0	0	0	0	0	0	0	0	0	0	0	0	0
R_6	0	0	0	0	0	-	0	-	-	-	-	0.33	0.38	0.01	-	-	0
R_7	0	0	0	0	0	0	0	0	0	0	0	0	0	0	0	0	0
R_8	0	0	0	0	0	0	0	-	0	0	0	0	0	0	-	-	0
R_9	0	0	0	0	0	-	0	-	-	-	0.03	0.31	0.34	0.33	-	-	0
R_{10}	0	0	0	0	0	-	0	-	-	-	0.002	0.33	0.02	0.02	-	-	0
R_{11}	0	0	0	0	0	0.04	0	0.35	0.06	0.34	-	0.32	0.34	0.33	-	-	0
R_{12}	0	0	0	0	0	0.61	0	0.46	0.35	0.96	0.96	-	0.02	0.02	0.56	0.39	0
R_{13}	0	0	0	0	0	0.42	0	-	-	-	-	0.33	-	0.01	-	-	0
R_{14}	0	0	0	0	0	-	0	-	0.25	-	0.03	0.32	0.34	-	-	-	0
R_{15}	0	0	0	0	0	0	0	0	0	0	0	0	0	0	-	0	0
R_{16}	0	0	0	0	0	0	0	0	0	0	0	0	0	0	0.62	-	0
R_{17}	0	0	0	0	0	0	0	0	0	0	0	0	0	0	0.61	0.23	0

Table.S3

Concentration sensitivity vs. V_{max}

	V_{max1}	V_{max2}	V_{max3}	V_{max4}	V_{max5}	V_{max6}	V_{max7}	V_{max8}	V_{max9}	V_{max10}	V_{max11}	V_{max12}	V_{max13}	V_{max14}	V_{max15}	V_{max16}	V_{max17}
Ser	0	0	0	0	0	0	0	0	0	0	0	0	0	0	0	0	0
PS	0	0	0	0	0	-	0	0.59	0.02	0.37	0.006	-	-	-	0.82	0.53	0
						0.33						0.31	0.27	0.002			
Etn	0	0	0	0	0	0	0	0	0	0	0	0	0	0	0	0	0
PEtn	0	0	0	0	0	0	0	0	0	0	0	0	0	0	0	0	0
PE	0	0	0	0	0	0.71	0	0.64	-	0.39	-	-	-	-	0.84	0.59	0
								0.16		0.02	0.30	0.23	0.20				
PC	0	0	0	0	0	0.02	0	0.55	0.03	-	-6e-	-	-	-	0.83	0.49	0
									0.65	4	0.33	0.005	0.004				
Cho	0	0	0	0	0	0	0	0	0	0	0	0	0	0	1.1	-	0
																0.65	
PCho	0	0	0	0	0	0	0	-	0	0	0	0	0	0	0.91	0.49	0
								0.50									

Table.S4

Concentration sensitivity vs. k_m

	K_{m1}	K_{m2}	K_{m3}	K_{m4}	K_{m5}	K_{m6}	K_{m7}	K_{m8}	K_{m9}	K_{m10}	K_{m11}	K_{m12}	K_{m13}	K_{m14}	K_{m15}	K_{m16}	K_{m17}
Ser	0	0	0	0	0	0	0	0	0	0	0	0	0	0	0	0	0
PS	0	0	0	0	0	0.33	0	-	-	-	-	0.31	0.27	0.002	-	-	0
							0.57	0.02	0.36	0.006					0.57	0.50	
Etn	0	0	0	0	0	0	0	0	0	0	0	0	0	0	0	0	0
PEtn	0	0	0	0	0	0	0	0	0	0	0	0	0	0	0	0	0
PE	0	0	0	0	0	-	0	-	0.160	-	0.02	0.30	0.23	0.20	-	-	0
						0.71		0.62		0.38					0.58	0.56	
PC	0	0	0	0	0	-	0	-	-	0.64	6e4	0.32	0.005	0.004	-	-	0
						0.02		0.52	0.032						0.58	0.45	
Cho	0	0	0	0	0	0	0	0	0	0	0	0	0	0	-	0.62	0
															0.66		
PCho	0	0	0	0	0	0	0	0.47	0	0	0	0	0	0	-	-	0
															0.61	0.46	

Appendix B

Differential quantification of DNA microarray expression

The choice of method used to identify differentially expressed genes (*Allison et al.*, 2006) can greatly affect the set of genes that are identified. Despite the wealth of available methods, there are fondness for two of approaches, namely the fold-change and the t-statistic. This is presumably because of their simplicity and interpretability. Given their tendency to use these methods, it is important to determine which is best in the analysis of real biological data.

Let X_{ij} and Y_{ij} denote the log2 expression levels of gene i in replicate j in the control and treatment, respectively. The ordinary two-sample t-statistic is defined as

$$T_i = (X_{ij} - Y_{ij}) / S_i$$

where S_i is the standard deviation of the replicates for gene i .

Fold change is a number describing how much a quantity changes going from an initial to a final value. For example, an initial value of 30 and a final value of 60 corresponds to a fold change of 2, or in common terms, a two-fold increase. Fold change is calculated simply as the ratio of the final value to the initial value, i.e. if the initial value is A and final value is B, the fold change is B/A. Fold change is often used in analysis of gene expression data in microarray and RNA-Seq experiments, for measuring change in the expression level of a gene here are two definitions of fold-change in the literature. The standard definition of the fold-change for gene i in control and treatment is given by (*Tusher et al.*, 2001).

$$FC_{ij} = X_{ij} / Y_{ij}$$

where X_{ij} and Y_{ij} are the raw expression levels of gene i in replicate j in the control and treatment, respectively.

On the other hand, in (*Guo et al.2006*), states the fold-change for gene i as

$$FC_i = X_i/Y_i$$

Fold-change results in more reproducible gene lists than do the ordinary and modified t-statistics (*Shi et al., 2006*),(*Guo et al.2006, MAQC Consortium 2006*). But in other case results from simulations (*Daniela et al.,2007*) suggests that whether fold-change or a modified t-statistic results in more accurate gene lists depends on whether one is interested in an absolute change in gene expression or in the change in gene expression relative to the underlying noise in the gene.

